University College Cork, Ireland
Coláiste na hOllscoile Corcaigh

The relevance of bacterial isoprenoid biosynthetic pathways for host-microbe interactions
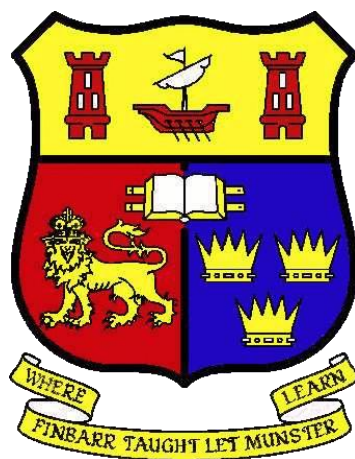
A Thesis Presented to the National University of Ireland

for the Degree of

Doctor of Philosophy

by

James Nolan B. Sc.

Student ID No. 106019978

October 2014

Supervisors: Dr. Cormac Gahan and Prof. Colin Hill

School of Microbiology

University College Cork

Head of Department: Professor Gerald Fitzgerald

CONTENTS

DECLARATION

I hereby declare that this thesis is my own work and has not been submitted for any other degree, either at University College Cork or elsewhere. Wherever contributions of others have been involved, every effort has been made to indicate this clearly, with reference to the scientific literature or acknowledgement of collaborative research or discussion.

Signed _____

James Nolan

Thesis Abstract

This thesis was undertaken to investigate the relevance of two bacterial isoprenoid biosynthetic pathways (Mevalonate (MVAL) and 2-C-methyl-$_D$-erythritol 4-phosphate (MEP)) for host-microbe interactions. We determined a significant reduction in microbial diversity in the murine gut microbiota (by next generation sequencing) following oral administration of a common anti-cholesterol drug Rosuvastatin (RSV) that targets mammalian and bacterial HMG-CoA reductase (HMG-R) for inhibition of MVAL formation. In tandem we identified significant hepatic and intestinal off-target alterations to the murine metabolome indicating alterations in inflammation, bile acid profiles and antimicrobial peptide synthesis with implications on community structure of the gastrointestinal microbiota in statin-treated animals. However we found no effect on local Short Chain Fatty Acid biosynthesis (metabolic health marker in our model). We demonstrated direct inhibition of bacterial growth *in-vitro* by RSV which correlated with reductions in bacterial MVAL formation. However this was only at high doses of RSV. Our observations demonstrate a significant RSV-associated impact on the gut microbiota prompting similar human analysis. Successful deletion of another MVAL pathway enzyme (HMG-CoA synthase (*mvaS*)) involved in *Listeria monocytogenes* EGDe isoprenoid biosynthesis determined that the enzyme is non-essential for normal growth and *in-vivo* pathogenesis of this pathogen. We highlight potential evidence for alternative means of synthesis of the HMG-CoA substrate that could render *mvaS* activity redundant under our test conditions. Finally, we showed by global gene expression analysis (Massive Analysis of cDNA Ends (MACE RNA-seq) a significant role for the penultimate MEP pathway metabolite (E)-4-hydroxy-3-methyl-2-but-2-enyl pyrophosphate (HMBPP) in significant up regulation of genes

of immunity and antigen presentation in THP-1 cells at nanomolar levels. We infected THP-1 cells with wild type or HMBPP under/over-producing *L. monoctyogenes* EGDe mutants and determined subtle effects of HMBPP upon overall host responses to *Listeria* infection. Overall our findings provide greater insights regarding bacterial isoprenoid biosynthetic pathways for host-microbe/microbe-host dialogue.

Chapter 1: Literature Review

3-hydroxy-3-methylglutaryl coenzyme A reductase (HMG-R): evolution, biochemistry, phylogenetics and the cholesterol-independent effects of statins

Contents

8. Statins and bile acids

8.1. Overview of cholesterol degradation and bile acid metabolism

8.2. Bile acid synthesis and regulation

8.3. Statins as mediators of bile acid synthesis

9. Short chain fatty acids and statins

9.1. Butyrate

9.2. Propionate

9.3. Acetate

10. Discussion

1. Abstract

3-hydroxy-3-methylglutaryl Co enzyme A reductase (HMG-R) is an important enzyme in the synthesis of mevalonate and subsequently the formation of isoprenoid compounds and cholesterol biosynthesis. Statins are lipid-lowering drugs that target the HMG-R enzyme for inhibition of the mevalonate pathway and cholesterol biosynthesis. Isoprenoids play a key role in cellular survival and the formation of integral cellular components such as the cell wall and cell membrane. In bacteria, isoprenoids are derived generally from one of two pathways: the classical mevalonate pathway or the alternate pathway via 2-C-methyl-D-erythritol 4-phosphate (MEP). Two different classes of HMG-R have been elucidated both biochemically and following bioinformatics analysis. Class 1 HMG-R are more sensitive to statin exposure than the Class 2 counterparts. Bioinformatic analysis of HMG-R was described to ascertain the distribution of the different classes of HMG-R in the gut microbiota. Biochemical analysis reveals the molecular level differences between both HMG-R classes and the associated tertiary structure of the enzyme. The historical use of statins and how they react with the target will also be discussed. Finally, cholesterol independent effects of statins associated with antimicrobial activity inflammation and immune response will be discussed to help ascertain the global impact of statin administration in the gut. The impact of statins on the bile acid biosynthetic regulatory network and on the production of short chain fatty acids will be analysed in light of implications on health and gut microbiota composition.

2. Introduction

2.1 Importance of isoprenoids

Isoprenoids are an important class of organic molecules that are ubiquitously found throughout a diverse range of organisms from eubacteria, archea and eukaryotes. At present, over 30,000 different isoprenoid derivatives are known. Their biological function is diverse in many micro-organisms forming membrane molecules such as hopanoids, sterols and electron transport molecules such as coenzyme Q. Isoprenoids also have wider functions involved in cellular transportation and regulation (Lange, Rujan *et al*. 2000; Wilding, Brown *et al*. 2000). Derivatives of isoprenoids such as farnesyl pyrophosphate (FPP) and geranyl pyrophosphate (GPP) are important compounds involved in metabolism as they form the backbone of many crucial products e.g. monoterpenes, sterols, farnesyl- and geranyl proteins, carotenoids, ubiquinones and Vitamin K2 (Holstein and Hohl 2004).

Isoprenoid biosynthesis generally occurs via one of two different pathways: the classical mevalonate pathway which is found generally in eukaryotic micro-organisms and a few prokaryotes and the alternate 2-C-methyl-D-erythritol 4-phosphate (MEP) pathway which is used by most prokaryotes (Goldstein and Brown 1990; Campos, Rodriguez-Concepcion *et al*. 2001; Hecht, Eisenreich *et al*. 2001; McAteer, Coulson *et al*. 2001) (Fig.1). *Listeria monocytogenes* is one such prokaryotic microorganism that has been well studied in our laboratory in terms of isoprenoid biosynthesis (Begley, Bron *et al.* 2008).

2.2. HMG-CoA reductase (HMG-R)

HMG-CoA reductase (HMG-R) is the major rate-limiting enzyme of the mevalonate pathway encoded by the *hmgR* gene (Fig. 1). This enzyme is the target of the class of drugs known as statins, which are used in the treatment of patients with hypercholesterolemia and elevated low-density lipoprotein (LDL) cholesterol in the bloodstream. Indeed, figures for 2010 suggest that 255.4 million statin scripts were prescribed in the United States of America (Borders-Hemphill 2010).

Analysis of the HMG-R enzyme revealed two different classes, each with their own distinct active site and enzymatic structure (Istvan 2001). These classes have been designated as Class 1 or Class 2 HMG-R isoforms. Comparisons of both enzymes elucidated highly conserved co-enzyme binding regions for nicotinamide adenine dinucleotide (NADH) and nicotinamide adenine dinucleotide phosphate (NAD(P)H) and variable binding sites for the substrate HMG-CoA.

Structural and sequence variations (discussed later in this review) between the two classes of enzyme have been proposed as evidence of divergent evolution occurring in the history of the HMG-CoA reductase enzyme (Istvan 2001). An appreciation of the differing biochemistry of these enzyme classes is significant as it is known that Class 1 enzymes are more sensitive than Class 2 HMG-R enzymes to statins (Bochar, Stauffacher *et al*. 1999; Hedl, Tabernero *et al*. 2004).

An evolutionary basis for the Mevalonate (MVAL) pathway and many other key catalytic enzymes such as HMG-R has been well described utilising modern day bioinformatics techniques (Neighbour-joining phylogenetic tree construction) shedding light on the origins of this pathway in biology (Fig.2). Previously, it was widely believed that the MVAL pathway mainly existed in higher organisms such as

mammals whilst the MEP pathway was largely present in bacteria. We have shown by extensive bioinformatics and phylogenetic analysis the existence of HMG-R (and indeed the MVAL pathway) in many gut bacterial species (including *Enterococcus faecalis, Enterococcus faecium* and *Lactobacillus johnsonii*) with the Class 2 HMG-R isoform and a number of other infectious bacterial species (including *Corynebacterium kroppenstedti*) with the Class 1 isoform (Fig.3).

Careful examination of different hypotheses for the ancestry of the Mevalonate pathway concluded that the origin of mevalonate pathway enzymes derives from a single common cenancestor in the past and subsequent evolution over time lead to genetic variations in the pathway. The MEP pathway as we know it today was absent in the cenancestor and may have been acquired overtime during a horizontal transfer or symbiotic event between bacteria and eukaryotes (Fig. 2) (Lombard and Moreira 2011).
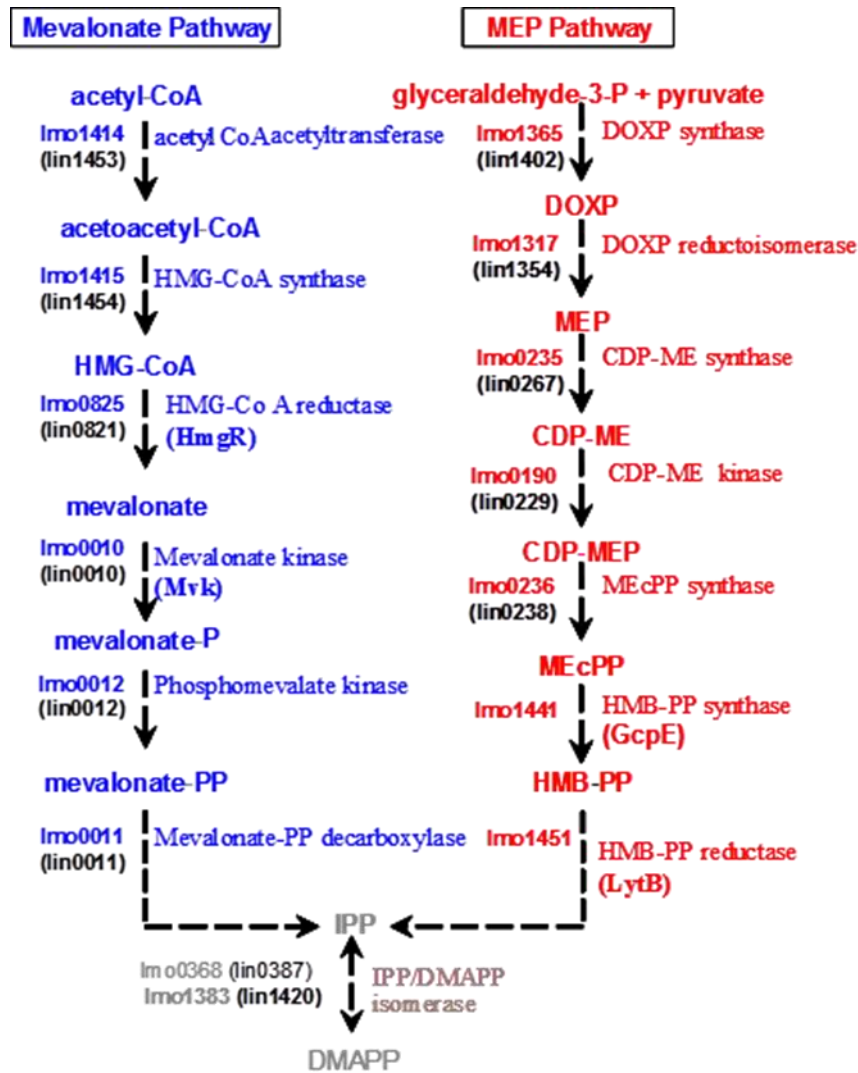
Fig.1. Schematic representation of the enzymes and metabolites involved in bacterial isoprenoid biosynthesis.

Illustrated are the MVAL and MEP isoprenoid biosynthetic pathways as described for the bacterium *L. monocytogenes* EGDe. The classical mevalonate pathway is indicated in blue and the MEP pathway in red. Homologues for corresponding genes in *L. innocua* Clip 11262 are indicated in black. This figure was taken from (Begley, Gahan *et al.* 2004) and was developed from the NCBI database.

3. Evolution of isoprenoid biosynthetic pathways

3.1 Mevalonate (MVAL) and MEP pathways

Historically the mevalonate pathway was originally discovered in eukaryotes and other higher organisms as the main biosynthetic route for isoprenoid precursors such as isopentenyl-pyrophosphate (IPP), dimethylallyl-pyrophosphate (DMAPP) (McGarvey and Croteau 1995). Subsequently, an alternative pathway (known as the MEP pathway) was later discovered in bacteria for the generation of isoprenoid precursors (Boucher, Huber *et al*. 2001; Kuzuyama 2002).

Evolutionary analysis of isoprenoid biosynthesis determined a hypothetical single common cenancestor organism which is believed to have given rise to the MVAL and MEP pathways in eukarya, bacteria and archaea (Fig. 2) (Lombard and Moreira 2011). This hypothesis suggests that over evolutionary time both pathways co-evolved in many different life forms and may point to why some microorganisms exclusively contain one or the other pathway. The MVAL pathway has been identified as the main biosynthetic route for isoprenoids for certain bacteria such as *S. aureus* (Balibar, Shen *et al*. 2009) and conversely the MEP pathway for other bacteria (such as *E. coli*) (Hintz, Reichenberg *et al*. 2001). Interestingly in our laboratory we identified a unique microorganism (*L. monocytogenes*) which is currently the only known utilizer of both pathways (Begley, Bron *et al*. 2008). An explanation for this anomaly is currently not well known but it is possible that host-microbe interactions (including virulence potential and immune stimulation) may determine the development of either pathway in many microorganisms (Boucher and Doolittle 2000; Heuston, Begley *et al*. 2012).
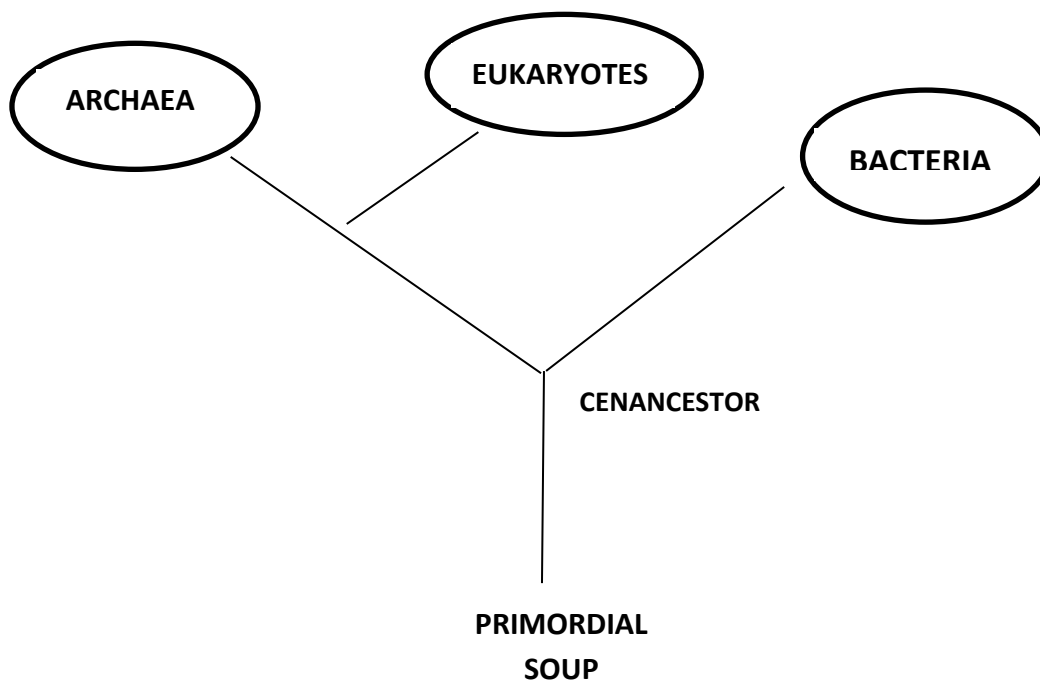
Fig. 2. The cenancestor hypothesis for the origin of isoprenoid biosynthesis.

For simplicity the subdivisions within the three main lineages (Archaea, Eukaryotes and Bacteria) have been excluded. Inheritance of the isoprenoid biosynthetic pathways is hypothesised to derive from a single common ancestral organism. Figure adapted from: (Lombard and Moreira 2011).

3.2. Phylogenetic and bioinformatics analysis of HMG-CoA reductase (HMG-R)

HMG-R, the target of anti-cholesterol drugs such as statins has become one of the most widely studied enzymes. HMG-R previously was categorised into two groups; Class 1 and Class 2 isoforms determined using sequence-based alignments (Lombard and Moreira 2011), (Istvan 2001). In this review, we used published sequences from the National Centre for Biotechnology Information (NCBI) GenBank database (http://www.ncbi.nlm.nih.gov/) for a variety of bacteria and other organisms that contain the HMG-R enzyme (with a particular focus on major gut dwelling microbes). Subsequently we performed molecular evolutionary genetics

15

analysis (MEGA) to calculate evolutionary distance and determine phylogenetic trees using sequence based alignments for both isoforms (Neighbour-Joining method) (Saitou and Nei 1987) confirming observations in the literature (Fig. 3).

We confirmed previous findings that Class 1 enzymes were mainly present in higher organisms such as humans (*Homo sapiens*), plant species (including *Arabdopsis*), and eukaryotic microorganisms (*Saccharomyces*) while Class 2 enzymes were present in bacterial species (including *E. faecalis* and *S. aureus*). One notable microorganism identified by our analysis was the bacterium *C. kroppenstedtii* DSM44385. This bacterium was unique in that we were successfully able to cultivate under our laboratory conditions as a representative Class 1 HMG-R microorganism (Tauch, Bischoff *et al.* 2004). Importantly *C. kroppenstedtii* (a lipophilic corynebacterial species) is a less pathogenic relative of *Corynebacterium. diptheriae* (the causative agent of diphtheria) and is generally safe to work with. We were successfully able to investigate the effect on growth of this bacterium when exposed to statin treatment (see Chapter 2).
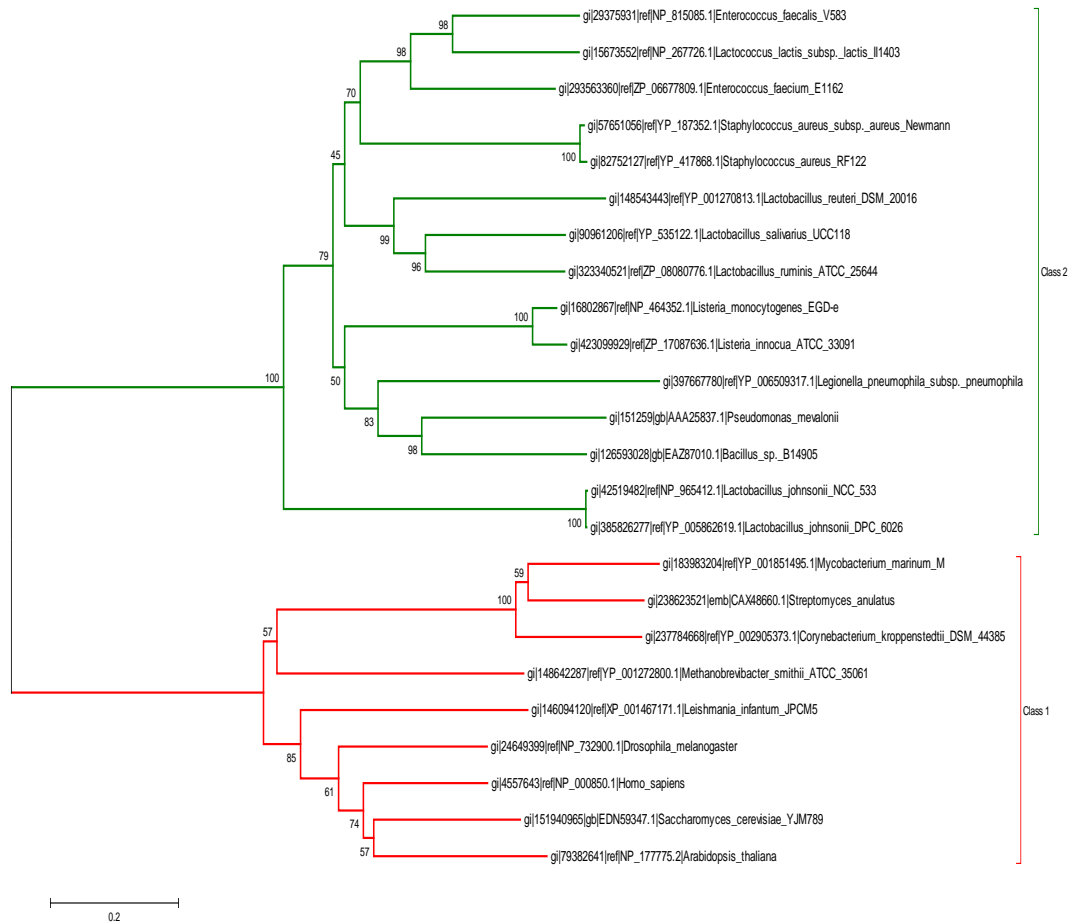
Fig.3. Phylogenetic analysis of Class 1 and Class 2 HMG-R enzymes in a variety of organisms.

Sequences were obtained from the National Centre for Biotechnology Information (NCBI) GenBank database. Evolutionary analysis was inferred using the Neighbour-Joining method. The bootstrap percentage value from 500 different replicates is given beside each branch and clustered together into representative taxa. Evolutionary distances were calculated based on a Poisson distribution and are represented in the number of amino acid substitutions per site. Twenty-four amino acids were analysed and positions containing gaps or missing data removed. Molecular evolutionary genetic analysis was carried out using MEGA5.

Further explorations into the structural and functional properties of HMG-R revealed greater insights into the enzymatic architecture for both isoforms in humans and bacteria (*Pseudomonas mevalonii*) (Istvan 2001; Istvan and Deisenhofer 2001). Based on this it was generally accepted that Class 1 HMG-R isoforms were human like whilst Class 2 isoforms were bacterial like. Subsequently we summarise previous findings regarding conserved amino acid sequences for both isoforms involved in coenzyme factor binding, substrate (HMG-CoA) binding (summarised in Table 1).

We summarise previous findings that binding of coenzyme factors (such as NADH or NAD(P)H) by HMG-R is one such important determinant for Class 1or Class 2 classification (Istvan 2001). Biochemical analysis determined that Class 1 enzymes use the phosphorylated form of the nicotinamide adenine dinucleotide phosphate molecule (NAD(P)H). In contrast Class 2 enzymes use the non-phosphorylated version (NADH) as an energy source (Kim, Stauffacher *et al.* 2000) (Table 1). We summarise previous findings that Class 1 enzymes contain the amino acid sequence (DAMGAN) for coenzyme factor binding but there is a substitution in the fifth amino acid from alanine to methionine for Class 2 enzymes (DAMGMN). Both classes of HMG-R enzymes encode identical conserved amino acid regions for substrate (HMG-CoA) binding (CXDKK) and dimerization motifs (ENVIG) (Istvan 2001).

Organism	HMG-R	Conserved sequence and function	
Homo sapiens		DAMGAN	NAD(P)H binding
Drosphila melanogaster			
Caenorhabditis elegans			
Dictyostelium discoideum			
Schistosoma mansomi			
Gossypium hirsutum (cotton)		CXDKK	HMG-CoA binding
Trypanosoma cruzi	**Class 1**		
Saccharomyces cerevisiae			
Methanococcus jannaschii		ENVIG	Conserved dimerization motif
Sulfolobus solfataricus			
Streptomyces griseosporeus			
Archaeoglobus fulgidus		DAMGMN	NADH binding
Staphylococcus aureus			
Enterococcus faecalis			
Streptoococcus pyogenes	**Class 2**	CXDKK	HMG-CoA binding
Borrelia burgdoferi			
Pseudomonas mevalonii		ENVIG	Conserved dimerization motif

Table 1. Structure and sequence alignments of Class 1 and Class 2 HMG-R enzymes.

Summary of important findings based on amino acid sequence alignments of Class 1 and Class 2 HMG-R enzymes. Conversed regions and associated functions were determined for both isoforms. This table summarises alignments performed by (Istvan 2001).

4. Cholesterol homeostasis and statins

Cholesterol is an essential mammalian biomolecule found in nearly every cell of the body, serving many essential physiological functions such as forming precursors of steroidal hormones, vitamin D as well as the synthesis of bile acids. Normal healthy adults naturally synthesize approximately 900mg of cholesterol per day in the body and absorb around 300mg per day from the diet. Approximately 10% of cholesterol is manufactured in the liver with the remaining 90% being generated in extrahepatic tissues (Dietschy, Turley *et al.* 1993)

Dietary cholesterol absorbed from the gut is converted by pancreatic lipase enzymes to free cholesterol and subsequently secreted as bile acids in the intestine. Bile acid accumulations in the intestine can be recycled and reabsorbed by the body with great efficiency (Bosner, Lange *et al.* 1999). The synthesis of cholesterol involves many different enzymes and intermediate metabolites (Fig. 4). The rate limiting and negative feedback control mechanism of this system involves the HMG-R enzyme which catalyses the initial reaction of the HMG-CoA to mevalonate, in cholesterol biosynthetic cascade.

Synthesis of cholesterol occurs following transport of acetyl CoA from the mitochondria to the cytosol of the cell. Two molecules of acetyl CoA fuse together in a condensation reaction forming acetoacetyl-CoA (acetoacetyl-CoA thiolase) (Iglesias and Diez 2003). HMG-CoA is subsequently formed by the fusion of a third acetyl-CoA unit by HMG-CoA synthase. Once formed, HMG-CoA is then moved to the endoplasmic reticulum membrane of the cell where it is reduced by the rate limiting enzyme HMG-CoA reductase to mevalonate. Sequential reactions by a

number of different enzymes phosphorylate mevalonate before it is decarboxylated to form IPP and DMAPP. Squalene synthase catalyses the formation of squalene from IPP and DMAPP, which is then finally converted to lanosterol and cholesterol (Iglesias and Diez 2003). Homeostasis of cholesterol can also be regulated naturally by monitoring the uptake of dietary cholesterol, via the conversion and excretion of bile acids from cholesterol and elimination into the faeces.

Cholesterol homeostasis can also be artificially regulated by the use of highly hepato-selective drugs called statins that target HMG-R. Rosuvastatin (RSV) is a superstatin which is one of the most effective available on the market because of its low lipophilicity (Davidson, Ma *et al*. 2002; Cheng-Lai 2003). RSV can be rapidly absorbed via the oral route and retain high bioavailability (approx. 20% initial dose). RSV is administered in its active form and is minimally metabolised by the body compared to other statins (White 2002).
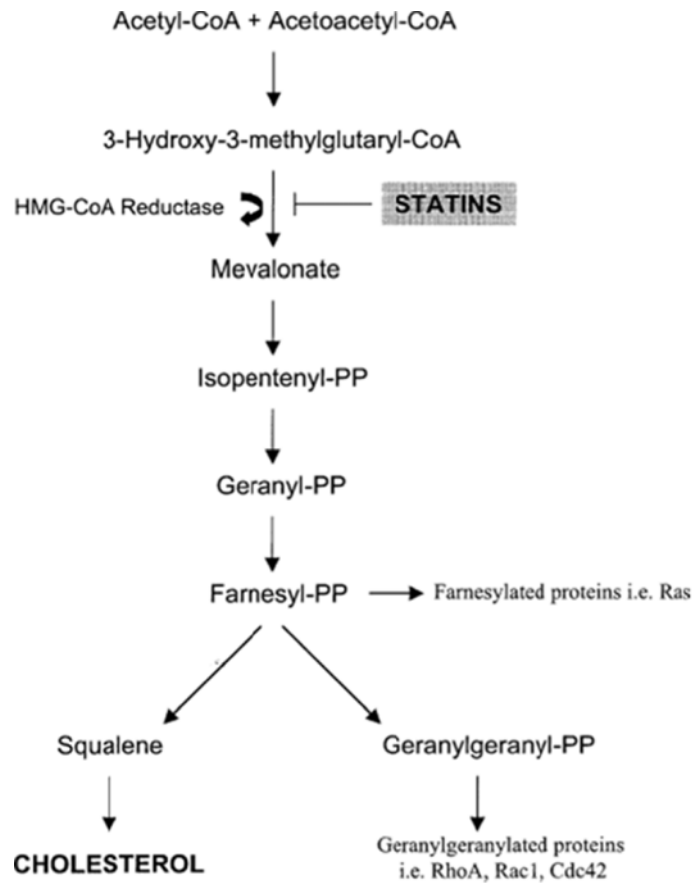
Fig.4. Cholesterol and geranylated/fernesylated protein biosynthesis in mammals.

The major metabolites of the cholesterol biosynthetic cascade are highlighted. Indicated is the major rate limiting enzyme HMG-CoA reductase (HMG-R) the major target of statins. Figure adapted from (Thurnher, Nussbaumer *et al.* 2012).

5.   Biochemistry of HMG-R

Previously we outlined the phylogenetics and bioinformatics of HMG-R and determined two distinct isoforms Class 1 and Class 2. We discuss how both enzymes have variations in their amino acids for important molecular functions such as co-enzyme factor binding (NADH/NAD(P)H). We will examine the precise molecular mechanisms involved in this interaction and determine the structure and folding of the HMG-R enzyme (below)

5.1. Interactions of HMG-R with co-enzyme factors

X-ray crystallography of the HMG-R protein confirms that class 1 enzymes favourably bind NAD(P)H whilst class 2 enzymes have a higher tendency to bind the NADH (Lawrence, Rodwell *et al*. 1995; Istvan 2001; Tabernero, Rodwell *et al*. 2003). Interestingly the orientation of the bound NAD(P) dihydronicotinamide ring structure differs in both enzymes. Relative to Class 1 enzymes the bound dihydronicotinamide ring in Class 2 enzymes is flipped at an angle 180º (Istvan 2001). Interaction of Class 2 HMG-R with NADH occurs via engagement of the amino acid residue phenylalanine (*Phe152*). However the interaction of Class 1 HMG-R with NAD(P)H involves a number of different amino acid residues at alternate positions including serine (*Ser626*), arginine (*Arg627*) and phenylalanine (*Phe628*) (Istvan 2002). This would suggest that modulation of HMG-R activity can be governed by phosphorylation states with respect to Class 1 and Class 2 enzymes.

5.2 Structure and folding of HMG-R

The polypepetide chain of the HMG-R enzyme can be divided into three main regions: the N-terminal membrane region, the C-terminal region and a short linking region connecting the catalytic and membrane regions. The N-terminal domain contains 339 amino acid residues integrated into the endoplasmic reticulum by membrane-spanning loops (eight in total) (Roitelman, Olender *et al.* 1992) (Fig. 5). This membrane region can sense elevated sterol levels in the cell and subsequently initiate degradation and repression of HMG-R (feedback regulation) (Skalnik, Narita *et al.* 1988). The C-terminal domain contains 548 amino acid residues and extends into the cytosol of the cell where it catalyses the formation of mevalonate (Liscum, Finer-Moore *et al.* 1985). The catalytic domain between Class 1 and Class 2 HMG-R enzymes is generally well conserved (up to 60% amino acid residue similarity) (Hampton, Dimster-Denk *et al.* 1996).

At the protein structure level the most striking difference between both HMG-R isoforms is the presence of a cis-loop conformation in the active site of the enzyme (Istvan 2001; Istvan 2002). Class 1 HMG-R enzymes exclusively contain this feature which plays an essential role in binding of the HMG-CoA substrate however it is completely absent from Class 2 HMG-R. Alternatively, it is known that Class 2 enzymes utilise neighbouring monomers in the active and recruiting specific lysine residues (*Lys267*), thus preserving orientation and functionality of the enzyme (Istvan 2001; Istvan 2002).
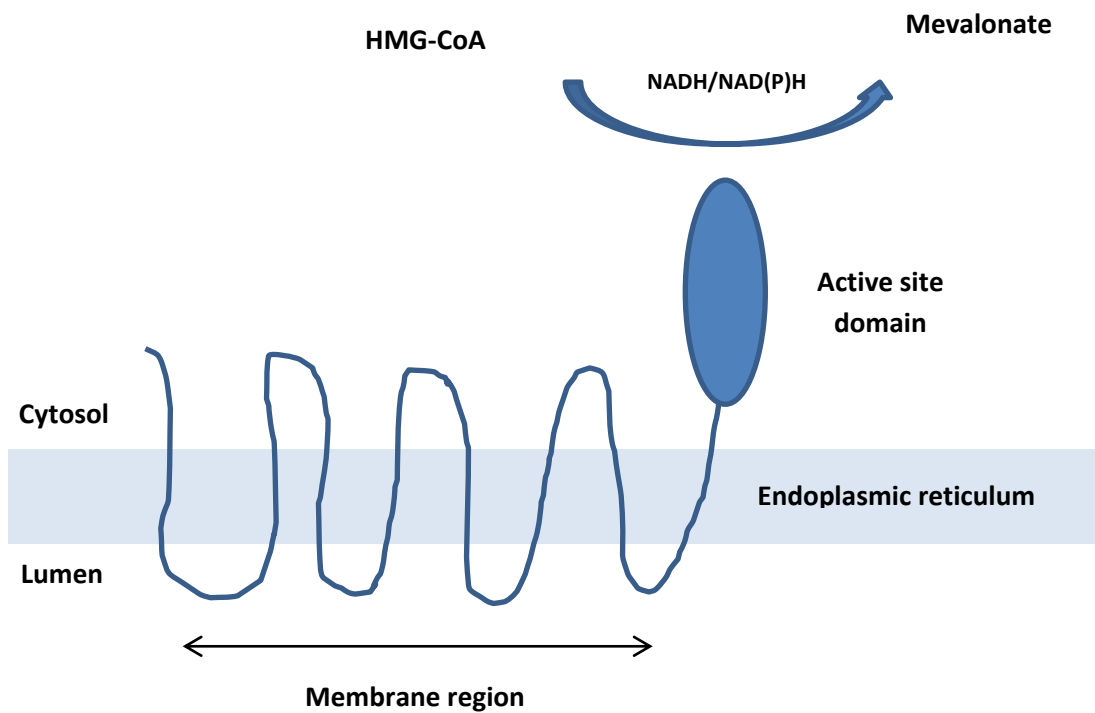
Fig.5. Simplistic illustration of the HMG-R enzyme.

The membrane region of HMG-R spans the endoplasmic reticulum of the cell and functions to sense sterol levels. The catalytic and active domain of the enzyme are present in the cytosol and derive energy from co-enzyme factors (NADH or NAD(P)H) to convert HMG-CoA into mevalonate. This image was adapted from: (DeBose-Boyd 2008).

6. Statins as HMG-R inhibitors

6.1 Mevastatin (compactin) the first naturally discovered statin

In the early 1970's, research began into microbial metabolites that had the ability to inhibit HMG-R, the important rate limiting enzyme in the biosynthesis of cholesterol. The first naturally discovered statin was mevastatin (or formerly compactin) found as a natural bi-product of some *Penicillium* species including: *Penicillium citrinum*, *Penicillium brevicompactum* and *Penicillium cyclopium,* (Brown, Smale *et al.* 1976; Endo, Kuroda *et al.* 1976; Doss, Chu *et al.* 1986). Mevastatin in its acidic form has a similar appearance to the core structure of the natural substrate of the HMG-R enzyme. This allows for competitive inhibition between the statin and HMG-CoA for the active site of the enzyme.

6.2 Diversity of statins

Currently, a large number of HMG-R inhibitors are widely available on the market to treat hypercholesterolemia including: atorvastatin, rosuvastatin, mevastatin, lovastatin, pravastatin and simvastatin (Fig. 6). These drugs have either been discovered in nature or were chemically synthesised and modified for increased activity. Statins have been shown to be extremely effective in reducing cholesterol in patients in particular lowering levels of low density lipoprotein (LDL) (Mabuchi, Sakai *et al.* 1983; Arad, Ramakrishnan *et al.* 1992; Davignon, Montigny *et al.* 1992).

Statin	Origin	Reference
Atorvastatin	Chemically synthesised	(Roth 2002)
Rosuvastatin	Chemically synthesised	(Watanabe, Koike *et al.* 1997)
Mevastatin	*Penicillium* spp.	(Endo, Kuroda *et al.* 1976)
Lovastatin	*Pleurotus ostreatus* (oyster mushroom)	(Bobek, Ozdin *et al.* 1998)
Pravastatin	Modified from lovasatin	(Endo, Kuroda *et al.* 1976)
Simvastatin	Modified from mevastatin	(Endo, Kuroda *et al.* 1976)
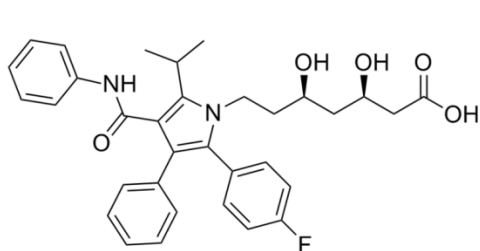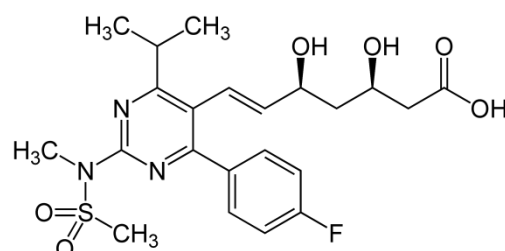
Atorvastatin   **Rosuvastatin**

Fig. 6. Statin diversity and their origins.

Described are six different statins (atorvastatin, rosuvastatin, mevastatin, lovastatin, pravastatin, and simvastatin) and their origins. Chemical structures for two commonly used statins are also illustrated (atorvastatin and rosuvastatin).

6.3. Competitive inhibition by statins

Statins inhibit the formation of mevalonate by reversibly and competitively binding the active site of the HMG-R. All statins share a HMG-like moiety in their chemical structure that mimics the natural substrate (HMG-CoA) for binding of the active site of HMG-R (Istvan and Deisenhofer 2001). Statins are large bulky molecules that bind tightly with HMG-R forming numerous strong Van der Waals attractions (Istvan 2002). Atorvastatin and rosuvastatin (RSV) are known to elicit very strong binding interactions with HMG-R (Blum 1994).

6.4. Antimicrobial activity of statins

It has been shown that both Class 1 and Class 2 HMG-R enzymes can be affected by statins. Increasingly statins are becoming linked with antimicrobial activity. Indeed Simvastatin has been identified as having a minimum inhibitory concentration (MIC) of 29.2mg/L against methicillin-sensitive strains of *S. aureus* and an MIC of 74.9mg/L against methicillin resistant strains (MRSA) (Jerwood and Cohen 2008). Similarly Atorvastatin proved beneficial in a hospital environment for the treatment of *C. difficile* in a number of patients (Park, Choi *et al.* 2013). Hence, it is reasonable to assume that there could be a possible effect on HMG-R containing microorganisms in the human gastro-intestinal as a result of long term prescription of these drugs (see Chapters 2 and 3 of this thesis).

7. Cholesterol-independent effects of statins

7.1. Statins promote formation of extracellular traps

Since the introduction of statins as a treatment for hypercholesterolemia, much research has been conducted into cholesterol-independent or off-target effects of statins. For instance, statins have been shown to improve endothelial function, decrease oxidative stress and inhibit the coagulation of blood (Liao and Laufs 2005). Statins have also been shown to engage the host human or murine immune system to increase the production of so-called DNA-based neutrophil or macrophage extracellular traps that are strongly antimicrobial (Chow, von Kockritz-Blickwede *et al.* 2010). These extracellular traps are the final end product of a cell death pathway and have become a key area of research as cholesterol-independent effectors of statins. These unique features of the immune response are composed largely of nuclear DNA, histones, antimicrobial peptides and proteases which are capable of engulfing and digesting many bacteria (Brinkmann, Reichard *et al*. 2004; von Kockritz-Blickwede and Nizet 2009). Extracellular trap release and antimicrobial activity has been shown to be dependent on the presence of reactive oxygen species (ROS) for activation when studied in macrophages and neutrophils (Brinkmann, Reichard *et al*. 2004; von Kockritz-Blickwede and Nizet 2009).

.

7.2. Antimicrobial peptides and mucins

The gastrointestinal tract of many mammals including humans and mice is composed of a mucosal layer, which constitutes a physical (celluar) and chemical barrier against the external environment from invading microorganisms. Antimicrobial peptides and the mucosal layer comprise the main front line defence of the gastrointestinal tract (Wehkamp, Koslowski *et al*. 2008; Hansson and Johansson 2010). Defensins and cathelicidins are among the most important antimicrobial peptides of the gut (Jager, Stange *et al*. 2010). In combination with the mucus layer of the colon which is composed of a sterile inner epithelial cell layer and a protective mucus (gel layer) that form a protective barrier. Mucin is secreted by a subset of mucin genes in the intestine namely: *MUC2, MUC5A, MUC5B, MUC6* and *MUC19*, of which *MUC2* is the main essential gene of the formation of this protective layer (Tytgat, Buller *et al*. 1994).

Defensins are antimicrobial small cationic peptides (3-5kDa) that are effective against gram positive and gram negative bacteria in the gastrointestinal lumen (Jager, Stange *et al*. 2010). Human and murine defensins share a low level of similarity at the amino acid level but at the secondary and tertiary levels of protein structure share remarkable similarity in structure and function (Bauer, Schweimer *et al*. 2001). Defensins are classified as either α-defensins or β-defensins based of their unique pattern of linkages between cysteine residues (Zhao and Lu 2014). The exact mechanism for the action of defensins is not yet known but it is believed that they might be able to integrate into the cell membrane of the invading bacterial cell, expanding the outer membrane and crushing the inner membrane, therefore disrupting the normal function of the cell (Papo and Shai 2003). Currently there is

no knowledge about the pleotropic effects of statins on defensins in human or murine models (see Chapter 3 of this thesis).

The second major antimicrobial peptides of the gastrointestinal tract are cathelicidins namely LL-37 (human) or its equivalent cathelicidin-like peptides (*CRAMP*) (murine). Cathelicidins are antimicrobial polypeptides usually 39-80 amino acid residues in size, comprised of a highly conserved cathelin domain and variable peptidic domain (Fig.7). They are found in the lysosomes of macrophages and other such iummune cells (Zanetti 2004).

Fig.7. Schematic diagram of the cathelin and peptidic domains of the antimicrobial peptide cathelicidin.

Illustrated are the disulphide bridges located in the cathelin domain of the CAMP antimicrobial peptide. This figure was adapted from: (Zanetti 2004).

Interestingly, the expression of cathelicidin in the gastrointestinal tract can be influenced by the bile acids including chenodeoxycholic acid and ursodeoxycholic acid which are influenced through nuclear hormone receptors in the liver namely the farnesoid X-receptor (FXR) and the vitamin D (VDR) receptors. These bile acids increase the induction of cathelicidin in the intestinal environment in combination with Vitamin D. This is indicative of cross-talk between in the liver and intestine that needs to be further investigated (D'Aldebert, Biyeyeme Bi Mve *et al*. 2009).

Chow and colleagues (Chow, von Kockritz-Blickwede *et al*. 2010) showed that *in-vitro*, PMA-treated human neutrophils, treated with 50μM mevastatin had dramatically enhanced neutrophil extracellular trap formation (2.5 fold) compared to vehicle controls. Neutrophils exhibited a much stronger ability to entrap and kill fluorescently labelled *S. aureus*, which could be quantified by fluorescently activated cell sorting (FACS) for the release of extracellular DNA (Fuchs, Abed *et al*. 2007). A murine model developed by (Bubeck Wardenburg, Patel *et al*. 2007; Chow, von Kockritz-Blickwede *et al*. 2010) to induce bacterial pneumonia in C57Bl/6 mice by intra nasal inoculation of *S. aureus* ($2x10^8$ CFU/animal sub-lethal dose) found that *in-vivo,* in alveolar sections the murine cathelicidin was significantly up regulated following treatment with 10μM simvastatin, up to 24 and 72 hours after infection with improved clearance of the bacteria compared to vehicle controls. This suggests that statins predispose cells to enter the cell death pathway for neutrophil extracellular trap formation in response to bacterial infection (Chow, von Kockritz-Blickwede *et al*. 2010). PAD-4 (peptidyl arginine deaminase 4) which catalyses the deamination of arginine residues in histones to citrullines facilitating chromatin decondensation (Wang, Li *et al*. 2009), has emerged as another potential biochemical marker of neutrophil extracellular traps, but treatment of a PAD-4 inhibitor failed to block enhanced neutrophil extracellular trap formation by simvastatin or mevastatin in such models.

7.3. T-helper cell class switching in the intestine caused by statins

Intra epithelial lymphocytes have the ability to secrete a wide variety of different cytokines including: IFNγ, TNFα, IL-2, IL-4, IL-6, IL-10, IL-15, IL-17, TGF-β1 (transforming growth factor) and KGF (keratinocyte growth factor). These lymphocytes contribute to mediating the inflammatory response through secretion of

cytokines and also in surveying the intestinal lumen for pathogenic microbes and other such infectious antigens (Barrett, Gajewski *et al*. 1992; Yang, Antony *et al*. 2004).

In a study by Zhang and colleagues (Zhang, Osawa *et al*. 2013), two commonly used statins simvastatin and lovastatin suppressed the intra epithelial lymphocyte production of T-helper class 1 cytokines (IFNγ, TNFα, TNFβ, IL-2) as well as the pro-inflammatory cytokine IL-4. Previously it has been reported that statins have the ability to induce a switch in the immunogenic response in *in-vitro* cultured lymphocytes from a T-helper cell class 1 mediated response to a T-helper class 2 mediated response promoting secretion of T_H2 specific cytokines (IL-4,IL5, IL-9, IL-10, IL-13 and TGF-β) (Youssef, Stuve *et al*. 2002). The T_H1 response is primarily associated in the gut with the cellular immune response of macrophages and lymphocytes to promote phagocytosis of invaders. Whilst the T_H2 response is strongly antibody-mediated and involves the accumulation of eosinophil cells (Romagnani 2000) which have been associated with defence against parasitic invaders and the allergenic response (Mowen and Glimcher 2004).

T-helper (T_H) cell cytokine class switching was also observed by Aktunc and colleagues (Aktunc, Kayhan *et al*. 2011) in the gastrointestinal tract of trinitrobezene sulfonic acid (TNBS-induced) inflammatory colitis in BALB/c mice. They observed that the hydrophobic statin, atorvastatin was able to alleviate clinical symptoms of colitis such as rectal bleeding, shortening of the colon often extended in colitis patients and improved histology of the cells lining the intestine. TNBS-induced colitis in mice promotes inflammatory bowel diseases attributed to the increased production of T_H1 and T_H17 specific pro-inflammatory cytokines: IFNγ, IL-6, IL-12, TNFα, IL-17 and IL-23 which are secreted by activated macrophages

and neutrophils (Gross, Andus *et al*. 1992; Plevy, Landers *et al*. 1997). In atorvastatin-treated colitis mice, it was noted that the T_H2 cytokine IL-10 suppressed the T_H1 cell response and promoted a T_H2 response. Other important proinflammatory cytokines such as IL-17 and IL-23 were also suppressed by statins. The T_H17 cell response is essential for enhancing T-cell priming and stimulating the production of IL-1, IL-6 and TNFα (Ikeda, Takeshima *et al*. 2008), which has been shown by (Aktunc, Kayhan *et al.* 2011). A representation of T_H cell differentiation into T_H cell subsets (T_{reg}, T_H1, T_H2 and T_H17) and effect of statins is depicted below (Fig.8), highlighting the major cytokines involved.
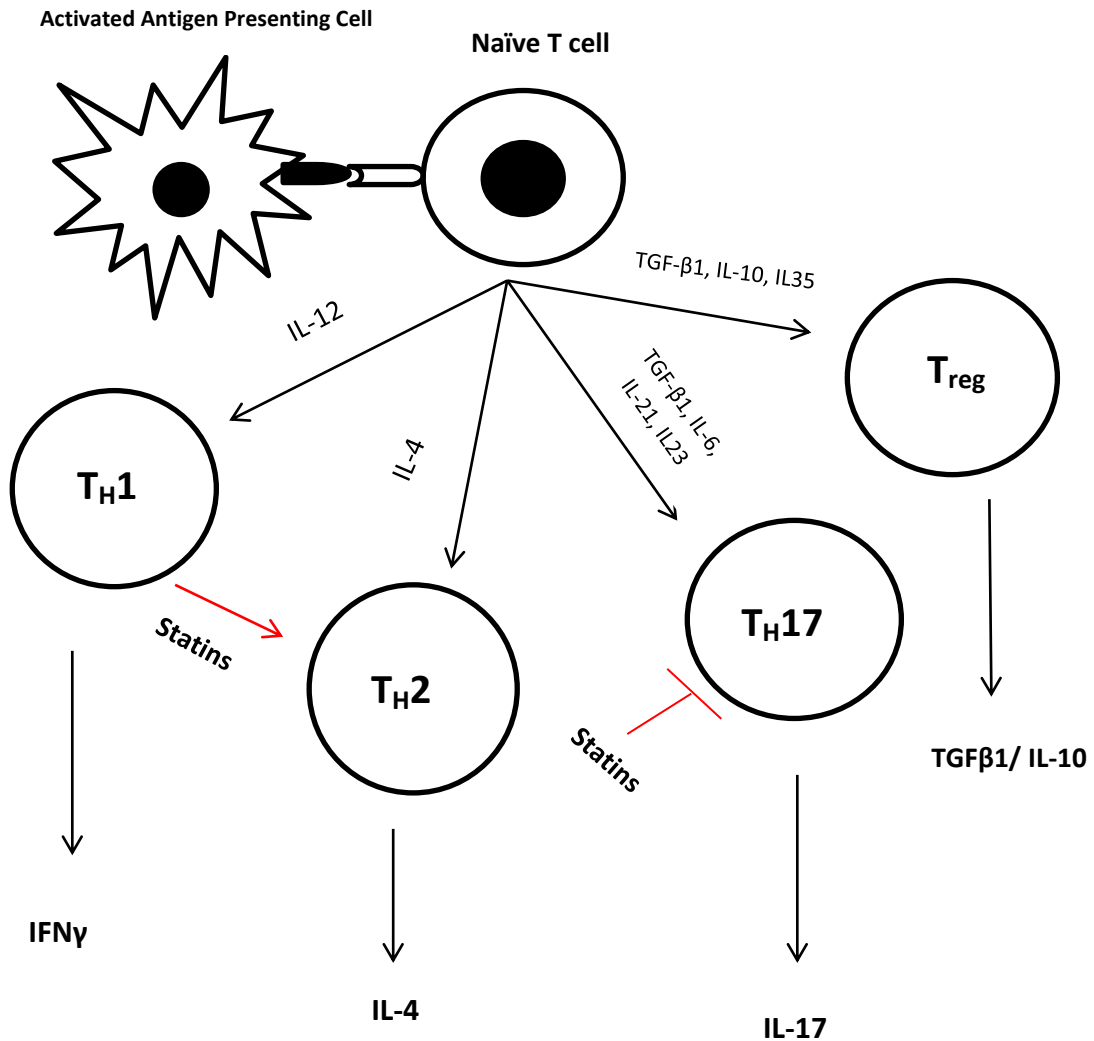
Fig.8. Presentation by antigen presenting cell to the surface of naïve T cells and subsequent cytokine mediated differentiation into T-helper cells (T$_H$1,2 and 17 and T$_{reg}$).

Indicated is the statin-mediated class switching of T$_H$1 to T$_H$2 cellular response and inhibition of T$_H$17 helper cell mediated immunity. Signature cytokines for each T cell response: T$_H$1 (IFNγ), T$_H$2 (IL-4), T$_H$17 and T$_{reg}$ (TGFβ1 and IL-10) are illustrated. The T$_H$1 response is generally cell-mediated and proinflammatory in comparison to the T$_H$2 response which is antibody-mediated and promote an allergenic and anti-parasitic response. Statins can also cause a suppression of the T$_H$17 response by inhibiting the cytokine IL-17. T$_{reg}$ cells are the major regulatory cells of the immune system and are generally unaffected by statins. This figure was adapted from: (Jutel and Akdis 2011).

7.4. RegIIIγ, Ang-4 antimicrobials and statins

Regenerating islet-derived protein 3 gamma (RegIIIγ) is a protein encoded by the *RegIIIγ* gene family secreted by Paneth cells in the small intestine of mice, its human counterpart is denoted as HIP/PAP (Laurine, Manival *et al.* 2005). RegIIIγ forms a C-type lectin protein (16kDa approx. in size) with conserved carbohydrate recognition domains (CRD's) that target surface exposed carbohydrate moieties in the peptidoglycan cell wall of gram positive bacteria. Binding of RegIIIγ to the surface of the bacterium, restricts colonisation and replication of the bacteria by interfering with normal cell function (Cash, Whitham *et al*. 2006). The peptidoglycan cell wall of bacteria consists of alternating α-linked N-acetylglucosamine (NAG) and N-acetylmuramic acid (NAM) residues that are cross-linked by short peptides and are recognised by the CRD's in RegIIIγ. Chitin which is structurally very similar to peptidoglycan with β-linked (NAG-NAM) residues is the main constituent of many fungal cell walls and is also recognised by RegIIIγ which prevents colonisation of fungal species in the intestine (Cash, Whitham *et al.* 2006). The expression of RegIIIγ in the intestine is largely governed by a direct interaction of microbial associated molecular patterns (MAMP's) such as the bacterial cell wall and signalling is directed through Toll-like receptors under the control of MyD88 (myeloid differentiation primary response protein 88) and the cytokine IL-22 (Gallo and Hooper 2012).

Another important antimicrobial compound secreted by Paneth cells in the intestine is Angiopoietin-4 (Ang-4) encoded by the gene *Ang-4* and its murine equivalent Ang-4-like peptide. Ang-4 is a class of RNase enzymes secreted by epithelial cells and is able to target both gram positive and gram negative bacteria,

currently there is not much known about the mode of action of Ang-4 in the defence of the gastrointestinal environment (Hooper, Stappenbeck *et al.* 2003). Angiogenin proteins have long been associated with the vascularisation (blood supply) of carcinogenic tumours (Fett, Strydom *et al.* 1985). Recently Ang-4 has been associated with defence of the intestine. Research conducted by Hooper and co-workers (Hooper, Stappenbeck *et al.* 2003) showed that Ang-4 is able to localise to the Paneth cell secretory granules and is exported into the gastrointestinal lumen in response to bacterial signals. They showed that exposure of gram negative *E. faecalis* and gram positive *L. monocytogenes* to 1µM Ang-4 exhibited a 99% reduction in the viable counts of both bacteria after 2 hours. However this effect appeared to be species specific as the commensal gut microbe *E. coli* K12 was found to be resistant to 10µM Ang-4 and similarly for the non-pathogenic bacteria *L. innocua.* Currently, there is little knowledge about the physiological concentration of Ang-4 in the lumen of the intestine, it is believed they might be secreted in a similar range to other antimicrobials such as defensins (1µM) (Ayabe, Satchell *et al.* 2000). Overall, previous work indicates a potential species-directed alteration of the gut microbial composition by Ang-4. As it stands, there is not much known about the cholesterol-independent effects of statins upon Paneth cell produced RegIIIγ and Ang-4 in the gastrointestinal environment. It has been shown that some statins (including RSV) are excreted into the intestine via the biliary route (Bergman, Forsell *et al.* 2006). As previously indicated statins elicit widespread effects on the host inflammatory immune response which could be suggestive of host-implicated alteration to the microbial composition of the gut.

8. Statins and bile acids

8.1. Overview of cholesterol degradation and bile acid metabolism

Currently, there is relatively little research carried out on the host effects of statins correlating interactions observed in the microbiota with similar alterations seen in the metabolome. Metabolomics is a powerful global biochemical tool for capturing net interactions between the microbiome and the environment namely the intestinal metabolome (Kaddurah-Daouk, Baillie *et al*. 2011). We discuss the metabolomics of bile acids and short chain fatty acids (SCFA's) with a view towards understanding their alterations in a statin-treated gastrointestinal environment.

In humans, cholesterol is an important biomolecule in the synthesis of bile acids (water soluble antimicrobial detergents), with chemical conversion to bile acids taking place via two pathways; the classic pathway via the enzyme 7α hydroxylase (*CYP7A1*) or the alternative (acidic) pathway involving the sterol mitochondrial associated 27-hydroxylase (*CYP27A1*) (Fig. 10). The classic pathway for bile acid synthesis occurs primarily in the liver, but the alternative pathway can occur in the brain and in the mitochondria of some cells (Chiang 2004). It is reasonable to assume that statins might have implications for the synthesis of bile acids by limiting available cholesterol.

The classic bile acid pathway is a complex system involving fourteen separate catalytic reactions that occur between the cytoplasm, microsomes, mitochondria and peroxisomes (Russell 2003). The classic pathway is able to synthesize two major primary bile acids cholic acid and chenodeoxycholic acid, which are subsequently conjugated with organic biomolecules glycine or organic acid taurine to form

conjugated bile acids that are secreted into the gastrointestinal tract and aid in the digestion of lipids and fats. The conjugation of bile acids is catalysed by the enzyme bile acid coenzyme A- amino acid N-acyltransferase. Conjugation of bile acids generally has the effect of improving their water solubility. The alternative pathway operates in a similar fashion utilising different cholesterol-associated enzymes to lead to formation of the primary bile acids (Chiang 2004).

As yet, a full understanding of the interplay between the classic and alternative pathway towards bile acid synthesis and homeostasis is not well characterised. It is hypothesised that the classic pathway is the main biosynthetic pathway in healthy humans and mammals (including mice) whereas the alternative pathway appears to be more active in patients with some forms of liver disease (Chiang 2004).

Cholesterol

CH₃ CH₂ CH₂ CH₃
CH CH₂ CH
CH₃ CH₃

HO
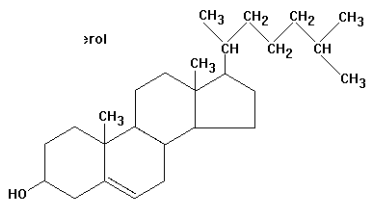
Classic pathway

Alternative pathway
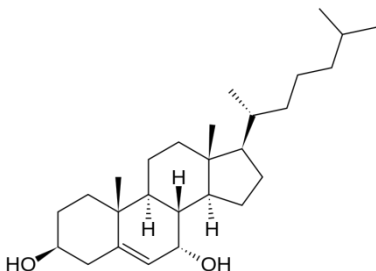
7α-hydroxycholesterol (*CYP7A1*)

HO OH
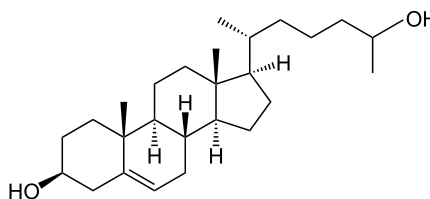
27-hydroxycholesterol (*CYP27A1*)

HO OH

Intermediate compounds (Classic pathway):

7α-hydroxy-4-cholesten-3-one

7α, 12α-dihydroxy-4-cholesten-3-one (*CYP8B1*)

5β-cholestan-3α, 7α, 12α-triol

3α, 7α, 12α-trihydroxy-5β-cholestanoic acid (*CYP27A1*)

5β-cholestan-3α, 7α-diol

3α, 7α-dihydroxy-5β-cholestanoic acid

Intermediate compounds (Alternative pathway):

3β, 7α-dihydroxy-5-cholestonic acid

7α-hydroxy-3-oxo-4-cholesronic acid

3α, 7α-dihydroxy-5β-cholestanoic acid (*CYP7B1*)

25-hydroxycholesterol

5-cholesten-3β,7α, 25-triol (*CYP8B1*)

24-hydroxycholesterol

5-cholesten-3β, 7α 24(S)-triol

OH O OH

HO OH

Cholic acid

O OH

HO OH
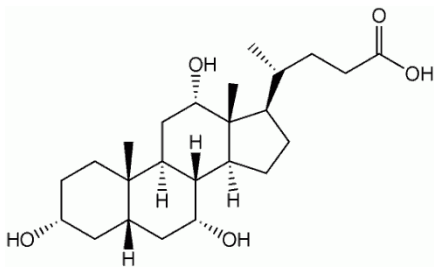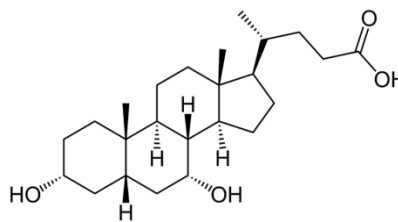
Chenodeoxycholic acid

Fig. 10. The synthesis of primary unconjugated bile acids cholic acid and chenodeoxycholic acid from cholesterol via the classic and alternative pathways including the major regulatory *CYP* genes.

Bile acid biosynthetic pathways are very complex reactions involving many different metabolites and major regulatory *CYP* genes. Shown here are the two main routes for bile acid synthesis; classic and alternative leading to the formation of cholic and chenodeoxycholic acid. This image was adapted from: (Chiang 2004)

8.2. Bile acid synthesis and regulation

The synthesis of bile acids occurs primarily in the liver which is mediated by a cytochrome P450-mediated (*CYP*) degradation and conversion of cholesterol involving 17 different enzymes and intermediary metabolites. The major rate limiting enzyme guarding the initial breakdown of cholesterol is cholesterol 7α-hydroxylase (*CYP7A1*) for the classical pathway of bile acid synthesis and the minor rate limiting enzyme sterol 27-hydroxylase (*CYP27A1*) for the alternative pathway (Russell 2003; Chiang 2004).

In humans, the dominant primary bile acids that emerge directly from the breakdown of cholesterol are cholic acid and chenodeoxycholic acid and in mice cholic acid and muricholic acid predominate (Hylemon and Harder 1998). During this complex multi-enzymatic system, cholesterol is hydroxylated forming precursor oxysterols (24,25 and 27-hydroxycholesterol) that are further modified with the addition of ring structures, oxidized and subsequently conjugated with amino acids prior to excretion into the intestine (Russell 2003). It is important to note that hydrophobic bile acids such as cholic acid (CA), chenoxydeoxycholic acid (CDCA), deoxycholic acid (DCA) and lithocholic acid (LCA) are strong inhibitors of bile acid synthesis whereas hydrophilic bile acids such as ursodeoxycholic acid (ursine) and β-muricholic acid promote bile acid synthesis through interactions with the *CYP7A1*

gene (Chiang 2002). Increasing the hydrophilicity of the total bile acid pool has the effect of reducing the absorption of dietary cholesterol in the intestine and is generally compensated by an increase in cholesterol synthesis (Li-Hawkins, Gafvels *et al.* 2002).

Another important aspect of regulation are nuclear receptors that are able to regulate the expression of genes involved in the biosynthesis of bile acids. The major nuclear receptors involved in bile acid synthesis regulation include: farnesoid X receptor (*FXR/NR1H4* in mice), liver X receptor (*LXR/NR1H4* in mice), pregnane X receptor (*PXR*) and the vitamin D receptor (*VDR*). These receptors are able to control regulation on the bile acid synthetic pathway by targeting regulatory genes in the network namely: (*CYP7A1, CYP27A1, CYP8B1, CYP7B1*) (Chiang 2003). In this review regulation over each of these genes will be discussed along with the complex network of interactions that occur to control bile acid synthesis.

CYP7A1 (cholesterol 7α-hydroxylase), the first rate limiting enzyme of bile acid synthesis and its regulation have been well described in both mice and humans (Lehmann, Kliewer *et al.* 1997; Stroup, Crestani *et al.* 1997; Chiang 2004). Regulation of this enzyme is complex and multifaceted with multiple regulatory factors involved. In mice, *CYP7A1* is regulated in the presence of high cholesterol by binding of a conserved bile acid response element (BARE-1) in the LXR receptor and inducing gene expression. However, in humans *CYP7A1* is not regulated by the LXR receptor under high cholesterol conditions, in this case a second conserved (BARE-2) element that binds alternate nuclear receptors HNF-4α and RARα to regulate bile acid synthesis. Mutations in the *CYP7A1* gene of *CPYP7A1 -/-* knockout mice have been associated with hypercholesterolemia and cholesterol build up (Pullinger, Eng *et al.* 2002). This leads to a high incidence of medical

complications of liver failure, vitamin deficiency and lipid malabsorption with an

reduction in the total bile acid present (Schwarz, Lund *et al*. 1996; Arnon,

Yoshimura *et al*. 1998). Suppression of *CYP7A1* can also be mediated by the FXR

nuclear receptor (*NR1H4* in mice) through signalling of the SHP nuclear receptor.

Excess accumulation of bile acids leads to repression of gene expression in *CYP7A1*

through a complex cascade of regulatory factors (Goodwin, Jones *et al*. 2000)

further stimulating bile acid conjugation and excretion into the intestine

(Ananthanarayanan, Balasubramanian *et al.* 2001). Regulation of *CYP7A1* inhibition

can also take place by a SHP-independent mechanism repressing expression via the

c-Jun N-terminus kinase (JNK) pathway, a full set of regulatory factors involved in

the JNK pathway has not yet been fully elucidated. It is believed that FXR, can also

induce activation of the Fibroblast Growth Factor 19 (*FGF-19*) leading to the JNK

pathway-mediated inhibition of *CYP7A1* (Stravitz, Vlahcevic *et al.* 1995). *CYP7A1*

has also been shown to be repressed by the pro-inflammatory cytokines TNFα and

IL-1β (Feingold, Spady *et al*. 1996). Statins, as potent inhibitors of the HMG-R

enzyme are also known to have cholesterol-independent effects on the inflammatory

response of the host which could have the potential to alter bile acid metabolism

through targeting of *CYP7A1* (cholesterol 7α- hydroxylase, (Ikeda, Takeshima *et al*.

2008).

   CYP27A1 (sterol 27- hydroxylase) which is the main enzyme involved in the

alternative (acidic) pathway is another important regulatory enzyme of bile acid

synthesis. It has been shown that in *CYP27A1*-/- knockout mice there is a dramatic

accumulation of precursor oxysterols (7α-hydroxycholesterol, 7α-hydroxy-4-

cholesten 3-one, 5β –cholestane 3α, 7α ,12α – triol) and cholesterol. Defective mice

also show a reduced synthesis of the primary bile acid chenodeoxycholic (CDCA).

CYP27A1 -/- mice have been shown to have a markedly reduced synthesis of bile acids and excretion into the faeces. Phenotypically these mice have engorged livers, high triglyceride levels with increased cholesterol absorption and synthesis (Rosen, Reshef *et al*. 1998; Repa, Lund *et al*. 2000).

CYP8B1 (sterol 12α- hydroxylase) is another important enzyme for the synthesis of primary bile acids and maintains homeostasis between cholic acid (CA) and chenodeoxycholic acid (CDCA). *CYP8B1* -/- knockout mice were found to have non-existent cholic acid synthesis, but had an increased expression of *CYP7A1*. This is potentially due to de-repression by increased muricholic acid. This suggests that *CYP8B1* is strongly regulated by the action of *CYP7A1* and muricholic acid (Li-Hawkins, Gafvels *et al*. 2002).

Finally, *CYP7B1* (oxysterol 7α – hydroxylase) has been described as one final potential regulated enzyme in the bile acid biosynthetic pathway. *CYP7B1* -/- knockout mice have been shown to have increased oxysterol precursor accumulation of 24, 25, and 27- hydroxycholesterol. However, these mice suffer a much less severe phenotype and clinical condition compared to *CYP7A1, CY27A1* and *CYP8B1* mutagenic mice (Setchell, Schwarz *et al*. 1998; Li-Hawkins, Lund *et al*. 2000).

8.3. Statins as mediators of bile acid synthesis

A powerful gas-chromatography and mass spectrometry platform was utilised by Kaddurah and colleagues (Kaddurah-Daouk, Baillie *et al*. 2011) to measure metabolites of cholesterol synthesis, dietary sterol absorption and bile acid formation in human plasma of Caucasian and African-American males and females with elevated cholesterol levels (160-400mg/dL) treated with the statin simvastatin (40mg/day) over a 6 week period. Bile acids and statins are known to share similar transporters in the liver and intestine and following this study the authors identified important bacterial-derived bile acids that were negatively correlated (i.e. poorly produced) as a result of positive statin-treatment to lower LDL-cholesterol. They indicate that pre-treatment levels of bile acids (and therefore the microbiota) were predictors of whether statins were effective in the host metabolome in relation to bile acid synthesis.

9. Short chain fatty acids and statins

9.1 Butyrate

Short chain fatty acids (SCFA's) are a sub class of short (up to six carbons) volatile fatty acids that are produced in the gastrointestinal tract following bacterial fermentation in most mammals. In this review, we discuss the importance of the SFCA's butyrate, propionate and acetate. These compounds in combination with trimethylamine, acetylaldehyde and inflammatory mediators are essential in maintaining the metabolic health of the host, through influences on satiety (feeling of being full), gut permeability and overall general immunity (Bergman 1990; Joyce and Gahan 2014).

Butyrate is synthesised in the gastrointestinal tract by pyruvate and acetyl CoA following the breakdown of complex carbohydrates (e.g. starch) (Louis and Flint 2009). Butyrate, is one of the most important short chain fatty acids produced by the fermentation of dietary fibre in the gastrointestinal tract and has been shown to have beneficial effects on the host, controlling normal cell differentiation and proliferation of enterocytes (preventing cancers and tumours of the large intestine) (Roediger 1980; Scheppach, Bartram *et al*. 1992). Butyrate has also been implicated in improving the defence barrier of the colon, decreasing oxidative stress and a reduction in inflammation through inhibition of $NF\text{-}_KB$ (major gene regulating expression of pro-inflammatory cytokines), as well as histone deacetylation (Hamer, Jonkers *et al.* 2008) and inhibition of IFNγ production (Klampfer, Huang *et al*. 2003). Butyrate has a very similar chemical structure to the molecule mevalonate and it is interesting to note that following oxidative metabolic conversion of butyrate to beta-hydroxybutyrate it is possible for the cell to establish precursors for the

synthesis of the HMG-CoA the substrate for mevalonate formation via HMG-CoA reductase (Velazquez, Jabbar *et al.* 1996). Very recently SCFA's (namely butyrate and propionate) have been shown to modulate intestinal gluconeogenesis for glucose and energy homeostasis through activation of important gut-brain regulatory circuits via fatty acid receptors such as FFRAR3 (De Vadder, Kovatcheva-Datchary *et al.* 2014).

Wachtershauser and co-workers (Wachtershauser, Akoglu *et al.* 2001) showed that mevastatin had a beneficial effect on the anti-proliferative ability of butyrate in a colorectal carcinoma model of Caco-2 epithelial cells. Co-culturing of Caco-2 cells with 1-2mM butyrate and 64µM mevastatin had a significant effect in reducing cell growth and proliferation in a dose and time dependent fashion over 5 days. This potentially demonstrates a synergistic interaction between butyrate and mevastatin in improving the disease state of cellular carcinoma.

Research conducted by Gaudier and co-workers (Gaudier, Jarry *et al.* 2004), showed that butyrate (2-5mM) was able to modulate the expression of mucin genes in epithelial goblet cells derived from a human colonic cell line (HT29-Cl.E) under glucose rich and glucose deprived conditions. They showed that under high glucose conditions butyrate significantly raised the expression of *MUC3* and *MUC5B* (1.6 fold), decreased *MUC5AC* expression and had no effect on the expression of *MUC2* control to untreated controls. Interestingly, under glucose deprived conditions there was a dramatic increase in the expression of all genes; *MUC5AC* expression was enhanced 3.7 fold and most strikingly *MUC2* expression was enhanced 23-fold following gene expression analysis. As previously indicated, *MUC2* has been described as the main mucin gene responsible for the formation of the protective mucosa barrier (Tytgat, Buller *et al.* 1994). Preliminary data from our lab suggests

that *MUC2* gene expression is significantly raised by qRT-PCR analysis in statin-treated C57Bl/6 mice fed on a high fat diet (see Chapter 3 of this thesis) Further research will need to be conducted to ascertain the potential for statins in butyrate-mediated *MUC2* expression or if statins can directly impact on the *MUC2* gene itself.

Culture-independent 16S rRNA analysis has revealed a great wealth of knowledge on the complexity of the gut microbiota in recent times. In general, strictly anaerobic unculturable gram positive *Firmicutes* such as *Lachnospiraceae, Ruminococcaecae* (Scott, Martin *et al*. 2014), *Roseburia* (Machiels, Joossens *et al*. 2013), *Eubacteria* and *Faecalibacterium prausnitzii* (Louis and Flint 2009) emerged as the most significant butyrate producers in mammals. As it stands, there is little knowledge about the direct interaction of HMG-R inhibitors (such as statins) against butyrate-producing anaerobes.

9.2. Propionate

Propionate, similar to butyrate has potential health benefits for the host. Propionate is mainly taken up by hepatocytes in the liver and has been shown to have anti-proliferative effects in carcinoma of the liver and anti-inflammatory effects in *in-vivo* colitis models and can even be used as energy source by gut cells (Cox, Jackson *et al*. 2009; Bindels, Porporato *et al.* 2012). Similarly to butyrate, much analysis of propionate-producing bacteria has been gathered through culture independent techniques and 16S rRNA analysis of the gut microbiota. The main bacterial genera that produce propionate in the gut include; *Bacteroides, Prevotella, Escherchia* and *Propionibacterium* (Hosseini, Grootaert *et al*. 2011).

9.3. Acetate

The SCFA acetate has traditionally been regarded as one of the end products of anaerobic fermentation which can be utilised by certain bacterial species such as *Faecalibacterium prausnitzii* and *Roseburia* spp. (accounting for 7% of total population in human faeces) for the formation of butyrate (Duncan, Holtrop *et al*. 2004). Also it has been shown that another important member of the gut microbiota namely *Coprococcus* (*Lachnospiraceae* genera) in particular *Coprococcus catus* GD/7 is a net acetate producer in the gut (Duncan, Holtrop *et al.* 2004). This was determined from investigating incorporation of ^{13}C-labelled acetate in batch anaerobic fermenters containing mixed bacterial populations from human faeces.

10. Discussion

3-hydroxy-3-methylglutaryl coenzyme A reductase (HMG-R) is a very important enzyme in the Mevalonate pathway for the synthesis of isoprenoids in bacteria and for cholesterol in humans. The presence of either the Mevalonate pathway or alternative 2-C-methyl-D-erythritol 4-phosphate (MEP) pathway has been well documented in many bacteria and other microorganisms. We have reviewed the biochemistry, evolution of both pathways and the phylogenetics of HMG-R enzymes as well as sensitivity to commonly used pharmaceutical anti-cholesterol drugs (statins) and explored their cholesterol-independent implications that affect host inflammation, immunogenic responses and the metabolome with a particular focus upon bile acids and SCFA's.

It is fascinating that bacteria produce isoprenoids via either the classical mevalonate pathway or the alternative MEP pathway. We suggest that much greater work is needed in order to understand the sensitivity of bacteria harbouring the classical pathway (and therefore the HMG-R enzyme) to statins. We hypothesize that long term statin use may impact upon the gut microbiota in humans through direct or indirect (off-target) mechanisms, a phenomenon that we examine in a mouse model in Chapters 2 and 3 of this thesis. We also suspect that bacteria expressing the alternative (MEP) pathway may stimulate local immune responses via the pathway intermediate HMBPP. In chapter 5 of this thesis we examine this concept.

References

Aktunc, E., B. Kayhan, et al. (2011). "The effect of atorvastatin and its role on systemic cytokine network in treatment of acute experimental colitis." Immunopharmacol Immunotoxicol **33**(4): 667-675.

Ananthanarayanan, M., N. Balasubramanian, et al. (2001). "Human bile salt export pump promoter is transactivated by the farnesoid X receptor/bile acid receptor." J Biol Chem **276**(31): 28857-28865.

Arad, Y., R. Ramakrishnan, et al. (1992). "Effects of lovastatin therapy on very-low-density lipoprotein triglyceride metabolism in subjects with combined hyperlipidemia: evidence for reduced assembly and secretion of triglyceride-rich lipoproteins." Metabolism **41**(5): 487-493.

Arnon, R., T. Yoshimura, et al. (1998). "Cholesterol 7-hydroxylase knockout mouse: a model for monohydroxy bile acid-related neonatal cholestasis." Gastroenterology **115**(5): 1223-1228.

Ayabe, T., D. P. Satchell, et al. (2000). "Secretion of microbicidal alpha-defensins by intestinal Paneth cells in response to bacteria." Nat Immunol **1**(2): 113-118.

Balibar, C. J., X. Shen, et al. (2009). "The mevalonate pathway of Staphylococcus aureus." J Bacteriol **191**(3): 851-861.

Barrett, T. A., T. F. Gajewski, et al. (1992). "Differential function of intestinal intraepithelial lymphocyte subsets." Journal of Immunology **149**(4): 1124-1130.

Bauer, F., K. Schweimer, et al. (2001). "Structure determination of human and murine beta-defensins reveals structural conservation in the absence of significant sequence similarity." Protein Sci **10**(12): 2470-2479.

Begley, M., P. A. Bron, et al. (2008). "Analysis of the isoprenoid biosynthesis pathways in Listeria monocytogenes reveals a role for the alternative 2-C-methyl-D-erythritol 4-phosphate pathway in murine infection." Infect Immun **76**(11): 5392-5401.

Begley, M., C. G. M. Gahan, et al. (2004). "The interplay between classical and alternative isoprenoid biosynthesis controls [gamma][delta] T cell bioactivity of Listeria monocytogenes." FEBS Letters **561**(1-3): 99-104.

Bergman, E., P. Forsell, et al. (2006). "Biliary secretion of rosuvastatin and bile acids in humans during the absorption phase." Eur J Pharm Sci **29**(3-4): 205-214.

Bergman, E. N. (1990). "Energy contributions of volatile fatty acids from the gastrointestinal tract in various species." Physiol Rev **70**(2): 567-590.

Bindels, L. B., P. Porporato, et al. (2012). "Gut microbiota-derived propionate reduces cancer cell proliferation in the liver." Br J Cancer **107**(8): 1337-1344.

Blum, C. B. (1994). "Comparison of properties of four inhibitors of 3-hydroxy-3-methylglutaryl-coenzyme A reductase." Am J Cardiol **73**(14): 3D-11D.

Bobek, P., L. Ozdin, et al. (1998). "Dose- and time-dependent hypocholesterolemic effect of oyster mushroom (Pleurotus ostreatus) in rats." Nutrition **14**(3): 282-286.

Bochar, D. A., C. V. Stauffacher, et al. (1999). "Sequence comparisons reveal two classes of 3-hydroxy-3-methylglutaryl coenzyme A reductase." Mol Genet Metab **66**(2): 122-127.

Borders-Hemphill, V. (2010). "Welchol and Crestor BPCA drug use review in the pediatric population." Center for DRug evaluation and research report, FDA.

Bosner, M. S., L. G. Lange, et al. (1999). "Percent cholesterol absorption in normal women and men quantified with dual stable isotopic tracers and negative ion mass spectrometry." J Lipid Res **40**(2): 302-308.

Boucher, Y. and W. F. Doolittle (2000). "The role of lateral gene transfer in the evolution of isoprenoid biosynthesis pathways." Mol Microbiol **37**(4): 703-716.

Boucher, Y., H. Huber, et al. (2001). "Bacterial origin for the isoprenoid biosynthesis enzyme HMG-CoA reductase of the archaeal orders Thermoplasmatales and Archaeoglobales." Mol Biol Evol **18**(7): 1378-1388.

Brinkmann, V., U. Reichard, et al. (2004). "Neutrophil extracellular traps kill bacteria." Science **303**(5663): 1532-1535.

Brown, A. G., T. C. Smale, et al. (1976). "Crystal and molecular structure of compactin, a new antifungal metabolite from Penicillium brevicompactum." J Chem Soc Perkin 1(11): 1165-1170.

Bubeck Wardenburg, J., R. J. Patel, et al. (2007). "Surface proteins and exotoxins are required for the pathogenesis of Staphylococcus aureus pneumonia." Infect Immun **75**(2): 1040-1044.

Campos, N., M. Rodriguez-Concepcion, et al. (2001). "Identification of gcpE as a novel gene of the 2-C-methyl-D-erythritol 4-phosphate pathway for isoprenoid biosynthesis in Escherichia coli." FEBS Lett **488**(3): 170-173.

Cash, H. L., C. V. Whitham, et al. (2006). "Symbiotic bacteria direct expression of an intestinal bactericidal lectin." Science **313**(5790): 1126-1130.

Cheng-Lai, A. (2003). "Rosuvastatin: a new HMG-CoA reductase inhibitor for the treatment of hypercholesterolemia." Heart Dis **5**(1): 72-78.

Chiang, J. Y. (2002). "Bile acid regulation of gene expression: roles of nuclear hormone receptors." Endocr Rev **23**(4): 443-463.

Chiang, J. Y. (2003). "Bile acid regulation of hepatic physiology: III. Bile acids and nuclear receptors." Am J Physiol Gastrointest Liver Physiol **284**(3): G349-356.

Chiang, J. Y. (2004). "Regulation of bile acid synthesis: pathways, nuclear receptors, and mechanisms." J Hepatol **40**(3): 539-551.

Chow, O. A., M. von Kockritz-Blickwede, et al. (2010). "Statins enhance formation of phagocyte extracellular traps." Cell Host Microbe **8**(5): 445-454.

Cox, M. A., J. Jackson, et al. (2009). "Short-chain fatty acids act as antiinflammatory mediators by regulating prostaglandin E(2) and cytokines." World J Gastroenterol **15**(44): 5549-5557.

D'Aldebert, E., M. J. Biyeyeme Bi Mve, et al. (2009). "Bile salts control the antimicrobial peptide cathelicidin through nuclear receptors in the human biliary epithelium." Gastroenterology **136**(4): 1435-1443.

Davidson, M., P. Ma, et al. (2002). "Comparison of effects on low-density lipoprotein cholesterol and high-density lipoprotein cholesterol with rosuvastatin versus atorvastatin in patients with type IIa or IIb hypercholesterolemia." Am J Cardiol **89**(3): 268-275.

Davignon, J., M. Montigny, et al. (1992). "HMG-CoA reductase inhibitors: a look back and a look ahead." Can J Cardiol **8**(8): 843-864.

De Vadder, F., P. Kovatcheva-Datchary, et al. (2014). "Microbiota-generated metabolites promote metabolic benefits via gut-brain neural circuits." Cell **156**(1-2): 84-96.

DeBose-Boyd, R. A. (2008). "Feedback regulation of cholesterol synthesis: sterol-accelerated ubiquitination and degradation of HMG CoA reductase." Cell Res **18**(6): 609-621.

Dietschy, J. M., S. D. Turley, et al. (1993). "Role of liver in the maintenance of cholesterol and low density lipoprotein homeostasis in different animal species, including humans." J Lipid Res **34**(10): 1637-1659.

Doss, S. L., C. K. Chu, et al. (1986). "Isolation of compactin (a hypocholestrolemic metabolite) from a new source: Penicillium cyclopium." J Nat Prod **49**(2): 357-358.

Duncan, S. H., G. Holtrop, et al. (2004). "Contribution of acetate to butyrate formation by human faecal bacteria." Br J Nutr **91**(6): 915-923.

Endo, A., M. Kuroda, et al. (1976). "Competitive inhibition of 3-hydroxy-3-methylglutaryl coenzyme A reductase by ML-236A and ML-236B fungal metabolites, having hypocholesterolemic activity." FEBS Lett **72**(2): 323-326.

Feingold, K. R., D. K. Spady, et al. (1996). "Endotoxin, TNF, and IL-1 decrease cholesterol 7 alpha-hydroxylase mRNA levels and activity." J Lipid Res **37**(2): 223-228.

Fett, J. W., D. J. Strydom, et al. (1985). "Isolation and characterization of angiogenin, an angiogenic protein from human carcinoma cells." Biochemistry **24**(20): 5480-5486.

Fuchs, T. A., U. Abed, et al. (2007). "Novel cell death program leads to neutrophil extracellular traps." J Cell Biol **176**(2): 231-241.

Gallo, R. L. and L. V. Hooper (2012). "Epithelial antimicrobial defence of the skin and intestine." Nat Rev Immunol **12**(7): 503-516.

Gaudier, E., A. Jarry, et al. (2004). "Butyrate specifically modulates MUC gene expression in intestinal epithelial goblet cells deprived of glucose." Am J Physiol Gastrointest Liver Physiol **287**(6): G1168-1174.

Goldstein, J. L. and M. S. Brown (1990). "Regulation of the mevalonate pathway." Nature **343**(6257): 425-430.

Goodwin, B., S. A. Jones, et al. (2000). "A regulatory cascade of the nuclear receptors FXR, SHP-1, and LRH-1 represses bile acid biosynthesis." Mol Cell **6**(3): 517-526.

Gross, V., T. Andus, et al. (1992). "Evidence for continuous stimulation of interleukin-6 production in Crohn's disease." Gastroenterology **102**(2): 514-519.

Hamer, H. M., D. Jonkers, et al. (2008). "Review article: the role of butyrate on colonic function." Aliment Pharmacol Ther **27**(2): 104-119.

Hampton, R., D. Dimster-Denk, et al. (1996). "The biology of HMG-CoA reductase: the pros of contra-regulation." Trends Biochem Sci **21**(4): 140-145.

Hansson, G. C. and M. E. Johansson (2010). "The inner of the two Muc2 mucin-dependent mucus layers in colon is devoid of bacteria." Gut Microbes **1**(1): 51-54.

Hecht, S., W. Eisenreich, et al. (2001). "Studies on the nonmevalonate pathway to terpenes: the role of the GcpE (IspG) protein." Proc Natl Acad Sci U S A **98**(26): 14837-14842.

Hedl, M., L. Tabernero, et al. (2004). "Class II 3-hydroxy-3-methylglutaryl coenzyme A reductases." J Bacteriol **186**(7): 1927-1932.

Heuston, S., M. Begley, et al. (2012). "Isoprenoid biosynthesis in bacterial pathogens." Microbiology **158**(Pt 6): 1389-1401.

Hintz, M., A. Reichenberg, et al. (2001). "Identification of (E)-4-hydroxy-3-methyl-but-2-enyl pyrophosphate as a major activator for human gammadelta T cells in Escherichia coli." FEBS Lett **509**(2): 317-322.

Holstein, S. A. and R. J. Hohl (2004). "Isoprenoids: remarkable diversity of form and function." Lipids **39**(4): 293-309.

Hooper, L. V., T. S. Stappenbeck, et al. (2003). "Angiogenins: a new class of microbicidal proteins involved in innate immunity." Nat Immunol **4**(3): 269-273.

Hosseini, E., C. Grootaert, et al. (2011). "Propionate as a health-promoting microbial metabolite in the human gut." Nutr Rev **69**(5): 245-258.

Hylemon, P. B. and J. Harder (1998). "Biotransformation of monoterpenes, bile acids, and other isoprenoids in anaerobic ecosystems." FEMS Microbiol Rev **22**(5): 475-488.

Iglesias, P. and J. J. Diez (2003). "New drugs for the treatment of hypercholesterolaemia." Expert Opin Investig Drugs **12**(11): 1777-1789.

Ikeda, M., F. Takeshima, et al. (2008). "Simvastatin attenuates trinitrobenzene sulfonic acid-induced colitis, but not oxazalone-induced colitis." Dig Dis Sci **53**(7): 1869-1875.

Istvan, E. S. (2001). "Bacterial and mammalian HMG-CoA reductases: related enzymes with distinct architectures." Current Opinion in Structural Biology **11**(6): 746-751.

Istvan, E. S. (2002). "Structural mechanism for statin inhibition of 3-hydroxy-3-methylglutaryl coenzyme A reductase." Am Heart J **144**(6 Suppl): S27-32.

Istvan, E. S. and J. Deisenhofer (2001). "Structural mechanism for statin inhibition of HMG-CoA reductase." Science **292**(5519): 1160-1164.

Jager, S., E. F. Stange, et al. (2010). "Antimicrobial peptides in gastrointestinal inflammation." Int J Inflam **2010**: 910283.

Jerwood, S. and J. Cohen (2008). "Unexpected antimicrobial effect of statins." J Antimicrob Chemother **61**(2): 362-364.

Joyce, S. A. and C. G. Gahan (2014). "The gut microbiota and the metabolic health of the host." Curr Opin Gastroenterol **30**(2): 120-127.

Jutel, M. and C. A. Akdis (2011). "T-cell subset regulation in atopy." Curr Allergy Asthma Rep **11**(2): 139-145.

Kaddurah-Daouk, R., R. A. Baillie, et al. (2011). "Enteric microbiome metabolites correlate with response to simvastatin treatment." PLoS One **6**(10): e25482.

Kim, D. Y., C. V. Stauffacher, et al. (2000). "Dual coenzyme specificity of Archaeoglobus fulgidus HMG-CoA reductase." Protein Sci **9**(6): 1226-1234.

Klampfer, L., J. Huang, et al. (2003). "Inhibition of interferon gamma signaling by the short chain fatty acid butyrate." Mol Cancer Res **1**(11): 855-862.

Kuzuyama, T. (2002). "Mevalonate and nonmevalonate pathways for the biosynthesis of isoprene units." Biosci Biotechnol Biochem **66**(8): 1619-1627.

Lange, B. M., T. Rujan, et al. (2000). "Isoprenoid biosynthesis: the evolution of two ancient and distinct pathways across genomes." Proc Natl Acad Sci U S A **97**(24): 13172-13177.

Laurine, E., X. Manival, et al. (2005). "PAP IB, a new member of the Reg gene family: cloning, expression, structural properties, and evolution by gene duplication." Biochim Biophys Acta **1727**(3): 177-187.

Lawrence, C. M., V. W. Rodwell, et al. (1995). "Crystal structure of Pseudomonas mevalonii HMG-CoA reductase at 3.0 angstrom resolution." Science **268**(5218): 1758-1762.

Lehmann, J. M., S. A. Kliewer, et al. (1997). "Activation of the nuclear receptor LXR by oxysterols defines a new hormone response pathway." J Biol Chem **272**(6): 3137-3140.

Li-Hawkins, J., M. Gafvels, et al. (2002). "Cholic acid mediates negative feedback regulation of bile acid synthesis in mice." J Clin Invest **110**(8): 1191-1200.

Li-Hawkins, J., E. G. Lund, et al. (2000). "Disruption of the oxysterol 7alpha-hydroxylase gene in mice." J Biol Chem **275**(22): 16536-16542.

Liao, J. K. and U. Laufs (2005). "Pleiotropic effects of statins." Annu Rev Pharmacol Toxicol **45**: 89-118.

Liscum, L., J. Finer-Moore, et al. (1985). "Domain structure of 3-hydroxy-3-methylglutaryl coenzyme A reductase, a glycoprotein of the endoplasmic reticulum." J Biol Chem **260**(1): 522-530.

Lombard, J. and D. Moreira (2011). "Origins and early evolution of the mevalonate pathway of isoprenoid biosynthesis in the three domains of life." Mol Biol Evol **28**(1): 87-99.

Louis, P. and H. J. Flint (2009). "Diversity, metabolism and microbial ecology of butyrate-producing bacteria from the human large intestine." FEMS Microbiol Lett **294**(1): 1-8.

Mabuchi, H., T. Sakai, et al. (1983). "Reduction of serum cholesterol in heterozygous patients with familial hypercholesterolemia. Additive effects of compactin and cholestyramine." N Engl J Med **308**(11): 609-613.

Machiels, K., M. Joossens, et al. (2013). "A decrease of the butyrate-producing species Roseburia hominis and Faecalibacterium prausnitzii defines dysbiosis in patients with ulcerative colitis." Gut.

McAteer, S., A. Coulson, et al. (2001). "The lytB gene of Escherichia coli is essential and specifies a product needed for isoprenoid biosynthesis." J Bacteriol **183**(24): 7403-7407.

McGarvey, D. J. and R. Croteau (1995). "Terpenoid metabolism." Plant Cell **7**(7): 1015-1026.

Mowen, K. A. and L. H. Glimcher (2004). "Signaling pathways in Th2 development." Immunol Rev **202**: 203-222.

Papo, N. and Y. Shai (2003). "Can we predict biological activity of antimicrobial peptides from their interactions with model phospholipid membranes?" Peptides **24**(11): 1693-1703.

Park, S. W., A. R. Choi, et al. (2013). "The effects of statins on the clinical outcomes of Clostridium difficile infection in hospitalised patients." Aliment Pharmacol Ther **38**(6): 619-627.

Plevy, S. E., C. J. Landers, et al. (1997). "A role for TNF-alpha and mucosal T helper-1 cytokines in the pathogenesis of Crohn's disease." J Immunol **159**(12): 6276-6282.

Pullinger, C. R., C. Eng, et al. (2002). "Human cholesterol 7alpha-hydroxylase (CYP7A1) deficiency has a hypercholesterolemic phenotype." J Clin Invest **110**(1): 109-117.

Repa, J. J., E. G. Lund, et al. (2000). "Disruption of the sterol 27-hydroxylase gene in mice results in hepatomegaly and hypertriglyceridemia. Reversal by cholic acid feeding." J Biol Chem **275**(50): 39685-39692.

Roediger, W. E. (1980). "Role of anaerobic bacteria in the metabolic welfare of the colonic mucosa in man." Gut **21**(9): 793-798.

Roitelman, J., E. H. Olender, et al. (1992). "Immunological evidence for eight spans in the membrane domain of 3-hydroxy-3-methylglutaryl coenzyme A reductase: implications for enzyme degradation in the endoplasmic reticulum." J Cell Biol **117**(5): 959-973.

Romagnani, S. (2000). "T-cell subsets (Th1 versus Th2)." Ann Allergy Asthma Immunol **85**(1): 9-18; quiz 18, 21.

Rosen, H., A. Reshef, et al. (1998). "Markedly reduced bile acid synthesis but maintained levels of cholesterol and vitamin D metabolites in mice with disrupted sterol 27-hydroxylase gene." J Biol Chem **273**(24): 14805-14812.

Roth, B. D. (2002). "The discovery and development of atorvastatin, a potent novel hypolipidemic agent." Prog Med Chem **40**: 1-22.

Russell, D. W. (2003). "The enzymes, regulation, and genetics of bile acid synthesis." Annu Rev Biochem **72**: 137-174.

Saitou, N. and M. Nei (1987). "The neighbor-joining method: a new method for reconstructing phylogenetic trees." Mol Biol Evol **4**(4): 406-425.

Scheppach, W., P. Bartram, et al. (1992). "Effect of short-chain fatty acids on the human colonic mucosa in vitro." JPEN J Parenter Enteral Nutr **16**(1): 43-48.

Schwarz, M., E. G. Lund, et al. (1996). "Disruption of cholesterol 7alpha-hydroxylase gene in mice. II. Bile acid deficiency is overcome by induction of oxysterol 7alpha-hydroxylase." J Biol Chem **271**(30): 18024-18031.

Scott, K. P., J. C. Martin, et al. (2014). "Prebiotic stimulation of human colonic butyrate-producing bacteria and bifidobacteria, in vitro." FEMS Microbiol Ecol **87**(1): 30-40.

Setchell, K. D., M. Schwarz, et al. (1998). "Identification of a new inborn error in bile acid synthesis: mutation of the oxysterol 7alpha-hydroxylase gene causes severe neonatal liver disease." J Clin Invest **102**(9): 1690-1703.

Skalnik, D. G., H. Narita, et al. (1988). "The membrane domain of 3-hydroxy-3-methylglutaryl-coenzyme A reductase confers endoplasmic reticulum localization and sterol-regulated degradation onto beta-galactosidase." J Biol Chem **263**(14): 6836-6841.

Stravitz, R. T., Z. R. Vlahcevic, et al. (1995). "Repression of cholesterol 7 alpha-hydroxylase transcription by bile acids is mediated through protein kinase C in primary cultures of rat hepatocytes." J Lipid Res **36**(6): 1359-1369.

Stroup, D., M. Crestani, et al. (1997). "Identification of a bile acid response element in the cholesterol 7 alpha-hydroxylase gene CYP7A." Am J Physiol **273**(2 Pt 1): G508-517.

Tabernero, L., V. W. Rodwell, et al. (2003). "Crystal structure of a statin bound to a class II hydroxymethylglutaryl-CoA reductase." J Biol Chem **278**(22): 19933-19938.

Tauch, A., N. Bischoff, et al. (2004). "Comparative genomics identified two conserved DNA modules in a corynebacterial plasmid family present in clinical isolates of the opportunistic human pathogen Corynebacterium jeikeium." Plasmid **52**(2): 102-118.

Thurnher, M., O. Nussbaumer, et al. (2012). "Novel aspects of mevalonate pathway inhibitors as antitumor agents." Clin Cancer Res **18**(13): 3524-3531.

Tytgat, K. M., H. A. Buller, et al. (1994). "Biosynthesis of human colonic mucin: Muc2 is the prominent secretory mucin." Gastroenterology **107**(5): 1352-1363.

Velazquez, O. C., A. Jabbar, et al. (1996). "Butyrate inhibits seeding and growth of colorectal metastases to the liver in mice." Surgery **120**(2): 440-447; discussion 447-448.

von Kockritz-Blickwede, M. and V. Nizet (2009). "Innate immunity turned inside-out: antimicrobial defense by phagocyte extracellular traps." J Mol Med (Berl) **87**(8): 775-783.

Wachtershauser, A., B. Akoglu, et al. (2001). "HMG-CoA reductase inhibitor mevastatin enhances the growth inhibitory effect of butyrate in the colorectal carcinoma cell line Caco-2." Carcinogenesis **22**(7): 1061-1067.

Wang, Y., M. Li, et al. (2009). "Histone hypercitrullination mediates chromatin decondensation and neutrophil extracellular trap formation." J Cell Biol **184**(2): 205-213.

Watanabe, M., H. Koike, et al. (1997). "Synthesis and biological activity of methanesulfonamide pyrimidine- and N-methanesulfonyl pyrrole-substituted 3,5-dihydroxy-6-heptenoates, a novel series of HMG-CoA reductase inhibitors." Bioorg Med Chem **5**(2): 437-444.

Wehkamp, J., M. Koslowski, et al. (2008). "Barrier dysfunction due to distinct defensin deficiencies in small intestinal and colonic Crohn's disease." Mucosal Immunol **1 Suppl 1**: S67-74.

White, C. M. (2002). "A review of the pharmacologic and pharmacokinetic aspects of rosuvastatin." J Clin Pharmacol **42**(9): 963-970.

Wilding, E. I., J. R. Brown, et al. (2000). "Identification, evolution, and essentiality of the mevalonate pathway for isopentenyl diphosphate biosynthesis in gram-positive cocci." J Bacteriol **182**(15): 4319-4327.

Yang, H., P. A. Antony, et al. (2004). "Intestinal Intraepithelial Lymphocyte γδ-T Cell-Derived Keratinocyte Growth Factor Modulates Epithelial Growth in the Mouse." Journal of Immunology **172**(7): 4151-4158.

Youssef, S., O. Stuve, et al. (2002). "The HMG-CoA reductase inhibitor, atorvastatin, promotes a Th2 bias and reverses paralysis in central nervous system autoimmune disease." Nature **420**(6911): 78-84.

Zanetti, M. (2004). "Cathelicidins, multifunctional peptides of the innate immunity." J Leukoc Biol **75**(1): 39-48.

Zhang, J., S. Osawa, et al. (2013). "Statins directly suppress cytokine production in murine intraepithelial lymphocytes." Cytokine **61**(2): 540-545.

Zhao, L. and W. Lu (2014). "Defensins in innate immunity." Curr Opin Hematol **21**(1): 37-42.

Chapter 2

The effects of Rosuvastatin on the murine gut microbiota and inhibition of bacterial mevalonate formation

* Research from this chapter currently under review:

Statins alter the community structure of the gastrointestinal microbiota

Nolan, J. A.[1,2], Skuse, P[3]., Govindarajan, K.[1,2], Patterson, E.[1,2,3] Konstantinidou, N.[2], Casey P. G.,[1] MacSharry, J.[1,2,4], Shanahan, F.[1], Stanton, C.[1,3], Hill, C.[1,2], Cotter, P.D. [1,3], Joyce, S. A.[1,2,4*], Gahan, C. G. M.[1,2,5*]

Abstract

Rosuvastatin (RSV) is part of a family of drug molecules used in the treatment of hypercholesterolemia. RSV inhibits the enzyme 3-hydroxy-3-methylglutaryl coenzyme A reductase (HMGR) which is involved in the conversion of HMG-CoA to mevalonate (MVAL). The enzyme is essential for the synthesis of cholesterol in mammals and essential isoprenoids in bacteria. Isoprenoids can be synthesised in bacteria by either a mevalonate-dependent "classical" pathway or a mevalonate-independent (2-C-methyl-D-erythritol 4-phosphate (MEP)) pathway. Bacteria with either pathways can be found in the gut environment leading us to hypothesise that statins may alter the community structure of the gut microbiota. Indeed, metagenomic pyrosequening of statin-treated mice revealed significant shifts in the microbial diversity of the caecum following treatment resulting in a significant reduction in physiologically relevant bacterial groups in the caecum and faeces (including the phylum *Proteobacteria* and the genera *Roseburia* and *Akkermansia*). The majority of bacteria affected by statin were negative for the presence of the HMGR enzyme, suggesting the gut microbiota might be altered indirectly. This finding prompted us to examine the effects of statins in bacteria *in-vitro*. HMGR-mediated inhibition by statins on growth and MVAL production appears to be dose dependent on administration of statin in certain bacterial species. No significant change was determined in caecal Short Chain Fatty Acid synthesis by RSV treatment. This study suggests that a commonly used statin (RSV) leads to an altered gut microbial composition in normal mice, a finding which should prompt further studies to investigate the implications of statins for gut microbial stability and health in humans.

Introduction

The gut microbiota encompasses vast numbers of microorganisms (10^{11} to 10^{12} g/ml) inhabiting the gastrointestinal tract and are integral to multiple physiological processes for the host. It is well known that microbial diversity in the gut is an important determinant of health and metabolic activity in the host (Kallus and Brandt 2012). The gut microbiota has been shown to affect host metabolism by driving increased energy utilisation from the diet, modulation of the immune system and associated physiological processes (Murphy, Cotter *et al*. 2010). Gut bacteria are well known to trigger innate immune responses in the host through key structural components of the cell such as lipopolysaccharide (LPS) (Sumbayev 2008).

The gastrointestinal tract is home to the largest reservoir of bacteria in the body extending from the mouth, oesophagus, stomach, small and large intestine to the rectum and anus. A bacterial population gradient exists along the length of this tract, with only 10^{3} microorganisms per ml in the duodenum compared to 10^{8} in the ileum. Low pH, bile acids and immunomodulatory factors represent the main reason for this gradient (Joyce and Gahan 2014)(Walter and Ley 2011). Generally humans and rodents share identical phyla in the distal gut microbiota namely, *Firmicutes, Bacteroidetes, Actinobacteria, Proteobacteria, Verrucomicrobia*, *Cyanobacteria*, TM7, *Fusobacteria* and *Spirochaetes.* It is well established that the phyla *Firmicutes* (20% approx.) and *Bacteroidetes* (80% approx.) are the two most dominant bacterial phyla in the gut microbiota of humans and rodents (Ley, Turnbaugh *et al.* 2006).

RSV is an example of a widely available statin used in the treatment of hypercholesterolemia worldwide (Johansen, Green *et al*. 2014). Statins inhibit the enzymatic activity of 3-hydroxy-3-methylglutaryl coenzyme A reductase (HMG-R),

an enzyme that catalyses the early rate limiting step in the synthesis of mevalonate, and subsequently the biosynthesis of cholesterol (Istvan 2002). As well as being an essential enzyme for the biosynthesis of cholesterol HMG-R is also important for the synthesis of isoprene subunits such as isopentenyl diphosphate (IPP) and dimethylallyl diphosphate (DMAPP) that form a much larger family of organic compounds named isoprenoids. These molecules form essential cellular metabolites in mammals and notably within bacteria (Heuston, Begley *et al.* 2012). Isoprenoids are essential for a wide variety of biological functions, including membrane forming molecules hopanoids, sterols and coenzyme Q in electron transport (Lange, Rujan et al. 2000; Wilding, Brown et al. 2000). We therefore hypothesized that RSV may influence the microbial community structure in the gut and upon individual bacteria species *in-vitro* through potential interactions with bacterial HMG-R.

Statins have been shown to elicit antibacterial effects (albeit at relatively high concentrations) (Jerwood and Cohen 2008) and have been proposed as potential alternatives to antibiotics (Motzkus-Feagans, Pakyz *et al.* 2012). However, only a subset of bacteria in the gut microbiota harbour the HMG-R enzyme (Lombard and Moreira 2011). The majority of bacterial species in the gut biosphere express an alternative (2-C-methyl-D-erythritol 4-phosphate (MEP)) pathway for isoprenoid biosynthesis and therefore lack the HMG-R isoform (Heuston, Begley *et al*. 2012). Reported antibacterial effects of statins have primarily been analysed in bacteria that possess HMG-R and to our knowledge a direct comparison of their effects upon a wide variety of bacteria is currently lacking.

Phylogenetic analysis of the HMG-R protein has revealed two distinct classes of enzyme, a Class 1 HMG-R isoform that is primarily found in higher organisms such as in mammals, as well as in many *Archaea* and *Actinobacteria*, and a Class 2

isoform that is generally limited to bacterial species (Lombard and Moreira 2011). Class 1 enzymes are seemingly found to be more sensitive to inhibition statins than their Class 2 counterparts (Bischoff and Rodwell 1996). This disparity in statin sensitivity is likely due to a combination of differential co-enzyme binding activity (NADH/NAD(P)H) and distinct conformational protein variation between both isoforms for substrate and indeed statin binding of both isoforms (Istvan and Deisenhofer 2001).

Previously unpublished data in our lab determined the *in-silico* distribution of isoprenoid biosynthetic pathways (including distribution of HMG-R) in the human gut microbiota (Konstantinidou 2012). The MetaHIT (European Metagenomics of the Human Intestinal Tract) catalogue of human metagenomic sequence data identified several gut bacterial species encoding enzymes with similarity to Class 1 and Class 2 HMG-R isoforms using respective driver sequences. The Class 1 isoform was categorised in many methanogenic bacterial species such as; *Methanothermus fervidus*, *Methanobrevibacter smithii*, the archeon *Acidianus hospitalis* and in the eukaryotic organism *Blastocystis hominis*. The Class 2 isoform was identified in a variety of important bacterial populations in the gut such as; *Coprococcus catus*, *Flavonifractor plautii* (*Firmicutes*) and a number of *Lactobacillus* species. This led us to hypothesise that long term statin treatment might inevitably have HMG-R target specific effects within the overall structure of the microbiota.

In this study we provided oral RSV to C57BL/6 mice fed a controlled high fat diet and examined the effects of treatment upon the community structure of the microbiota. C57BL/6 mice provided us with an excellent model for examining the potential effects of RSV on gut bacteria as this mouse species has been extensively

studied under a variety of dietary conditions for alterations to the microbiota (Clarke, Murphy *et al*. 2012; Patterson, RM *et al.* 2014). A number of key microbial groups (including the phylum *Proteobacteria* and the genera *Roseburia* and *Akkermansia*) were significantly reduced in the caecum and/or faeces of statin-treated animals. Interestingly the phyla affected were negative for the presence of HMG-R suggesting that the effects of statins in this instance were indirect (see Chapter 3). Indeed in-vitro susceptibility testing of a number of both gut representative HMGR positive and HMGR negative bacteria revealed that statins were effective antimicrobials only at relatively high concentrations. Evidence is presented that RSV effectively targeted the production of mevalonate (MVAL) (most likely through inhibition of HMG-R activity) when used at high concentrations.

Materials and Methods

C57BL/6 murine RSV administration study:

Adult, female 8-12 week old C57BL/6 (n=20) mice were obtained from Harlan, UK
and housed under pathogen-free conditions. Ethical approval was obtained through
the animal experimental ethics committee (AEEC). Mice were fed a High Fat
Western diet (D12451- Research Diets Inc.) and were acclimatized for two weeks
prior to statin administration. One group of mice (n=10) were orally administered *ad
libitum* sterile drinking water with 62.6mg/L dissolved Rosuvastatin Calcium Salt
(Kemprotec Ltd.), the control group (n=10) received untreated sterile water.
Consumption and dosage were calculated giving a final RSV concentration of
0.5mg/ body weight /8ml daily consumption (Famer and Crisby 2007). Drinking
water was replaced regularly to maintain drug efficacy. Mice were humanely
sacrificed under anaesthesia after one month intervention. Standard procedures for
collection of blood (large retro optical sinus), organ dissection (liver, ileum and
caecum) and faecal pellets were utilised. Tissues for gene expression analysis were
preserved in RNAlater (Ambion), organs were flash frozen in liquid nitrogen, and
serum was separated from blood by centrifugation (2,000g /10mins at 4º C). Murine
specimens were maintained at -80ºC for long term storage.

HDL/LDL and Total Cholesterol Quantification:

Murine serum HDL and LDL cholesterol were measured using the (BioVision) HDL
and LDL/VLDL cholesterol quantification kit (Catalog #K613-100) with
measurements carried out according to the manufacturers guidelines.

Microbial DNA extraction, amplification and high throughput DNA sequencing:

Total metagenomic DNA was extracted from individual faecal and caecal (content) samples of RSV treated and control mice using the QIamp DNA Stool Mini Kit (Qiagen), after an additional bead-beating step. Bacterial composition was determined by sequencing of 16S rRNA amplicons (V4-V5 region; 408nt long) generated by a separate PCR reaction for each sample (in triplicate) using universal 16S primers. Forward primers (5'-AYTGGGYDTAAAGNG), with attached molecular identifier tags between the 454 adapter sequence and target-specific primer sequence, and the reverse primer V5 (5'-CCGTCAATTYYTTTRAGTTT) (Claesson, Wang *et al.* 2010) were used along with Biomix Red (Bioline, London UK) (Table 1). The template DNA was amplified under the following PCR conditions for 35 cycles: 94˚C for 2 mins and 1 min respectively (initialization and denaturation), 56˚C for 60 secs (annealing) and 72˚C for 60 secs (elongation), proceeded by a final elongation stage of 2 mins. Negative control reactions with PCR grade water in place of template DNA were used to confirm lack of contamination. Amplicons were pooled and cleaned using the AMPure XP purification system (Beckman and Coulter, Takeley, UK) and DNA concentration was determined using the NANODROP 3300 Fluorospectrometer (Thermo Scientific) coupled with the Quant-it™ Picogreen® dsDNA Assay Kit (Invitrogen). Equal volumes of each sample were then pooled together and underwent a final cleaning and quantification stage. Amplicons were sequenced at the 454 sequencing centre (Branford, CT, USA) with the Roche GS FLX Titanium platform.

Sample	Clamp	Barcode	Oligo
Fusion45bc1L	CCATCTCATCCCTGCGTGTCTCCGACTCAG	AGAGAGAG	AYTGGGYDTAAAGNG
Fusion45bc2L	CCATCTCATCCCTGCGTGTCTCCGACTCAG	AGAGATGC	AYTGGGYDTAAAGNG
Fusion45bc3L	CCATCTCATCCCTGCGTGTCTCCGACTCAG	AGAGCAGC	AYTGGGYDTAAAGNG
Fusion45bc4L	CCATCTCATCCCTGCGTGTCTCCGACTCAG	AGAGCATG	AYTGGGYDTAAAGNG
Fusion45bc5L	CCATCTCATCCCTGCGTGTCTCCGACTCAG	AGATCATC	AYTGGGYDTAAAGNG
Fusion45bc6L	CCATCTCATCCCTGCGTGTCTCCGACTCAG	AGATCTGC	AYTGGGYDTAAAGNG
Fusion45bc7L	CCATCTCATCCCTGCGTGTCTCCGACTCAG	AGATGAGC	AYTGGGYDTAAAGNG
Fusion45bc8L	CCATCTCATCCCTGCGTGTCTCCGACTCAG	AGATGATG	AYTGGGYDTAAAGNG
Fusion45bc9L	CCATCTCATCCCTGCGTGTCTCCGACTCAG	AGATGCAG	AYTGGGYDTAAAGNG
Fusion45bc10L	CCATCTCATCCCTGCGTGTCTCCGACTCAG	AGATGCTC	AYTGGGYDTAAAGNG
Fusion45bc11L	CCATCTCATCCCTGCGTGTCTCCGACTCAG	AGCAGAGC	AYTGGGYDTAAAGNG
Fusion45bc12L	CCATCTCATCCCTGCGTGTCTCCGACTCAG	AGCAGATG	AYTGGGYDTAAAGNG
Fusion45bc13L	CCATCTCATCCCTGCGTGTCTCCGACTCAG	AGCAGCAG	AYTGGGYDTAAAGNG
Fusion45bc14L	CCATCTCATCCCTGCGTGTCTCCGACTCAG	AGCAGCTC	AYTGGGYDTAAAGNG
Fusion45bc15L	CCATCTCATCCCTGCGTGTCTCCGACTCAG	AGCATCTG	AYTGGGYDTAAAGNG
Fusion45bc16L	CCATCTCATCCCTGCGTGTCTCCGACTCAG	AGCATGAG	AYTGGGYDTAAAGNG
Fusion45bc17L	CCATCTCATCCCTGCGTGTCTCCGACTCAG	AGCTCAGC	AYTGGGYDTAAAGNG
Fusion45bc18L	CCATCTCATCCCTGCGTGTCTCCGACTCAG	AGCTCATG	AYTGGGYDTAAAGNG
Fusion45bc19L	CCATCTCATCCCTGCGTGTCTCCGACTCAG	AGCTGATC	AYTGGGYDTAAAGNG
Fusion45bc20L	CCATCTCATCCCTGCGTGTCTCCGACTCAG	AGCTGCTG	AYTGGGYDTAAAGNG
Fusion45bc21L	CCATCTCATCCCTGCGTGTCTCCGACTCAG	ATCAGATC	AYTGGGYDTAAAGNG
Fusion45bc22L	CCATCTCATCCCTGCGTGTCTCCGACTCAG	ATCAGCTG	AYTGGGYDTAAAGNG
Fusion45bc23L	CCATCTCATCCCTGCGTGTCTCCGACTCAG	ATCATCAG	AYTGGGYDTAAAGNG
Fusion45bc24L	CCATCTCATCCCTGCGTGTCTCCGACTCAG	ATCATCTC	AYTGGGYDTAAAGNG
Fusion45bc25L	CCATCTCATCCCTGCGTGTCTCCGACTCAG	ATCTCATC	AYTGGGYDTAAAGNG
Fusion45bc26L	CCATCTCATCCCTGCGTGTCTCCGACTCAG	ATCTCTGC	AYTGGGYDTAAAGNG
Fusion45bc27L	CCATCTCATCCCTGCGTGTCTCCGACTCAG	ATCTGAGC	AYTGGGYDTAAAGNG
Fusion45bc28L	CCATCTCATCCCTGCGTGTCTCCGACTCAG	ATCTGATG	AYTGGGYDTAAAGNG
Fusion45bc29L	CCATCTCATCCCTGCGTGTCTCCGACTCAG	ATCTGCAG	AYTGGGYDTAAAGNG
Fusion45bc30L	CCATCTCATCCCTGCGTGTCTCCGACTCAG	ATCTGCTC	AYTGGGYDTAAAGNG
Fusion45bc31L	CCATCTCATCCCTGCGTGTCTCCGACTCAG	ATGAGAGC	AYTGGGYDTAAAGNG
Fusion45bc32L	CCATCTCATCCCTGCGTGTCTCCGACTCAG	ATGAGATG	AYTGGGYDTAAAGNG
Fusion45bc33L	CCATCTCATCCCTGCGTGTCTCCGACTCAG	ATGAGCAG	AYTGGGYDTAAAGNG
Fusion45bc34L	CCATCTCATCCCTGCGTGTCTCCGACTCAG	ATGAGCTC	AYTGGGYDTAAAGNG
Fusion45bc35L	CCATCTCATCCCTGCGTGTCTCCGACTCAG	ATGATCTG	AYTGGGYDTAAAGNG
Fusion45bc36L	CCATCTCATCCCTGCGTGTCTCCGACTCAG	ATGATGAG	AYTGGGYDTAAAGNG
V5-reverse	CCTATCCCCTGTGTGCCTTGGCAGTCTCAG	408bp	5' CCGTCAATTYYTTTRAGTTT-3'

Table 1. Barcoding of faecal and caecal genomic DNA samples for control and RSV-treated animals.

16s rRNA analysis bacterial composition analysis was carried out using universal "tagged" 16S primers targeted to the 16S gene from a genomic DNA template. The forward primer: 5'-AYTGGGYDTAAAGNG-3' was barcoded with a unique identifier for each biological sample between the forward primer and 454 adapter sequence (clamp). Amplicons were generated by PCR reaction with the V5 region reverse primer: 5'-CCGTCAATTYYTTTRAGTTT-3' for up to 98% sequence coverage.

Bioinformatic and taxonomic analysis

Raw sequencing reads were 'de-noised' using traditional techniques implemented in the Ribosomal Database Project Pyrosequencing (RDP) Pipeline and ambiguous bases, non-exact primer matches and reads shorter than 150bp were excluded. Trimmed FASTA files were then BLASTed against a previously published 16S-specific database using default parameters. The resulting files were then parsed using the MEGAN software package, which assigns reads to the National Centre for Biotechnology Information (NCBI) taxonomies via the lowest common ancestor algorithm. Results were filtered prior to tree construction and summarization by the use of bit scores from within MEGAN where a cut-off bit score of 86 was employed (Urich, Lanzen *et al*. 2008; Rea, Dobson *et al*. 2011). The QIIME software suite was employed to achieve clustering of sequence reads into operational taxonomic units (OTUs) (Caporaso, Kuczynski *et al.* 2010). Chimeric OTUs were removed using the ChimeraSlayer program (Haas, Gevers *et al*. 2011) and phylogenetic trees constructed using the FastTreeMP tool (Price, Dehal *et al*. 2010). Beta diversity values were calculated based on Bray Curtis, weighted and unweighted UniFrac distances, and the KING viewer was used to visualise resulting PCoA plots (Huson, Richter *et al.* 2007; Chen, Davis *et al*. 2009). Sequence reads were deposited in the European Nucleotide Archive (EHA) under the accession number PRJEB5192. This work was undertaken in conjugation by our lab and our collaborators at the Teagasc Food Research Centre, Biosciences Department, Moorepark, Fermoy, Cork, Ireland.

RSV preparation for in-vitro growth experiments:

RSV calcium salt was dissolved in appropriate growth media to a final near saturated concentration of 3mg/ml. Vortexing and gentle heating were applied to ensure complete dissolution. Sterilisation was performed by means of filtration (0.2μm). Subsequent dilution was performed with sterile media as required.

Bacterial strains and growth conditions:

Bacterial growth media and conditions were observed as follows: *Enterococcus* (GM17 broth), *Staphylococcus aureus* (Brain Heart Infusion (BHI) broth), *L. monocytogenes* (BHI broth), *Escherichia coli* (BHI or Luria Bertani (LB) broth) and *Corynebacterium kroppenstedtii* (BHI Yeast Tween (BYT) complex media) (Tauch, Bischoff *et al*. 2004) grown shaking aerobically at 37ºC. For anaerobic bacteria *Bifidobacteria* (Reinforced Clostridial Media (RCM)), cultures were under anaerobic conditions in a modular atmosphere controlled environment. For solid media (1.5%) agar was added.

In-vitro bacterial growth curves:

Bacterial growth was monitored in a TECAN GENios ™ Microplate reader. Overnight cultures were measured using a BioPhotometer (eppendorf) and (10X 4X 45mm) cuvette. An optical density (OD_{600}) of 1 was determined for each bacteria and pelleted by centrifugation (13,000rpm/5mins) and resuspended in 1ml of broth. Cultures were diluted 1:20 giving a starting OD_{600} of 0.05 for growth. 200μL was dispensed per well of a 96-well plate in triplicate and growth monitored every hour. Bacteria were exposed to three different concentrations of media dissolved RSV (filter sterilised): 0.0005mg/ml, also 0.5mg/ml and 3mg/ml.

Mevalonate (MVAL) extraction from bacterial cells and growth media:

Cultures were set up in triplicate for a number of HMGR positive (*E. faecalis, E. faecium, L. monocytogenes, C. kroppenstedtii* and *S. aureus*) and HMGR negative bacteria (*E.coli* and *B. infantis*) in appropriate growth media with the same starting OD used for growth curve analysis. Bacteria were incubated for 24 hours with a number of different RSV doses (Control (0mg/ml), 0.5mg/ml and 2mg/ml) until stationary growth phase was reached. At this time, optical density readings were taken for normalisation of data relative to an OD of 1. 560μL was aliquoted into tubes from each sample and subsequently the cellular and supernatant fractions were separated by centrifugation into separate tubes (13,000rpm/5mins). Bacterial cell pellets were resuspended in an equivalent volume of PBS. Deuterated internal standard (mevalonolactone-4,4,5,5-d_4 (d_4-MVAL) (CDN isotopes Canada) was added to both cellular and supernatant fractions prior to extraction. MVAL extraction was performed by acidification (addition of 140μL of HCl) with thorough vortexing (45s) and subsequent addition of 560μL of ethyl acetate to each sample with final vortexing at top speed for 5mins. Organic layer (containing ethyl acetate/MVAL/internal standard) and aqueous layer separation was performed by final centrifugation (13,000rpm/5mins). The organic layer was finally transferred carefully to fresh tubes, ethyl acetate evaporated off and resuspended in 140μL of Mobile Phase A (water + 5mmol/L ammonium formate, pH adjusted to 2.5 (formic acid)) for MVAL quantification.

Ultra Performance Liquid chromatography Mass Spectrometry (UPLC-MS):

MVAL was detected and quantified on a Waters G2 Q-TOF LC-MS ® system following a procedure described by Waldron and colleagues (Waldron and Webster 2011). Following conversion to the lactone version, MVAL was detected on the LC-MS system in positive ion mode with tetra-deuterated d4-MVAL as the internal standard. The identity of MVAL was confirmed by its accurate mass obtained on the instrument corresponding to the protonated version of the analyte. The size to charge ratio (m/z) of MVAL occurred at approximately 131.3Da and for the internal standard at 135.1Da. The chromatography column was supplied by Sigma Aldrich® (Ascentis Express F5 column, 10 cm x 2.1 mm, 2.1 um particle size). A solvent gradient was set up using Mobile Phases A and B. Mobile phase A: water + 5 mM ammonium formate pH adjusted to pH 2.5 with formic acid and B: methanol + 5 mM ammonium formate pH adjusted to pH 3.0 with formic acid. The retention time on the instrument was approximately 2.5 minutes. The following parameters were observed using the MassLynx software package for running of the instrument. M.S. tune file: Polarity: ES+. Analyser: Resolution mode, Capillary voltage: 3kV, Sample cone: 80, Extraction cone: 2, Source Temperature: 120ºC, Desolvation Temperature: 450ºC, Cone Gas Flow (L/Hr): 50, Desolvation Gas Flow (L/Hr): 800. Sample infusion flow rate: 10μL/min by injection. Calibration (m/z range) of the instrument was performed using the reference compound: Leucine Enkephalin. The following UPLC conditions were observed on the instrument: Run Time: 5mins, Solvent A: water + 5mM ammonium formate (pH 2.5), Solvent B: methanol + 5mM ammonium formate (pH 3). Low pressure limit: 0 psi, High pressure limit: 15,000 psi. Washing of the Waters Acquity AutoSampler was carried out as follows; weak solvent wash: water + 0.1% formic acid, wash volume: 600μL, strong solvent wash: 50:50

methanol and water. Strong wash volume: 200µL. Target column temperature: 40ºC

and Target sample temperature: 4ºC. The following MS functions were observed in

general for running samples on the instrument: Function 1: Scans in function: 79,

Cycle time: 1.014 secs, Scan duration: 1 sec, Inter Scan Delay: 0.014 sec, Start-End

time: 0-5mins, Ionization mode: ES+, Data type: Enhanced Mass, Function type:

TOF MS, Mass Range: 100-1000. Function 2: Scans in function: 13, Cycle Time:

1.1 secs, Scan duration: 1 sec, Inter Scan Delay: 0.1 sec, Start-End time: 0-5mins,

Ionization mode: Enhanced Accurate Mass, Function type: TOF MS and Mass

Range: 100-1000.

MVAL chromatogram and standard curve:

 MVAL quantification was determined by means of a standard curve a range of run

on the instrument. MVAL was assayed using a range of concentrations (20µg/ml to

3.125ng/ml) with a final internal standard concentration of 5µg/ml (Fig. 1).

Chromatograph peaks for MVAL and D4-MVAL internal standard peaks are

illustrated below (Fig. 2).
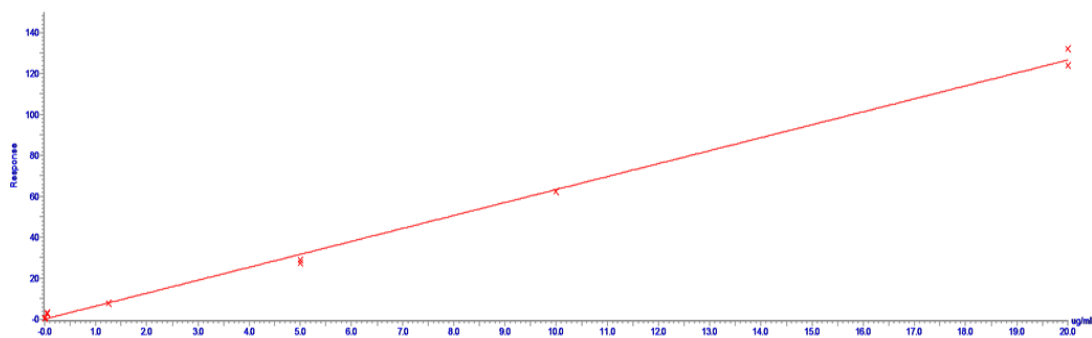
Fig. 1. MVAL standard curve (20µg/ml-3.125ng/ml) with R^2 of the line equal to 0.997725
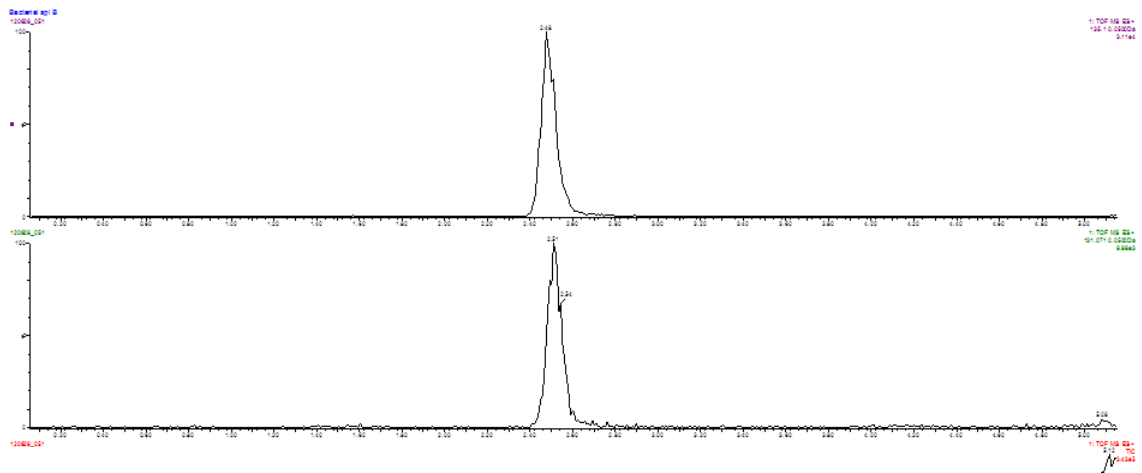
Fig.2. Chromatogram peaks for analyte MVAL (above) and internal standard D4-MVAL (below)

Analysis of short chain fatty acids

Short chain fatty acid (SCFA) analysis was performed according to a previously described protocol (Wall, Marques *et al*. 2012). Briefly, caecal content (30-40mg) was vortex-mixed with 1ml Milli-Q water and incubated at room temperature for 10mins and subsequently centrifuged at 10,000g for 5mins to pellet bacteria and other solids. The supernatant was filtered, transferred to a clear gas chromatography (GC) vial and 2-ethylbutyric acid (Sigma-Aldrich) was added as an internal standard. Standard solutions of 10.0mmol/L, 8.0mmol/L, 6.0mmol/L, 4.0mmol/L, 1.0mmol/L and 0.5mmol/L of acetic acid, propionic acid, isobutyric acid and butyric acid (Sigma-Aldrich), respectively were used for calibration. The concentrations of SCFA were measured using a Varian 3800 GC-flame-ionization system fitted with a ZB-FFAP column (30m X 0.32mm X 0.25µm; Phenomenex, Macclesfield, Cheshire, UK). Initial oven temperature was set at 100ºC for 30secs and raised to 180ºC at 8ºC per min and subsequently held for 1min, then increased to 200ºC at 20ºC per min and finally held at 200ºC for 5mins. Helium was used as the carrier gas at a flow rate of 1.3ml/min. The temperature of injector and the detector were set at

240ºC and 250ºC respectively. A standard curve was constructed with different concentrations of a standard mix containing acetic acid, propionic acid, isobutyric acid and N-butyric acid (Sigma-Aldrich). Peaks were integrated using the Varian Star Chromatography Workstation v6.0 software. This work was carried out in conjugation by our lab and our collaborators at the Teagasc Food Research Centre, Biosciences Department, Moorepark, Fermoy, Cork, Ireland.

Results

LDL and Total cholesterol was significantly lowered in statin treated animals:

Murine serum HDL/LDL and Total Cholesterol were measured for control and statin-treated animals by means of the BioVision HDL and LDL/VLDL cholesterol quantification kit following manufacturer's guidelines. RSV significantly lowered LDL (***p=0.001) and Total Cholesterol (*p=0.042) in the treated animals (Fig. 3).

C57BL/6 High Fat diet and RSV
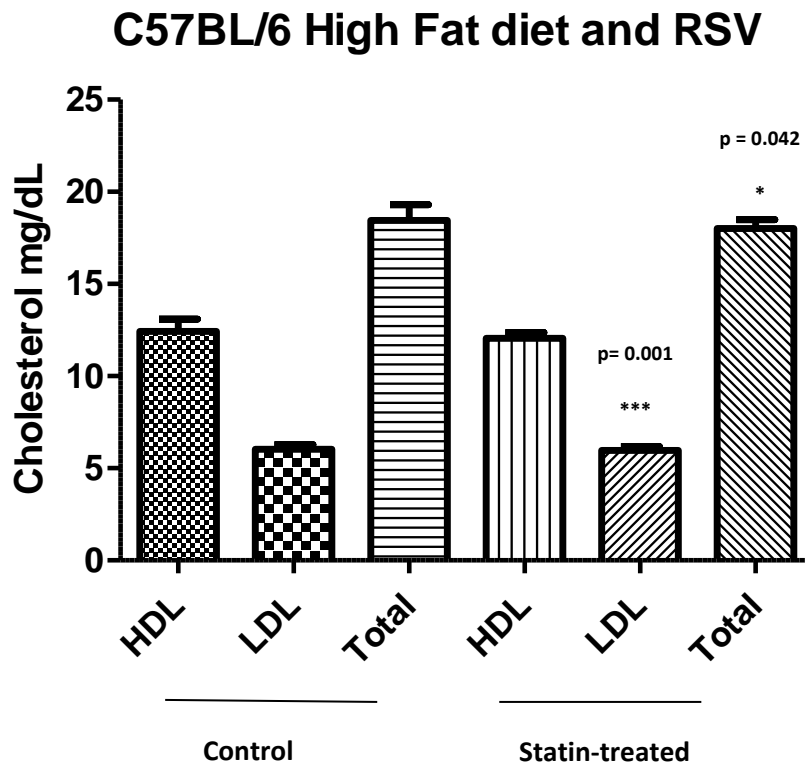
Fig.3. Serum HDL, LDL and Total cholesterol (mg/dL) for control and statin-treated animals

Serum HDL, LDL and Total Cholesterol levels were determined for control (n=10) and statin-treated (n=10) mice. Error bars the represent standard deviation from the mean. LDL (***p=0.001) and Total Cholesterol (*p=0.042) were found to be significantly lower in statin-treated animals.

RSV significantly impacts the composition and diversity of the gut microbiota:
A total of 683,749 V4-V5 16s rRNA sequence reads were generated during the
sequencing process corresponding to an average of 170,937 reads per group or
17,535 reads per animal. α-diversity values for species richness (Chao1), observed
species and phylogenetic diversity were found to be significantly lower
(***p<0.0001) in the statin treated animals (HF+ROS) compared to the control
group (HF+H20) in samples of caecal origin (Fig.4). No significant changes in α-
diversity were observed in samples of faecal origin. Principal coordinate (β-
diversity) analysis based upon unweighted UniFrac distances (Fig.5A and B)
revealed a distant clustering between the two groups in samples of both caecal (Fig.
5A) and faecal origin (Fig. 5B). Phylogenetic analysis (green and red flux charts)
(Fig. 6 A and B) revealed several significant microbial populations changes in
relative abundance due to RSV. Presence of HMG-R in significantly altered
bacteria was determined by GenBank and BLASTp analysis using the HMGR driver
sequence from *L. monocytogenes* EGDe (NP_464352.1) and designated HMGR+, in
both caecum and faeces. A complete phylogenetic breakdown for phyla, family and
genus levels of speciation are illustrated in pie charts (Fig.8).

Flux chart analysis of the caecum (Fig.6A) revealed no significant changes in
the phylum of statin-treated mice. At the family level there was a significant increase
in the proportion of the family *Lachnospiraceae* (HMGR+) (*p=0.02), and a
decrease in RF9 (*p=0.046) in statin-treated animals. At the genus level, *Rikenella*
(p=0.028), and *Coprococcus* (HMGR+) (**p=0.010) a member of the
Lachnospiraceae family were increased in the presence of RSV. Other bacterial
genera such as *Erysipelotrichaceae* IS (**p=0.002) and *Roseburia* (***p=0.001)
were significantly reduced (Fig.6A).

Flux chart analysis of the faeces revealed overall decreases in the phylum, family and genus bacterial groups in the gut microbiota of statin-treated mice. At the phylum level, *Proteobacteria* (*p=0.041), *Tenericutes* (**p=0.009) and *Verrucomicrobia* (*p=0.024) were significantly reduced in the presence of RSV (Fig. 6B). At the family level, significant decreases were observed in the proportions of *Desulfovibrionaceae* (*p=0.022), *Coriobacteriaceae* (*p=0.029) and *Akkermansiaeae* (*p=0.024) for the statin-treated animals (Fig. 6B). At the genus level, *Bilophila* (*p=0.022), *Erysipelotrichaceae Incertae Sedis* (***p=0.001), *Roseburia* (**p=0.008), *Enterorhabdus* (*p=0.036) and *Akkermansia* (*p=0.024) proportions were found to be significantly decreased by RSV (Fig. 6B). HMG-R was absent in all of the bacterial groups identified.

Our data suggests, a significant reduction in the biodiversity of the caecum (α-diversity) and distant clustering of bacterial populations (PCA plots) in the presence of RSV relative to control mice. Flux analysis revealed widespread alteration in numerous bacterial phyla, family and genera in both the caecum and faeces of treated animals. The majority of these changes led to a reduction in bacterial populations. However, significant increases were observed in known HMG-R +ve bacteria (as determined in our lab) in the family *Lachnospiraceae* genera *Coprococcus.* This contradicted our initial hypothesis that RSV would target HMGR containing bacteria in the gut microbiota and led us to believe the effect is indirect at the physiological relevant dose used in our study. Chapter 3 of this thesis will explore the mediating host factors of this indirect effect.
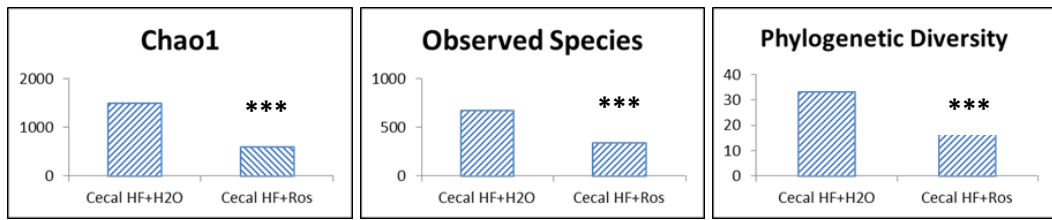
Fig. 4. Reduced α-diversity in the caecum of statin treated (HF+Ros) mice relative to control (HF+H₂O) mice.

Chao1, Observed species and Phylogenetic diversity testing revealed a significantly lower abundance of bacterial taxa (***p<0.0001) in the caecum of statin-treated mice. α-diversity analysis revealed no significant differences in faeces.
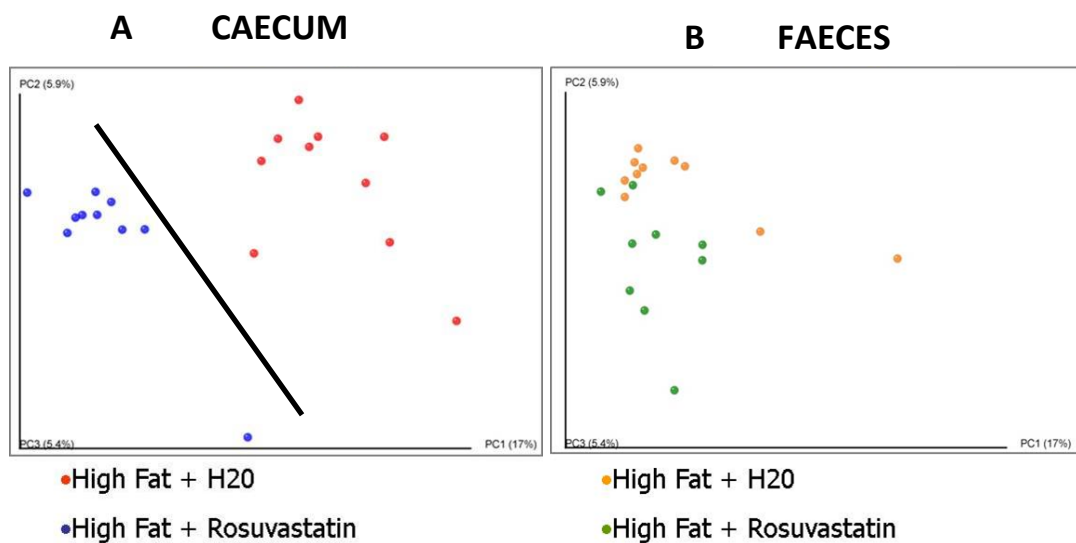
Fig.5. PCA analysis of control and statin-treated mice in caecum and faeces.

Principle coordinate analysis (PCA) (β-diversity) revealed a distinctive clustering of whole microbial communities in the caecum in the presence of RSV relative to control mice. Clustering in the faeces had less spatial separation. β-diversity represents a means to analyse presence or absence of bacterial populations.
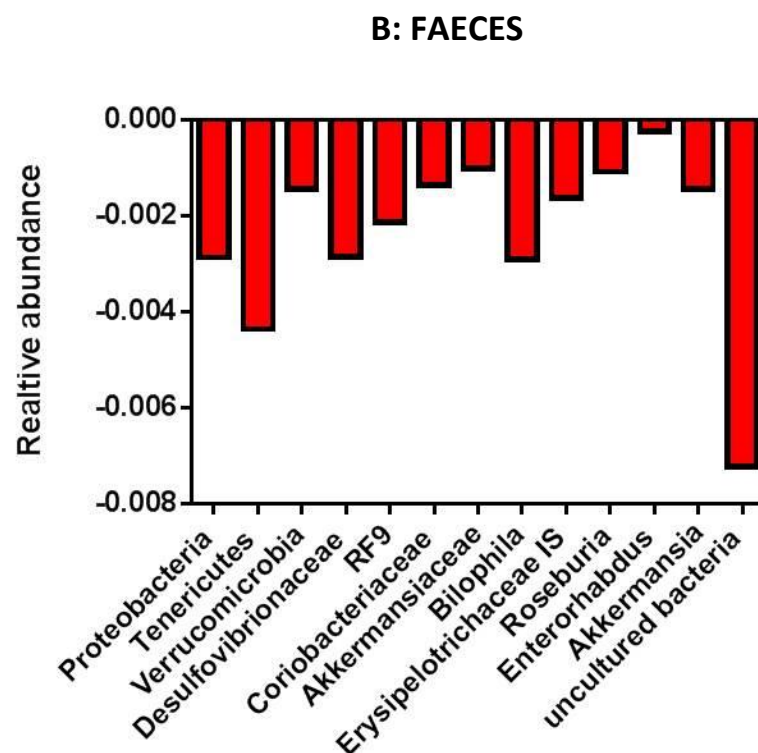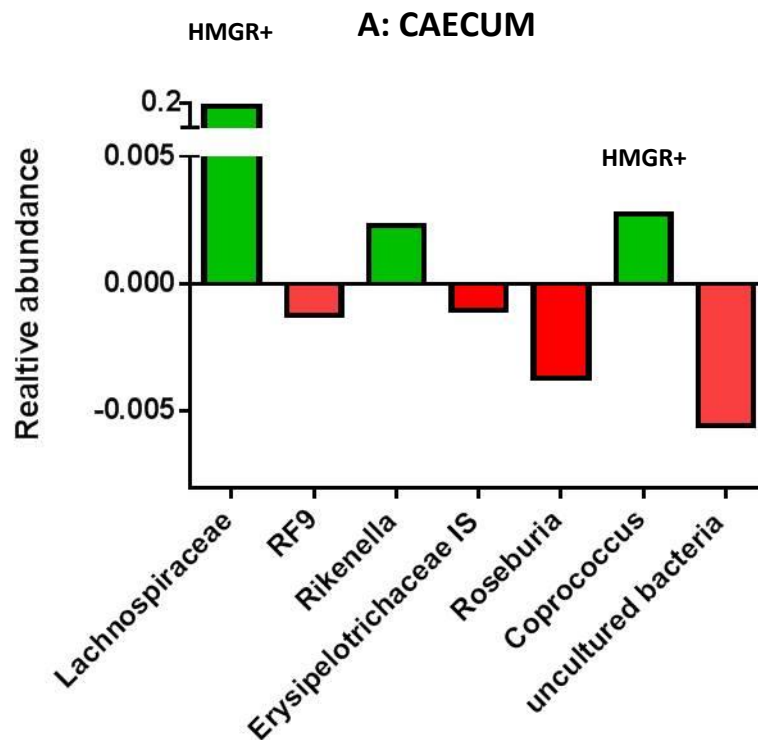
Fig.6. Phylogenetic (flux chart analysis) in the caecum and faeces of statin treated animals relative to control.

Green bars indicate a significant increase in the statin-treated group of particular bacterial phyla, family or genus determined by the Kruskall Wallis algorithm

(p<0.05). Conversely, red bars denote significant decreases in populations in the presence of RSV. At the phylum level there were significant changes in the caecum At the family level, *Lachnospiraceae* (HMGR+ve) was increased, *RF9* was decreased At the genus level, *Rikenella* and *Coprococcus* (HMGR+ve) were increased as well as reductions in the genera *Erysipelotrichaceae IS* and *Roseburia* In the faeces, a reduction in many bacterial populations was observed. Reductions were seen for phylum level (*Proteobacteria*, *Tenericutes* and *Verrucomicrobia*), family level (*Desulfovibrionaceae*, *RF9*, *Coriobacteraceae* and *Akkermansiaceae*) and genus level (*Bilophila*, *Erysipelotrichaceae IS*, *Roseburia*, *Enterorhabdus* and *Akkermansia*) in the presence of RSV. HMGR+ denoted presence or absence of HMG-R in each bacterial population. The majority of bacteria were negative for the presence of HMG-R.

Phylum level

Cecal HF+H20 Cecal HF+RSV Fecal HF+H20 Fecal HF+RSV

Proteobacteria Bacteroidetes Actinobacteria Firmicutes Tenericutes Deferribacteres Verrucomicrobia Candidate division TM7 Other

Family level

Cecal HF+H20 Cecal HF+RSV Fecal HF+H20 Fecal HF+RSV

Desulfovibrionaceae S24-7 Bacteroidaceae
Rikenellaceae Porphyromonadaceae Bifidobacteriaceae
Streptococcaceae Lactobacillaceae Erysipelotrichaceae
Lachnospiraceae Peptostreptococcaceae (Clostridiales) Ruminococcaceae
Family XIII Incertae Sedis Peptococcaceae RF9
Deferribacteraceae Coriobacteriaceae Clostridiaceae
Akkermansiaceae Rhodospirillaceae Other

85

Fig.7. Complete microbial map of the faecal and caecal microbiota of control (HF+H₂O) and statin treated (HF+RSV) mice as determined by 16s rRNA analysis.

RSV significantly affects growth of HMGR+ve bacteria at high levels:

In-vitro susceptibility testing of HMGR+ve (*S. aureus*, *E. faecalis*, *E. faecium* and *L. monocytogenes*) and HMGR-ve bacteria (*E. coli*) (Fig.8) determined a reduction in bacterial growth only at the highest levels of RSV tested. RSV only inhibited growth of HMGR+ve bacteria and had no effect on HMGR-ve of the strains tested. Sensitivity was most pronounced in the exponential phase of growth.

HMGR +ve bacteria:

Staphylococcus aureus Newmann
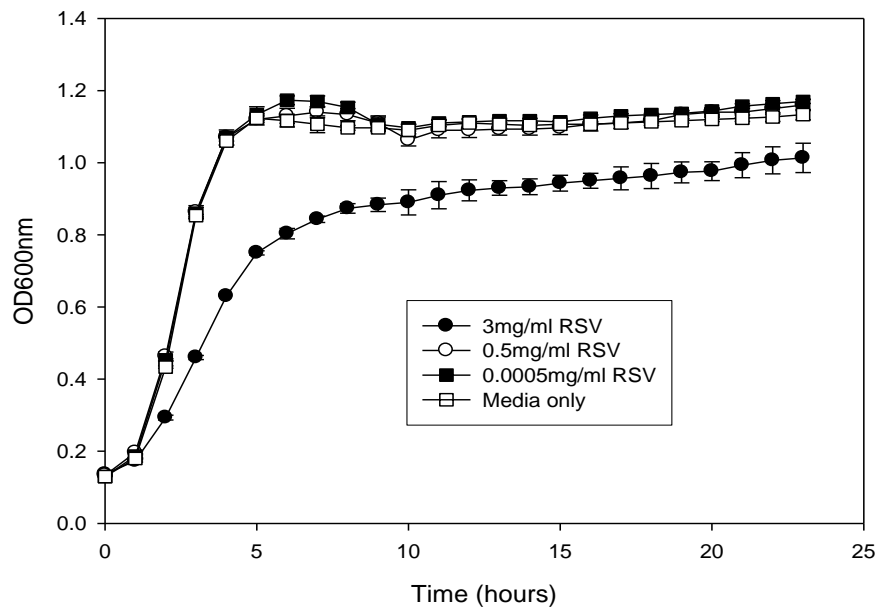
Enterococcus faecium DOTX16
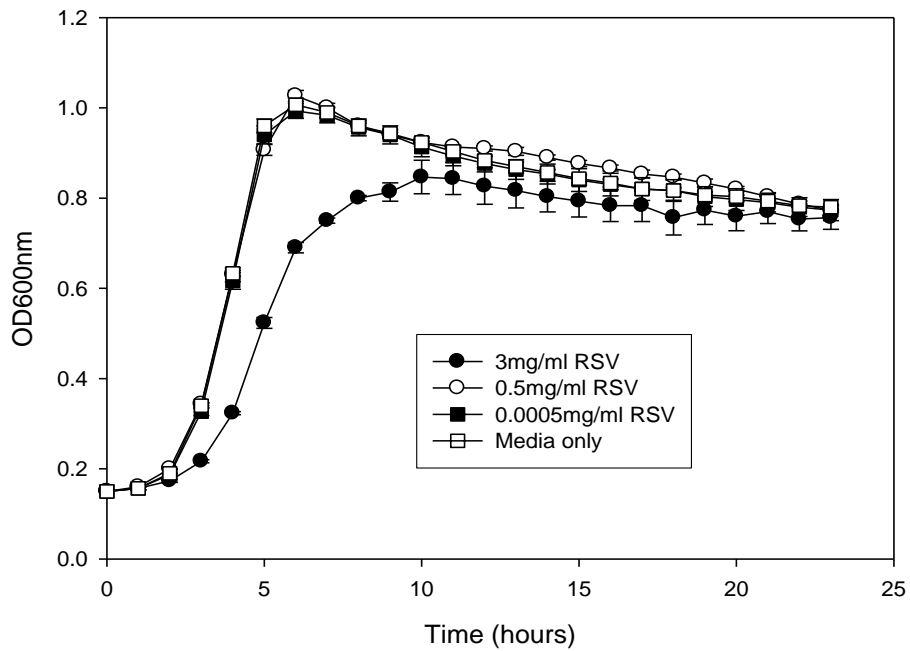
Enterococcus faecalis V583
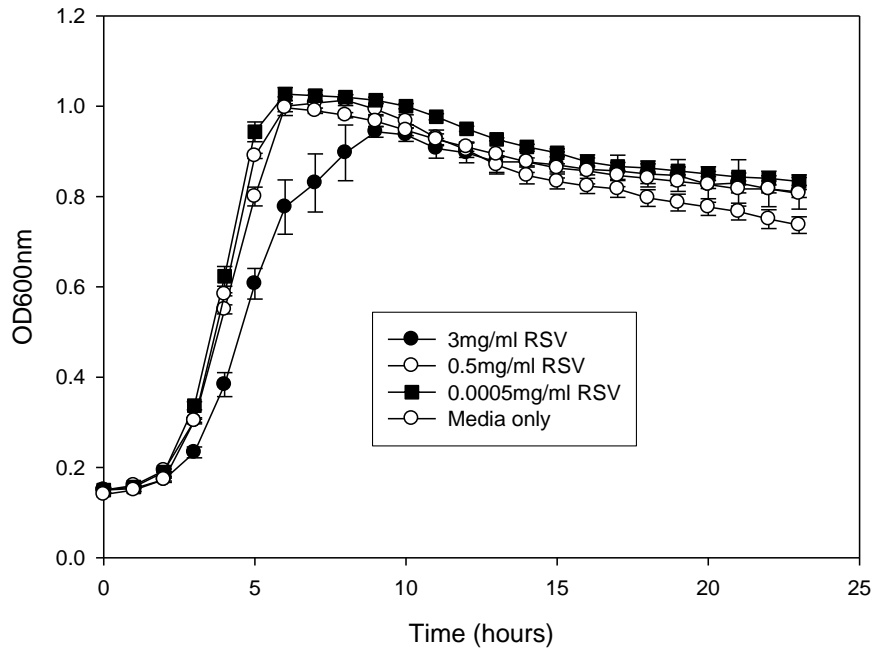
Listeria monocytogenes EGDe
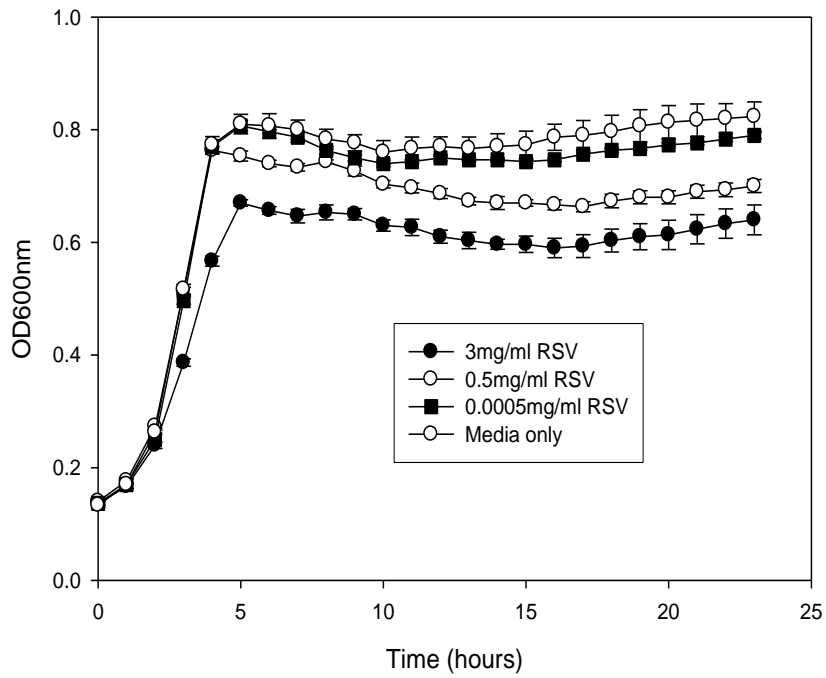
HMGR-ve bacteria:

Escherichia coli Nistle
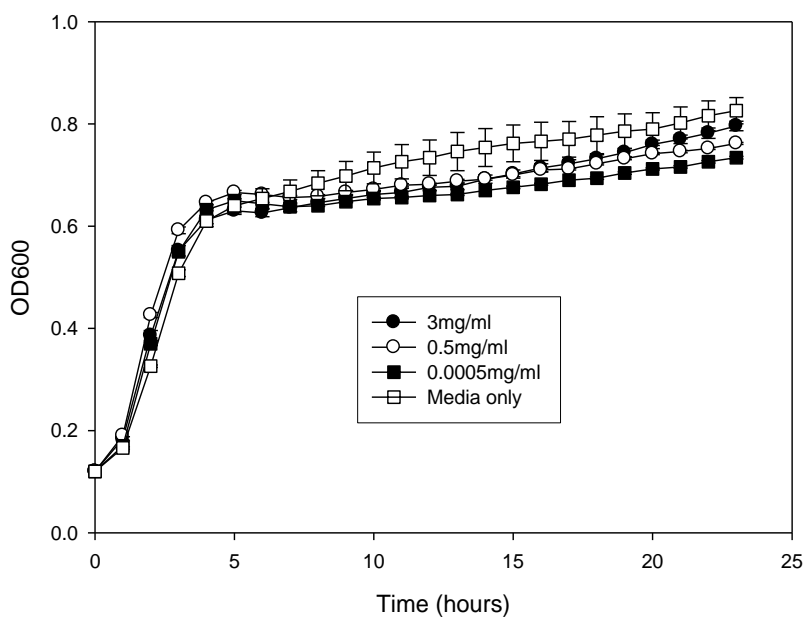
Escherichia coli K12 MG1655
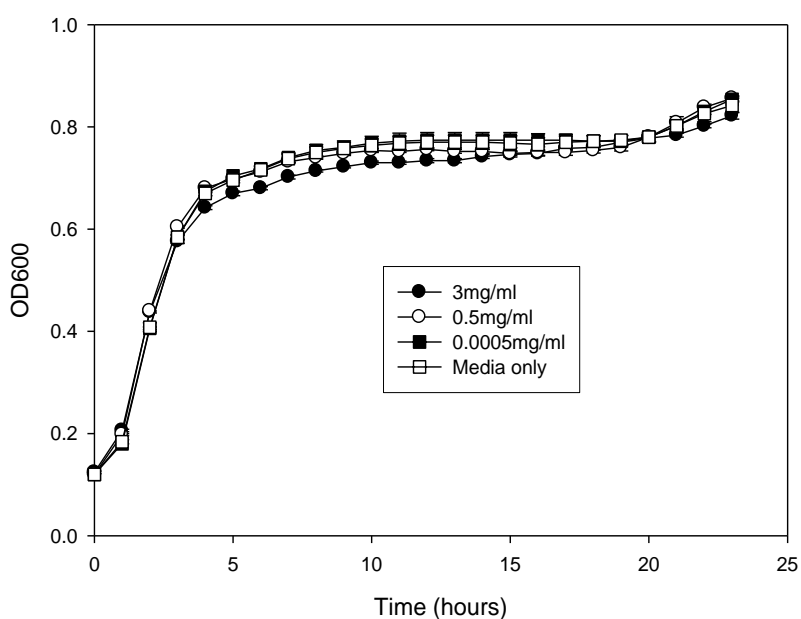
Fig. 8. *In- vitro* susceptibility of HMGR+ bacteria (*Staphylococcus aureus*, *Enterococcus faecium*, *Enterococcus. faecalis* and *Listeria monocytogenes*) and HMGR- bacteria (*Escherichia coli*) against RSV.
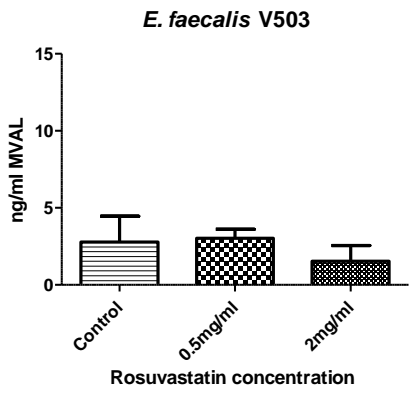
Dark circles denote (3mg/ml) media dissolved RSV, white circles (0.5mg/ml), black squares (0.0005mg/ml) RSV and white squares controls. Growth was monitored by optical density (OD600) over 24 hours and errors represent the standard deviation from the mean of a number of repeated experiments.

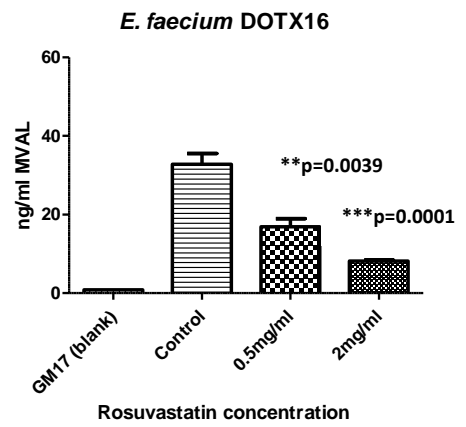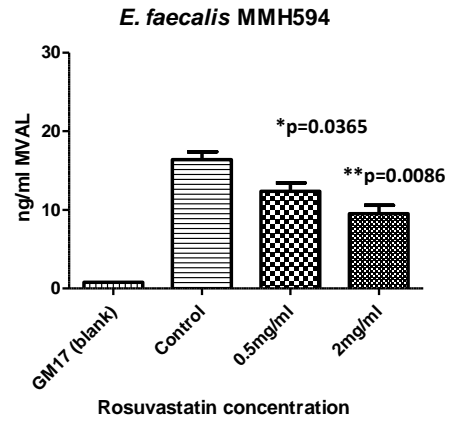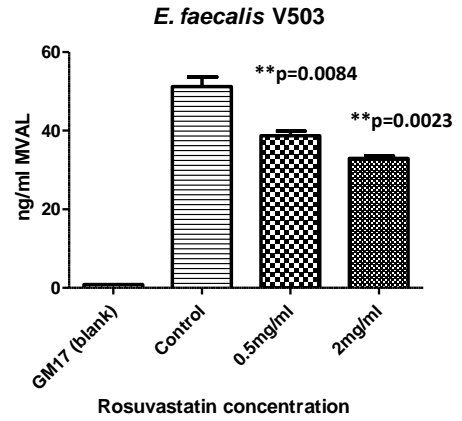*RSV significantly lowered mevalonate (MVAL) in supernatant of HMGR+ve bacteria:*

Mevalonate (MVAL) was quantified in cellular and supernatant fractions of HMGR+ve bacteria (*S. aureus, E. faecalis, E. faecium, L. monocytogenes, C. kroppenstedtii*) and HMGR-ve bacteria (*E. coli* and *B. infantis*) by UPLC-MS (see Materials and Methods) (Fig.9). Supernatant fractions contained significantly higher proportions of MVAL compared to cellular fractions. RSV significantly lowered the production of MVAL in a dose dependent fashion in the supernatant of HMGR+ve with respect to controls (Fig.9). HMGR-ve bacteria produced significantly lower levels of MVAL compared to HMGR+ve bacteria and this was unaffected by RSV.
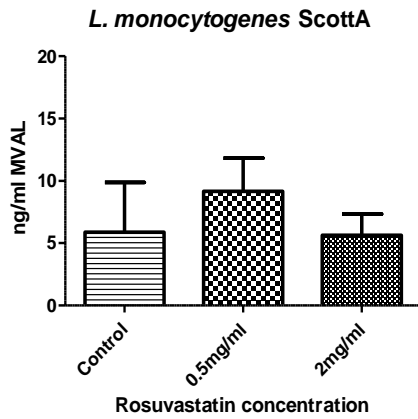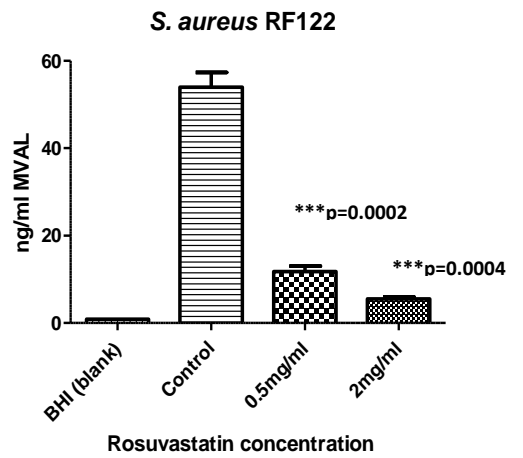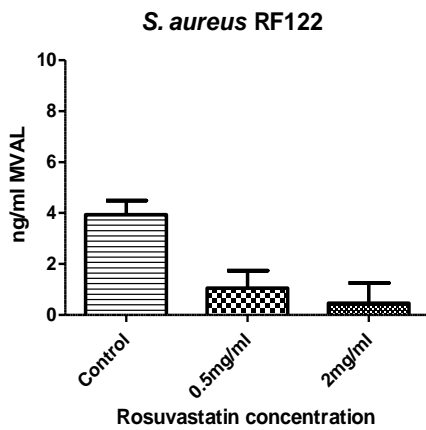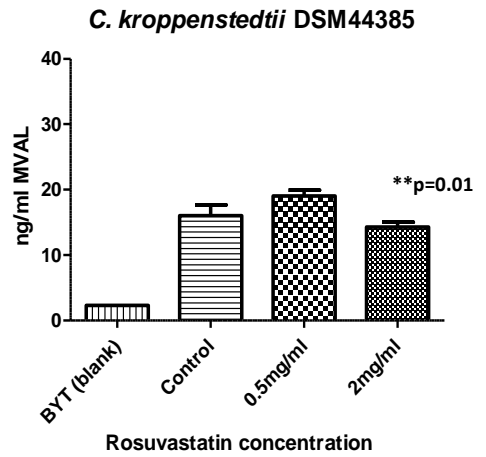
HMGR +ve BACTERIA:

CELLULAR FRACTION:

E. faecalis V503

E. faecalis MMH594

E. faecium DOTX16

E. faecium E1162

SUPERNATANT FRACTION:

E. faecalis V503

E. faecalis MMH594

E. faecium DOTX16

E. faecium E1162
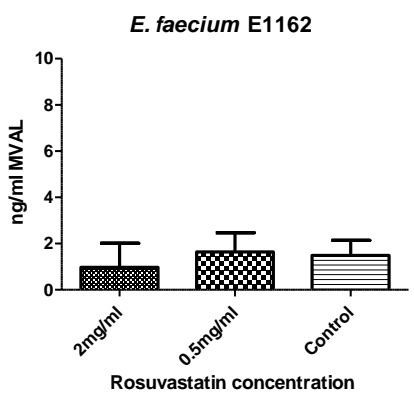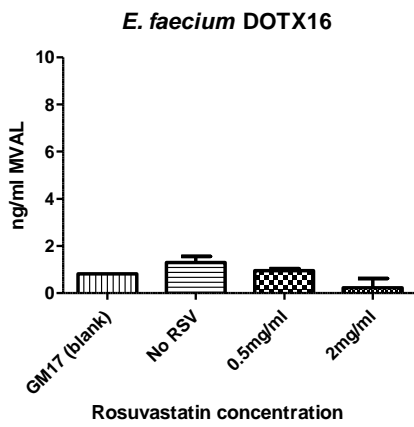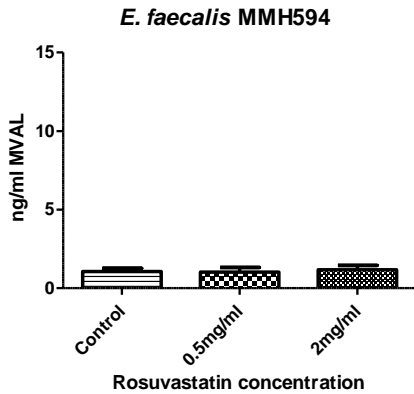
CELLULAR FRACTION:

SUPERNATANT FRACTION:

L. monocytogenes ScottA

L. monocytogenes ScottA

C. kroppenstedtii DSM44385

C. kroppenstedtii DSM44385

S. aureus RF122

S. aureus RF122

HMGR –ve BACTERIA:

CELLULAR FRACTION:

E. coli K12 MG1655

SUPERNATANT FRACTION:

E. coli K12 MG1655

Bif. infantis ATCC 15697

### *Bif. infantis* ATCC 15697
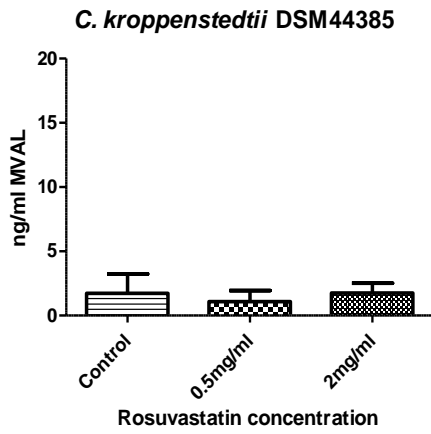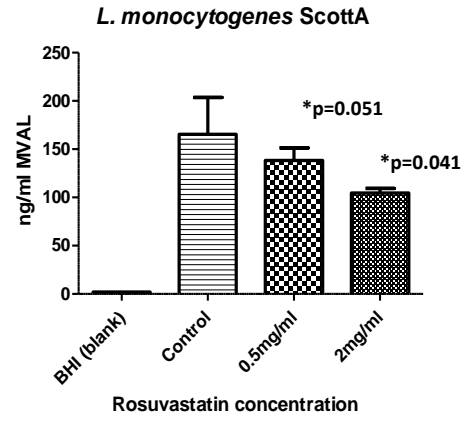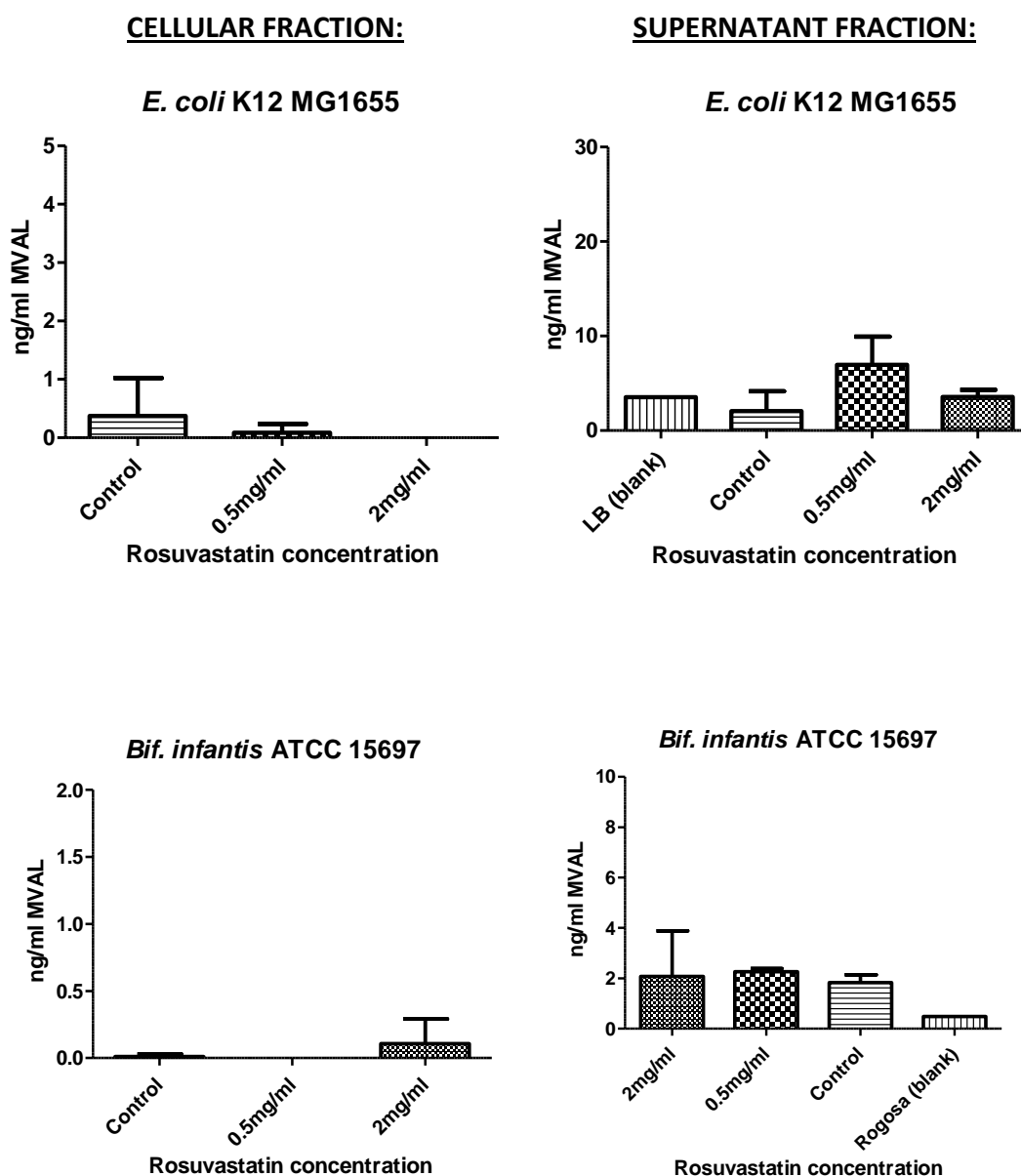
Fig.9. UPLC-MS analysis of (cellular and supernatant) bacterial MVAL production in response to RSV.

Normalised MVAL (ng/ml) determination of the HMGR+ve bacteria (*E. faecalis, E. faecium, L. monocytogenes*, *C. kroppenstedtii*, and *S. aureus*) and HMGR-ve bacteria (*E. coli* and *B. infantis*) by UPLC-MS. Cellular (left column) and supernatant MVAL (right column). Error bars represent standard deviation from mean of a number of repeated experiments and statistical significance compared to controls was calculated by the Student's T-test.

.

Impact of statins upon microbial SCFA production in mice

The reduction in key microbial species (described above) and the links between SCFA and positive health indicators are well described (see Chapter 1). This prompted us to examine the impact of RSV upon microbial production of SCFA. The concentrations of butyrate, iso-butyrate, propionate and acetate in the caecal contents of RSV treated and control animals were determined (Fig. 10). The results indicate that despite the significant alterations in the microbiota community structure there is no significant impact upon net production of key SCFAs in our experimental system.
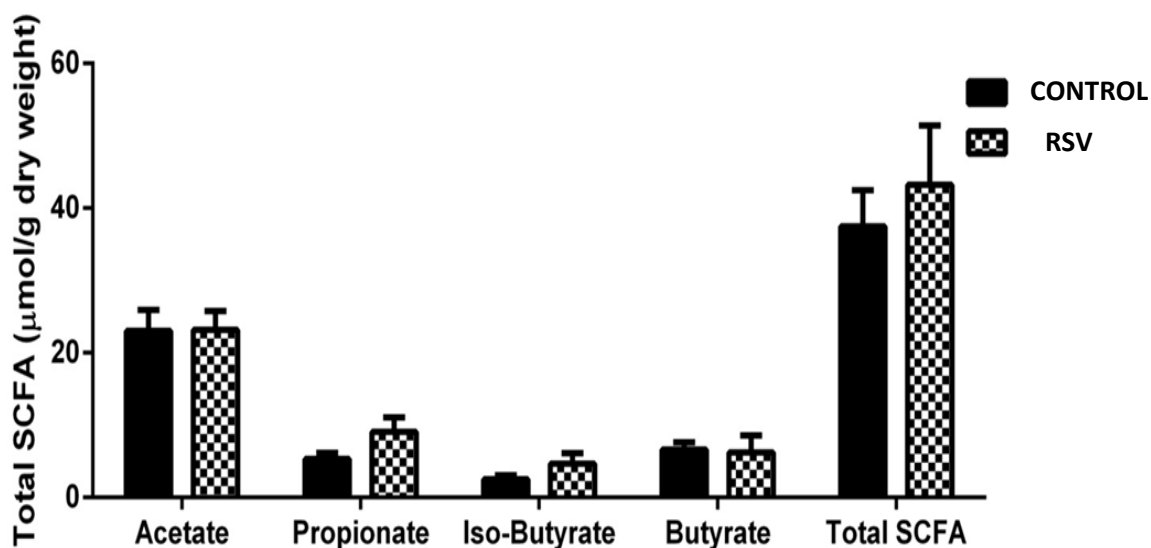
Fig. 10. RSV does not significantly alter the synthesis of short chain fatty acids in the caecum of mice.

Gas-liquid chromatography was used to analyse levels of short chain fatty acids (acetate, propionate, iso-butyrate, butyrate and total short chain fatty acids) in the caecum of RSV-treated mice and control animals. No significant differences detected between control and RSV-treated animals for any of the SCFA analysed.

Discussion

Exposure to xenobiotics has the potential to significantly alter the community structure within the host microbiota (Maurice, Haiser *et al*. 2013) in turn potentially shifting metabolic parameters in the host. Significant numbers of patients worldwide take daily medications to regulate chronic conditions (including hypercholesterolemia, depression and gastric acidity). However, with notable exceptions (Davey, Cotter *et al*. 2013; Maurice, Haiser *et al*. 2013; Patterson and Turnbaugh 2014), relatively little is known about the impact of these long term medications upon the host microbiota. Statins target the HMG-R protein in the mammalian host reducing the formation of cholesterol to regulate systemic cholesterol levels (Istvan 2002) and also have off-target effects upon the host including the potential to regulate host inflammation (Liao and Laufs 2005; Thongtang, Diffenderfer *et al*. 2013; Nenseter, Aukrust *et al*. 2014) (see Chapter 3). We therefore hypothesized that long term administration of statins might influence the composition of the microbiota either through a direct effect upon bacteria which possess an HMG-R isoform or through other processes linked to inflammation or bile acid metabolism (see Chapter 3). Herein we demonstrate that exposure to oral RSV in mice significantly reduces the diversity of the gut microbial community through a mechanism that is likely to be indirect, reflecting the pleiotropic effects of RSV upon host physiological processes.

Following administration of RSV to mice we noted a significant reduction in the overall phylogenetic diversity within the microbial community of the caecum relative to control mice. Significant flux was observed in specific groups both in the

caecum and faeces with a reduction in the family *Erysipelotrichaceae* and genus *Roseburia* in both compartments. These bacterial populations are well known to be associated with the production of Short Chain Fatty Acids (for example butyrate) and the beneficial health status of the host (Machiels, Joossens *et al*. 2013; Zhao, Wu *et al*. 2013) (see Chapter 1 also).

In faeces there was a significant relative reduction in numerous clusters including *Proteobacteria* and *Tenericutes*, in *Bilophila* species within the family *Desulfovibrionaceae,* as well as a reduction in the *Akkermansiaceae* within the phylum *Verrucomicrobia*. The phylum *Proteobacteria* are a well reported gram negative bacterial population in the gut associated with inflammation via interaction with the endotoxin lipopolysaccharide (LPS) (Yue, Ma *et al*. 2012). Similarly we determined a statin-associated reduction in the gram positive bacterial genus *Enterorhabdus* which has been shown in murine studies to be pro-inflammatory (Clavel, Charrier *et al*. 2009). The phylum *Akkermansiaceae* has been shown by a number of groups to be strongly anti-inflammatory in the gut and improves gut barrier defence via mediation of the endocannabinoid system (Alhouayek, Lambert *et al*. 2011; Hansen, Rosenkilde *et al*. 2011). Further interpretation of inflammatory role of RSV in the gastrointestinal environment will be discussed in Chapter 3. Also interestingly in our model, we observed a decline in the phylum *Tenericutes* which contain a recently discovered class of bacteria (*Mollicutes*) that are generally more prevalent in conventional mice fed a high fat diet (Turnbaugh, Backhed *et al.* 2008).

A number of the genera identified as altered by RSV in our model have been previously associated with physiological parameters in the host. For instance, *Bilophila wadsworthia* has been previously associated with causation of colitis in mouse models (Devkota, Wang *et al.* 2012; Joyce and Gahan 2014). *Akkermansia*

muciniphila (a mucin-degrading bacteria) has been associated with a lean phenotype in both human (Cani and Everard 2014) and murine models (Everard, Belzer *et al.* 2013). *A. muciniphila* is well described as a gram negative bacterial species that colonises the mammalian gut early in life and can represent up to 3% of the total microbiota (Derrien, Collado *et al.* 2008). Also of interest, we observed a significant reduction in the phylum *Desulfovibrionaceae* which form part of major sulphate reducing microorganisms in the gut that can form a significant proportion (up to 50%) of the distal microbiome with *Desulfovibrio piger* contributing the largest cohort. This sulphate reduction process has beneficial implications for energy utilisation and metabolic processes in the host (Rey, Gonzalez *et al.* 2013).

Most notably members of the *Lachnospiraceae* (including *Coprococcus* and *Roseburia*) which are associated with butyrate production in the gut and are associated with improved health status were determined by flux analysis to be increased by RSV (Duncan, Hold *et al.* 2002; Duncan, Holtrop *et al.* 2004; Louis and Flint 2009; Claesson, Wang *et al.* 2010; Reichardt, Duncan *et al.* 2014). However despite significant alterations to the caecal and faecal microbiota we failed to detect alterations in gastrointestinal SCFA production. This finding may reflect the fact that the *Lachnopiraceae* group is increased in the caecum of these animals while other populations of SCFA producers are decreased.

The most significant changes seen in RSV treated animals were to organisms which lack the mevalonate pathway for isoprenoid biosynthesis and therefore do not possess the HMG-R enzyme. Indeed *Coprococcus spp.*, which we have shown to possess the *hmgR* gene (and other enzymes in this pathway), were increased by RSV treatment. Other bacterial families which we and others have shown to possess the mevalonate pathway (Lombard and Moreira 2011; Heuston, Begley *et al.* 2012) such

as *Lactobacillaceae* and *Enterococcaceae* (Hedl, Sutherlin *et al.* 2002) were not statistically altered through RSV administration in our study. This suggests that the impact of long-term RSV administration on the microbial community is indirect and not through inhibition of organisms that possess HMG-R. This supposition is supported by our finding that cultivable gut organisms which possess a mevalonate pathway (including *Enterococcus* species and *Listeria* species) are not susceptible to physiological concentrations of RSV *in vitro*. This supports previous analysis by Masadeh and coworkers (Masadeh, Mhaidat *et al.* 2012) which found that *Enterococcus* and *S. aureus* isolates display a minimum inhibitory concentration (MIC) for RSV which is approximately one thousand fold higher than a physiologically relevant dose for an average patient.

This finding was also supported when we analysed inhibition of MVAL (the product of HMG-R activity) formation in a number of cultivable bacteria. We developed a UPLC-MS approach to quantify MAVL in microbial samples. As expected we confirmed significant MVAL levels in HMGR+ve bacteria (*E. faecalis, E. faecium, L. monocytogenes*, *C. kroppenstedtii* and *S. aureus*) and marginal biosynthesis in HMGR-ve bacteria (*E. coli* and *B. infantis*).We demonstrated a significant reduction in HMGR+ve bacterial MVAL when cultures were exposed to RSV and these effects were dose dependent. These and previously mentioned findings confirm that relatively high levels of statins are required to directly inhibit bacterial growth (and MVAL) through targeting of the HMG-R enzyme.

Surprisingly, MVAL was predominantly detected in the supernatant of HMGR+ve bacteria and not in the cellular fraction. Previous studies in our lab (Heuston, Begley *et al.* 2012) (see also Chapter 4) have shown that exogenous MVAL can rescue the growth of HMG-R mutant in *L. monocytogenes* EGDe. The

combined studies suggest that MVAL is readily transported into the bacterial cell and is also secreted into the growth media. Further studies examining the mechanisms of microbial MVAL transport are warranted.

In conclusion, the current study demonstrates that RSV can significantly alter the community structure of the gut microbiota in our murine model. When examined in greater detail antimicrobial activity of this statin only appears to relate to inhibition of HMG-R activity at relatively high levels of this drug. However it is clear that observed perturbations to the gut microbiota are more likely due to a host (indirect) effect of RSV further manipulating the bacterial structure of the gastrointestinal environment which we further examine in Chapter 3 of this thesis. The current study should prompt further analysis to determine the effects of long-term use of statins upon the gut microbial community and host health.

References

Alhouayek, M., D. M. Lambert, et al. (2011). "Increasing endogenous 2-arachidonoylglycerol levels counteracts colitis and related systemic inflammation." FASEB J **25**(8): 2711-2721.

Bischoff, K. M. and V. W. Rodwell (1996). "3-Hydroxy-3-methylglutaryl-coenzyme A reductase from Haloferax volcanii: purification, characterization, and expression in Escherichia coli." J Bacteriol **178**(1): 19-23.

Cani, P. D. and A. Everard (2014). "[Akkermansia muciniphila: a novel target controlling obesity, type 2 diabetes and inflammation?]." Med Sci (Paris) **30**(2): 125-127.

Caporaso, J. G., J. Kuczynski, et al. (2010). "QIIME allows analysis of high-throughput community sequencing data." Nat Methods **7**(5): 335-336.

Chen, V. B., I. W. Davis, et al. (2009). "KING (Kinemage, Next Generation): a versatile interactive molecular and scientific visualization program." Protein Sci **18**(11): 2403-2409.

Claesson, M. J., Q. Wang, et al. (2010). "Comparison of two next-generation sequencing technologies for resolving highly complex microbiota composition using tandem variable 16S rRNA gene regions." Nucleic Acids Res **38**(22): e200.

Clarke, S. F., E. F. Murphy, et al. (2012). "The gut microbiota and its relationship to diet and obesity: new insights." Gut Microbes **3**(3): 186-202.

Clavel, T., C. Charrier, et al. (2009). "Isolation of bacteria from the ileal mucosa of TNFdeltaARE mice and description of Enterorhabdus mucosicola gen. nov., sp. nov." Int J Syst Evol Microbiol **59**(Pt 7): 1805-1812.

Davey, K. J., P. D. Cotter, et al. (2013). "Antipsychotics and the gut microbiome: olanzapine-induced metabolic dysfunction is attenuated by antibiotic administration in the rat." Transl Psychiatry **3**: e309.

Derrien, M., M. C. Collado, et al. (2008). "The Mucin degrader Akkermansia muciniphila is an abundant resident of the human intestinal tract." Appl Environ Microbiol **74**(5): 1646-1648.

Devkota, S., Y. Wang, et al. (2012). "Dietary-fat-induced taurocholic acid promotes pathobiont expansion and colitis in Il10-/- mice." Nature **487**(7405): 104-108.

Duncan, S. H., G. L. Hold, et al. (2002). "Roseburia intestinalis sp. nov., a novel saccharolytic, butyrate-producing bacterium from human faeces." Int J Syst Evol Microbiol **52**(Pt 5): 1615-1620.

Duncan, S. H., G. Holtrop, et al. (2004). "Contribution of acetate to butyrate formation by human faecal bacteria." Br J Nutr **91**(6): 915-923.

Everard, A., C. Belzer, et al. (2013). "Cross-talk between Akkermansia muciniphila and intestinal epithelium controls diet-induced obesity." Proc Natl Acad Sci U S A **110**(22): 9066-9071.

Famer, D. and M. Crisby (2007). "Rosuvastatin reduces gliosis and the accelerated weight gain observed in WT and ApoE-/- mice exposed to a high cholesterol diet." Neurosci Lett **419**(1): 68-73.

Haas, B. J., D. Gevers, et al. (2011). "Chimeric 16S rRNA sequence formation and detection in Sanger and 454-pyrosequenced PCR amplicons." Genome Res **21**(3): 494-504.

Hansen, K. B., M. M. Rosenkilde, et al. (2011). "2-Oleoyl glycerol is a GPR119 agonist and signals GLP-1 release in humans." J Clin Endocrinol Metab **96**(9): E1409-1417.

Hedl, M., A. Sutherlin, et al. (2002). "Enterococcus faecalis acetoacetyl-coenzyme A thiolase/3-hydroxy-3-methylglutaryl-coenzyme A reductase, a dual-function protein of isopentenyl diphosphate biosynthesis." J Bacteriol **184**(8): 2116-2122.

Heuston, S., M. Begley, et al. (2012). "HmgR, a key enzyme in the mevalonate pathway for isoprenoid biosynthesis, is essential for growth of Listeria monocytogenes EGDe." Microbiology **158**(Pt 7): 1684-1693.

Heuston, S., M. Begley, et al. (2012). "Isoprenoid biosynthesis in bacterial pathogens." Microbiology **158**(Pt 6): 1389-1401.

Huson, D. H., D. C. Richter, et al. (2007). "Dendroscope: An interactive viewer for large phylogenetic trees." BMC Bioinformatics **8**: 460.

Istvan, E. S. (2002). "Structural mechanism for statin inhibition of 3-hydroxy-3-methylglutaryl coenzyme A reductase." Am Heart J **144**(6 Suppl): S27-32.

Istvan, E. S. and J. Deisenhofer (2001). "Structural mechanism for statin inhibition of HMG-CoA reductase." Science **292**(5519): 1160-1164.

Jerwood, S. and J. Cohen (2008). "Unexpected antimicrobial effect of statins." J Antimicrob Chemother **61**(2): 362-364.

Johansen, M. E., L. A. Green, et al. (2014). "Cardiovascular risk and statin use in the United States." Ann Fam Med **12**(3): 215-223.

Joyce, S. A. and C. G. Gahan (2014). "The gut microbiota and the metabolic health of the host." Curr Opin Gastroenterol **30**(2): 120-127.

Kallus, S. J. and L. J. Brandt (2012). "The intestinal microbiota and obesity." J Clin Gastroenterol **46**(1): 16-24.

Konstantinidou, N. (2012). "In-silico analysis of isoprenoid biosynthetic pathways in the human gut microbiota." MSc thesis (Bioinformatics), University College Cork.

Lange, B. M., T. Rujan, et al. (2000). "Isoprenoid biosynthesis: the evolution of two ancient and distinct pathways across genomes." Proc Natl Acad Sci U S A **97**(24): 13172-13177.

Ley, R. E., P. J. Turnbaugh, et al. (2006). "Microbial ecology: human gut microbes associated with obesity." Nature **444**(7122): 1022-1023.

Liao, J. K. and U. Laufs (2005). "Pleiotropic effects of statins." Annu Rev Pharmacol Toxicol **45**: 89-118.

Lombard, J. and D. Moreira (2011). "Origins and early evolution of the mevalonate pathway of isoprenoid biosynthesis in the three domains of life." Mol Biol Evol **28**(1): 87-99.

Louis, P. and H. J. Flint (2009). "Diversity, metabolism and microbial ecology of butyrate-producing bacteria from the human large intestine." FEMS Microbiol Lett **294**(1): 1-8.

Machiels, K., M. Joossens, et al. (2013). "A decrease of the butyrate-producing species Roseburia hominis and Faecalibacterium prausnitzii defines dysbiosis in patients with ulcerative colitis." Gut.

Masadeh, M., N. Mhaidat, et al. (2012). "Antibacterial activity of statins: a comparative study of atorvastatin, simvastatin, and rosuvastatin." Ann Clin Microbiol Antimicrob **11**: 13.

Maurice, C. F., H. J. Haiser, et al. (2013). "Xenobiotics shape the physiology and gene expression of the active human gut microbiome." Cell **152**(1-2): 39-50.

Motzkus-Feagans, C. A., A. Pakyz, et al. (2012). "Statin use and the risk of Clostridium difficile in academic medical centres." Gut **61**(11): 1538-1542.

Murphy, E. F., P. D. Cotter, et al. (2010). "Composition and energy harvesting capacity of the gut microbiota: relationship to diet, obesity and time in mouse models." Gut **59**(12): 1635-1642.

Nenseter, M. S., P. Aukrust, et al. (2014). "Low level of inflammatory marker in hyperhomocysteinemic patients on statin therapy." Scand J Clin Lab Invest **74**(1): 1-7.

Patterson, A. D. and P. J. Turnbaugh (2014). "Microbial Determinants of Biochemical Individuality and Their Impact on Toxicology and Pharmacology." Cell Metab.

Patterson, E., O. D. RM, et al. (2014). "Impact of dietary fatty acids on metabolic activity and host intestinal microbiota composition in C57BL/6J mice." Br J Nutr: 1-13.

Price, M. N., P. S. Dehal, et al. (2010). "FastTree 2--approximately maximum-likelihood trees for large alignments." PLoS One **5**(3): e9490.

Rea, M. C., A. Dobson, et al. (2011). "Effect of broad- and narrow-spectrum antimicrobials on Clostridium difficile and microbial diversity in a model of the distal colon." Proc Natl Acad Sci U S A **108 Suppl 1**: 4639-4644.

Reichardt, N., S. H. Duncan, et al. (2014). "Phylogenetic distribution of three pathways for propionate production within the human gut microbiota." ISME J **8**(6): 1352.

Rey, F. E., M. D. Gonzalez, et al. (2013). "Metabolic niche of a prominent sulfate-reducing human gut bacterium." Proc Natl Acad Sci U S A **110**(33): 13582-13587.

Sumbayev, V. V. (2008). "LPS-induced Toll-like receptor 4 signalling triggers cross-talk of apoptosis signal-regulating kinase 1 (ASK1) and HIF-1alpha protein." FEBS Lett **582**(2): 319-326.

Tauch, A., N. Bischoff, et al. (2004). "Comparative genomics identified two conserved DNA modules in a corynebacterial plasmid family present in clinical isolates of the opportunistic human pathogen Corynebacterium jeikeium." Plasmid **52**(2): 102-118.

Thongtang, N., M. R. Diffenderfer, et al. (2013). "Effects of atorvastatin on human C-reactive protein metabolism." Atherosclerosis **226**(2): 466-470.

Turnbaugh, P. J., F. Backhed, et al. (2008). "Diet-induced obesity is linked to marked but reversible alterations in the mouse distal gut microbiome." Cell Host Microbe **3**(4): 213-223.

Urich, T., A. Lanzen, et al. (2008). "Simultaneous assessment of soil microbial community structure and function through analysis of the meta-transcriptome." PLoS One **3**(6): e2527.

Waldron, J. and C. Webster (2011). "Liquid chromatography-tandem mass spectrometry method for the measurement of serum mevalonic acid: a novel marker of hydroxymethylglutaryl coenzyme A reductase inhibition by statins." <u>Ann Clin Biochem</u> **48**(Pt 3): 223-232.

Wall, R., T. M. Marques, et al. (2012). "Contrasting effects of Bifidobacterium breve NCIMB 702258 and Bifidobacterium breve DPC 6330 on the composition of murine brain fatty acids and gut microbiota." <u>Am J Clin Nutr</u> **95**(5): 1278-1287.

Walter, J. and R. Ley (2011). "The human gut microbiome: ecology and recent evolutionary changes." <u>Annu Rev Microbiol</u> **65**: 411-429.

Wilding, E. I., J. R. Brown, et al. (2000). "Identification, evolution, and essentiality of the mevalonate pathway for isopentenyl diphosphate biosynthesis in gram-positive cocci." <u>J Bacteriol</u> **182**(15): 4319-4327.

Yue, C., B. Ma, et al. (2012). "Lipopolysaccharide-induced bacterial translocation is intestine site-specific and associates with intestinal mucosal inflammation." <u>Inflammation</u> **35**(6): 1880-1888.

Zhao, Y., J. Wu, et al. (2013). "Gut microbiota composition modifies fecal metabolic profiles in mice." <u>J Proteome Res</u> **12**(6): 2987-2999.

Chapter 3

The effects of rosuvastatin on the murine host: inflammation, bile acids and antimicrobial peptides

Statins alter the community structure of the gastrointestinal microbiota

Nolan, J. A.[1,2], Skuse, P[3]., Govindarajan, K.[1,2], Patterson, E.[1,2,3] Konstantinidou, N.[2], Casey P. G.,[1] MacSharry, J.[1,2,4], Shanahan, F.[1], Stanton, C.[1,3], Hill, C.[1,2], Cotter, P.D. [1,3], Joyce, S. A.[1,2,4*], Gahan, C. G. M.[1,2,5*]

Abstract

Rosuvastatin (RSV) is a widely prescribed drug that is used for treating hypercholesterolemia. RSV acts by targeting the enzyme 3-hydroxy-3-methylglutaryl co enzyme A reductase (HMG-R) and blocking the formation of mevalonate (MVAL), a key intermediate in cholesterol biosynthesis. We have shown that HMG-R is essential for isoprenoid biosynthesis in a number of bacteria that inhabit the gut. Previously, we have demonstrated that treating mice with RSV can significantly alter the community structure of the gut microbiota. Treatment predominantly affected bacteria negative for HMG-R suggesting an indirect effect of RSV upon the microbiota. In this chapter we examined how RSV might affect microbe-host regulatory circuits that are known to impact upon microbiota composition. We show that RSV significantly affects hepatic and ileal gene expression of a number of inflammatory markers including *TNFα, IL-1β* and cellular adhesion molecules (*ICAM-1* and *Itgal*). qRT-PCR analysis revealed a significant increase in markers of antimicrobial activity in the gut (including *RegIIIγ, CAMP, iNOS2* and *MUC2*) that are likely to influence alterations in the gut microbiota. UPLC-MS analysis of bile acids revealed significant alterations in total and individual bile acids (including CA and CDCA), a finding that mirrored changes in the hepatic expression of genes encoding enzymes involved in bile acid synthesis (including *CYP27A1* and *CYP8B1*). RSV administration in germ free mice indicated the importance of the microbiota for host metabolomic processes. These findings in combination with those of Chapter 2 should prompt further investigation in humans.

Introduction

Statins (including Rosuvastatin (RSV)) are important drugs for the treatment of hypercholesterolemia (Johansen, Green *et al.* 2014). RSV is a potent inhibitor of 3-hydroxy-3-methylglutaryl co enzyme A reductase (HMG-R) activity (Istvan 2002). RSV has been reported as being amongst the most potent of the statins in terms of lowering serum LDL cholesterol and triglycerides (Vijan and Hayward 2004).

Statins have pleiotropic effects upon host metabolism in higher organisms (Liao and Laufs 2005). They lower markers of inflammation (Thongtang, Diffenderfer *et al*. 2013; Nenseter, Aukrust *et al*. 2014) and this activity may be relevant in lowering the risk of cardiovascular disease (Mora and Ridker 2006). Statins decrease production of pro-inflammatory cytokines in a variety of cell types (Ortego, Bustos *et al.* 1999; Rosenson, Tangney *et al*. 1999; Zhang, Osawa *et al*. 2013) and also display anti-oxidant effects through alterations in both reactive oxygen and reactive nitrogen species (Tokuhara, Habara *et al*. 2013; Song, Liu *et al*. 2014) (see Chapter 1).

These pleiotropic effects of statins upon host physiological processes and the reported antibacterial effects of these drugs (Jerwood and Cohen 2008) led us to evaluate the impact of statin treatment upon the gastrointestinal microbiota (see Chapter 2). We administered RSV to mice and demonstrated highly significant changes to the community structure of the microbiota in both the caecum and the faeces of these animals (as determined by V4 16s rRNA sequencing) relative to untreated controls. Analysis of microbial changes revealed significant reductions in physiologically relevant genera including *Roseburia* and *Akkermansia* species.

Microbial genera that were reduced in statin-treated mice were generally negative for HMG-R indicating that the activity of the statin on the microbial populations in the gut was indirect (see Chapter 2).

We hypothesised that off-target effects of RSV might influence physiological parameters in the host that are known to impact upon the composition of the microbiota. We therefore examined the impact of RSV treatment on bile acid synthesis and ileal and hepatic gene expression changes as a result of statin treatment. The data indicate that RSV reduces hepatic expression of genes associated with inflammation in the host, supporting recent studies that statins reduce markers of systemic inflammation (see Chapter 1). However we determined that specific inflammatory markers are increased in the ileum of RSV-treated mice and may correlate with the changes in the microbiota witnessed previously (see Chapter 2).

Bile acid synthesis has emerged as an example of a microbe-host regulated circuit that is known to directly influence microbial composition in the gut and in turn is influenced by the gut microbiota. In particular the effects of certain bile acids (such as cholic acid (CA)) have been shown in rodents to modulate the gut microbiota (Islam, Fukiya *et al.* 2011). That study showed that oral administration of cholic acid to rats significantly alters the composition of the gut microbiota promoting an increase in *Firmicutes* (in particular an outgrowth of specific *Clostridium* and *Erysipelotrichi* clusters) and an increase in *Proteobacteria* (in particular *E. coli*) (Islam, Fukiya *et al.* 2011). Research conducted by our group has also highlighted the importance of bile acids within wider implications for host lipid and cholesterol metabolism (and weight gain) in rodent models. In particular our laboratory analysed the activity of bile salt hydrolase (BSH) enzymes which form the basis of a specific microbe-host dialogue in the gut (Joyce, MacSharry *et al*.

2014). We hypothesized the profound potential for RSV to impact upon these microbe-host interactions (Chapter 2) leading to concomitant effects on the gut microbiota. However the precise structure of the microbiota underpinning this phenomenon needs to be investigated. Overall we demonstrate significant alterations in the microbiota of statin-treated mice which are coincident with alterations to host bile acid metabolism and gut inflammatory markers.

Materials and Methods

Quantitative RT-PCR (qRT-PCR) for target genes:

RNA was extracted from liver and ileum specimens using the RNAeasy Plus Universal Kit (Qiagen). Primers for RT-PCR were designed for targets (Table 1) using the Roche Probe Finder® v2.5 web based software and performed using the Roche Universal Probe Library for Mouse (Roche#04869877001). Complementary (cDNA) was synthesised by reverse transcription using Roche® reverse transcriptase enzyme (Roche) using the Applied Biosystems® Veriti 96-well thermal cycler under the following conditions (25ºC/10mins, 55ºC/30mins, 85ºC/5mins and held forever at 4ºC). qRT-PCR amplifications were performed on the Roche® LightCycler480 system in 384-well lightcycler480 plates (Roche) with the Roche 2X LG480 mastermix. Relative changes in gene expression were determined using the $2^{\Delta\Delta C}$ method (Livak and Schmittgen 2001) with beta-actin as the housekeeping or reference gene.

Genes	UPL Probe	Left primer sequence	Right primer sequence
Cyp3a	#12	tgaatatgaaacttgctctcactaaaa	ccttgtctgcttaatttcagaggt
Cyp7a1	#4	aagcaagcttggaactcactg	tttcttggtcttgaaaattacttcc
Cyp7b1	#1	tcatttgtagtgaatgtgcttttct	ggcagaacataaaaccatattagagg
Cyp8b1	#9	aactcaaccaggccatgc	gcacccagactcgaacctt
Cyp27a1	#66	cctcacctatgggatcttcatc	tttaaggcatccgtgtagagc
CYP46a1	#1	ccattgactttcaaccctgac	gtaagtgaaccgtggcttgg
Padi4	#1	aggccaagatgaacagagtga	aggccttccacatagaagtctg
NFκB	#3	cttatgaggccccgagcta	cccaaaactgcatttggaac
TNFα	#49	tcttctcattcctgcttgtgg	ggtctgggccatagaactga
CCL20	#73	aactgggtgaaaagggctgt	gtccaattccatcccaaaaa
TGF-β1	#4	caccatccatgacatgaacc	ccgcacacagcagttcttc
TLR2	#50	taggggcttcacttctctgc	ttctgaccggtgatgcaat
ICAM-1	#6	tggtagacagcatttaccctca	ggccaccatcctgttctg
Itgal	#78	ccccagacttttgctactgg	cgtgtgtccaggttgtagctc
Itgb2	#32	cccagtgtgagtgtcagtgc	tcccaatgtagccagactca
ROS	#2	ctctggagcaaaccactctgt	ggctgttgttgtaccaatcca
iNOS2	#3	ggagcctttagacctcaacaga	aaggtgagctgaacgaggag
Reg3γ	#89	ccccgtataaccatcaccat	ggcatctttcttggcaactt
MUC2	#12	gacgcctgtgacctctcaat	ggtgcttgaaagggtggtag
CAMP	#20	gccctttcggttcaagaaa	ccaatcttctccccaccttt
IL-1β	#38	agttgacggaccccaaaag	agctggatgctctcatcagg
IL-18	#46	caaaccttccaaatcacttcct	tccttgaagttgacgcaaga
IL-17A	#34	gattttcagcaaggaatgtgg	cattgtggagggcagacaat
ACTB	#106	ttgctgacaggatgcagaag	tgatcttgatcttcatggtgct

Table 1. Probe library primers for RSV intervention study target genes

Bile acid extraction

Bile acids were extracted from serum, liver and faecal samples using a previously outlined method (Swann, Want *et al.* 2011) with modifications (Joyce, MacSharry *et al*. 2014). 100μL of plasma was added to 50% ice-cold methanol (Sigma-Aldrich). The extract was thoroughly combined and centrifuged (6,000g/10mins at 4ºC). Extraction was performed with addition of 5% acetonitrile (Sigma-Aldrich), the resulting supernatant was dried under vacuum and reconstituted in 150μL ice-cold 50% methanol. Liver and faecal bile acids were similarly extracted by first homogenising the samples in 2ml screw cap tubes containing silica beads with the Roche MagnaLyser® and then subsequently adding acetonitrile.

Internal standards and chemicals

Standards for conjugated bile acids and non-conjugated bile acids were purchased from Sigma-Aldrich or Steraloids. Tetra-deuterated d_4-2,2,4,4 – cholic acid (D-2452) and d_4-2,2,4,4 –chenodeoxycholic acid (D-2772) were obtained from CDN isotopes Inc.® HPLC-grade methanol, acetonitrile, water, ammonium acetate, ammonium formate, ammonium hydroxide, formic acid and acetic acid were supplied by Fischer Scientific®. All bile acid standards were constituted as 1mg/ml solution. Stock solutions of individual bile acids were combined 50:50 in methanol/water and prepared to final concentration of 40μg/ml in a total volume of 1ml. Subsequent dilutions were performed to obtain a desired standard curve.

UPLC-MS analysis of murine bile acids

UPLC-MS was performed using a method outlined by (Swann, Want *et al.* 2011), with certain modifications. 5µL of extracted bile acids was injected onto a 50mm T3 Acquity column (Waters) and eluted using a 20min gradient of 100% mobile phase A to 100% mobile phase B. (A=0.1% formic acid in water, B=0.1% formic acid in methanol). The flow rate on the instrument was 400µL/min and column temperature (50ºC). Samples were analysed with the Acquity UPLC system (Waters) coupled online to an LCT Premier mass spectrometer (Waters) in negative electrospray mode with a scan range of 50-1,000 m/z. Bile acids strongly ionize in negative mode, resulting in a prominent [M-H] negative ion. Capillary voltage was 2.4kV, sample cone was 35V, desolvation temperature was 350ºC, source temperature was 120ºC and desolvation gas flow was 900L/hour. Principal component analysis (PCA) was performed using Markerlynx (Waters) by limiting elemental numbers (C, H, N and S) to detect individual analytes. A template of defined known molecular weight masses was applied to allow bile acid detection specifically. Each analyte was identified according to its mass and specific retention time (Table 2). Standard curves were performed   with known bile acids and each bile acid analyte was quantified thusly, normalisation was determined using deuterated internal standards (Appendix to Chapter 3). This work was carried out by collaboration within our own lab (SAJ).

Analyte	Negative ion mass	RT (min 25 m^{-1})	Chemical formula
Taurine	124.0068	0.75	$C_{24}H_7NO_3S$
Cholic acid	407.2797	11.76	$C_{24}H_{40}O_5$
Chenodeoxycholic acid	391.2848	17.63	$C_{24}H_{40}O_4$
Lithocholic acid	375.2855	21.72	$C_{24}H_{40}O_3$
Deoxycholic acid	391.2848	18.86	$C_{24}H_{40}O_4$
Dehydrocholic acid	401.239	1.71	$C_{24}H_{34}O_5$
Ursodeoxycholic acid	391.2848	9.04	$C_{24}H_{40}O_4$
Hyodeoxycholic acid	391.2848	10.04	$C_{24}H_{40}O_4$
α-muricholic acid	407.2898	5.5	$C_{24}H_{40}O_5$
β-muricholic acid	407.2898	6.44	$C_{24}H_{40}O_5$
ω-muricholic acid	407.2898	5.86	$C_{24}H_{40}O_5$
Taurocholic acid	515.2838	4.95	$C_{26}H_{45}NO_7S$
Taurochenodeoxycholic acid	498.2889	8.64	$C_{26}H_{44}NO_6S$
Taurolithocholic acid	482.294	14.74	$C_{26}H_{45}NO_5S$
Taurodeoxycholic acid	498.2889	3.54	$C_{26}H_{44}NNaO$
Tauroursodeoxycholic acid	498.2889	8.64	$C_{26}H_{44}NO_6S$
Taurohyodeoxycholic acid	498.2889	3.49	$C_{26}H_{43}NO_5$
Tauroα-muricholic acid	514.2838	1.79	$C_{26}H_{45}NO_7S$
Tauroβ-muricholic acid	514.2838	1.69	$C_{26}H_{45}NO_7S$
Tauroω-muricholic acid	514.2838	1.89	$C_{26}H_{45}NO_7S$
D4 cholic acid	411.3053	11.97	$C_{24}D_4H_{36}O_5$
D4 chenodeoxycholic acid	427.6565	17.82	$C_{24}D_4H_{36}O_4$
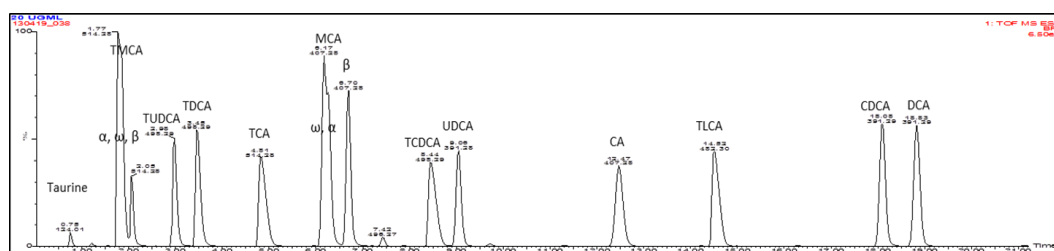
Table 2. UPLC bile acid analysis for RSV intervention study

MSD cytokine analysis:

Meso Scale Discovery (MSD)® (10 spot MULTI-SPOT plates®) multi-plex cytokine assay (Cat# N05048A-1 – Proinflammatory Panel 1 (mouse)) platform was used to determine the effect of RSV in liver and plasma cytokines for the RSV intervention study (as well as complementary Germ Free animal study). Protein expression of pro-inflammatory cytokines (including IL-1β and TNFα) was determined in control statin treated mice. MSD utilises 96-well plate precoated with capture antibodies with independent well-defined spots in each well per cytokine. Plasma and liver are added as a solution containing detection antibodies conjugated to chemiluminescent labels (MSD SULFO-TAGS®). Plasma samples can be directly added to MSD. Liver extractions were performed as follows: 100mg liver tissue placed into 2ml (Magna Lyser®) tubes containing prefilled ceramic beads (Roche#03358941001) with 1ml of homogenization solution added (50ml PBS+10% Foetal Bovine Serum+2 Protease Cocktail Inhibitor Tablets (Sigma-Aldrich S8830)). Tubes were subjected to 5X rounds of 6,000rpm/30s shakes (MagnaLyser). Subsequently, tubes were centrifuged at 10,000g for 10mins at 4ºC with supernatant aspirated off into fresh tubes. The MSD instruction manual, manufacturer guidelines and supplied reagents were used for cytokine analysis. Analytes in each sample bind capture antibodies and are immobilised onto the working electrode surface completing the (SULFO TAG-Analyte-Capture Antibody-Working Electrode) sandwich. MSD read buffer is added to each well creating the appropriate chemical environment for electrochemiluminescence when appropriate voltage is applied to the electrodes causing the emission of light. MSD platform measures light intensity and quantifies based on a standard curve for each cytokine (Appendix to Chapter 3).

Germ Free (GF) statin trial:

Neonatal Swiss Webster (SW) mice were delivered from adult female mice by caesarean section under completely sterile conditions and housed in a germ free incubation unit under ethical approval sought through the Alimentary Pharmabiotic Centre, University College Cork. Mice were reared post-caesarean in gnotobiotic units and fed by artificial lactation with sterile artificial milk substitutes for up to 21 days. Subsequently, mice were weaned and switched onto a sterile solid chow diet and given sterile water *ad libitum* (Yi and Li 2012). Mice were allowed to reach adulthood (8-12 weeks) prior to commencing statin intervention. GF mice (n=7) were administered (62.6mg/L) rosuvastatin *ad libitum* in the drinking water (GF+RSV) (Famer and Crisby 2007) for 19 days, with control mice (GF) (n=5) just receiving sterile water. The GF trial was conducted in a similar manner to the convention C57BL/6 statin trial (as described above). At regular intervals during the entire time course of trial the weight was recorded for each individual mouse. At the end of the trial, mice were humanely sacrificed and biological samples were collected for analysis. Segments of the liver and ileum were harvested for qRT-PCR gene expression analysis (as described above) and stored in RNAlater (Ambion). Serum plasma, liver, faecal pellets and the gall bladder were harvested for UPLC-MS bile acid analysis (as described above). Faecal and ileum samples were taken in order to determine if any microbial colonization had occurred. Indeed, weekly throughout the trial faecal pellets were taken and examined for microbial content throughout the trial. This GF model will enable us to determine if physiological alterations in conventional C57BL/6 mice were due to a host response or a microbiota response to RSV.

.

Statistical analysis

Data for all variables were normally distributed by the standard deviation from the mean values in most cases. Statistical significance was determined as a p-value less than 0.05 inclusive of technical and biological replicates.

RESULTS

Oral RSV modulates gut defensins and local and systemic cytokines in C57Bl/6J mice:

Microbiological analysis indicated an indirect effect of RSV upon the microbiota (Chapter 2). Such an indirect effect could be mediated through host physiological processes. To assess this possibility qRT-PCR was utilised to determine gene expression changes in RSV treated animals and we investigated host systems which are known to impact upon gut microbial community structure including inflammation (Everard, Belzer *et al*. 2013) mucin production (Bergstrom, Kristensen *et al*. 2012; Sommer, Adam *et al*. 2014), production of nitric oxide synthase (NOS) (Qiao, Sun *et al*. 2013) and defensin production (Mukherjee, Vaishnava *et al*. 2008; Ostaff, Stange *et al*. 2013). The data indicated a general reduction in expression of genes encoding systemic inflammatory markers in statin-treated animals (including *TNFα, CCL20, IL-1β,IL-18, NF-κB*) (Fig.1A). Levels of TNFα and IL-1β proteins were significantly reduced in the plasma and liver respectively as measured by the mesoscale discovery (MSD) assay (Fig.1C). A reduction in hepatic expression of genes encoding cellular adhesion molecules (*ICAM-1* and *Itgal*) were also determined (Fig. 1A). In contrast, expression of genes encoding inflammatory markers (including *TNFα, CCL20, IL-1β, IL-18, TGF-β1, IL-17A*) and adhesion molecules (*ICAM-1* and *Itgal*) were increased locally in the ileum of statin-treated animals (Fig. 1B). The genes encoding the antimicrobial peptides *RegIIIγ* and *CAMP* were significantly increased in the ileum in statin-treated animals (Fig. 1B). Transcription of the genes encoding inducible nitric oxide synthase (*iNOS2*), and the common mucosal mucin (*MUC2*) were also significantly elevated in statin-treated animals (Fig. 1B). In all cases, relative changes in gene expression are indicated

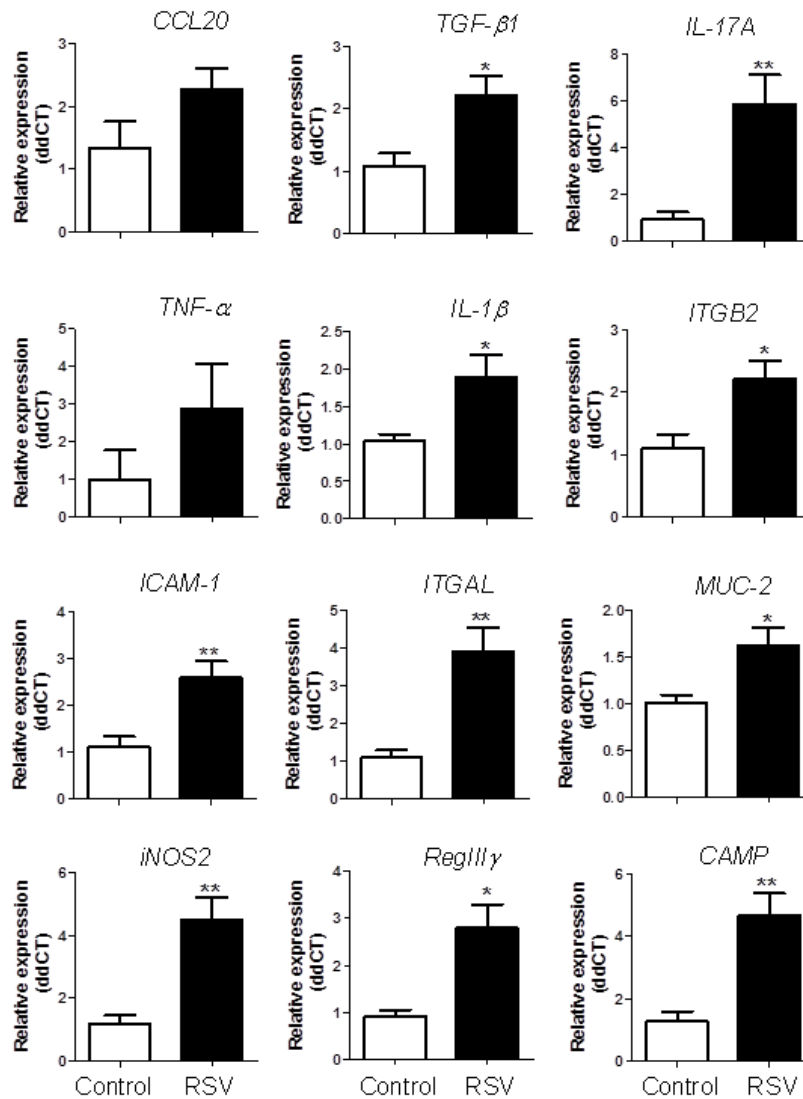using beta-actin as reference gene. Data is presented as means +/- SEM; *P<0.05, **P<0.01, ***P<0.005.

LIVER:
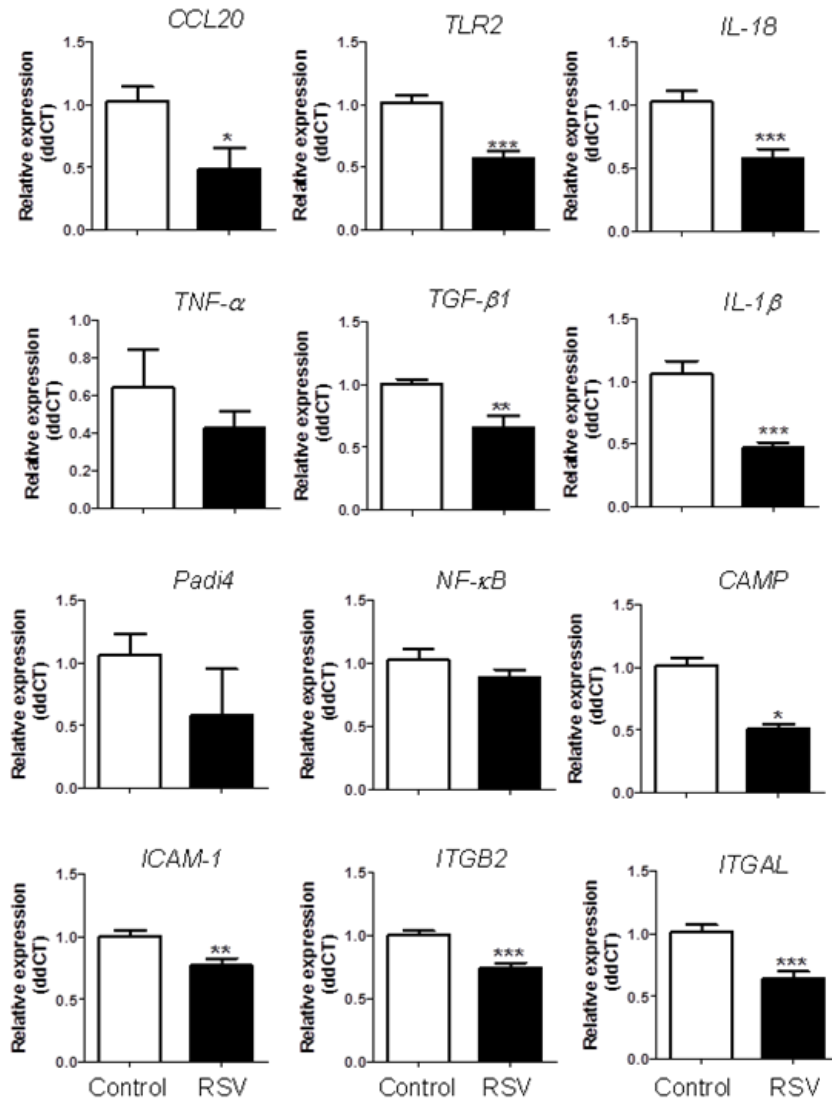
Fig. 1A. Gene expression profiles of selected genes in the liver of control mice or mice administered RSV.

qRT-PCR amplifications were performed on a Roche Lightcycler480 system using appropriate primers. Data is presented as means +/- SEM; *P<0.05, **P<0.01, ***P<0.005.
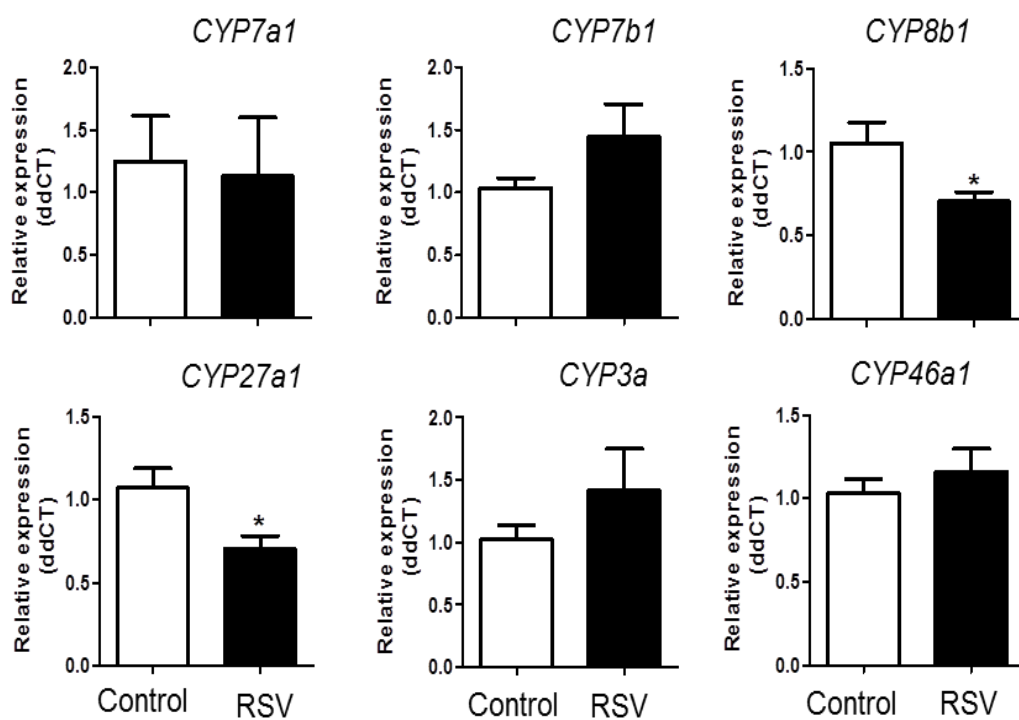
ILEUM:

Fig.1B. Gene expression profiles of selected genes in the terminal ileum of control mice or mice administered RSV.

qRT-PCR amplifications were performed on a Roche Lightcycler480 system using appropriate primers. Data is presented as means +/- SEM; *P<0.05, **P<0.01
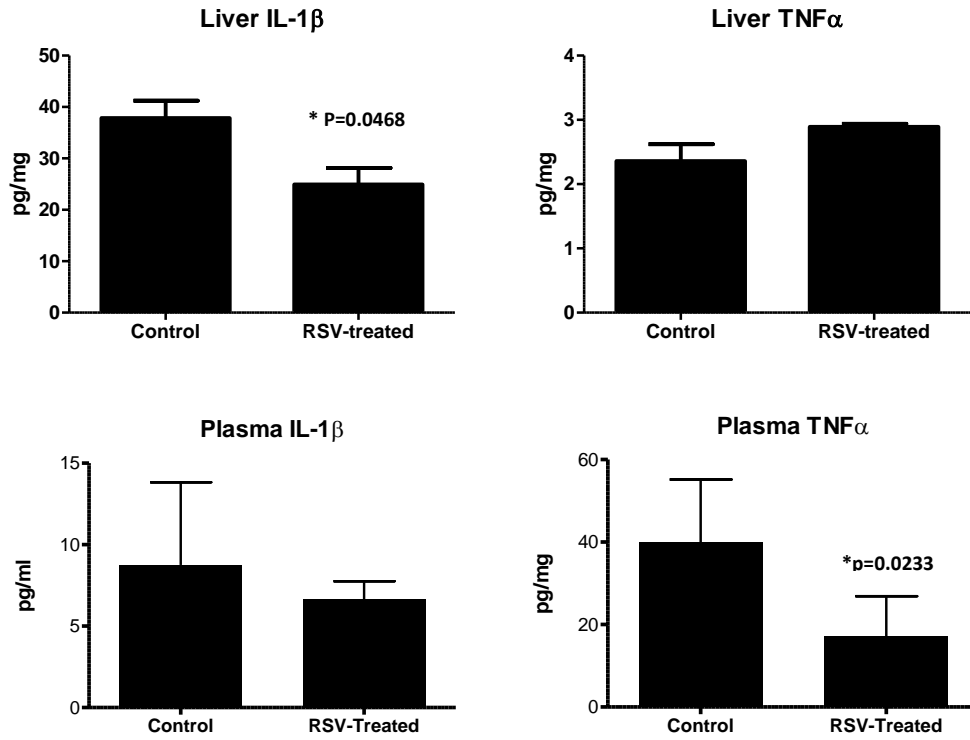
Fig. 1C. MSD analysis of hepatic and plasma cytokine levels.

MSD assays were carried out according to the manufacturer's instructions (Meso Scale Discovery, Rockville, MD). Data are indicated as means +/- SD from the mean. P values (*P<0.05) indicate significance relative to control mice.

RSV modulates changes in bile acid levels in mice

Bile acids (BAs) are formed through pathways downstream of cholesterol biosynthesis in the liver and released as components of bile into the duodenum (Begley, Gahan *et al.* 2005). BAs can alter the microbial content of the gut through impacts upon individual microorganisms and ratios of various BAs in the gut are likely to influence microbiota composition (Islam, Fukiya *et al*. 2011; Yokota, Fukiya *et al*. 2012; Joyce, MacSharry *et al.* 2014). In our model RSV significantly reduced the hepatic expression of *Cyp8b1* and *Cyp27a1* genes which encode enzymes regulating the rate of conversion of 7α-hydroxycholesterol to cholic acid (CA) (*Cyp8b1*) or chenodeoxycholic acid (CDCA) (*Cyp27a1*) (Fig.2A). We utilised a UPLC-MS approach to determine the precise levels of individual BAs (see Table 2) and examined the effects of RSV upon individual BA ratios in murine faeces (Fig. 2 B, C), liver (Fig. 2 D, E) and plasma (Fig 3 A, B). PCA analysis demonstrated significant shifts in BA profiles in the faeces and plasma following long-term statin administration (Fig 4). In particular, RSV led to a significant reduction in faecal and hepatic levels of CA and CDCA which agrees with gene expression analysis (Fig. 2 B, C, D, E).

LIVER:

Fig.2 A. Gene expression profiles of hepatic genes encoding key enzymes in the biosynthesis of BAs in control mice or mice administered RSV.

qRT-PCR amplifications performed on a Roche Lightcycler480 system using appropriate primers. Relative changes in gene expression are indicated using beta-actin as reference gene. Data presented as means +/- SEM; *P < 0.05.
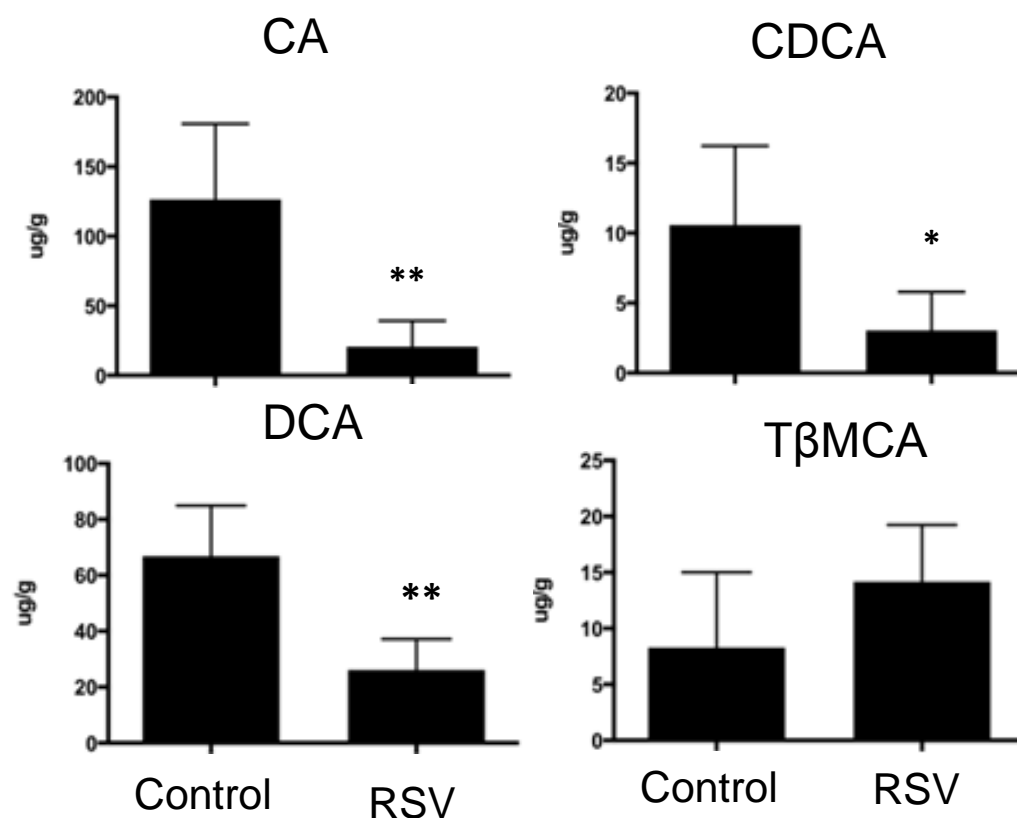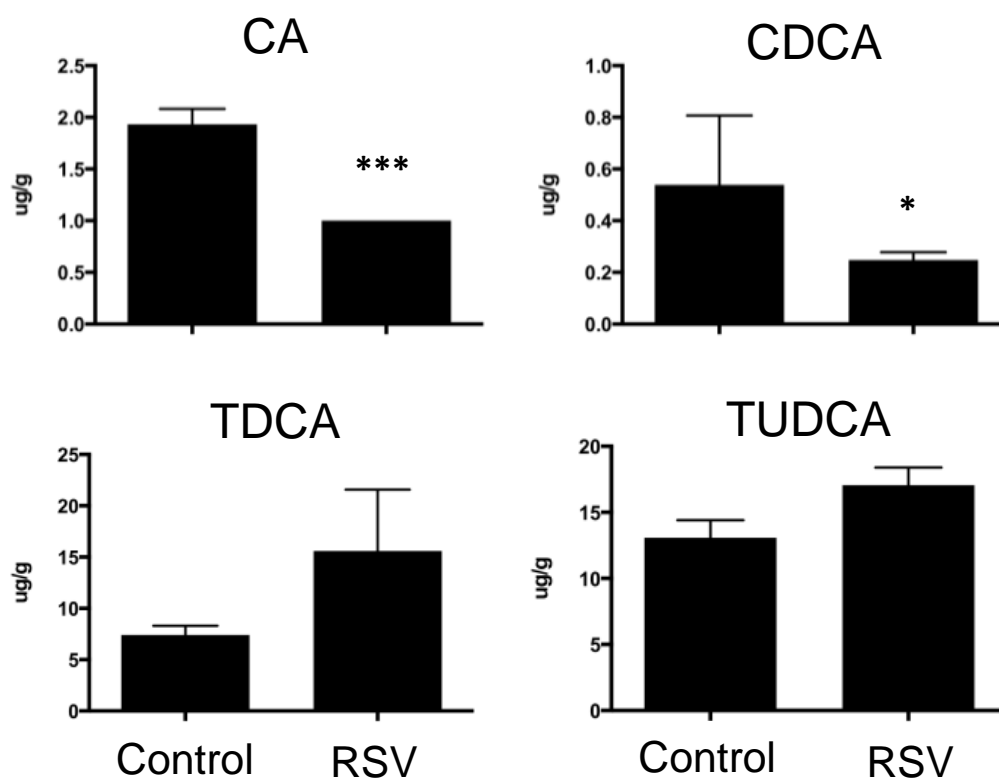
.

FAECES:
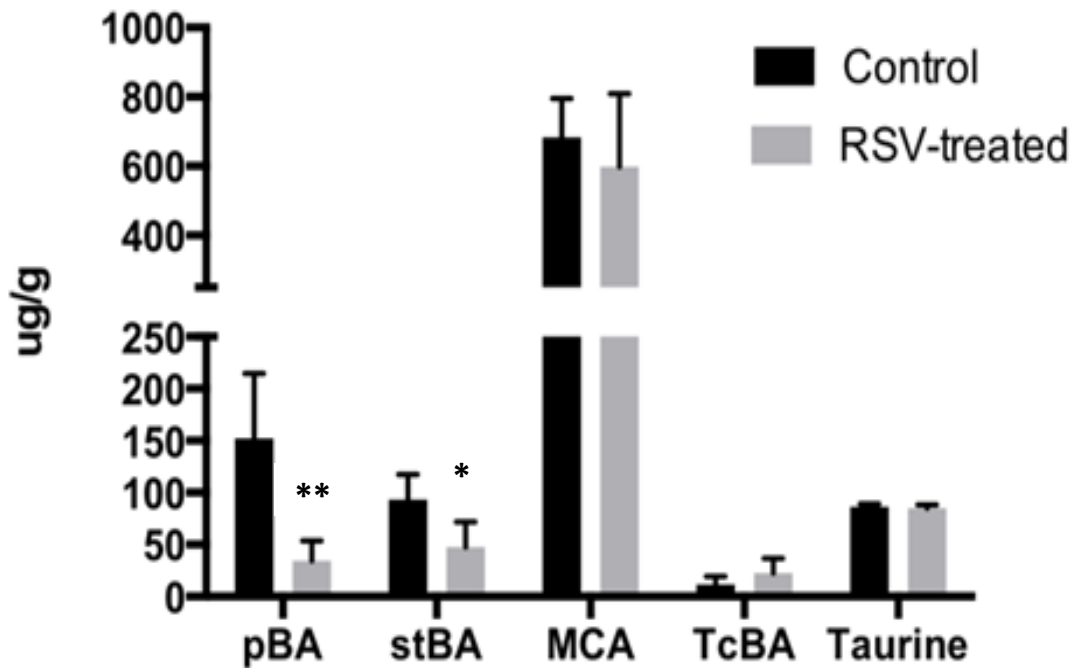
Fig. 2 B. UPLC-MS analysis of specific BAs in the faeces of control and RSV-treated mice.

Figure represents a summary of specific BA groups including primary BAs (pBA), secondary and tertiary BAs (stBA), muricholic acids (MCA), tauro-conjugated BAs (TcBA) and free taurine. Data are indicated as means +/- SD from the mean; *P < 0.05, **P < 0.005.
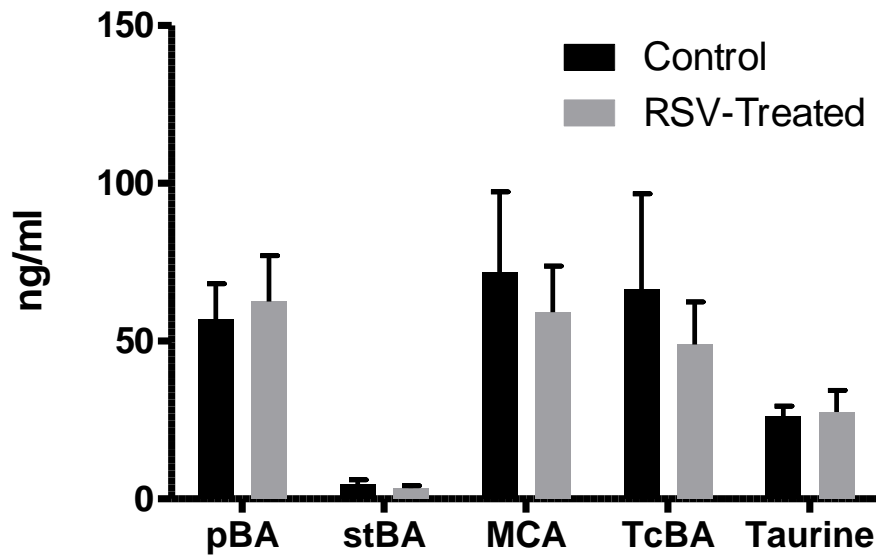
FAECES:

Fig. 2 C. Precise levels of selected BAs in faeces of control and RSV-treated mice.

Individual graphs indicate levels of Cholic acid (CA), Chenodeoxycholic acid (CDCA), Deoxycholic acid (DCA) and tauro-beta-Muricholic acid (TβMCA). Data are indicated as means +/- SD from the mean; *P < 0.05, **P < 0.005.

LIVER:
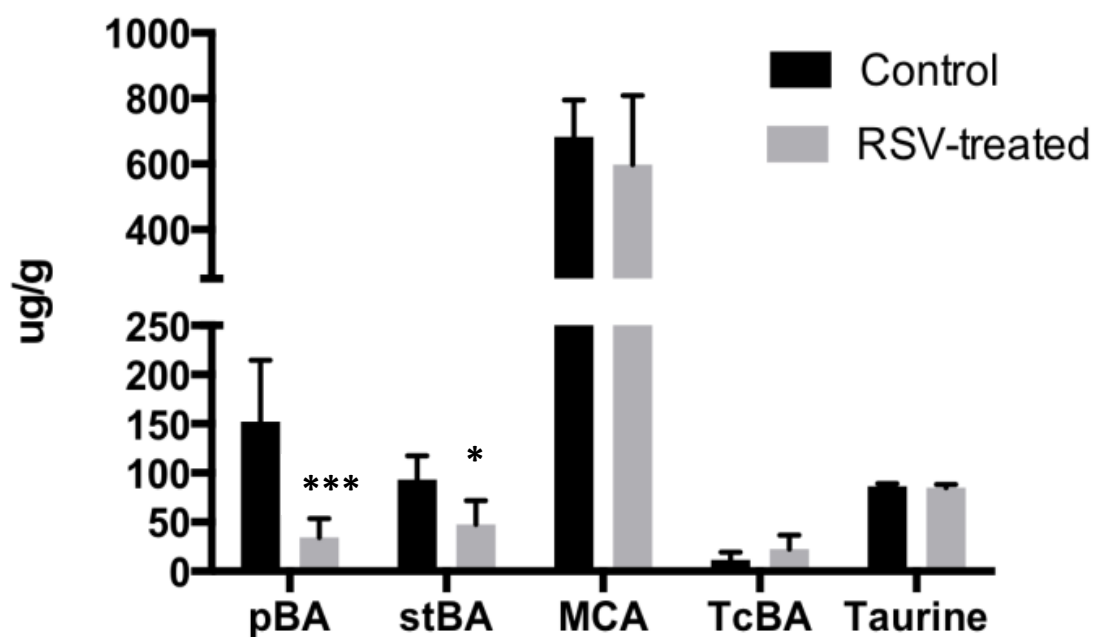
Fig. 2 D. UPLC-MS analysis of specific BAs in the livers of control and RSV-treated mice.

Figure represents a summary of specific BA groups including primary BAs (pBA), secondary and tertiary BAs (stBA), muricholic acids (MCA), tauro-conjugated BAs (TcBA) and free taurine. Data are indicated as means +/- SD from the mean; *P < 0.05, ***P < 0.0001.

LIVER:

Fig. 2 E. Precise levels of selected BAs in livers of control and RSV-treated mice.

Individual graphs indicate levels of Cholic acid (CA), Chenodeoxycholic acid (CDCA), taurodeoxycholic acid (TDCA) and tauro-urso-deoxycholic acid (TUDCA). Data are indicated as means +/- SD from the mean; *P < 0.05, ***P< 0.0001.

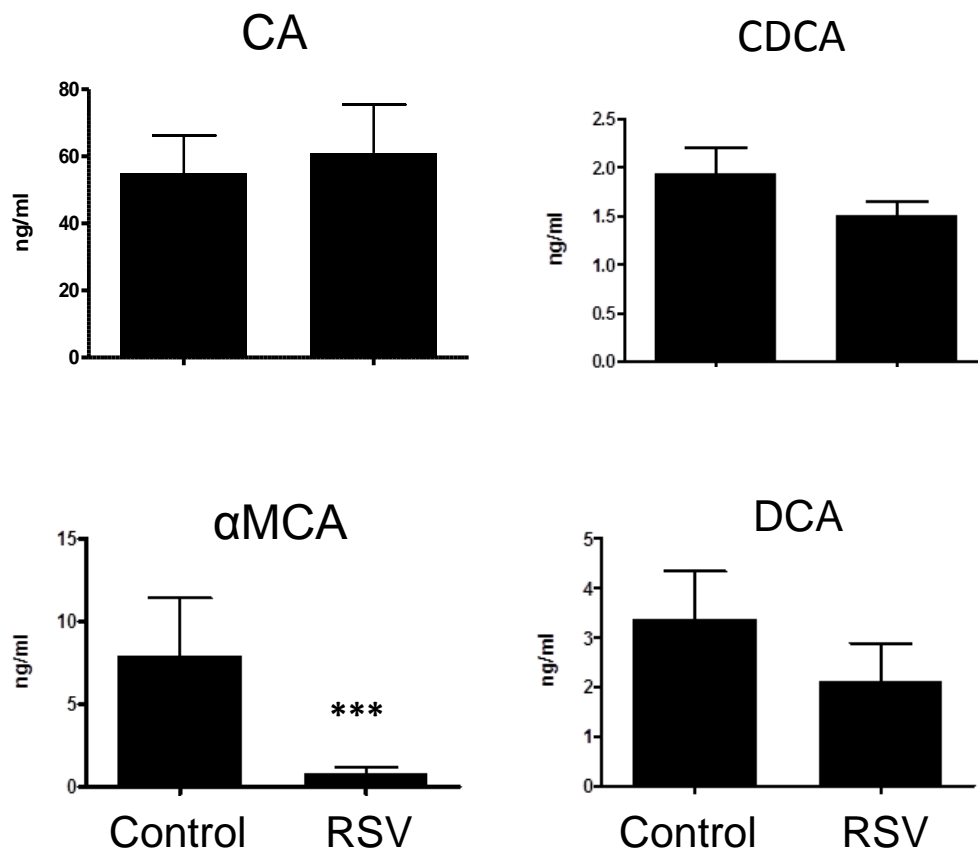**PLASMA:**

Fig. 3 A. UPLC-MS analysis of specific BAs in the plasma of control and RSV-treated mice.

Figure represents a summary of specific BA groups including primary BAs (pBA), secondary and tertiary BAs (stBA), muricholic acids (MCA), tauro-conjugated BAs (TcBA) and free taurine. Data are indicated as means +/- SD from the mean; *P < 0.05, ***P < 0.0001.
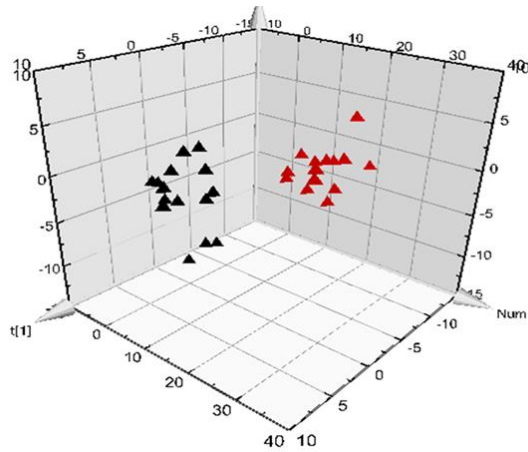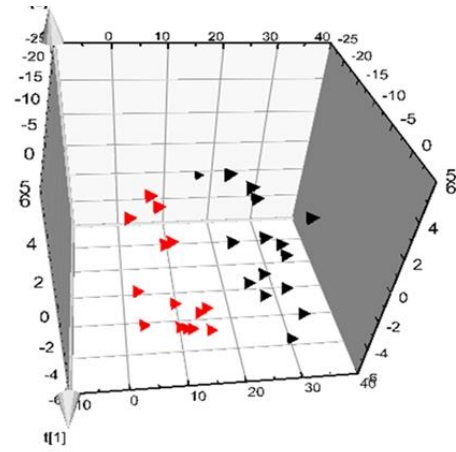
Fig. 3 B. Precise levels of selected BAs in plasma of control and RSV-treated mice.

Individual graphs indicate levels of Cholic acid (CA), Chenodeoxycholic acid (CDCA), alpha-muricholic acid (αMCA) and deoxycholic acid (DCA). Data are indicated as means +/- SD from the mean; *P < 0.05, ***P< 0.0001.
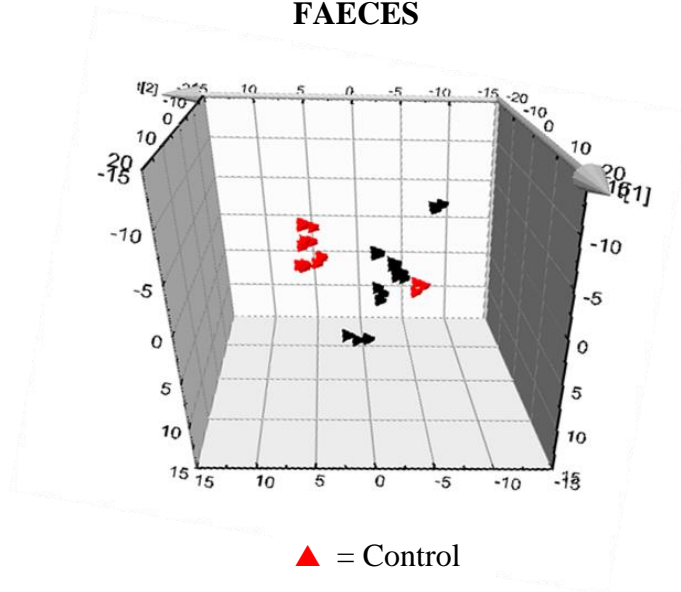
LIVER

PLASMA

FAECES

▲ = Control

▲ = RSV

Fig. 4. Principle Co-ordinates analysis (PCA) revealed significant shifts in liver and plasma BA profiles following long-term RSV administration of C57BL/6 mice.

PCA analysis of total BA profiles in C57BL/6 mice demonstrated a significant profile shift in the liver and plasma comparing control and RSV-treated mice. Faecal BA profiles were not as significantly altered following treatment.

No significant differences were detected from the analysis of a number of individual faecal bile acids: lithocholic acid (LCA), taurolithocholic acid (TLCA), taurodeoxycholic acid (TDCA), tauroursodeoxycholic acid (TUDCA), α-muricholic acid (αMCA), tauro-α-muricholic acid (TαMCA), β-muricholic acid (βMCA), tauro-β-muricholic acid (TβMCA), ω-muricholic acid (ωMCA), tauro-ω-muricholic acid (TωMCA) or taurochenodeoxycholic acid (TCDCA), (Appendix to Chapter 3).
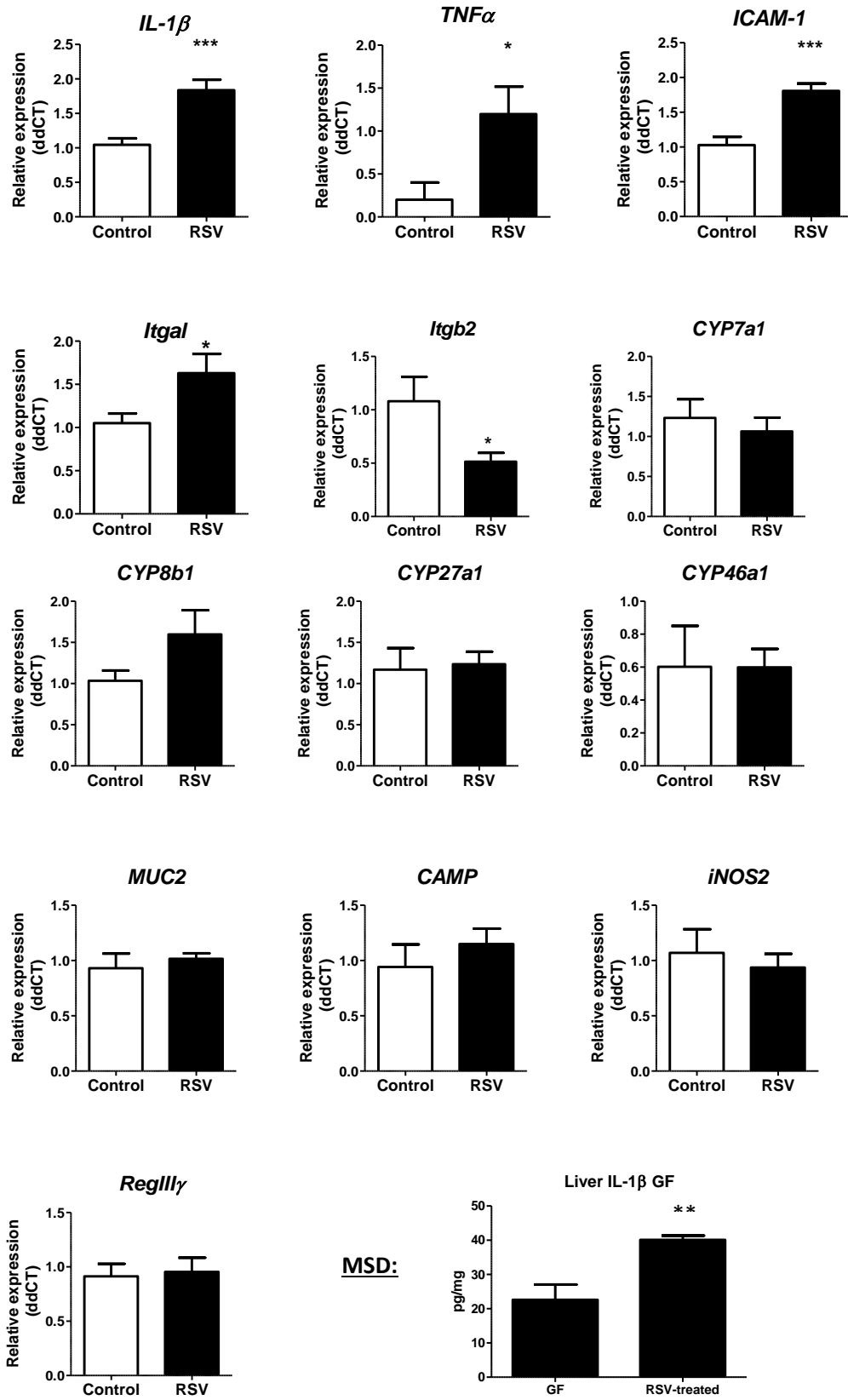
No significant differences were detected in a number of individual hepatic bile acids; deoxycholic acid (DCA), taurocholic acid (TCA), ursodeoxycholic acid (UDCA), taurochenodeoxycholic acid (TCDCA), tauro-conjugated muricholic acid (TcMCA), α-muricholic acid (αMCA) and ω-muricholic acid (ωMCA), (Appendix to Chapter 3). Lithocholic acid (LCA) was not detectable in the liver.

RSV did not significantly affect the precise levels of a number of plasma bile acids: deoxycholic acid (DCA), taurocholic acid (TCA), ursodeoxycholic acid (UDCA), taurodeoxycholic acid, (TDCA), taurochenodeoxycholic acid (TCDCA), tauro-conjugated muricholic acid (TcMCA), β-muricholic acid (βMCA) and ω-muricholic acid (ωMCA) (Appendix to Chapter 3). Lithocholic acid (LCA) or taurolithocholic acid (TLCA) were not detected in the plasma of mice.

Oral RSV modulation in germ-free (GF) mice:

Further to the C57BL/6 murine RSV administration study described in this chapter, a similar study was performed in germ free control and RSV-treated animals (see Materials and Methods). RSV significantly increased expression of inflammatory markers in the liver (*IL-1β, TNFα, ICAM-1* and *Itgal*) and ileum (*Itgb2*) of statin treated animals (Fig 5). Levels of IL-1β protein were significantly increased in the liver of GF animals as determined by MSD (Fig.5). RSV did not modulate genes involved in hepatic BA synthesis (*CYP7a1, CYP7b1, CYP8b1, CYP27a1* and *CYP46a1*) in germ free animals (Fig. 5). Genes encoding antimicrobial peptides (*RegIIIγ* and *CAMP*), inducible nitric oxide synthase (*iNOS2*) and the common mucosal mucin gene (*MUC2*) were not affected in the ileum of germ free animals (Fig.5).

GF LIVER AND ILEUM:

IL-1β

TNFα

ICAM-1

Itgal

Itgb2

CYP7a1

CYP8b1

CYP27a1

CYP46a1

MUC2

CAMP

iNOS2

RegIIIγ



MSD:

Liver IL-1β GF

134

Fig. 5. Host gene expression analysis of RSV upon hepatic and gastrointestinal inflammatory markers, bile acid and antimicrobial genes in GF mice.

Gene expression profiles of selected genes in the liver (*IL-1β, TNFα, ICAM-1, Itgal, CYP7a1, CYP8b1, CYP27a1, CYP46a1*) and ileum (*Itgb2, MUC2, CAMP, RegIIIγ*) of control mice or mice administered RSV. qRT-PCR amplifications performed on a Roche Lightcycler480 system using appropriate primers. Relative changes in gene expression are indicated using beta-actin as reference gene. In all cases data are presented as means +/- SEM; *P < 0.05, **P < 0.01, ***P < 0.005.

RSV did not affect hepatic, circulating, bilary or faecal primary bile acids synthesis in GF mice:

Gene expression analysis of GF control and RSV-treated mice revealed no signifcant effect for genes (*CYP7a1, CYP7b1, CYP8b1, CYP27a1* and *CYP46a1*) involved in hepatic BA synthesis (Fig. 5). This was confirmed by UPLC-MS analysis of individual primary BA's (CA and CDCA) as well for MCA (Fig. 6) and for total primary (pBA), tauroconjugated (TcBA) and secondary (stBA) BA's (Fig. 7).
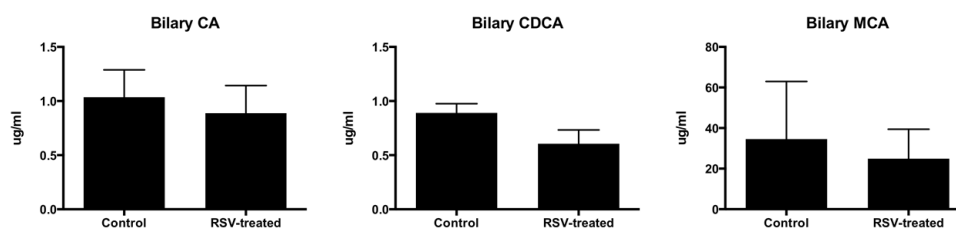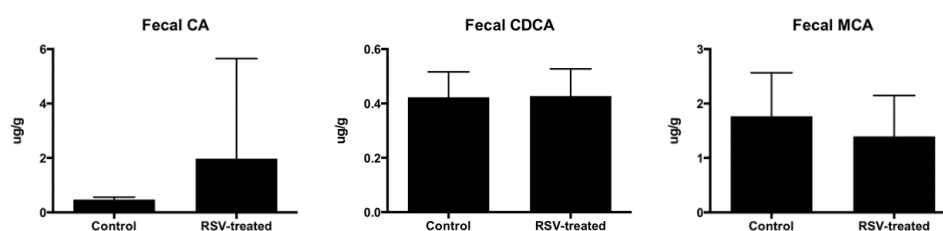
LIVER:
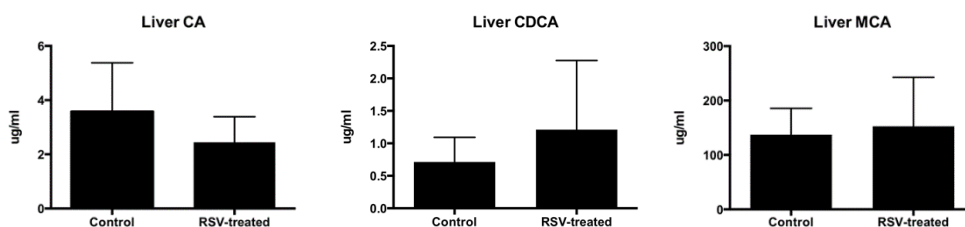
PLASMA:
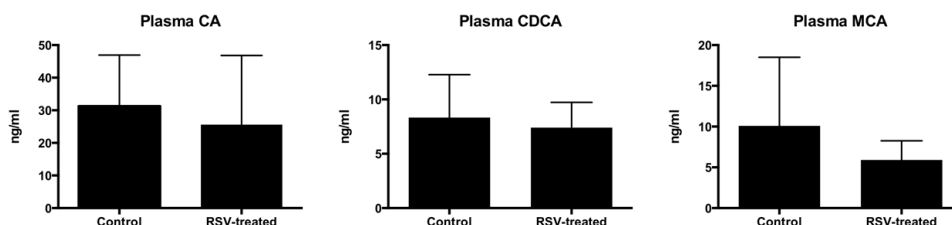
GALL BLADDER:

FAECES:

Fig.6. **Precise levels of selected BAs in liver, plasma, gall bladder and faeces of control and RSV-treated GF mice.**

Individual graphs indicate levels of Cholic acid (CA), Chenodeoxycholic acid (CDCA), muricholic acid (MCA) in GF liver, plasma, gall bladder and faeces. RSV had no effect on indicated BA's. Data are indicated as means +/- SD from the mean; *P < 0.05.

RSV did not affect total primary, secondary and tauroconjugated BA's in GF mice:

GF mice were unaffected by RSV for individual synthesis of BA's (CA, CDCA and

MCA) (Fig.6). UPLC-MS analysis of total primary (pBA), secondary (stBA) and

tauroconjugated (TcBA) confirmed this result in liver, plasma, gall bladder and faces

of GF mice (Fig.7).

136
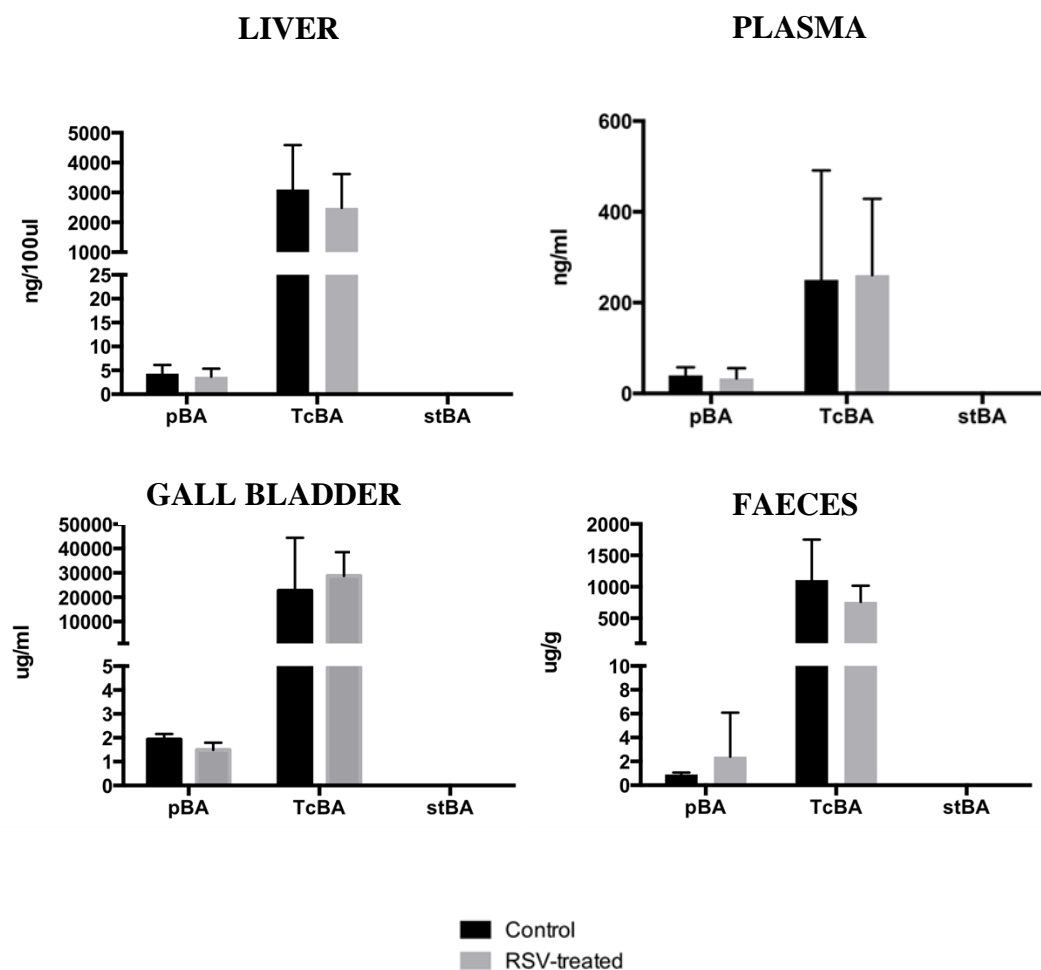
Fig. 7. UPLC-MS analysis of total primary, secondary and tauroconjugated BA's in control and RSV-treated GF mice.

Graphs indicate levels of total primary (pBA), secondary (stBA) and tauroconjugated (TcBA) BA's in control and RSV-treated GF mice (liver, plasma, gall bladder and faeces). RSV had no effect on indicated BA's. Data are indicated as means +/- SD from the mean with a value for *P < 0.05 denoting significance.

RSV did not affect synthesis of a number of other individual BA's:

UPLC-MS analysis of hepatic, circulating, biliary and faecal BA's including

tauroconjugated muricholic acid (TcMCA), taurocholic acid (TCA),

taurochenodeoxycholic acid (TCDCA) or free taurine determined no effect of RSV

in GF mice (Appendix to Chapter 3).

RSV did not modulate bile acid profiles in GF mice:

Individual UPLC-MS (BA) analysis revealed no significant effect of RSV on the primary BA's (CA and CDCA) and MCA (Fig. 6) as well for total primary, secondary and tauroconjugated BA's (Fig.7) and a number of other BA's (Appendix to Chapter 3). This finding was confirmed by PCA analysis for total hepatic, circulating, biliary and faecal BA signatures in control and RSV-treated GF mice (Fig. 8). This was confirmed by UPLC-MS analysis of individual BA's.

LIVER   **PLASMA**

GALL BLADDER   **FAECES**

▲ = Control

▲ = RSV
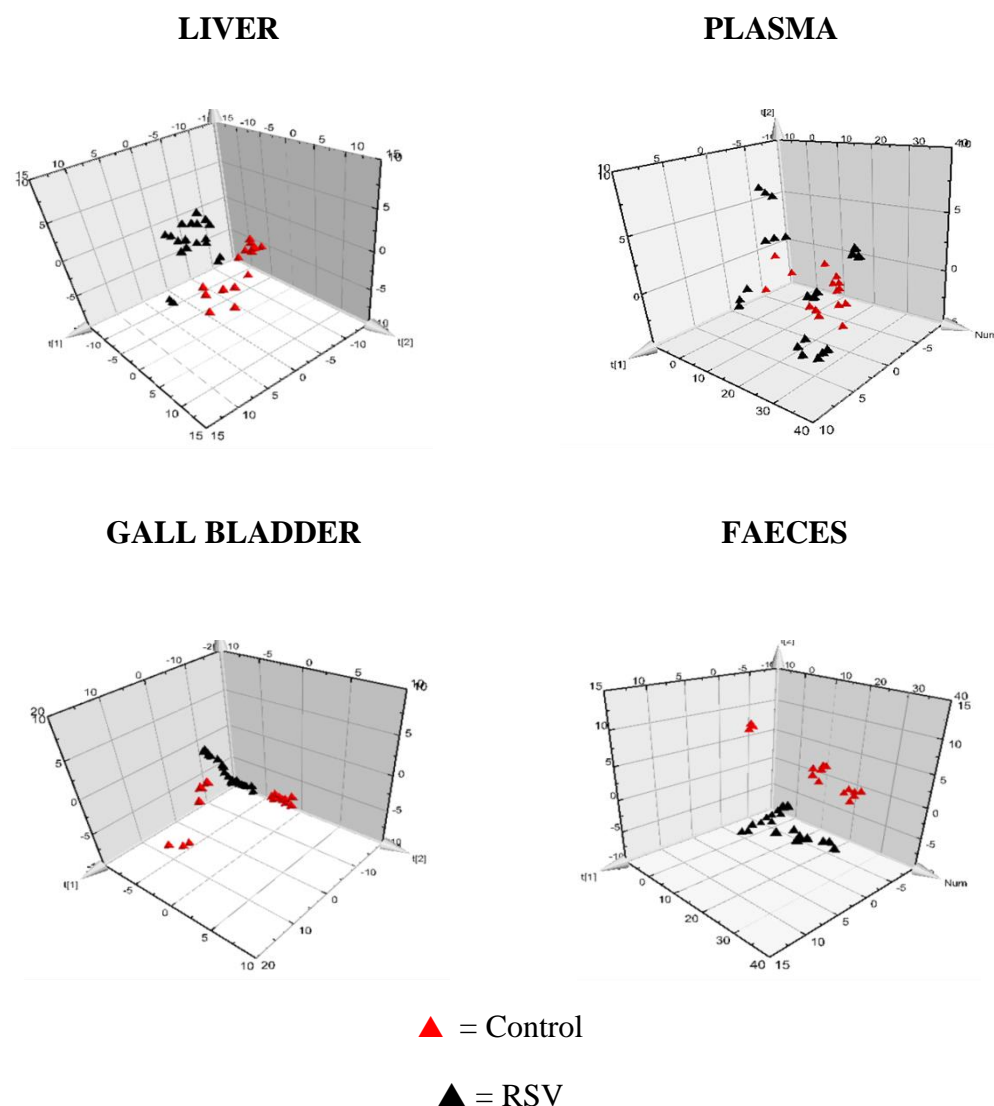
Fig. 8. Principle Component Analysis (PCA) of hepatic, circulating, bilial and faecal BA profiles of control and RSV-treated GF mice.UPLC-MS determined no significant shift in BA signatures (liver, plasma, gall bladder and faeces) in GF mice.

Discussion

In addition to lowering systemic cholesterol levels in mammals, statins have been shown to affect markers of inflammation (Nenseter, Aukrust *et al.* 2014) and the efficacy of statins is influenced by bile acid profiles (as a marker of microbiota composition and activity) (Kaddurah-Daouk, Baillie *et al.* 2011). Indeed RSV has been shown to be secreted into the gastrointestinal tract of patients via the biliary route after initial treatment (Bergman, Forsell *et al.* 2006). As these physiological processes may influence microbiota composition we examined these parameters in our model. We show that markers of inflammation (hepatic expression of genes encoding *TNFα, CCL20, IL-1β*, *TLR2* and *IL-18*) were reduced following RSV treatment. Indeed it has been similarly reported that RSV in rodents reduced cytokine mediated (for example TNFα) inflammation following liver trauma and sepsis (Awad and El Sharif 2010).

Contrastingly we observed a significant increase in the gene expression of both proinflammatory cytokines (such as *IL-1β* and *IL-17A*) combined with an increase in cellular adhesion molecules (such as *ICAM-1*, *Itgal* and *Itgb2*) as well as powerful anti-inflammatory mediators of inflammation (*TGF-β, iNOS2*) in the ileum of RSV treated C57BL/6 mice. We propose whilst statins generally have anti-inflammatory effects in the intestine (Bereswill, Munoz *et al.* 2010), it is likely that observed pro-inflammatory increases in our model are masked by the effects of TGF-β and other such anti-inflammatory agents such as nitric oxide (NO). TGF-β is a strong anti-inflammatory cytokine which is a major up regulator of mucosal T_{reg} cells (with potent immune suppression activity) in murine colitis models and is essential in maintaining inflammatory homeostasis (Ruemmele and Garnier-

Lengline 2013). We observed a significant increase in the expression of this cytokine in our statin model. Similarly, increased nitric oxide release (NO) attributed to statin exposure in other murine models has been shown to promote anti-inflammatory activity in atherosclerotic cases (Momi, Monopoli *et al*. 2012). We determined a significant increase in the mucosal expression of *iNOS2* in our statin model. With respect to other studies that show the anti-inflammatory effects of statins in the intestines (in particular artificially induced colitis models) (Naito, Katada *et al*. 2006), we accept that statins generally exhibit beneficial effects with regard to inflammation, however these effects were only shown in extreme (disease state) cases where cytokine levels (in particular serum TNFα) were artificially elevated (Jahovic, Gedik *et al.* 2006). Further studies should be prompted in models which examine statins in non-inflamed as well as non-induced cases further examining immune homeostasis.

Importantly, we demonstrate a significant increase in the expression of genes encoding antimicrobial peptides (*RegIIIγ* and *CAMP*) which have known functions in regulating the local composition of the microbiota (Vaishnava, Yamamoto *et al*. 2011; Wan, van der Does *et al*. 2014) (see Chapter 1 and 2 also). RegIIIγ and CAMP respectively mediate the gut microbiota by directly inhibiting bacterial cell wall synthesis (Cash, Whitham *et al*. 2006) and normal functioning of the cell membrane (Thennarasu, Tan *et al*. 2010). Interestingly other groups have shown the induction of mucosal cathelicidin by statin (simvastatin) treatment (Bubeck Wardenburg, Patel *et al*. 2007; Chow, von Kockritz-Blickwede *et al*. 2010). Also *in vitro* models the anti-microbial activity of neutrophils is also enhanced following statin exposure (mevastatin) (Chow, von Kockritz-Blickwede *et al*. 2010). We noted significant increase in local expression of *iNOS2* and the mucin gene (*MUC2*), factors which

are likely to impact locally upon the composition of the microbiota (Jager, Stange *et al.* 2010). Interestingly there is evidence that expression of antimicrobial peptides (such CAMP) can be influenced within the gastrointestinal tract by the presence of bile acids such as chenodeoxycholic acid (CDCA) and ursodeoxycholic acid (UDCA) via concomitant interactions with nuclear hormone receptors in human biliary epithelium (D'Aldebert, Biyeyeme Bi Mve *et al.* 2009).

It has previously been shown that oral administration of cholic acid (CA) to rats significantly alters the composition of the gut microbiota promoting an increase in *Firmicutes* (in particular an outgrowth of specific *Clostridia* and *Erysipelotrichi* clusters) and an increase in *Proteobacteria* (in particular *E. coli*) (Islam, Fukiya *et al.* 2011; Yokota, Fukiya *et al.* 2012). In our study RSV administration in mice reduced expression of *Cyp8b1* and *Cyp27a1* in the liver and reduced overall levels of hepatic and faecal CA and CDCA. We note a concomitant effect on the microbiota which is broadly the opposite to that seen in CA-treated animals (Islam, Fukiya *et al.* 2011), notably a decrease in specific *Firmicutes* groups including specific *Clostridial* clusters (*Roseburia* species) and *Erysipelotrichaceae* and a decrease in the *Proteobacteria* (see Chapter 2).

In our study we therefore show that RSV treatment resulted in a reduction in the synthesis of primary bile acids (including CA) which correlates with alterations to the microbiota that may reflect these changes. Whilst inflammation and BA profiles are known to exert a powerful influence upon the microbiota we recognise that other physiological parameters (including regulation of local cholesterol levels (Martinez, Wallace *et al.* 2009; Martinez, Perdicaro *et al.* 2013) may also potentially influence the structure of the gut microbial community in our model.

We wished to examine whether some of the off-target effects of RSV are mediated directly in the host or are dependent upon specific host-microbe interactions in the gut. We therefore administered a sterile RSV formulation orally to germ free mice and measured selected physiological parameters in these animals. We noted an increase in the local expression of hepatic inflammatory markers (*IL-1β, TNFα, ICAM-1* and *Itgal*) and subsequently confirmed this by MSD protein analysis. This contrasted with an observed decrease in the expression of these same inflammatory markers in our conventional mouse model. Interestingly, hepatic expression of the intracellular adhesion molecule (*ICAM-1*) has been shown to be only constitutively expressed in the presence of a functional enteric microflora (Komatsu, Berg *et al*. 2000). *ICAM-1* expression is also strongly up regulated in the presence of other pro-inflammatory cytokines (in particular *IL-1β*) (Henninger, Panes *et al.* 1997) which we observed in our study. Similarly gut defensins including RegIIIγ are known to be influenced by the gut microbiota are generally poorly expressed in germ free animals (Vaishnava, Yamamoto *et al*. 2011; Natividad, Hayes *et al*. 2013; Joyce, MacSharry *et al*. 2014) and in our study we saw no effect of statins on these parameters in the absence of gut bacteria. We conclude that statins affect these parameters only in the presence of the gut microbiota through affecting the interplay between host and microbe with direct consequences for the community structure of the microbiota.

RSV had no effect on the local hepatic expression of bile acid regulatory genes (*CYP7a1, CYP7b1, CYP8b1, CYP27a1* or *CYP46a1*) in our GF murine model. This observation correlated with UPLC-MS analysis of individual (CA and CDCA) and total (primary and tauroconjugated) bile acids in the liver, plasma, gall bladder and faeces between control and RSV-treated animals. This is unsurprising as the gut

microbiota in human and murine models is well described as essential for bile acid metabolism (Narushima, Itoh *et al*. 1999; Bhowmik, An *et al*. 2012).

Overall we show that RSV significantly influences the community structure of the gut microbiota most likely by altering the subtle interplay between microbe and host leading to changes in local gene expression and bile acid profiles that feedback further upon the microbiota. Microbial symbiosis in the gut is characterized by significant microbe-host and host-microbe feedback systems that influence both entities. For instance, whilst RegIIIγ plays a major role in moderating the mucosal microbiota (Vaishnava, Yamamoto *et al*. 2011) direct alterations to gut microbiota composition can alter the expression of RegIIIγ (Delzenne, Neyrinck et al. 2011; Swann, Want *et al.* 2011). Similarly bile acid synthesis in the host both influences and is influenced by the microbiota (Islam, Fukiya *et al*. 2011; Devkota, Wang *et al.* 2012; Yokota, Fukiya *et al*. 2012).

In the current study we demonstrate that statins significantly alter the gut microbiota in mice with attendant alterations to bile acid profiles and local gene expression profiles. Whilst we see no alterations in local SCFA production in our model (Chapter 2) the overall health implications of our findings are unclear and should prompt further studies in humans.

References

Awad, A. S. and A. El Sharif (2010). "Immunomodulatory effects of rosuvastatin on hepatic ischemia/reperfusion induced injury." Immunopharmacol Immunotoxicol **32**(4): 555-561.

Begley, M., C. G. Gahan, et al. (2005). "The interaction between bacteria and bile." FEMS Microbiol Rev **29**(4): 625-651.

Bereswill, S., M. Munoz, et al. (2010). "Anti-inflammatory effects of resveratrol, curcumin and simvastatin in acute small intestinal inflammation." PLoS One **5**(12): e15099.

Bergman, E., P. Forsell, et al. (2006). "Biliary secretion of rosuvastatin and bile acids in humans during the absorption phase." Eur J Pharm Sci **29**(3-4): 205-214.

Bergstrom, A., M. B. Kristensen, et al. (2012). "Nature of bacterial colonization influences transcription of mucin genes in mice during the first week of life." BMC Res Notes **5**: 402.

Bhowmik, S. K., J. H. An, et al. (2012). "Alteration of bile acid metabolism in pseudo germ-free rats [corrected]." Arch Pharm Res **35**(11): 1969-1977.

Bubeck Wardenburg, J., R. J. Patel, et al. (2007). "Surface proteins and exotoxins are required for the pathogenesis of Staphylococcus aureus pneumonia." Infect Immun **75**(2): 1040-1044.

Cash, H. L., C. V. Whitham, et al. (2006). "Symbiotic bacteria direct expression of an intestinal bactericidal lectin." Science **313**(5790): 1126-1130.

Chow, O. A., M. von Kockritz-Blickwede, et al. (2010). "Statins enhance formation of phagocyte extracellular traps." Cell Host Microbe **8**(5): 445-454.

D'Aldebert, E., M. J. Biyeyeme Bi Mve, et al. (2009). "Bile salts control the antimicrobial peptide cathelicidin through nuclear receptors in the human biliary epithelium." Gastroenterology **136**(4): 1435-1443.

Delzenne, N. M., A. M. Neyrinck, et al. (2011). "Targeting gut microbiota in obesity: effects of prebiotics and probiotics." Nat Rev Endocrinol **7**(11): 639-646.

Devkota, S., Y. Wang, et al. (2012). "Dietary-fat-induced taurocholic acid promotes pathobiont expansion and colitis in Il10-/- mice." Nature **487**(7405): 104-108.

Everard, A., C. Belzer, et al. (2013). "Cross-talk between Akkermansia muciniphila and intestinal epithelium controls diet-induced obesity." Proc Natl Acad Sci U S A **110**(22): 9066-9071.

Famer, D. and M. Crisby (2007). "Rosuvastatin reduces gliosis and the accelerated weight gain observed in WT and ApoE-/- mice exposed to a high cholesterol diet." Neurosci Lett **419**(1): 68-73.

Henninger, D. D., J. Panes, et al. (1997). "Cytokine-induced VCAM-1 and ICAM-1 expression in different organs of the mouse." J Immunol **158**(4): 1825-1832.

Islam, K. B., S. Fukiya, et al. (2011). "Bile acid is a host factor that regulates the composition of the cecal microbiota in rats." Gastroenterology **141**(5): 1773-1781.

Istvan, E. S. (2002). "Structural mechanism for statin inhibition of 3-hydroxy-3-methylglutaryl coenzyme A reductase." Am Heart J **144**(6 Suppl): S27-32.

Jager, S., E. F. Stange, et al. (2010). "Antimicrobial peptides in gastrointestinal inflammation." Int J Inflam **2010**: 910283.

Jahovic, N., N. Gedik, et al. (2006). "Effects of statins on experimental colitis in normocholesterolemic rats." Scand J Gastroenterol **41**(8): 954-962.

Jerwood, S. and J. Cohen (2008). "Unexpected antimicrobial effect of statins." J Antimicrob Chemother **61**(2): 362-364.

Johansen, M. E., L. A. Green, et al. (2014). "Cardiovascular risk and statin use in the United States." Ann Fam Med **12**(3): 215-223.

Joyce, S. A., J. MacSharry, et al. (2014). "Regulation of host weight gain and lipid metabolism by bacterial bile acid modification in the gut." Proc Natl Acad Sci U S A **111**(20): 7421-7426.

Kaddurah-Daouk, R., R. A. Baillie, et al. (2011). "Enteric microbiome metabolites correlate with response to simvastatin treatment." PLoS One **6**(10): e25482.

Komatsu, S., R. D. Berg, et al. (2000). "Enteric microflora contribute to constitutive ICAM-1 expression on vascular endothelial cells." Am J Physiol Gastrointest Liver Physiol **279**(1): G186-191.

Liao, J. K. and U. Laufs (2005). "Pleiotropic effects of statins." Annu Rev Pharmacol Toxicol **45**: 89-118.

Livak, K. J. and T. D. Schmittgen (2001). "Analysis of relative gene expression data using real-time quantitative PCR and the 2(-Delta Delta C(T)) Method." Methods **25**(4): 402-408.

Martinez, I., D. J. Perdicaro, et al. (2013). "Diet-induced alterations of host cholesterol metabolism are likely to affect the gut microbiota composition in hamsters." Appl Environ Microbiol **79**(2): 516-524.

Martinez, I., G. Wallace, et al. (2009). "Diet-induced metabolic improvements in a hamster model of hypercholesterolemia are strongly linked to alterations of the gut microbiota." Appl Environ Microbiol **75**(12): 4175-4184.

Momi, S., A. Monopoli, et al. (2012). "Nitric oxide enhances the anti-inflammatory and anti-atherogenic activity of atorvastatin in a mouse model of accelerated atherosclerosis." Cardiovasc Res **94**(3): 428-438.

Mora, S. and P. M. Ridker (2006). "Justification for the Use of Statins in Primary Prevention: An Intervention Trial Evaluating Rosuvastatin (JUPITER)--Can C-Reactive Protein Be Used to Target Statin Therapy in Primary Prevention?" The American Journal of Cardiology **97**(2, Supplement 1): 33-41.

Mukherjee, S., S. Vaishnava, et al. (2008). "Multi-layered regulation of intestinal antimicrobial defense." Cell Mol Life Sci **65**(19): 3019-3027.

Naito, Y., K. Katada, et al. (2006). "Rosuvastatin, a new HMG-CoA reductase inhibitor, reduces the colonic inflammatory response in dextran sulfate sodium-induced colitis in mice." Int J Mol Med **17**(6): 997-1004.

Narushima, S., K. Itoh, et al. (1999). "Absence of cecal secondary bile acids in gnotobiotic mice associated with two human intestinal bacteria with the ability to dehydroxylate bile acids in vitro." Microbiol Immunol **43**(9): 893-897.

Natividad, J. M., C. L. Hayes, et al. (2013). "Differential induction of antimicrobial REGIII by the intestinal microbiota and Bifidobacterium breve NCC2950." Appl Environ Microbiol **79**(24): 7745-7754.

Nenseter, M. S., P. Aukrust, et al. (2014). "Low level of inflammatory marker in hyperhomocysteinemic patients on statin therapy." Scand J Clin Lab Invest **74**(1): 1-7.

Ortego, M., C. Bustos, et al. (1999). "Atorvastatin reduces NF-kappaB activation and chemokine expression in vascular smooth muscle cells and mononuclear cells." Atherosclerosis **147**(2): 253-261.

Ostaff, M. J., E. F. Stange, et al. (2013). "Antimicrobial peptides and gut microbiota in homeostasis and pathology." EMBO Mol Med **5**(10): 1465-1483.

Qiao, Y., J. Sun, et al. (2013). "Alterations of the gut microbiota in high-fat diet mice is strongly linked to oxidative stress." Appl Microbiol Biotechnol **97**(4): 1689-1697.

Rosenson, R. S., C. C. Tangney, et al. (1999). "Inhibition of proinflammatory cytokine production by pravastatin." Lancet **353**(9157): 983-984.

Ruemmele, F. M. and H. Garnier-Lengline (2013). "Transforming growth factor and intestinal inflammation: the role of nutrition." Nestle Nutr Inst Workshop Ser **77**: 91-98.

Sommer, F., N. Adam, et al. (2014). "Altered mucus glycosylation in core 1 O-glycan-deficient mice affects microbiota composition and intestinal architecture." PLoS One **9**(1): e85254.

Song, X., B. C. Liu, et al. (2014). "Lovastatin inhibits human B lymphoma cell proliferation by reducing intracellular ROS and TRPC6 expression." <u>Biochim Biophys Acta</u> **1843**(5): 894-901.

Swann, J. R., E. J. Want, et al. (2011). "Systemic gut microbial modulation of bile acid metabolism in host tissue compartments." <u>Proc Natl Acad Sci U S A</u> **108 Suppl 1**: 4523-4530.

Thennarasu, S., A. Tan, et al. (2010). "Antimicrobial and membrane disrupting activities of a peptide derived from the human cathelicidin antimicrobial peptide LL37." <u>Biophys J</u> **98**(2): 248-257.

Thongtang, N., M. R. Diffenderfer, et al. (2013). "Effects of atorvastatin on human C-reactive protein metabolism." <u>Atherosclerosis</u> **226**(2): 466-470.

Tokuhara, K., K. Habara, et al. (2013). "Fluvastatin inhibits the induction of inducible nitric oxide synthase, an inflammatory biomarker, in hepatocytes." <u>Hepatol Res</u> **43**(7): 775-784.

Vaishnava, S., M. Yamamoto, et al. (2011). "The antibacterial lectin RegIIIgamma promotes the spatial segregation of microbiota and host in the intestine." <u>Science</u> **334**(6053): 255-258.

Vijan, S. and R. A. Hayward (2004). "Pharmacologic lipid-lowering therapy in type 2 diabetes mellitus: background paper for the American College of Physicians." <u>Ann Intern Med</u> **140**(8): 650-658.

Wan, M., A. M. van der Does, et al. (2014). "Antimicrobial peptide LL-37 promotes bacterial phagocytosis by human macrophages." <u>J Leukoc Biol</u> **95**(6): 971-981.

Yi, P. and L. Li (2012). "The germfree murine animal: an important animal model for research on the relationship between gut microbiota and the host." <u>Vet Microbiol</u> **157**(1-2): 1-7.

Yokota, A., S. Fukiya, et al. (2012). "Is bile acid a determinant of the gut microbiota on a high-fat diet?" <u>Gut Microbes</u> **3**(5): 455-459.

Zhang, J., S. Osawa, et al. (2013). "Statins directly suppress cytokine production in murine intraepithelial lymphocytes." <u>Cytokine</u> **61**(2): 540-545.

Chapter 4

HMG-CoA synthase (*mvaS*) involved in isoprenoid biosynthesis is non- essential for the normal growth of *Listeria monocytogenes* EGDe

Abstract

HMG-CoA synthase is the second enzyme of the "classical" mevalonate pathway for isoprenoid biosynthesis in *Listeria monocytogenes* EGDe that catalyses the formation of HMG-CoA. Isoprenoids are essential organic molecules that help to form major cellular structures (cell wall and cell membrane) of bacteria and are involved in important metabolic activities of the cell. *L. monocytogenes* is a unique micro-organism as it also possesses an alternative biosynthetic pathway for isoprenoid biosynthesis namely the MEP (methylerythritol 4-phosphate) pathway. Previously, it has been shown that deleting the third enzyme (HMG-CoA reductase) of the mevalonate pathway in *L. monocytogenes* EGDe, results in a mutant that is dependent upon the addition of mevalonate for normal growth. However, in the current study deletion of the gene for HMG-CoA synthase (*mvaS*) did not affect growth in complex and defined media compared to the wild type or significantly impair virulence of the mutant in cell culture or in a murine model. Deletion of this gene did not significantly predispose the cells to antibiotic or cell wall stresses compared to the wild type. The HMG-Co reductase inhibitor Rosuvastatin did not significantly impair growth of the knockout mutant. Overall this work demonstrates that HMG-CoA synthase is not essential in *L. monocytogenes* and suggests the existence of other enzymes that may support this isoprenoid biosynthetic pathway.

Introduction

HMG-CoA synthase (*mvaS*) (lmo1415) is the second enzyme reaction in the mevalonate-dependent isoprenoid biosynthetic pathway that catalyses the conversion of acetoacetyl-CoA to 3-hydroxy-3-methylglutaryl CoA (HMG-CoA). Isoprenoids are a large family of compounds synthesised by many living organisms on the planet. These terpenoids are essential to the growth and survival of many organisms by being integral cellular components such as the cell wall and cell membrane (bactoprenol and hopanoids), electron transport chain (ubiquinone and menaquinone), and components of the photosynthetic pathway (chlorophyll, bacteriophyll, rhodopsins and catenoids) (Rodríguez-Concepción and Boronat 2013). In the majority of the bacterial kingdom, the common isoprenoid building blocks are formed via the MEP (methylerythritol 4-phosphate) pathway. This pathway is absent in the archaeal kingdom as well as in higher eukaryotes such as fungi and humans. In this case, the isoprenoid precursors are generated by a different pathway, the mevalonate pathway, which is biochemically distinct from the MEP pathway (Perez-Gil and Rodriguez-Concepcion 2013) & (Rodríguez-Concepción and Boronat 2013). Bacteria are unique in that some utilise either pathway and the foodborne pathogen *L. monocytogenes,* has been found to contain a complete sets of enzymes of both pathways in the genome (Fig. 1) (Begley, Gahan *et al*. 2004). *Listeria innocua* a non-pathogenic close relative of *L. monocytogenes* was found to be lack the genes *gcpE* and *lytB* of the MEP pathway but contains a full set of genes for the mevalonate pathway (Begley, Bron *et al.* 2008).

L. monocytogenes is a gram positive bacterium that is the cause of listeriosis in patients in particular those that have a suppressed immune system. *L. monocytogenes* is a non-sporeforming facultative anaerobic rod. It is capable of

growing at temperatures between -0.4ºC - 50ºC. The bacterium is catalase positive/oxidase negative and expresses a β-hemolysin on blood agar. It has been associated with the contamination of ready to eat foods including meat and dairy products. Upon infection, *L. monocytogenes* is able to cause meningtitis, septicaemia and even abortion in pregnant females (Farber and Peterkin 1991).

Previous work in our lab has shown that the rate limiting enzyme HMG-Co A reductase (*hmgR*) is essential for growth and survival of *L. monocytogenes* EGDe (Heuston, Begley *et al*. 2012). However it was unclear whether the entire pathway is essential for viability in this organism. Therefore the splicing by overlap extension (SOE) PCR technique (Leenhouts, Venema *et al*. 1998) was used to generate a precise deletion mutant in another gene in this pathway (*mvaS*) in *L. monocytogenes* EGDe. This mutant allowed us to examine if the enzyme HMG-CoA synthase (*mvaS*) is essential in *L. monocytogenes* EGDe for growth and virulence and permitted comparison with mutants in the mevalonate pathway, (*hmgR* (lmo0825)) or MEP pathway (*gcpE* (lmo1441) and *lytB* (lmo1451)) that have been generated previously.
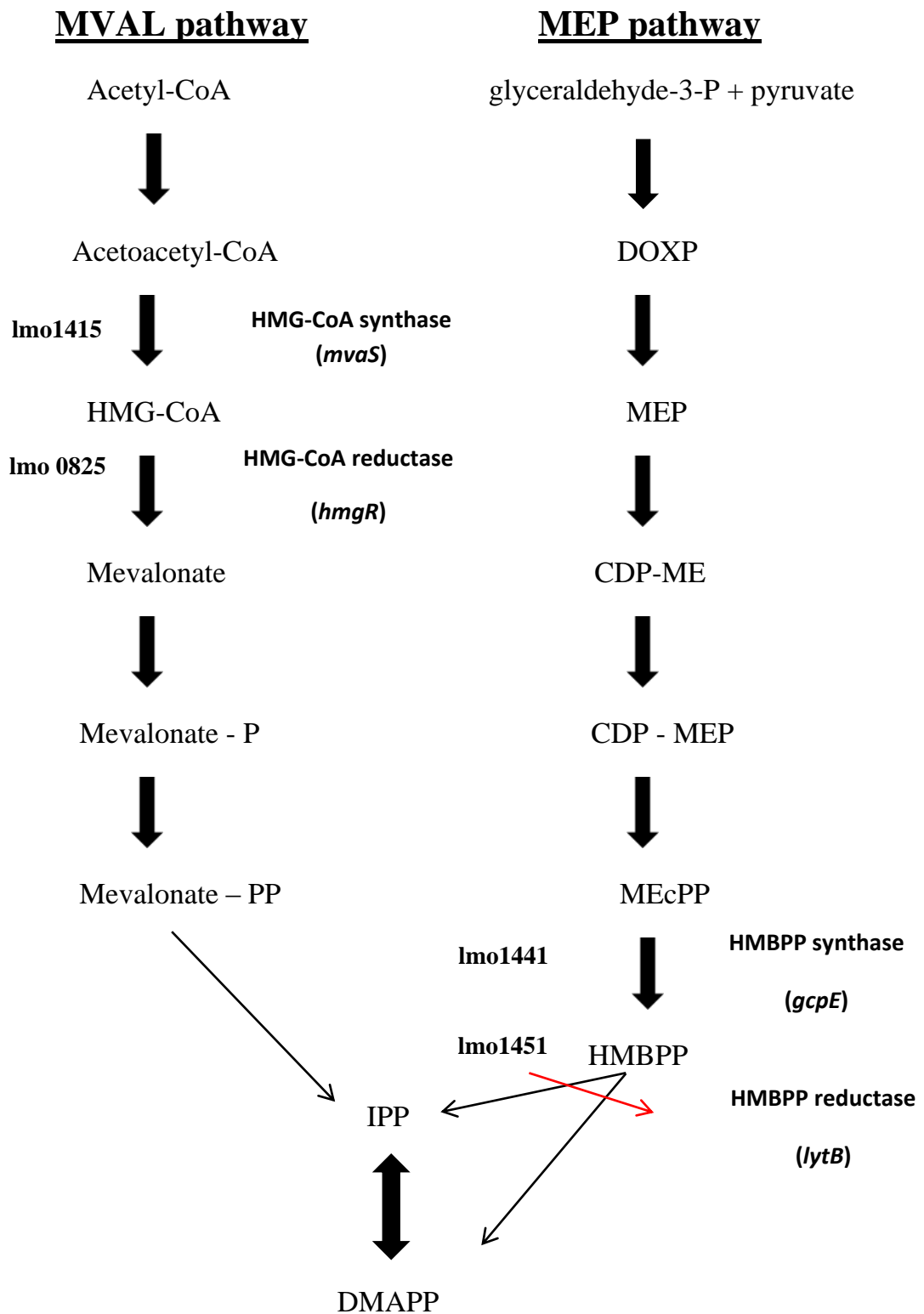
Fig. 1. The metabolites, enzymes and genes involved in the mevalonate and MEP pathways for isoprenoid biosynthesis in *Listeria monocytogenes* EGDe.

The essential pathway enzymes HMG-CoA synthase and HMG-CoA reductase are highlighted and NCBI annotated. This figure was modified from (Begley, Gahan *et al*. 2004)

Materials and Methods

Bacterial strains, media, chemicals and other growth reagents:

The pORI280 based *repA* negative system was used during this study in an attempt to create a clean deletion mutant in *L. monocytogenes* EGDe in HMG-CoA synthase (*lmo*1415). The *repA* positive strain *Escherichia coli* EC101 was used as a cloning host during the creation of the deletion mutant construct and was grown routinely at 37ºC in Luria Bertani (LB) medium with shaking (Reid 1991). *L. monocytogenes* EGDe was grown in Brain Heart Infusion (BHI) media (Oxoid) also at 37ºC with shaking. For agar plates, 1.5% agar technical from Merck was used. Antibiotic selection during the study was as follows: *E. coli* EC101 (250µg/ml erythromycin), *L. monocytogenes* EGDe-pVE6007 (7.5µg/ml chloramphenicol) and *L. monocytogenes* EGDe (5µg/ml erythromycin). For the transformant selection, 100µg/ml X-gal (5-bromo-4-chloro-3-indolyl-β-D-galactopyranoside) was added to the media (Sigma Aldrich).

Mevalonate preparation:

Mevalonate was prepared to 1M total concentration by dissolving Mevalonolactone powder (Sigma Aldrich) in deionised water and subsequently hydrolysed with an equal volume of 2M sodium hydroxide (NaOH) at 37ºC shaking. Following filter sterilisation, the 1M mevalonate solution was aliquoted and stored at -20ºC ready for use. In this study, mevalonate was always used at a final concentration of 0.001M as it is exogenously taken up by a mevalonate-deficient mutant (Δ*hmgR*) in *L. monocytogenes EGD*e (Heuston, Begley *et al*. 2012) and we predicted that this

would support the growth of the (*mvaS*) HMG-CoA synthase clean deletion mutant-if required.

Genetic manipulations:

Plasmid DNA was isolated from bacterial cultures using the QIAGEN QIAprep Miniprep spin kit ®. For the cloning reactions the proofreading enzyme KOD Hot Start DNA polymerase (Novagen) was used, to carry out consecutive polymerase chain reactions during the SOEing PCR procedure. *L. monocytogenes* EGDe genomic DNA used as the template and was extracted using the GenElute bacterial genomic miniprep kit (Sigma Aldrich). Hyperladder 1® from BioLine® was used as the standard molecular weight marker during the entire study. Restriction enzymes for the cloning reactions were supplied by New England BioLabs®. The four overlapping oligonucleotide primers used during the experimented were synthesised to our specifications by MWG-BioTech®. All other reagents and chemicals used during this work were ordered from Sigma Aldrich.

pORI280 chromosomal mutagenesis:

Splicing by overlap extension (SOE) PCR technique was used to generate two fragments of approximately 600bp in length. The first fragment (AB) was generated upstream of the gene to be deleted and contained the ATG start codon and the second fragment (CD) generated downstream beginning with the stop codon TAA. Two sets of primers were designed such that the two fragments would overlap forming AB fragment (lmo1414For_Xba1/lmo1414RevOL) and CD fragment (lmo1416FOL/1416R_Pst1). The 1.2kb ABCD product was generated following three subsequent PCR reactions. In the first reaction, 1μL of diluted *L. monocytogenes* EGDe genomic DNA (10-50ng DNA) was used as the template to

generate the initial PCR fragments. The reaction conditions for KOD polymerase were as follows; hot start 95ºC for 5mins, 95ºC for 30secs, 55ºC for 30secs, 70ºC for 45secs repeated for 35 cycles, final extension 70ºC for 2mins and held at 4ºC. These initial fragments were then combined in a 1:1 ratio in a primerless PCR reaction as follows; 95ºC for 1min, 55ºC for 1min and 70ºC for 1min this was repeated for 10 cycles. The final PCR reaction was used to amplify the ABCD fragment using the lmo1414For_Xba1 and lmo1416R_Pst1 primers; initial denaturation 95ºC for 1min, 95ºC for 1min, 55ºC for 30secs, 70ºC for 30secs repeated for 35 cycles, 70º for 2mins final extension and held at 4ºC forever. The SOEing PCR product was subsequently digested with the appropriate restriction.

The long fragment was visualised a gel and sequenced by GATC BioTech in the forward and reverse directions to ensure the accuracy of the ABCD product. An ATP-dependent ligation reaction using T4-DNA ligase (Roche) was carried out to unite the digested fragments and plasmids. The plasmid containing the insert pORI280:Δlmo1415 (*mvaS*) was first electroporated into electro-competent *E. coli* EC101 (see below), using the BioRad Gene Pulser ® electroporator set at the following conditions: (cuvette size 0.2cm; resistance 200Ώ; voltage 2.5kV; capacitance 25µF). Cells were revived by incubation with nutrient S.O.C. media shaking at 37ºC for 1hour. Subsequently, cells were plated on LB agar plates supplemented with 250µg/ml erythromycin. Colonies were then selected and grown overnight in appropriate broth and antibiotic at 37ºC with shaking. Plasmid extraction was then carried out to isolate plasmid containing the insert. Electrocompetent *L. monocytogenes* EGDe cells were prepared (see below) ready for electroporation with the purified plasmid construct.

Electrocompetent E. coli EC101 cell preparation and electroporation:

From a freshly streaked out LB agar plate, a single colony of *E. coli* EC101 was grown overnight shaking at 37ºC. Into 200mls of LB broth, 2ml (1% inoculum) was placed into a sterile 250ml conical flask and grown shaking at 37ºC for approx. 3-4 hours to an OD600 of 0.5-1 measured regularly throughout growth. The flask was then chilled on ice for 15 mins and centrifuged in sterile bottles at 4,000rpm for 15 mins at 4ºC. The pellet was washed twice in 100mls of cold sterile water at 4ºC twice and finally placed into 50ml falcon tubes and centrifuged as before. 5ml of a 10% (v/v) sterile glycerol solution was then used to resuspend once more and then finally in a volume of 750μL. The cells were dispensed into 50μL aliquots and stored at -80ºC ready for use.

L. monocytogenes EGDe competent cell preparation and electroporation:

A 10ml culture of *L. monocytogenes* EGD-pVE6007 was grown overnight in BHI broth (Oxoid) at 37ºC shaking, in the presence of 7.5μg/ml chloramphenicol. Into a sterile conical flask, 2ml of overnight culture was added to 100ml BHI broth supplemented with 0.5M sucrose (filter sterilised) and 7.5μg/ml chloramphenicol. The flask was grown shaking at 37ºC for 2-3 hours to an OD600 of 0.2-0.3. 100μL of Penicillin G antibiotic (10μg/ml final concentration) was added to the flask and left to incubate for a further 2 hours. Subsequently, the bacterial culture was centrifuged at 7,000rpm for 10 mins at 4ºC in 250ml bottles and the supernatant discarded. The cells were washed twice in a solution of 1mM ice-cold HEPES and 0.5M sucrose in a volume of 100ml decanted and then 55ml and decanted again. After washing, cells were resuspended in a final volume of 200-300μL HEPES/sucrose and dispensed into 50μL aliquots and stored at -80ºC ready to be

used. The plasmid containing insert (pOR1280-Δl*mo*1415) was electroporated into *L. monocytogenes* EGDe-pVE6007 competent cells, with a helper plasmid providing RepA *in-trans* to allow replication of pORI280. The following electroporation conditions were used: (cuvette size: 0.2cm; resistance 400Ω; voltage 1.8-2kV and capacitance 25µF). Cells were revived by incubation at 30ºC without shaking with 2ml ice-cold 0.5M sucrose/BHI broth for 2 hours statically and spread plated onto BHI plates supplemented with 5µg/ml erythromycin, 100ug/ml X-gal and 0.001M mevalonolactone incubated at 30ºC for 48hours. Individual light blue and dark blue colonies were selected from the transformation plates. The integration of pORI280 by a single crossover event was stimulated by streaking selected colonies and onto BHI plates supplemented with erythromycin, X-gal and mevalonolactone and incubated at 37ºC for 24hours. The loss of the pVE6007 helper plasmid was confirmed by replica plating onto BHI agar containing 5µg/ml erythromycin or 7.5µg/ml chloramphenicol. Chloramphenicol sensitive colonies were subsequently selected for plasmid excision and curing by statically passaging cultures diluted 1:1000 for five successive passages and at 37ºC in plain BHI broth supplemented with mevalonolactone, each passage was spread plate onto BHI plates containing X-gal. Each passage was diluted 10^{-5} in BHI broth and 100µL spread on BHI agar supplemented with 100µg/ml and incubated for 24 hours at 37ºC. White colonies were screened by colony PCR with primers external to the deletion region (lmo1415OutFwd: 5'-catctgttaaaccatcaattaac – 3' /lmo1415OutRev: 5'-accgatcctttcgatattcgc – 3') and compared to wild-type *L. monocytogenes* EGDe for the presence of the deleted gene and confirmed by sequencing. Colonies were patch inoculated on BHI agar containing erythromycin, sensitivity to the antibiotic confirmed loss (curing) of the pORI280 plasmid.

Complementation of the Δlmo1415 deletion mutant:

The HMG-CoA synthase deletion mutant in *L. monocytogenes* EGDe was complemented using the pPL2 plasmid (Lauer, Chow *et al*. 2002). pPL2 is a site specific integration vector that can be used to complement gene deletions is *L. monocytogenes* EGDe. pPL2-*lmo*1415 was created using the primer pair (*lmo*1415CompF_Kpn1/*lmo*1415CompR_Spe1) to amplify a PCR fragment of approx.1.2kb in length containing the promoter region and start/stop codons of the HMG-CoA synthase gene and then electroporated into DH5α cells. This was then extracted, purified and transformed into HMG-CoA synthase (Δlmo1415) *lmo*EGDe deletion mutant. Transformants were selected using chloramphenicol as the selectable marker. The correct insert was verified and checked by PCR and sequencing. Primers external to the multiple cloning site were used to screen for the presence of the complemented gene (pPL2MCS_FWD: 5'- acgtcaatacgactcact-3' and pPL2MCS_REV: 5'-gaatggcagaaattcgaaagc-3').

Escherichia coli	
EC101	Cloning host RepA+ integrated in the *glgB* gene
DH5α	Cloning host for complementation
Listeria monocytogenes	
EGDe	Wild type of serotype ½a, sequenced genome
EGDe-Δlmo1415	EGDe with entire HMG-CoA synthase gene deleted
EGDe::pEV6007	EGDe transformed with temperature sensitive helper plasmid
Plasmids	
pORI280	Erythromycin/Chloramphenicol resistant, RepA-gene replacement vector, lacZ expressor 5.3kb in size
pEV6007	Erythromycin resistant, Temperature sensitive helper plasmid supplies RepA in *trans*
pPL2	Chloramphenicol resistant, Site specific *Listeria* integration vector

Table 1. Bacterial strains and plasmids used in this study

Primers	5'-3' sequence
pORI280 system	
lmo1414For_Xba1	atatt**tctaga**ggattgatttcttcaccggctagctcggg
lmo1414RevOL	cggtttttttttgattacatatgtaagctcaagtcctttatattttatttg
lmo1416ForOL	gacttgagcttacatatgtaatcaaaaaaaaccgactaggctaaatcagc
lmo1416R_Pst1	atatt**ctgcag**gcacgtaatggccacagttagtcatatgg
pPL2 complementation	
lmo1415CompF_Kpn1	aagg**ggtacc**tgctttaatagcgatttgtc
lmo1415CompR_Spe1	ggggcgcagtacatgct**actagt**agga
Muliple cloning site primers	
pORI280_FWD	tatcgatgcatgccatggtacc
pORI280_REV	cgccagggttttcccagtcacgac

Table 2. Oligonucleotides used in this study with restriction sites highlighted in bold.

Growth curve analysis in normal growth media:

L. monocytogenes EGDe wild and the clean deletion mutant Δ*mvaS* (HMG-Co A

synthase), were grown in BHI (Brain Heart Infusion) broth overnight, shaking at

37ºC. Overnight cultures of each strain were measured using a BioPhotometer

(Eppendorf) and (10X4X45mm) polystyrene cuvettes (STARSTEDT). An OD_{600} of

1 was determined for each strain and pelleted by centrifugation at 13,000rpm for 5

mins and subsequently resuspended in 1ml of BHI broth. A 1:20 dilution was used

to a give a starting optical density of (OD_{600}= 0.05) for growth. 200μL was placed

into each well of a 96-well plate in triplicate and growth was monitored every hour,

over 24 hours. A multiscan microtitre plate reader (TECAN GENios® microplate

reader) and Magellan® software package were used to determine growth of the

bacterial strains. Growth was compared to that of the wild type as well other mevalonate and MEP mutants generated in our lab (Δlmo0825 (*hmgR*), Δlmo1441 (*gcpE*) and Δlmo1451 (*lytB*)). Exogenous mevalonate (0.001M) was added to support the growth of the mevalonate-dependent mutant Δlmo0825 (*hmgR*). Growth curves were correlated with spot plating of bacterial cultures on solid BHI (1.2%) agar grown overnight at 37ºC.

Growth curve analysis in defined media (DM):

Similar growth curves in the microtitre plate performed using BHI media were repeated using a chemically defined growth media for *L. monocytogenes* (Premaratne, Lin *et al.* 1991). Stock solutions: Na_2HPO4/KH_2PO_4, $MgSO_4$, Glucose, Fe-citrate, Amino acids (leucine, isoleucine, valine, methionine, arginine and glycine) were prepared in sterile water and autoclaved, Vitamins (riboflavin, biotin, thiamine prepared in 96% ethanol and combined with sterile water and an alcohol solution of thiotic acid). Fresh cysteine and glutamine stocks were prepared in sterile water and filter sterilised each time. Stock solutions were added to an appropriate volume of sterile water and used as the DM for monitoring the growth of *L. monocytogenes* EGDe wild and the deletion mutants.

Murine macrophage (J774.A1) uptake and survival assay:

J774.A1 macrophage cells were routinely maintained and grown in Dulbecco Modified Eagle Medium (DMEM) (Sigma-Aldrich), supplemented with 10% (v/v) Foetal Bovine Serum (Gibco) and 1% (v/v) Penicillin-Streptomycin (Sigma-Aldrich) in a 37ºC incubator supplemented with 5% CO_2. For all the uptake and survival assays, antibiotic-free media was used. Cells were routinely passaged 1:5 or 1:10, old media was removed and the cell monolayer washed with sterile Phosphate

Buffered Saline (PBS) (Sigma-Aldrich). Cells were removed from the monolayer by scraping using a Cell Scraper (STARSTEDT) and transferred to a fresh T175 tissue culture flask (STARSTEDT). Cells were counted using a haemocytometer and trypan blue exclusion to a cell density of 5×10^5 cells/ml of media and seeded into each well of a 24-well tissue culture plate (STARSTEDT) in triplicate. Cells were allowed grow to a confluency of 70-80% over 48 hours. 24 hours prior to the assay cells were incubated in antibiotic free media.

Overnight cultures of wild type *L. monocytogenes* EGDe and deletion mutants strains were grown overnight at 37ºC shaking and in the case of the Δlmo0825 (*hmgR*) supplemented mevalonate. One ml of overnight culture was subsequently pelleted by centrifugation and then washed in PBS and diluted to final concentration of 5×10^6 CFU/ml and resuspended in plain DMEM giving a multiplicity of infection (M.O.I. = 10) for the assay.

The antibiotic-free DMEM was removed from the J774 cells in each well and washed once with sterile PBS, to which 1ml of bacteria suspension was added and incubated for 1 hour at 37ºC/5% CO_2 to allow internalisation of the bacteria into the macrophage cells. Subsequently, the bacterial inoculum was removed and the monolayer washed once with sterile PBS. 50µg/ml gentamicin (Sigma) was resuspended in plain DMEM and applied to the monolayer and incubated one further hour to kill extracellular bacteria. This was then followed by lysis and scraping of the entire monolayer with a blue tip into ice cold sterile water containing 0.1% TritonX-100 in a sterile tube. 100µl of this lysate was serially diluted and plated onto BHI agar and in the case of the Δlmo0825 (*hmgR*) mutant supplemented with 0.001M mevalonate, which was incubated at 37ºC overnight. Bacterial counts were performed (CFU/ml) for the time points T0, T7 and T24 hours.

Effects of the HMG-CoA reductase inhibitor Rosuvastatin (RSV) on the growth of
L. monocytogenes WT and deletion mutants:

Rosuvastatin calcium salt (CAS:147098-20-2) was obtained from KEMPROTEC

Ltd, (11 Pennyman Green, Maltby, Middlesborough, TSB 0BX UK), as a pure solid

powder. RSV was dissolved to a maximum soluble concentration of 3mg/ml for *in-*

vitro experimentation and subsequently filter sterilised (0.2µm). Growth curves were

performed in a similar manner as outlined previously in BHI and DM media growth

experiments in the microtitre plate reader. A range of RSV concentrations were used

(0.0005mg/ml), (0.5mg/ml) and (3mg/ml) were dissolved in sterile BHI broth.

Growth rates were compared for the following strains: *L. monocytogenes EGDe*

wild, Δlmo1415 (*mvaS*), Δlmo0825 (*hmgR*), Δlmo1441(*gcpE*) and Δlmo1451(l*ytB*)

over 24 hours at 37ºC.

Triton X-100 cell wall stress autolytic assay:

Overnight cultures of *L. monocytogenes* EGDe wild type and the deletion mutant

Δlmo1415 (*mvaS*) were grown at 37ºC shaking. The protocol for the Triton X-100

autolytic assay was conducted as previously decribed (Popowska, Kusio *et al*. 2009).

Bacterial cultures were pelleted by centrifugation and washed once with fresh BHI

media and grown to log phase ($OD_{600} = 0.6$). Bacterial cells were harvested by

spinning at 7000g for 12mins and washed once with sterile PBS and finally

resuspended to an OD600 of 0.8 in lysis buffer. (50mM Trizma-Hydrochloride

(Tris-HCl) (Sigma-Aldrich) pH adjusted with 2M Sodium Hydroxide (NaOH) to pH

7.5. containing 0.1% Triton X-100). Incubations were performed shaking at 37ºC

and cell lysis was measured as a percentage decline in the optical density (OD_{600})

using the BioPhotometer. Readings were recorded at T0, T30, T60, T90, T120, T150, T180 and T210mins and plotted as a declining curve on Sigma Plot®.

Effect of cell wall antibiotics Penicillin G and Ampicillin:

L. monocytogenes EGDe wild type clean deletion mutants (Δlmo1415 (*mvaS*) and Δlmo0825 (*hmgR*)) were examined by disk diffusion assay for sensitivity to Penicillin G and Ampicillin (cell wall synthesis inhibitors). Individual colonies were selected from overnight BHI agar plates and grown in Mueller-Hinton (MH) broth (Fluka Analytical). The bacterial suspension was thoroughly mixed and swabbed onto the surface of MH plates. Antibiotic disks Penicillin (2 units) and Ampicillin (10μg) were placed on the surface of the agar with a sterilised forceps and incubated inverted for 24 hours at 37ºC. Zones of clearance (bacterial inhibition) surrounding each disk were measured with a Vernier Callipers (mm) and conducted in triplicate for each strain.

Oxidative stress (Hydrogen peroxide) disk assay:

Overnight cultures of *L. monocytogenes* wild type and mutants Δlmo1415 (*mvaS*) and lmo0825 (*hmgR*) were grown shaking at 37ºC in BHI broth. Fresh BHI broth was inoculated with a 2% overnight culture and grown to an OD600=0.2 (log phase). 33.3% (v/v) hydrogen peroxide solution (Sigma-Aldrich) was prepared and autoclaved. Sterile filter disks (Sigma) were aseptically placed on the surface of a BHI plates. 10 and 20μL of the hydrogen peroxide solution was placed on the surface of each disk. 5mls molten BHI agar (0.75%) was inoculated with 10% bacterial suspension thoroughly combined and overlaid on the agar. Plates were incubated overnight at 37ºC and zones of clearance measured.

Enumeration of bacterial inoculum for BALB/c intraperitoneal infections:

L. monocytogenes EGDe wild type, Δlmo1415 (*mvaS*) mutant and the complemented strain *lmo*EGDeΔlmo1415::pPL2(lmo1415) were grown overnight at 37ºC shaking in BHI broth. For the complemented strain media was supplemented with 7.5μg/ml chloramphenicol. Bacterial cells were harvested by centrifugation (8,000rpm for 5mins) and cell pellets were then resuspended in equal aliquots of PBS. Optical density (OD600) was determined on the BioPhotometer and serial dilutions performed to obtain a final bacterial inoculum of $4x10^4$CFU/200μL injection volume.

BALB/c intra-peritoneal in-vivo competition study:

8-12 week old female BALB/c mice (n=6 per strain) were inoculated with $1 X 10^6$CFU/ml bacteria by injection (200μL) via the intra-peritoneal route. 3 days post infection mice were humanely sacrificed and spleens and livers homogenized in 5ml of PBS, serial dilutions were performed and plated onto BHI agar. CFU/ml was determined for each strain for *in-vivo* survival of the bacteria per mouse. All murine studies were conducted with relevant legislation and approved by the animal ethics committee at University College Cork.

Bioinformatic and KEGG pathway analysis of Δlmo1415 deletion mutant:

Bioinformatic analysis was carried out on the HMG-CoA synthase gene using information provided by the National Center for Biotechnology Information (NCBI) database, Pasteur Institute ListiList and Basic Local Alignment Search Tool (BLASTn, nucleotide query and BLASTx, translated query). The accession number (NP_464940.1) for HMG-CoA synthase (lmo1415) in *L. monocytogenes* EGDe was

used to gather information on the length of the gene and encoded protein, the presence of any other similar copies of the gene in the *L. monocytogenes* EGDe genome. The Kyoto Encyclopedia of Genes and Genomes (KEGG®) was used to elucidate potential other metabolic pathways that involve HMG-CoA synthase and its product HMG-CoA under the entry (EC: 2.3.3.10) in *L. monocytogenes* EGDe.

Statistical analysis:

Analysis of statistical in this study was performed for a number of technical and biological replicates and variance was determined via the Student's T-test. Statistical significance was determined based on a p-value from the mean values (+/- SEM; *P < 0.05, **P < 0.01 and ***P< 0.001).

Results

Bioinformatic analysis of the lmo1415 HMG-CoA synthase gene in L. monocytogenes EGDe:

L. monocytogenes is a unique bacterial pathogen in that it contains a complete set of genes for the mevalonate and MEP pathways for isoprenoid biosynthesis (Fig.1.). The gene lmo1415 is predicted to encode HMG-CoA synthase, the second enzyme in the mevalonate pathway which was selected for deletion. Bioinformatic analysis of HMG-CoA synthase revealed a 388 amino acid (1167bp) protein on the positive strand, with a HMG-CoA synthase superfamily domain, 3 active site domains and multiple dimer interface sites that are distributed along the full length of the conserved domain of the protein (Fig.2). HMG-CoA synthase from this analysis belongs to a family of condensing enzymes that catalyse reactions either by carboxylation or non-carboxylation in a claisen like condensation reaction. Members of this family share strong structural similarity and are all involved in the synthesis or degradation of fatty acids and even in the production polyketides.
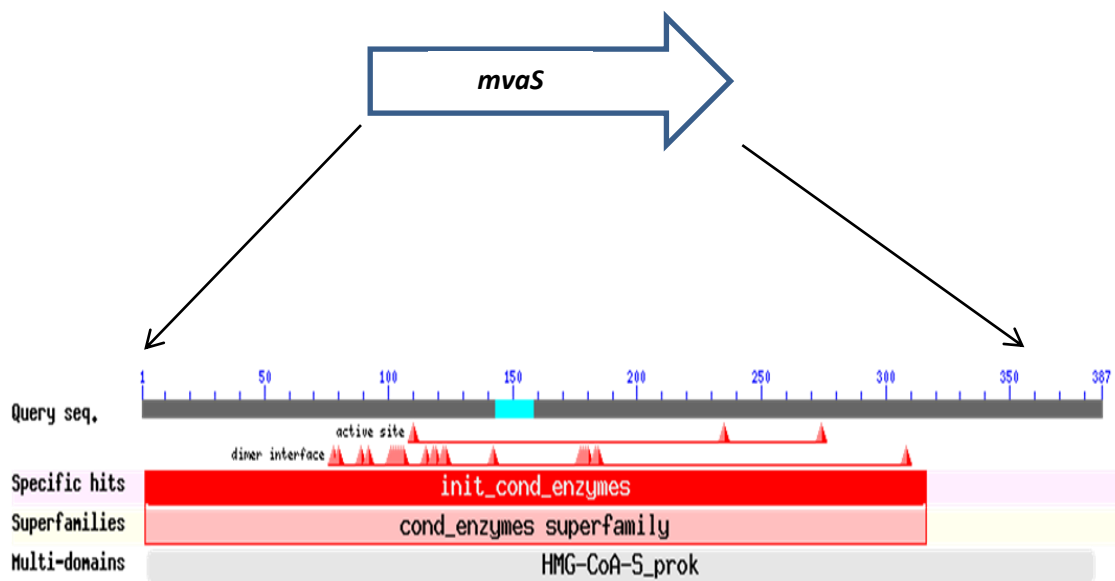
Fig.2. Conserved domains of the HMG-CoA synthase protein of *L. monocytogenes* EGDe in the Mevalonate pathway of isoprenoid biosynthesis

Three active site domains and multiple dimer interface sites were found with the HMG-Co A synthase superfamily/condensing enzyme domains.

Creation of a HMG-CoA synthase deletion mutant in L. monocytogenes EGDe:

In this study, the splicing by overlap extension (SOE) PCR method (Fig. 3.) (Horton 1995) was used to delete the lmo1415 HMG-CoA synthase gene in

L. monocytogenes EGDe, as a means to determine if this gene is essential to the lifecycle of the pathogen. Previous work in our lab (Heuston, Begley *et al.* 2012) created a clean deletion mutant in the third enzyme in the mevalonate pathway of *L. monocytogenes* EGDe lmo0825 (HMG-CoA reductase), which proved to be essential in growth and survival of the wild type compared to the mutant variant.
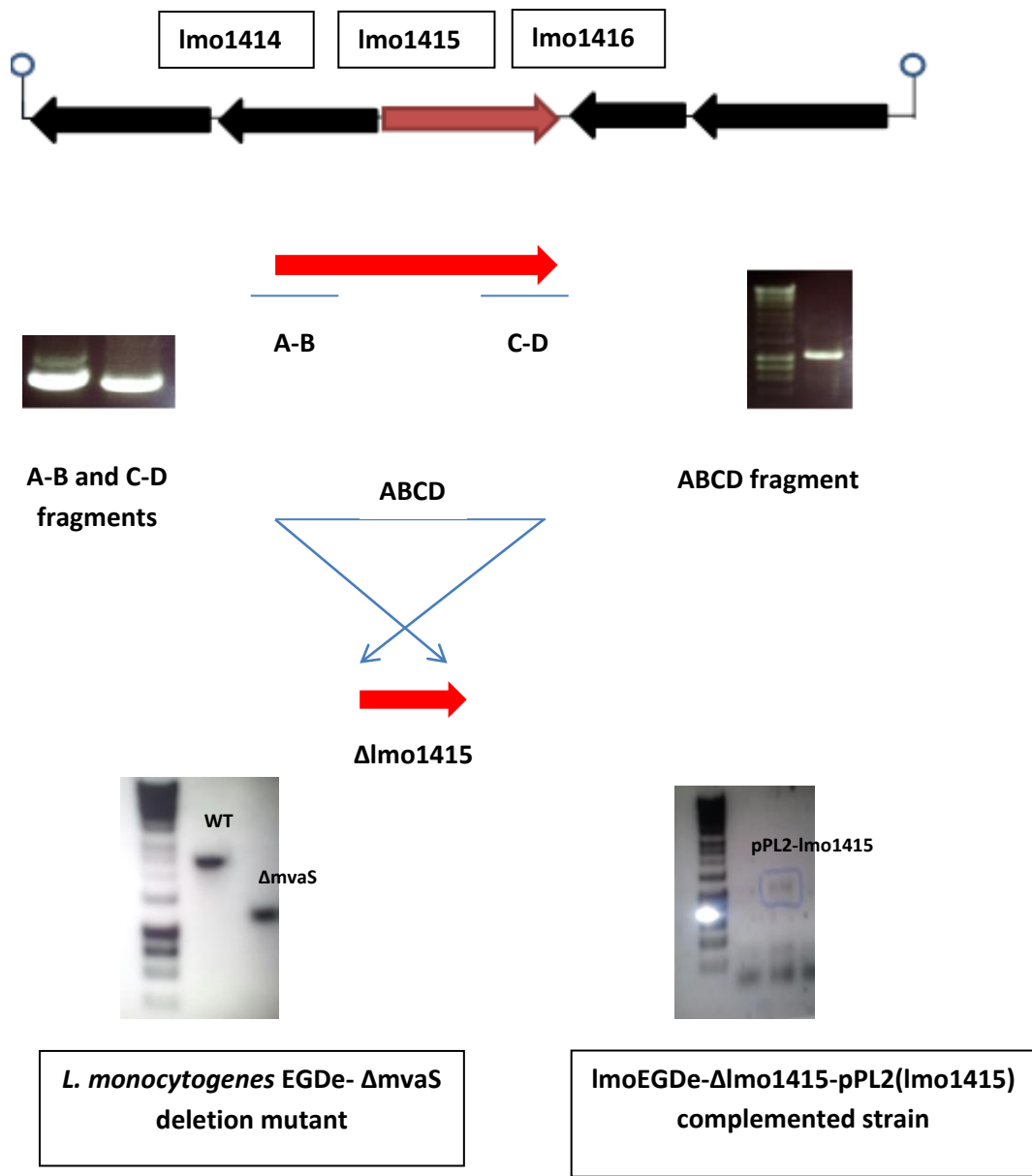
Fig. 3. Genetic organisation of the HMG-CoA synthase (lmo1415) and surrounding genes in *Listeria monocytogenes* EGDe including schematic of SOEing procedure.

Illustrated above is a diagram depicting the organisation and orientation of the

lmo1415 gene in *L. monocytogenes* EGDe and its neighbouring genes lmo1414 and

lmo1416. The gene to be deleted is highlighted in red and the neighbouring genes

are indicated in black. The splicing by overlap extension (SOE) technique is

described (Horton 1995). Following restriction digestion, the fragment was cloned

into the site specific integrating vector pORI280. The vector pORI280 requires to be

co-transformed with a helper plasmid pVE6007 into *L. monocytogenes* EGDe. Chromosomal integration in both cases is temperature sensitive at 37ºC. Deletion mutants were screened by colony PCR using primers external to the deleted region and compared to the wild type strain.

KEGG pathway analysis of HMG-CoA synthase and HMG-CoA:

KEGG pathway analysis of HMG-CoA synthase and HMG-CoA (S)-3-hydroxy-3-methylglutaryl-CoA (EC:2.3.3.10) (below) in *L. monocytogenes* EGDe genera revealed a complex subset of biological reactions involved including: (lmo00280 (valine, leucine and isoleucine degradation), lmo00650 (butanoate metabolism), lmo00900 (terpenoid backbone biosynthesis i.e. mevalonate and MEP pathways (Fig. 1), lmo01100 (metabolic pathways) and lmo01110 (biosynthesis of secondary metabolites). The pathway for the degradation of valine, leucine and isoleucine revealed another potential enzyme (EC:4.2.1.18 (methylglutaconyl-CoA hydratase)) that may provide an alternative route for the synthesis of HMG-CoA. This degradation pathway was also found to exist in a wide variety of other bacteria. This could potentially be an alternative route for HMG-CoA substrate in *L. monocytogenes* EGDe but as of yet is not defined.

(A): KEGG pathway analysis of *mvaS* in *L. monocytogenes* EGDe:

Entry	lmo1415　　　　CDS　　　　T00066
Definition	hypothetical protein
	K01641　　hydroxymethylglutaryl-CoA synthase [EC:2.3.3.10]
Organism	lmo Listeria monocytogenes EGD-e
	lmo00072　　Synthesis and degradation of ketone bodies lmo00280　　Valine, leucine and isoleucine degradation lmo00650　　Butanoate metabolism lmo00900　　Terpenoid backbone biosynthesis lmo01100　　Metabolic pathways lmo01110　　Biosynthesis of secondary metabolites

(B): Bacterial Valine, leucine and isoleucine degradation:
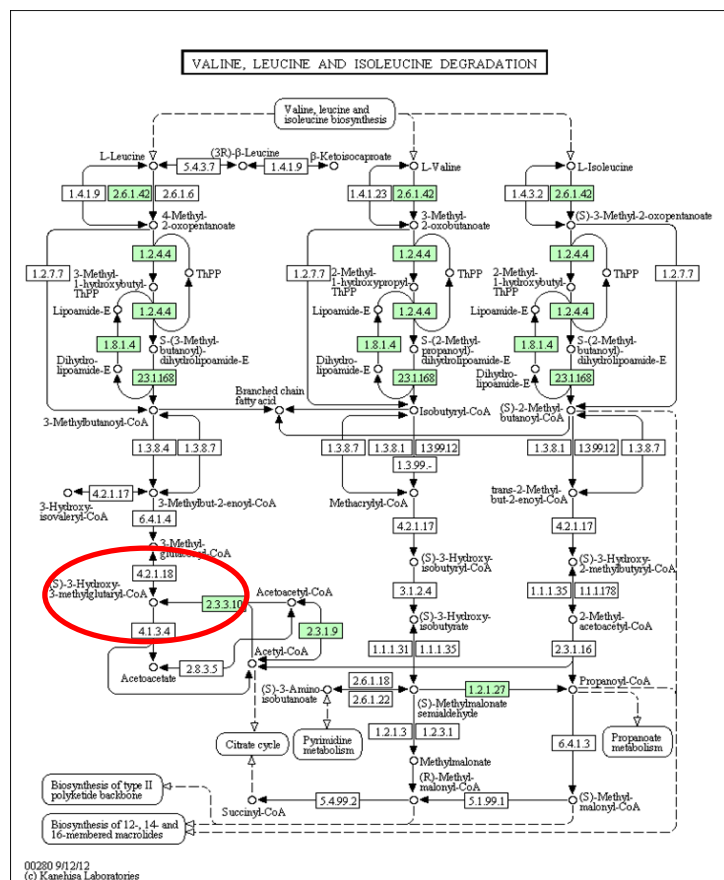
Fig. 4. KEGG pathway analysis of HMG-CoA synthase and its product HMG-CoA (S)-3-hydroxymethylglutaryl-CoA in *Listeria* and other bacteria.

KEGG pathway analysis of the enzyme HMG-CoA synthase (EC:2.3.3.10) in *Listeria* revealed a wide range of biochemical pathways including: terpenoid backbone synthesis (mevalonate and MEP pathways) as well as the degradation of valine, leucine and isoleucine. It should be noted that this degradation pathway also exists in a wide variety of other bacterial species and not just in *L. monocytogenes* EGDe. Highlighted is the enzyme HMG-CoA synthase (EC:4.3.3.10) and the enzyme denoted (EC:4.2.1.18 – methylglutaconyl-CoA hydratase) for a potential alternative route of HMG-CoA synthesis.

Growth characteristics of L. monocytogenes EGDe wild and mevalonate/MEP deletion mutants in normal growth media:

Cultures of wild type *L. monocytogenes* EGDe and mutants Δ*mvaS* (lmo1415), Δ*hmgR* (lmo0825), Δ*gcpE* (lmo1441) and Δ*lytB* (lmo1451) were grown to late stationary phase (24 hours) in a microtitre plate reader to profile growth of each strain in BHI (see materials and methods) (Fig.5). Growth curves and statistical analysis were performed using Sigma Plot software package.

BHI growth curve WT vs. mutant *Listeria monocytogenes* EGDe

Legend:
- ● lmo EGDe wild-type
- ○ lmo EGDe- lmo1415 (MvaS)
- ■ lmo EGDe- lmo 0825 (HmgR)
- □ lmo EGDe- lmo 0825 (HmgR) + 0.001M MVAL
- ▲ lmo EGDe-lmo1441 (GcpE)
- △ lmo EGDe-lmo1451 (LytB)
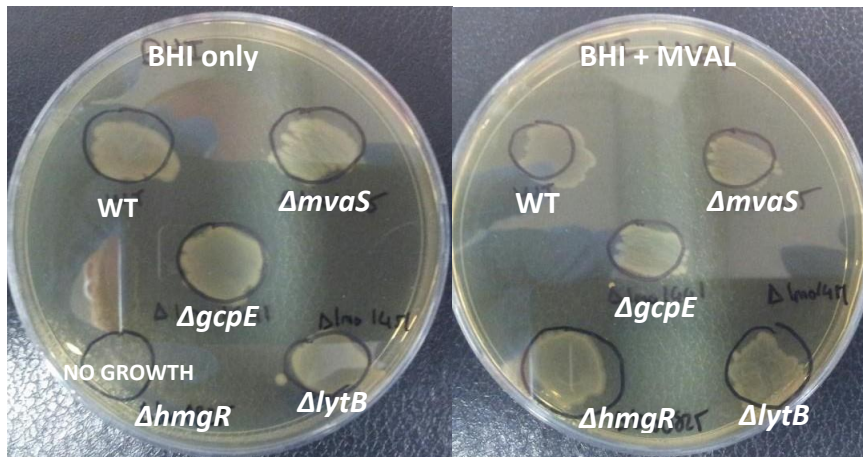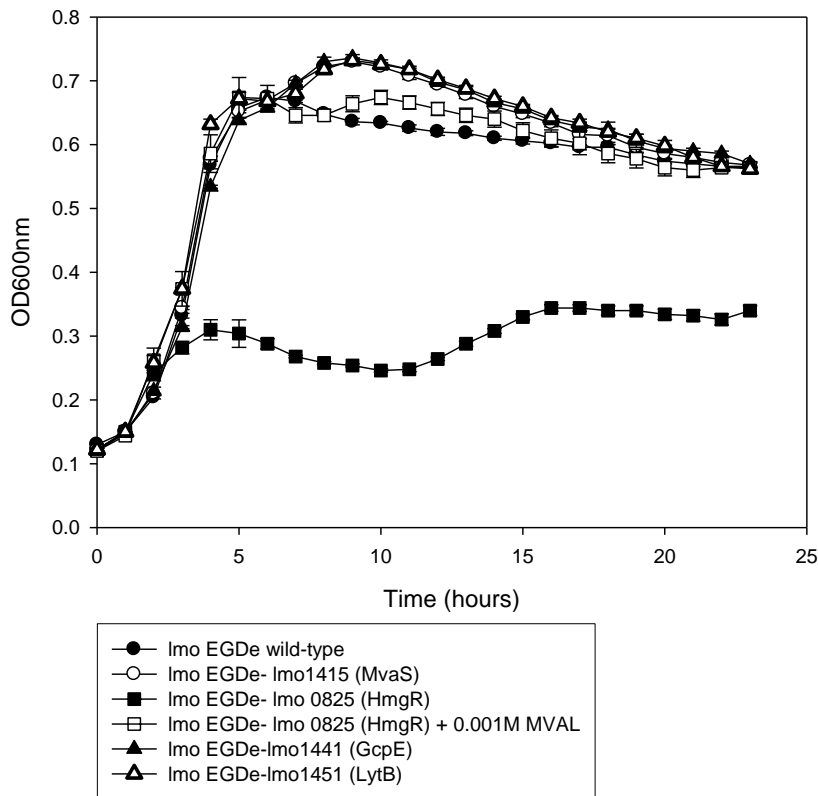
Fig.5. **Growth curve analysis of *L. monocytogenes* EGDe wild type and mevalonate and MEP pathway mutants BHI media.**

Cultures of wild type *L. monocytogenes* EGDe and deletions mutants lmo1415, lmo0825, lmo1441 and lmo1451 were grown and monitored in BHI broth (with or without 0.001M mevalonate (MVAL)) over 24 hours to late stationary phase in a microtitre plate reader. With the exception of the un-supplemented lmo0825 mutant all strains reached a similar final OD600 of 0.6-0.7, with similar profiles of growth. This suggests that the *mvaS* deletion is capable of normal growth under lab

conditions without supplementation. Replica plating of all strains onto BHI or BHI+MVAL agar confirmed this finding.

Growth characteristics of L. monocytogenes EGDe and mutant strains in DM:

Growth experiments were similarly performed using a chemically defined media (DM) for *L. monocytogenes* EGDe (Premaratne, Lin *et al*. 1991). Wild type and mutant cultures were again grown to late stationary phase (24hours) in triplicate and repeated a number of times. Graphs were plotted and statistical analysis performed using Sigma Plot.

DM growth curve WT vs. mutant *Listeria monocytogenes* EGDe
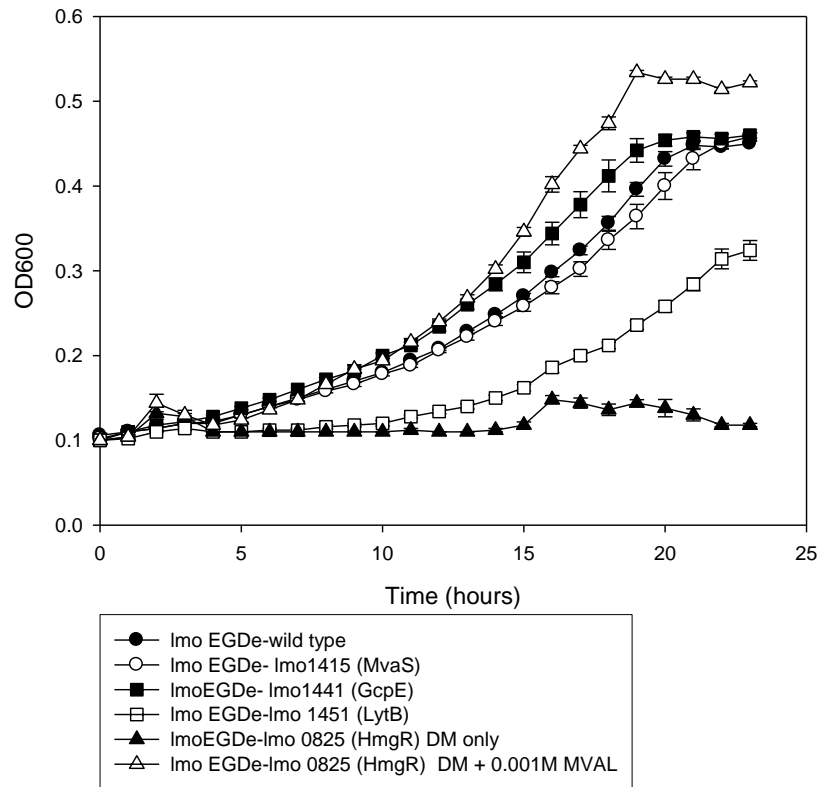
Fig.6. Growth curve analysis of *L. monocytogenes* EGDe wild type and deletion mutants Δ*mvaS* (lmo1415), Δ*hmgR* (lmo0825), Δ*gcpE* (lmo1441) and Δ*lytB* (lmo1451) in defined growth media over 24 hours.

DM was able to support the growth of the wild type, lmo1415, lmo1441, lmo0825(+MVAL) and reach a similar final optical density OD600 = 0.4-0.5. The lmo1451 mutant had a reduced capacity for growth in DM only reaching a final OD600=0.3. Un-supplemented lmo0825 was not capable of growth in DM.

HMG-CoA synthase deletion mutant is not affected in virulence in J774
macrophages compared to wild type and other mutants:

In-vitro uptake and survival of the lmo1415 gene deletion mutant was not affected in

murine J774 macrophages compared to the wild type *L. monocytogenes* strain and

other mutant strains tested (Fig. 7). 5 X 10^5 J774.A1 macrophage cells/ml were

infected with $5x10^6$ CFU/ml (M.O.I. = 10). All mutants were not affected in their

initial uptake by the macrophages at T0 hours determined by bacterial counts

(average log CFU/ml) compared to the wild type strain. After 7 hours, there was no

statistical difference in the ability of all strains to survive intracellularly in the

macrophages. The extended time point T24 hours was determined and again there

was no significant difference in any of the strains.

J774 macrophage assay T0 hours

J774 macrophage assay T7 hours

J774 macrophage assay T24 hours
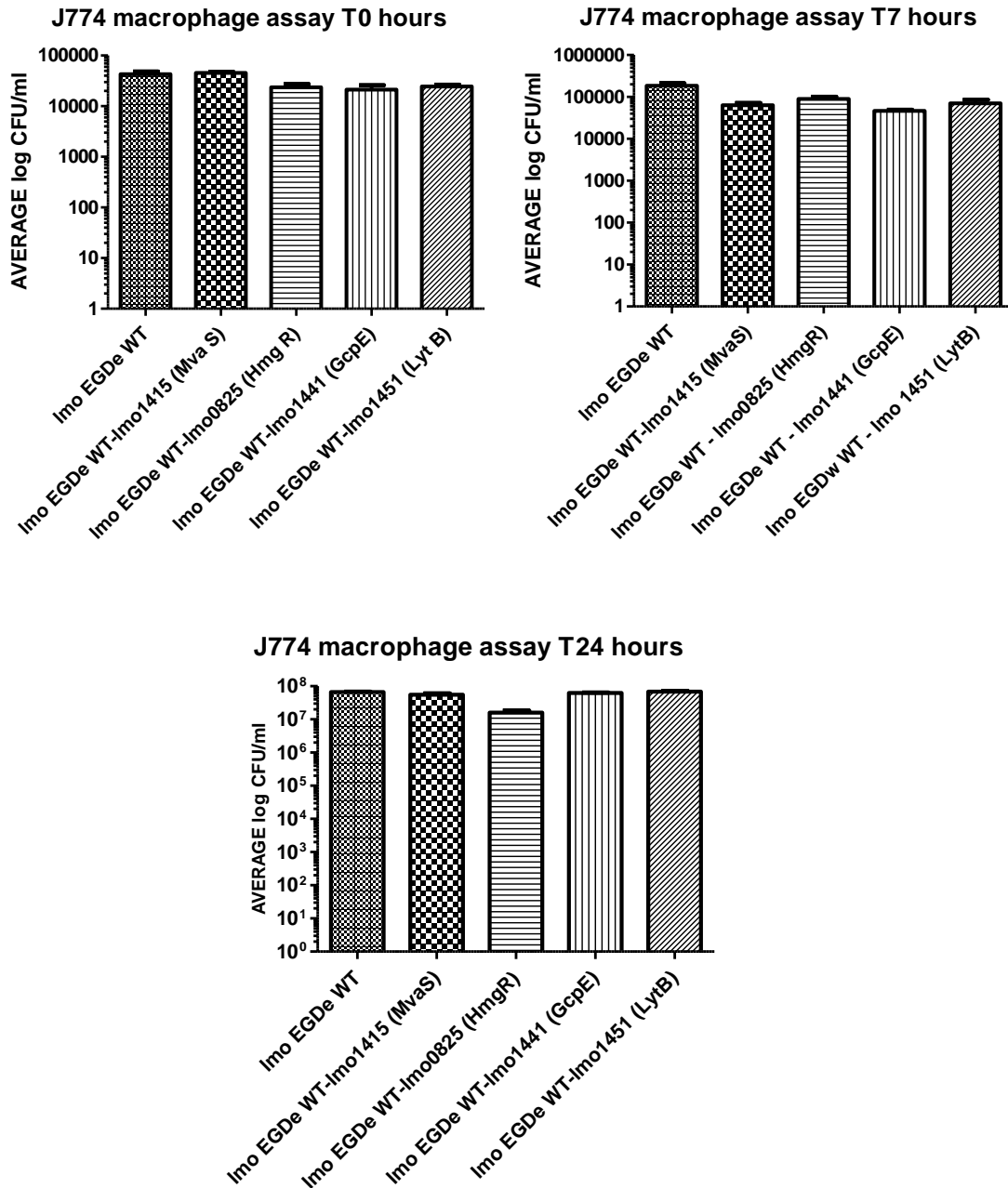
Fig. 7. *In-vitro* **uptake and survival of** *L. monocytogenes* **EGDe wild type and deletion mutants** *ΔmvaS* **(lmo1415),** *ΔhmgR* **(lmo0825),** *ΔgcpE* **(lmo1441) and** *ΔlytB* **(lmo1451) in J774.A1 macrophages.**

Bacterial numbers are calculated per average log CFU/ml after T0, T7 and T24 hours infection with wild type and deletion mutants. Error bars represent the standard deviation from the mean of a number of replica experiments. There was no statistical difference in any of the strains compared to the wild type by the Student's T-test.

Growth of ΔmvaS deletion mutant was not significantly affected by the HMG-CoA reductase inhibitor Rosuvastatin (RSV):

Growth analysis was performed on *L. monocytogenes* EGDe wild type and the

ΔmvaS (lmo1415) deletion mutant in BHI broth containing varying concentrations of

Rosuvastatin (see materials and methods) and controls without added RSV. Growth

was monitored to late stationary phase.
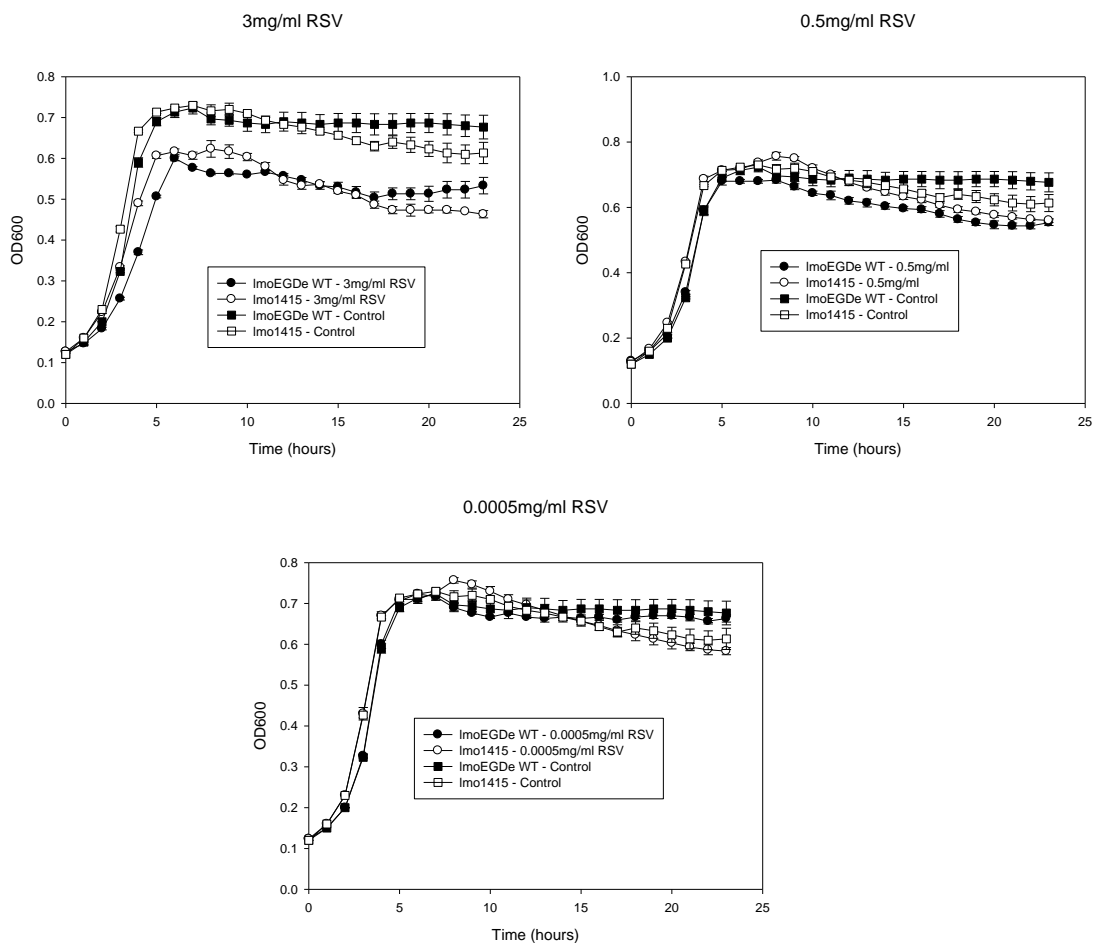
Fig.8. Effect on growth of the HMG-CoA reductase inhibitor Rosuvastatin (RSV) on the growth of wild type *L. monocytogenes* EGDe and *ΔmvaS* (lmo1415) deletion mutant.

Wild type *L. monocytogenes* EGDe wild type and the *ΔmvaS* (lmo1415) deletion mutant were grown and monitored to late stationary phase (24hours) in BHI broth containing: (3mg/ml; 0.5mg/ml and 0.0005mg/ml) dissolved RSV. Error bars were generated based on the standard deviation from the mean value from a number of replica experiments. Inhibition by RSV only occurs at very high levels (3mg/ml), perturbing growth between 0.1 and 0.15 OD600 at the stationary phase of growth is

reached compared to controls. There was no significant difference in the growth of wild type vs. lmo1415 deletion mutant both were equally sensitive.

HMG-CoA reductase is the third rate limiting enzyme of the mevalonate pathway for isoprenoid biosynthesis and cholesterol metabolism and is the target for the treatment of hypercholesterolemia clinically by the drugs commonly known as statins (Istvan and Deisenhofer 2001). *L. monocytogenes* EGDe has been described as carrying a Class 2 HMG-CoA reductase enzyme (see Chapter 1) and according to (Jerwood and Cohen 2008) statins have been shown to possess antimicrobial activity against bacteria that utilise the mevalonate pathway for isoprenoid biosynthesis. HMG-CoA synthase precedes the target for statins and should be sensitive to statin exposure as HMG-CoA reductase. However, in our study we find little evidence of increased sensitivity of our deletion mutant.

No difference in wild type and ΔmvaS mutant sensitivity to cell wall autolysis:

HMG-CoA synthase is an important enzyme in the mevalonate pathway for isoprenoid biosynthesis that play a key role in forming major structures of the cell, such the cell membrane and cell wall. An autolytic Triton X-100 (see materials and methods) cell wall stress assay was performed on wild type *L. monocytogenes* EGDe and *ΔmvaS* deletion mutant to compare vulnerability. Previously, it was shown by (Heuston, Begley *et al*. 2012) that a deletion of the HMG-CoA reductase gene predisposed the bacterial cell to autolytic cell death from Triton X-100, with almost a 58% decline in optical density after 30mins. In our experiment, both the wild type and lmo1415 mutant displayed identical sensitivity over the time course. A 50-60% reduction in OD600 was attained between T90-T120mins and T210mins a final decline to 20% of both strains was observed.

Triton x-100 autolysis assay
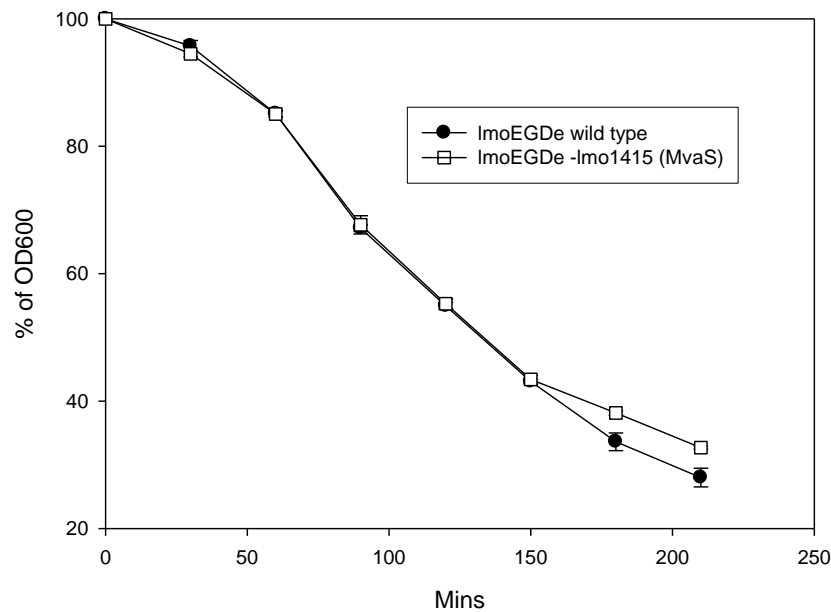
**Fig. 9. Triton X-100 induced cell wall autolysis of wild type *L. monocytogenes*
EGDe and *ΔmvaS* (lmo1415) deletion mutant.**

Autolysis was determined as a % reduction in the optical density from an initial
OD600 of 0.8, over the time course T0, T30, T90, T120, T150, T180 and T210
mins. Error bars represent the standard deviation from the mean value of a number
of replicated experiments. Both wild type and mutant strains display identical
sensitivity to Triton X-100. There was no statistical significant effect over the course
of the experiment.

*Effect of oxidative stress on L. monocytogenes EGDe wild type and ΔmvaS
(lmo1415) and ΔhmgR (lmo0825) deletion mutants:*

L. monocytogenes EGDe wild type and the deletion mutants were examined for their

sensitivity to hydrogen peroxide induced oxidative stress (Table 3). Hydrogen

peroxide is a cytolytic oxidative antimicrobial compound that is commonly secreted

by macrophages (Jorens, Matthys *et al*. 1995) . Oxidative compounds such as nitric

oxide (iNOS) are known to have antimicrobial effects when the immune system is

triggered following bacterial infection. Wild type and mutant strains were exposed to

10 or 20μL 33.3% (v/v) hydrogen peroxide in blank filter disks (see materials and

methods). It was observed that wild type and lmo1415 deletion mutant shared similar vulnerability to oxidative stress by hydrogen peroxide in both 10 and 20μL disks. The lmo0825 mutant exhibited the most significant inhibition (15+/-0.164mm) which was similarly observed by (Heuston, Begley *et al.* 2012).

Strain	10μL (mm)	20μL (mm)
lmoEGDe wild type	10.6 +/- 0.155	13.567 +/- 0.163
Δlmo1415	10.567 +/- 0.121	13.3633 +/- 0.248
Δlmo0825	10.833 +/- 0.216	15.0 +/- 0.164*
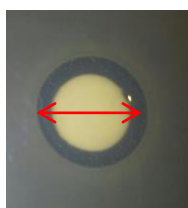
Zone of inhibition

Table 3. **Hydrogen peroxide disk assay comparing the effect of oxidative stress on the growth of *L. monocytogenes* EGDe wild type and mevalonate pathway mutants.**

L. monocytogenes EGDe wild type and the mevalonate pathway mutants lmo1415 and lmo0825 were grown to log phase and inoculated into molten BHI agar and incubated in the presence of 10 or 20μL of 33.3% (v/v) hydrogen peroxide. Zones of inhibition around the filter disks were measured using a Vernier Callipers in mm. Average values are expressed as +/- the standard deviation from the mean value of a number of replicated experiments. Statistical significance was determined via the Student's T-test and an asterisk (*) denotes a p-value less than 0.05. Inhibition of growth was more pronounced in 20μL hydrogen peroxide compared to 10μL. Only the *ΔhmgR* (lmo0825) deletion mutant had a significant degree of inhibition compared to the wild type strain. The *ΔmvaS* (lmo1415) mutant showed very similar sensitivity to the wild type strain.

Penicillin G and Ampicillin cell wall antibiotic sensitivity is not increased by the deletion of HMG-CoA synthase:

L. monocytogenes EGDe wild type and the mevalonate pathway deletion mutants

ΔmvaS (lmo1415) and *ΔhmgR* (lmo0825), were examined for sensitivity to Penicillin

G and Ampicillin (see Materials and Methods). Zones of clearance around the disk

were measured using a Vernier Callipers in mm and results from a number of

repeated experiments were tabulated in Table 4 below.

Strain	P2(mm)	Amp10 (mm)
EGDe wild type	22.83 +/- 0.279	29.083 +/- 0.232
ΔmvaS (lmo1415)	22.167 +/- 0.48	28.933 +/- 0.314
ΔhmgR (lmo0825)	27.383 +/- 0.366*	31.95 +/- 0.547*

Table 4. Penicillin G and Ampicillin antimicrobial sensitivity of *L. monocytogenes* EGDe wild type and mevalonate pathway mutants.

Zones of clearance surrounding P2 and Amp10 antibiotic disks were measured using Vernier Callipers. Average values are expressed +/- the standard deviation from the mean value of a number of replicated experiments. Statistical significance was determined via the Student's T-test an asterisk (*) denotes a p-value less than 0.05. The *ΔhmgR* (lmo0825) mutant was most sensitive compared to the wild type.

***In-vivo survival and virulence comparing L. monocytogenes wild type, ΔmvaS
(lmo1415) mutant and pPL2 complemented strain in a murine model:***

The virulence potential of the *ΔmvaS* (lmo1415) mutant and complementation strain
were examined by intraperitoneal injection (200μL) with 1 X 10^6 CFU/ml bacteria
into the abdominal cavity of BALB/c mice. Post-gastrointestinal phase virulence
was assessed 3 days following infection by determining bacterial numbers in the
spleen and liver of each animal. Average log CFU/ml for each mouse was
determined by plating on BHI agar and graphed as a vertical scatter plot using
GraphPad Prism5®.
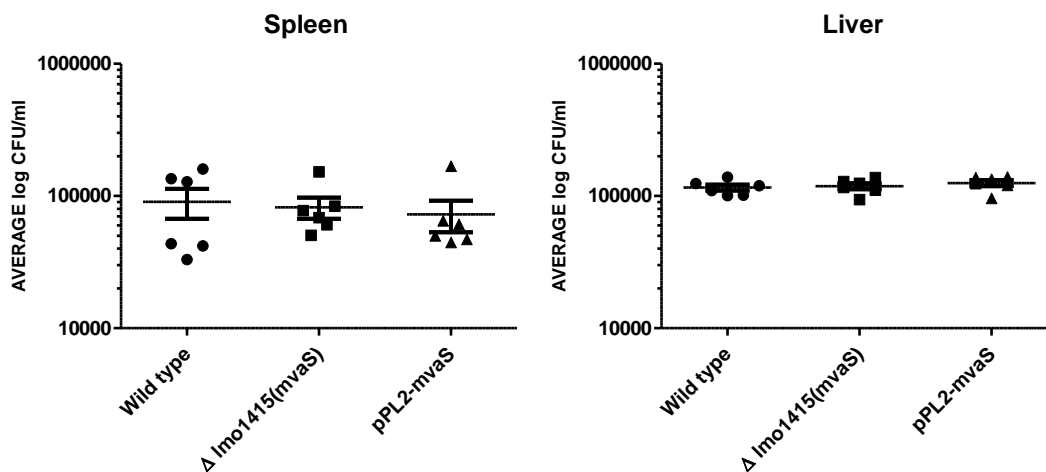
**Fig.10. Murine intraperitoneal infections of the spleen and liver with wild type
L. monocytogenes EGDe, *ΔmvaS* (lmo1415) deletion mutant and complemented
(pPL2) strain.**

Bacterial enumeration of wild type *L. monocytogenes* EGDe (●), *ΔmvaS* (lmo1415)
mutant (■) and pPL2 complemented strain (▲), 3 days post murine intraperitoneal
infection of the spleen and liver. Bacterial numbers are expressed as average log
CFU/ml for each strain. On average, approx. $1x10^5$ CFU/ml live bacteria was
recovered from the spleen and liver of all 3 animal groups. Error bars represent the
standard deviation from the mean of n=6 mice per group. There was no statistical
difference between the virulence of the wild type and mutant strains or the
complement strain as determined by the Student's T-test. Spleen: (WT vs. Δlmo1415
p=0.7749, WT vs. pPL2 p=0.7244), Liver: (WT vs. Δlmo1415 p=0.6495, WT vs.
pPL2 p=0.0695). Statistical significance was determined as a p-value less than 0.05.

Discussion

The main aim of this study was to create a clean deletion mutant in the gene lmo1415 (HMG-CoA synthase) of *L. monocytogenes* EGDe in an attempt to elucidate if this enzyme is essential for the normal growth and virulence of this foodborne pathogen. *L. monocytogenes* is a highly unusual micro-organism in that it possesses genes encoding two different pathways enzymes for isoprnoid biosynthesis (Fig.1), namely the mevalonate and methylerythritol 4-phosphate (MEP) pathways (Begley, Gahan *et al*. 2004). Isoprenoids and in particular the end metabolite of the pathway isopentenyl pyrophosphate (IPP) are utilised for essential components and biochemical processes within the cell.

Previously, it was shown in our lab by Heuston *et. al*. (Heuston, Begley *et al*. 2012) that a deletion mutant in the gene lmo0825 (encoding HMG-CoA reductase) of *L. monocytogenes* is dependent upon the addition of exogenous mevalonate to support normal growth of the bacteria in normal media. This suggested that HMG-CoA reductase is a critical enzyme for cell viability and indicated that perhaps the mevalonate pathway rather than the MEP pathway is central to survival in this organism. Herein we wished to determine if another enzyme in the mevalonate pathway (HMG-CoA synthase) is also essential for survival of the pathogen.

Initial work in this study focussed on generating a clean deletion mutant in the lmo1415 gene for HMG-CoA synthase by using the spicing by overlap extension (SOE) PCR technique described by Horton and co-workers (Horton 1995). We successfully created a mutant using the pORI280 *rep*A- plasmid (Monk, Gahan *et al*. 2008) integration system which permitted double crossover and gene replacement with a mutated gene fragment. Interestingly, growth experiment analysis of *ΔmvaS*

(lmo1415) mutant in normal growth media (Fig.5.) and defined media (Fig.6.) revealed that knockout of the HMG-CoA synthase gene in did not adversely affect growth compared to the wild type and MEP pathway mutants *ΔgcpE* (lmo1441) and *ΔlytB* (lmo1451). In contrast, only the *ΔhmgR* (lmo0825) mutant required the addition of mevalonate to accommodate growth. This study suggests that the gene encoding HMG-CoA synthase is non-essential for the normal growth *of L. monocytogenes* EGDe despite the gene encoding the downstream enzyme of the pathway (HMG-CoA reductase), previously being shown to be a key enzyme (Heuston, Begley *et al*. 2012).

The *ΔmvaS* (lmo1415) mutant was examined phenotypically in order to determine the potential effect of the mutation upon growth and survival under different environmental conditions. In particular mutation of HMG-CoA reductase has previously been shown to influence susceptibility to Triton-X induced cell wall autolysis, hydrogen peroxide mediated oxidative stress of the cell and sensitivity to cell wall synthesis antibiotics indicating that it plays a role in resistance to cell envelope stresses (Heuston, Begley *et al.* 2012). In contrast, our *ΔmvaS* mutant was affected under similar conditions. Deletion of HMG-CoA synthase did not significantly increase susceptibility to Triton-X (Fig.9.), hydrogen peroxide (Table 3) or the cell wall antibiotics Penicillin or Ampicillin (Table 4) comparable to the wild type *L. monocytogenes* EGDe. Similarly, we determined no difference between the HMG-CoA synthase mutant in their ability to infect J774 macrophages (Fig. 7.) or ability to infect mice (Fig.10.). Likewise, we found no increased sensitivity of HMG-CoA synthase mutant when exposed to a commonly used HMG-CoA reductase inhibitor (Rosuvastatin) under normal growth conditions compared to the wild type (Fig.8.).

Collectively the data suggest the possibility of an alternative enzyme capable of generating HMG-CoA in *L. monocytogenes* but currently improperly annotated within the EGDe genome. Analysis of KEGG pathways for bacterial synthesis of HMG-CoA (Fig.4.) highlights an alternative means of generating this substrate that potentially proceeds in other bacterial species and *L. monocytogenes* EGDe via the activity of methylglutaconyl-CoA hydratase (E.C. 4.2.1.18) involved in the degradation of valine, leucine and isoleucine (lmo00280). Extensive KEGG pathway and bioinformatics searches of *Listeria* genomes failed to identify a properly annotated homologue of this enzyme in *L.monocytogenes* EGDe. Bioinformatic analysis of the methylglutaconyl-CoA hydratase only revealed presence of this enzyme in a more distantly related *Listeria* species (*L. fleischmanni*) which was likely used for construction of the KEGG pathway for valine, leucine and isoleucine degradation for *Listeria* genomes (data not shown). It is possible that an alternative mechanism exists for providing the substrate in *L. monocytogenes* EGDe which renders the HMG-CoA synthase enzyme redundant at least under the conditions tested here which may involve methylglutaconyl-CoA hydratase. Further to this, extensive bioinformatics analysis of the HMG-CoA synthase enzyme determined only a single functional copy of this gene (*mvaS*) in the *L. monocytogenes* EGDe genome by Basic Local Alignment Search Tool (BLAST) analysis that was deleted in this study (data not shown). In order to investigate this hypothesis further I suggest that future studies could generate a transposon bank within the HMG-CoA synthase mutant and analyse this bank for clones incapable of growth in the absence of mevalonate.

References

Begley, M., P. A. Bron, et al. (2008). "Analysis of the isoprenoid biosynthesis pathways in Listeria monocytogenes reveals a role for the alternative 2-C-methyl-D-erythritol 4-phosphate pathway in murine infection." Infect Immun **76**(11): 5392-5401.

Begley, M., C. G. M. Gahan, et al. (2004). "The interplay between classical and alternative isoprenoid biosynthesis controls [gamma][delta] T cell bioactivity of Listeria monocytogenes." FEBS Letters **561**(1-3): 99-104.

Farber, J. M. and P. I. Peterkin (1991). "Listeria monocytogenes, a food-borne pathogen." Microbiol Rev **55**(3): 476-511.

Heuston, S., M. Begley, et al. (2012). "HmgR, a key enzyme in the mevalonate pathway for isoprenoid biosynthesis, is essential for growth of Listeria monocytogenes EGDe." Microbiology **158**(Pt 7): 1684-1693.

Horton, R. M. (1995). "PCR-mediated recombination and mutagenesis. SOEing together tailor-made genes." Mol Biotechnol **3**(2): 93-99.

Istvan, E. S. and J. Deisenhofer (2001). "Structural mechanism for statin inhibition of HMG-CoA reductase." Science **292**(5519): 1160-1164.

Jerwood, S. and J. Cohen (2008). "Unexpected antimicrobial effect of statins." J Antimicrob Chemother **61**(2): 362-364.

Jorens, P. G., K. E. Matthys, et al. (1995). "Modulation of nitric oxide synthase activity in macrophages." Mediators Inflamm **4**(2): 75-89.

Lauer, P., M. Y. Chow, et al. (2002). "Construction, characterization, and use of two Listeria monocytogenes site-specific phage integration vectors." J Bacteriol **184**(15): 4177-4186.

Leenhouts, K., G. Venema, et al. (1998). "A lactococcal pWV01-based integration toolbox for bacteria." Methods in Cell Science **20**(1-4): 35-50.

Monk, I. R., C. G. Gahan, et al. (2008). "Tools for functional postgenomic analysis of listeria monocytogenes." Appl Environ Microbiol **74**(13): 3921-3934.

Perez-Gil, J. and M. Rodriguez-Concepcion (2013). "Metabolic plasticity for isoprenoid biosynthesis in bacteria." Biochem J **452**(1): 19-25.

Popowska, M., M. Kusio, et al. (2009). "Inactivation of the wall-associated de-N-acetylase (PgdA) of Listeria monocytogenes results in greater susceptibility of the cells to induced autolysis." J Microbiol Biotechnol **19**(9): 932-945.

Premaratne, R. J., W. J. Lin, et al. (1991). "Development of an improved chemically defined minimal medium for Listeria monocytogenes." Appl Environ Microbiol **57**(10): 3046-3048.

Reid, G. A. (1991). "Molecular cloning: A laboratory manual, 2nd edn: by J. Sambrook, E. F. Fritsch and T. Maniatis, Cold Spring Harbor Laboratory Press, 1989. $115.00 (3 vols; 1659 pages) ISBN 0 87969 309 6." Trends in Biotechnology **9**(1): 213-214.

Rodríguez-Concepción, M. and A. Boronat (2013). Isoprenoid Biosynthesis in Prokaryotic Organisms. Isoprenoid Synthesis in Plants and Microorganisms. T. J. Bach and M. Rohmer, Springer New York**:** 1-16.

Chapter 5

The effects of (E)-4-hydroxy -3-methyl-but-2-enyl pyrophosphate (HMBPP): a potential pathogen associated molecular pattern (PAMP) on human THP-1 cells

* A manuscript is currently being prepared based on research conducted in this chapter for publication.

Abstract

We examined the bacterial metabolite (E)-4-hyroxy-3-methyl-but-2-enyl pyrophosphate (HMBPP), a potential pathogen associated molecular pattern (PAMP) as a mediator of immunity in antigen presenting cells. HMBPP is a key intermediary metabolite of the 2-C-methyl-$_D$-erythritol 4-phosphate (MEP) pathway in the bacterial non mevalonate pathway for isoprenoid biosynthesis. We show by MACE RNA-seq analysis that a biologically relevant concentration of exogenous HMBPP is able to elicit significant gene expression activation in "dendritic-like" THP-1 cells without a cellular permeabilisation agent and does not significantly impair cell viability. HMBPP significantly activated genes (including *CCL4*, *IL-17D, TNFAIP6, CCL22, FCGR2B, FCGR3B, TRAIL-R*) involved in a number of immune and antigenic presentation pathways; (cytokine-cytokine receptor interactions, phagosome formation, apoptosis, toll-like receptor signalling, NFκB signalling and MAPK signalling pathways). Further qRT-PCR analysis of HMBPP-activated genes in THP-1 cells infected, with wild type and HMBPP under-producing (*ΔgcpE*) and HMBPP over-producing (Δ*lytB*) mutant *L. monocytogenes* EGDe strains showed that HMBPP likely plays a small yet important role in overall bacterial infection through other biological PAMPS's most likely mask its effect. Our data suggest that HMBPP is an important signalling molecule potentially priming antigen presenting cells for stimulation of a γδ T-cells response during bacterial infection.

Introduction

(E)-4-hydroxy-3-methyl-2-but-2-enyl pyrophosphate (HMBPP) is the last small metabolite molecule (<500Da) of the 2-C-methyl-$_D$- erythritol 4-phosphate (MEP) pathway utilised by many bacterial and protozoan species known to infect mammals (humans) either systemically in the case of malaria (*Plasmodium falciparum*) (Rekittke, Olkhova *et al.* 2013) or via the gastrointestinal tract (for example *L. monocytogenes*) (Ryan-Payseur, Frencher *et al.* 2012). The MEP pathway exists as an alternative to the mevalonate pathway for the formation of IPP (isopentyl diphosphate) and DMAPP (dimethylallyl diphosphate) (Fig. 1), which are essential five carbon isoprene precursors leading to the formation of isoprenoid biomolecules (Begley, Gahan *et al.* 2004). Isoprenoids and their derivatives play functional and metabolic roles in many aspects of biology; for example as a part of cellular organelles, electron transport pathways, signal transduction pathways, mating pheromones and even in photosynthesis to name a few (Sacchettini and Poulter 1997).

Amslinger and colleagues (Amslinger, Hecht *et al.* 2007) have shown that HMBPP can activate Vγ9/Vδ2 human T cells *in-vitro* at concentrations as low as $EC_{50} = 70pM$ (10^{-12} moles) in the presence of antigen presenting cells (APCs). The isoprene molecule IPP was generally found to be 150 times less stimulatory for Vγ9/Vδ2 human T cells compared to HMBPP in the presence of APCs (Eberl, Altincicek *et al.* 2002). This was determined comparing wild type and *ΔlytB* (for HMBPP conversion) *Escherichia coli,* a microorganism that exclusively utilises the MEP pathway. HMBPP was released from the bacterial cultures by sonication and filtered (Millipore) of live cells producing low weight molecular extracts. Exposure of these extracts to γδ T-cells (in the presence of APCs) resulted in reduced

expansion and proliferation for the *ΔlytB* mutant compared to the wild type,

affirming the strong immune potential of HMBPP (Eberl, Altincicek *et al.* 2002).
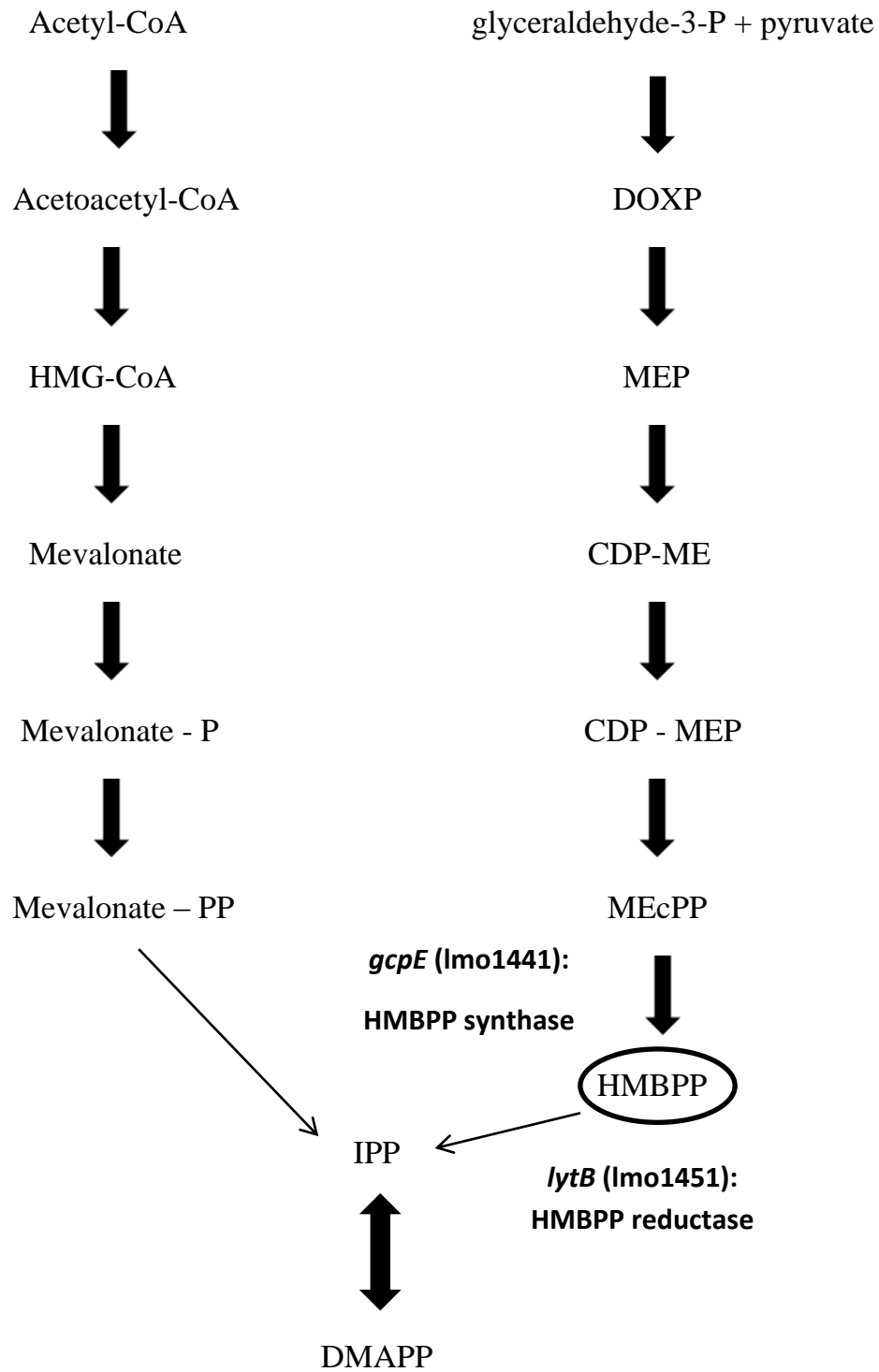
**Fig.1. Formation of IPP/DMAPP, during isoprenoid biosynthesis via the mevalonate pathway or the MEP pathway.**

Highlighted; the penultimate metabolite of the MEP pathway (HMBPP), a major immunostimulator of Vγ9/Vδ T cells, HMBPP synthase (*gcpE*) for HMBPP synthesis from MEcPP and HMBPP reductase (*lytB*) for HMBPP conversion to IPP as characterised in *L. monocytogenes* EGDe. Figure was adapted from (Begley, Gahan *et al*. 2004).

HMBPP essentially meets all the criteria to be considered a pathogen associated molecular pattern (PAMP); it can be produced by certain pathogenic microorganisms such as those that cause malaria and listeriosis (as previously mentioned) but also by other infectious bacteria of the gastrointestinal tract such as *Helicobacter pylori*, *Escherichia coli* 0157, *Salmonella enterica* and even *Legionella pneumophila* (Eberl and Moser 2009).

HMBPP has a small molecular weight of around 260gmol^{-1} and is a major stimulator of the immune system via Vγ9/Vδ2 T cells as previously mentioned. However, at the moment there is very little known concerning the ability of APCs to process and present HMBPP to T-cells following bacterial phagocytosis (Fig. 2) (Hepworth and Sonnenberg 2014). It is estimated that sonicated lysates of *E. coli* and *L. monocytogenes* generally contain around 200-300mM of HMBPP (Eberl, Roberts *et* al. 2009). Despite this relatively high bacterial concentration numerous studies suggest nanomolar concentrations of HMBPP (EC$_{50}$ of 0.1nM) potently activate γδ T-cells in presence of APCs (Hintz, Reichenberg *et al*. 2001; Eberl, Hintz *et al.* 2003).

THP-1 human monocytic cell line were utilised to examine the molecular response in the antigen presenting cell to HMBPP. THP-1 cells are an immortalised cell line derived from an acute monocytic leukaemia patient that can be differentiated by the addition PMA and IL-4 into "dendritic-like" APCs. Cell viability, MACE RNA-seq and qRT-PCR analysis was performed following

exposure to HMBPP. Host genes induced by HMBPP were subsequently examined

in THP-1 cells infected with wild type, *ΔgcpE* (HMBPP under-producing), *ΔlytB*

(HMBPP over-producing), *L. monocytogenes* EGDe mutants.
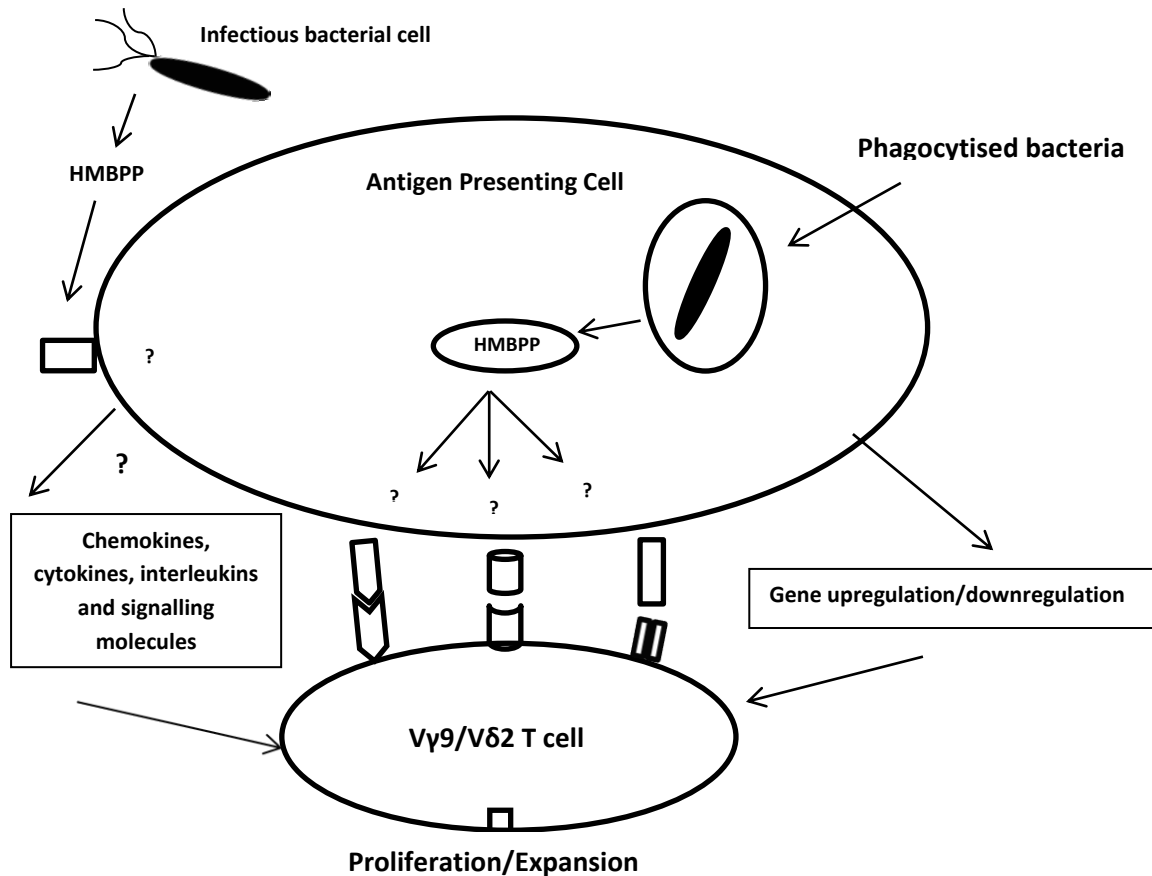
Fig.2. Representation of a HMBPP-producing bacterium infecting an antigen presenting cell. The bacterial cell is engulfed by the phagocytic cell. HMBPP is released following engulfment or recognised at the cell surface of the APC cell triggers HMBPP-specific activation and processing of this pathogen associated molecular pattern (PAMP) at the cell surface which is recognised by Vγ9/Vδ2 T cell eliciting proliferation and expansion. Much remains to be discovered about the cellular interactions between cells of the innate immune response (dendritic cells) and HMBPP. This figure was modified from; (Bonneville and Scotet 2006)

Materials and Methods

Culturing of THP-1 cells:

THP- 1 ATCC TIB-202 (human monocytic) immortalised cells derived from an acute monocytic leukaemia patient were obtained from frozen stocks at University College Cork. Cells were routinely cultured and maintained in RPMI-1640 media (Sigma Alrdich) supplemented with 10% (v/v) (FBS) Foetal Bovine Serum (Gibco) and 1% (v/v) Penicillin-Streptomycin (P/S) (Sigma Aldrich). Media was changed on average every 2-3 days by centrifuging the cell suspension at 250rcf/g for 5mins and aspirating off the old media. The cell pellet was subsequently resuspended in RPMI-1640 supplemented media and seeded into fresh tissue culture flasks (Sarstedt), cells were counted by Trypan Blue exclusion (haemocytometry) and maintained at a cell density never more confluent than 2×10^6 cells/ml. The cells were grown at 37ºC in a 5% CO_2 supplemented incubator and monitored regularly under the inverted light microscope.

Differentiation of THP-1 cells:

For this study, THP-1 cells were differentiated into "dendritic-like" cells by the addition of 10ng/ml PMA (Phorbal 12-myristate 13-acetate) (Sigma Aldrich) and 20ng/ml IL-4 (human interleukin 4) to RPMI-1640 supplemented media with FBS and P/S and incubation over 96 hours at 37ºC with 5% CO_2. PMA was obtained in a powder form and resuspended in sterile chloroform at 0.1mg/ml and similarly for IL-4 which was resuspended as a 10µg/ml solution in sterile water. Following, cell counting by the haemocytometer the required cell density was determined and the cell suspension centrifuged to obtain a cell pellet which was, subsequently

resuspended in differentiation media. Cells were monitored regularly under the inverted light microscope to observe the establishment of a "dendritic-like" cell monolayer.

Preparation of HMBPP and the digitonin permeabilisation buffer:

(E)-4-hydroxy-3-methyl-but-2- enyl pyrophosphate (HMBPP) was obtained from Echelon® (675 Arapeen Drive, Suite 302, Salt Lake City, UT 84108) (Product code: I-M055) in powder form as an ammonium salt and resuspended in endotoxin-free sterile water to a working concentration of 1mg/ml. Serial dilutions for cell culture work were performed in Phosphate Buffered Saline (PBS) (Sigma Aldrich) to obtain nano molar concentrations of HMBPP. In order to aid uptake of HMBPP by "dendritic-like" cells, a digitonin permeabilisation buffer was prepared (Woodward, Iavarone *et al*. 2010) allowing permeability across the cell membrane. Digitonin was ordered in a powder form (Sigma Aldrich, Product code: D5628) and resuspended in 96% sterile ethanol to a stock concentration of 10mg/ml and stored at -20ºC ready for use. Other stock solutions for the permeabilisation buffer were prepared as follows: Bovine Serum Albumin (BSA) 20% (w/v), HEPES 1M, Potassium chloride (KCl) 1M, Magnesium chloride ($MgCl_2$) 1M, Dithiothreitol (DTT) 1M, Sucrose (1M), Adenosine tri phosphate (ATP) 0.1M and Guanosine-5'-triphosphate (GTP) 0.1M in sterile water and filter sterilised using a 0.22µm filtration apparatus. The digitonin permeabilisation solution was subsequently prepared in sterile PBS at the following final concentrations: (BSA (0.2%), HEPES (50mM), KCl (100mM), $MgCl_2$ (3mM), DTT (0.1nM), Sucrose (85mM), ATP (1mM), GTP (0.1mM)). A 10X volume of digitonin mixture was combined with HMBPP to obtain final desired concentration of phosphoantigen. Cell culture media was aspirated off the cells and subsequently 50µL of combined mixture added for cell viability testing (96-well

plate) or 500μL for RNA extractions (6-well plate). Cells were incubated for 30mins at 37ºC with 5% CO_2 and afterwards the solution was removed and fresh RMPI-1640 media supplemented with FBS and P/S added. Cells were incubated over 24 hours and analysed for cell viability or RNA extraction (qRT-PCR).

CellTitre-Glo® Luminescent Cell Viability assay:

The CellTiter-Glo® luminescent cell viability assay was purchased from Promega® (Cat No#G7570) and used to determine the number of viable cells in our cell culture assays. Viability was quantified using the luciferase reaction to measure ATP formed by viable cells. Levels of ATP measured directly correlate with cell viability. If cells lose membrane integrity, and are killed as a result of HMBPP or digitonin treatment, they will lose the ability to synthesize ATP and endogenous ATPases will destroy any remaining ATP in the sample. For this study, 50,000 differentiated (dendritic-like) cells/cm^2 were seeded in a total volume of 100μL cell culture media (as above) directly into each well (Thermo Scientific® white flat bottom nunclon delta surface 96-well plate Cat No# 136101) and incubated for 96hours. A range of HMBPP concentrations were tested on the cells: 0.05nM, 0.1nM and 1nm for cell viability. A number of controls were also assayed (untreated cells, digitonin control (1) - complete digitonin buffer without HMBPP, digitonin control (2) - digitonin buffer without added ATP/GTP or HMBPP and HMBPP diluted in PBS only)). ATP/GTP controls were analysed for cell viability analysis of the digitonin buffer. Prior to the assay being carried out , the Cell Titre Glo® substrate and Cell Titre Glo® buffer were combined in a 1:1 ratio to form the Cell Titre Glo® reagent providing luciferin, luciferase and other reagents required to lyse the cells, inhibit endogenous ATPases and allow for the bioluminescent reaction to occur. Following treatment with HMBPP/digitonin (see above), 100μL (equal volume) of the Cell

Titre Glo® reagent was applied to the treated cells, the plate was covered with tinfoil to protect from light and thoroughly mixed on an orbital shaker at 200rpm for 2mins to induce cell lysis. The plate was incubated at room temperature for 10mins to stabilize luminescent signal and read on a microtitre plate reading installed with the Promega® Cell Titre Glo software. Results were recorded and graphed as RLU (relative light units) using the Graph Pad Prism5 ® software package. Statistical analysis was performed on the different test groups via the Student's T-test.

RNA extraction from THP-1 cells:

In a similar manner, to the cell viability assays, 50,000cells/cm^2 were seeded into each well of 6-well plate (Sarstedt) in a total volume of 2ml cell media. The differentiation and treatment of the cells with HMBPP/digitionin was carried out as described previously. 1nM HMBPP was chosen for this study based on the optimal cell viability readings. The following groups were used for MACE RNA-seq analysis: (untreated cells, digitonin only control, HMBPP treated only and HMBPP + digitonin). Total RNA extractions were performed 24 hours following treatment of "dendritic-like" cells with HMBPP by lysing the cell monolayer with Lysis Buffer from the BIOLINE® ISOLATE RNA mini kit and following the instructions outlined in the manual (Cat. No. BIO-52043) and then quantified on the NanoDrop ® and stored at -80ºC to preserve samples.

Massive Analysis of cDNA Ends (MACE) RNA-seq analysis:

MACE (Massive Analysis of cDNA Ends) is an accurate deep sequencing-based technology for high-resolution, global gene expression profiling (Zawada, Rogacev *et al.* 2014). MACE analysis of RNA samples in this study was performed by Genxpro GmbH, Altenhöferallee 3, 60438 Frankfurt am Main, Germany. MACE is as a digital gene expression analysis method, in which each cDNA molecule is represented by one cDNA fragment (tag) of 94 base pairs, originating from a region approximately 100-500 base pairs upstream from the 3' end (poly-A tail) of the transcript. MACE is a high resolution gene expression analysis method that is capable of revealing differential expression in low abundance transcripts that might not otherwise be detected using conventional microarrays. MACE RNA-seq provides 20 times greater sequencing depth compared with other methods (Asmann, Klee *et al*. 2009). For preparation of the MACE library, 2µg/sample total RNA was extracted from cells (UCC), cDNA was synthesised by first and second strand synthesis (SuperScript® 3 First-Strand Synthesis System (Life Technologies Gmbh)) with modified and barcoded poly-T adapters for binding Illumina Hiseq2000 flow cell and biotinylated at the 5' end (Genxpro). Subsequently, biotinylated cDNA are fragmented into approximately 250 base pair segments and are bound to streptavidin beads (Genxpro). TrueQuant adapters were ligated onto each of the fragments (Genxpro). For quantification of gene expression, MACE reads in the library were poly-A trimmed and the marked quality (Genxpro). Reads were mapped onto the human genome using the Novoalign® software package (http://novocraft.com/) (Genxpro). Mapped coordinates were overlapped with the RefSeq® annotation track system via the UCSC table browser (http://genome.ucsc.edu/cgi-bin/hgTables?command=start). The DEseq® package

was used to normalise and test differential gene expression using statistical programming language R (www.r-project.org/) (Anders and Huber 2010) (Genxpro). Gene ontology (GO) enrichment analysis was performed using the GO-enrichment analysis toolkit (http://genxpro.ath.cx) based on the Fischer's exact test for differentially expressed transcripts with a p-value less than 0.05 (Genxpro). Differentially expressed genes from MACE RNA-seq analysis were organised by Genes Ontology designation and associated KEGG pathways using GATHER® (http://gather.genome.duke.edu), Duke University, NC, USA) and Subio® (Subio Inc., Japan) (UCC in collaboration with Dr. John Mac Sharry (JMS)). Differentially expressed genes in the dataset were screened for significance by initial stringent criteria reducing to 1.5 fold differential and *P*<0.05 cut off (UCC). Functional classification and annotation chart analysis was carried out using the web-based resources, GATHER® (http://gather.genome.duke.edu). Pathway visualisation was carried out using Subio software to identify the differentially expressed genes between assays (UCC). MACE RNA-seq analysis was confirmed by qRT-PCR analysis for selected altered genes (*CCL4, IL-17D, TNFAIP6, CCL22, FCGR2B* and *FCGR3B*).

Microscopy of THP-1 cells:

Light microscope images were taken of differentiated "dendritic-like" THP-1 cells treated and untreated with HMBPP or digitonin under the Nikon Eclipse TE2000-S and Olympus DP70 inverted light microscope and camera at 10X magnification. Cells were examined for dendritic cell morphology and an adherent pattern to the cell monolayer. Any changes in cell morphology were recorded.

L. monocytogenes EGDe infection of THP-1 cells:

THP-1 cells were routinely maintained and differentiated for bacterial infection as described previously. 5×10^5 cells/ml were seeded into 6-well cell culture plates (SARSTEDT) in a total volume of 2ml of RPMI-1640 media. After 96 hours differentiation, cells were infected with 5×10^6 CFU/ml overnight cultures of PBS-washed and DMEM-resuspended (no antibiotic), *L. monocytogenes* EGDe wild type, lmo1441 (Δ*gcpE*) HMBPP-under producing mutant, lmo1451 (Δ*lytB*) HMBPP-overproducing mutant and mock infection to a multiplicity of infection of (1:10) in triplicate. Bacteria were allowed to internalise for 2 hours at 37ºC/5% CO_2. Subsequently inoculum was removed and monolayer was washed once with 2ml PBS. 2ml gentamicin (50µg/ml) (Sigma-Aldrich) was resuspended in DMEM, applied to the monolayer and incubated for a further hour. The monolayer was washed twice with PBS and incubated for a further 5 hours post infection with plain DMEM. Post infection media was removed from cells and RNA was extracted as previously described above using the BIOLINE® ISOLATE RNA mini kit. qRT-PCR analysis was subsequently performed on potential genes altered by HMBPP (Table 1). Bacterial counts (CFU/ml) were also performed by cell lysis of the monolayer with 0.1% (v/v) Triton X-100, serial dilution and spread plating on BHI agar.

Reverse Transcription (RT) and cDNA synthesis:

Total RNA extracted from the THP-1 cell assay system. Complementary DNA (cDNA) synthesis was performed using the Applied Biosystems® Veriti 96-well thermal cycler. Transcriptor reverse transcriptase enzyme, a random (nonamer) primer, deoxynucleoside triphosphates (dNTP's) and RNase inhibitor (all Roche®)

were used for the reaction. 100ng of RNA in 10μL PCR grade water (Roche) was diluted for each sample. Master mix was made up with 5X Transcriptor buffer (Roche #3531287001), Protector RNase inhibitor (Roche #3335402001), PCR nucleotide mix (Roche #11814362001) in a total volume of 20μL per reaction as follows: (4μL Transcriptor RT buffer, 2μL nucleotide mix, 1μl Transcriptor RT enzyme, 3μL Random primer) to which the 10μL of RNA sample was to the PCR tube. Control negative RT reactions (without RT enzyme or RNA) were performed to check for potential contamination. RT reaction was carried out under the following conditions (10mins at 25ºC, 30mins at 55ºC, 5 mins at 85ºC and held at 4ºC forever).

Probe library primer design for qRT-PCR:

Left (L) and Right (R) primers were subsequently designed for qRT-PCR analysis. The Human Gene Compendium® (http://www.genecards.org) was searched for potential matches including potential intron spliced variants (exons) for candidate genes and reference mRNA sequence obtained from the National Centre for Biotechnology Information (NCBI) RefSeq database. PCR primer pairs were designed using the Roche ProbeFinder® Version 2.5 web based software package (design centre) for candidate human genes (see below)

Primer	Sequence
hACTB_PL64_L	ccaaccgcgagaagatga
hACTB_PL64_R	ccagaggcgtacagggatag
hCCL4_PL40_L	ctctccagcgctctcagc
hCCL4_PL40_R	accacaaagttgcgaggaag
hIL17D_PL27_L	cctgaagcctactgcctgtg
hIL17D_Pl27_R	acggtgggcatgtagacag
hTNFAIP6_PL34_L	ggccatctcgcaacttaca
hTNFAIP6_PL34_R	cagcacagacatgaaatccaa
hCCL22_PL51_L	cgtggtgaaacacttctactgg
hCCL22_PL51_R	ccttatccctgaaggttagcaa
hFCGR2B_PL14_L	ctgcaggaaaaagcggatt
hFCGR2B_PL14_R	ggtttctcagggagggtctct
hFCGR3B_PL9_L	gggcttgttgggagtaaaaa
hFCGR3B_PL9_R	acttggtacccaggtggaga

Quantitative Real Time PCR (qRT-PCR) and mRNA expression:

qRT-PCR was performed on the Roche® LightCycler 480 system and analysed

using the Roche® LightCycler software package. Reactions were carried out using

384-well white lightcycler480 plates (Roche#4729749001) in a total volume of

10μL and were performed as follows: (5μL 2X LG480 mastermix, 1μL L+R primers

(combined), 0.1μL PL probe, 2.9μL PCR grade water and 1μL cDNA sample).

Negative no RT (reverse transcriptase) and no RNA controls were also analysed by

RT-PCR, to verify primer amplification and exclude probability of contamination.

The "housekeeping" gene beta-actin (β-Actin) was analysed as an invariant

endogenous control or reference gene for data normalization in gene quantification

analysis. Thermocycling conditions were as follows: 95ºC for 10mins initial

denaturation and activation of Taq polymerase followed by 45 cycles of 95ºC for

10secs, 50ºC for 20secs and 72ºC for 30secs with a ramping rate of 4.4ºC/second,

2.2ºC/second and 4.4ºC/second respectively, Fluorescence was measured once at

each 50ºC stage.

qRT-PCR statistical analysis and interpretation:

The C_t (threshold cycle value) was obtained for each gene of interest and for the housekeeping gene (β-actin) for each treatment group (Control, HMBPP, Digitonin and HMBPP + Digitonin) in the Roche® LightCycler 480. The C_t value represents the cycle number for the amplification curve fluorescence signal to cross the threshold and exceed background levels. The C_t value is inversely proportional to the quantity of target mRNA in each sample. C_t values below 35 cycles were generally regarded as acceptable reads for amplification. The $2^{-\Delta\Delta Ct}$ method (Livak and Schmittgen 2001) was used to calculate relative changes in gene expression. Statistical analysis was performed using the GraphPad prism software package

Results

Cell viability analysis of HMBPP and/or digitonin-treated THP-1 cells:

 THP-1 cells (50,000cells/cm^2) were treated with a range of concentrations of (E)-4-hydroxy-3-methyl-but-2-enyl pyrophosphate (HMBPP): 0.05nM, 0.1nM and 1nM with and without complete digitonin (1) or digitonin (2) excluding ATP/GTP (see Materials and Methods). Cell viability was measured using Promega CellTitre-Glo® luminescent cell viability assay kit (see Materials and Methods). Cell viability was read in a 96-well plate by luminescence RLU (relative light units) statistical analysis performed using the Student's T-test (Fig. 3 (A and B)).
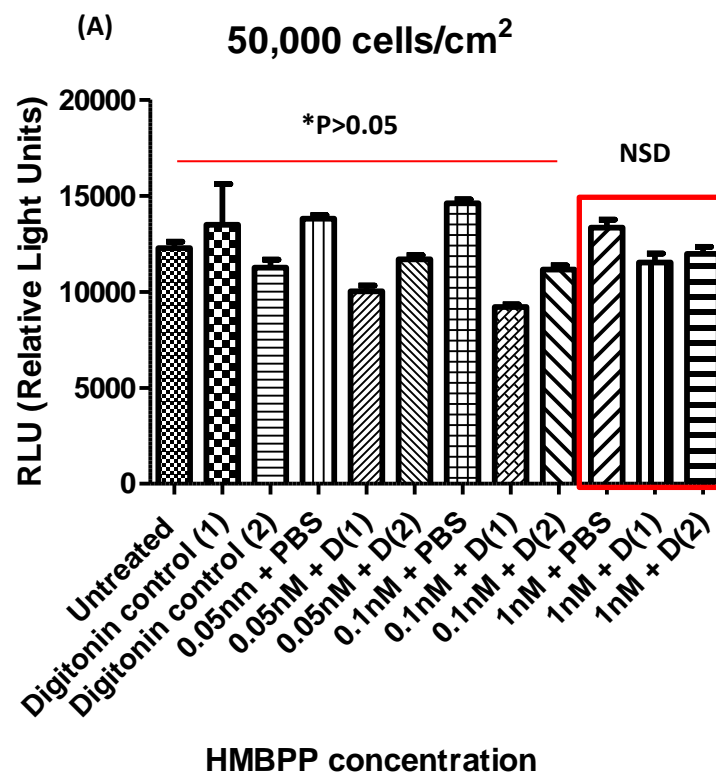
Fig. 3 (A). Cell viability analysis of THP-1 cells against 0.05, 0.1 and 1nM HMBPP with and without digitonin and with and without exogenous ATP/GTP.

50,000cells/cm^2 of THP-1 cells were exposed to HMBPP/digitonin treatment for 24 hours and examined for cell viability. Cellular ATP was measured using the Promega® CellTitre Glo cell viability assay kit for untreated THP-1 cells, HMBPP only, complete digitonin buffer (1) and digitonin buffer (2) without ATP/GTP. 0.05nM, 0.1nM and 1nM HMBPP was tested in this assay. Cell viability was determined in RLU (relative light units). 1nM HMBPP was found to give the most optimal cell viability readings for further analysis. NSD = No significant difference.
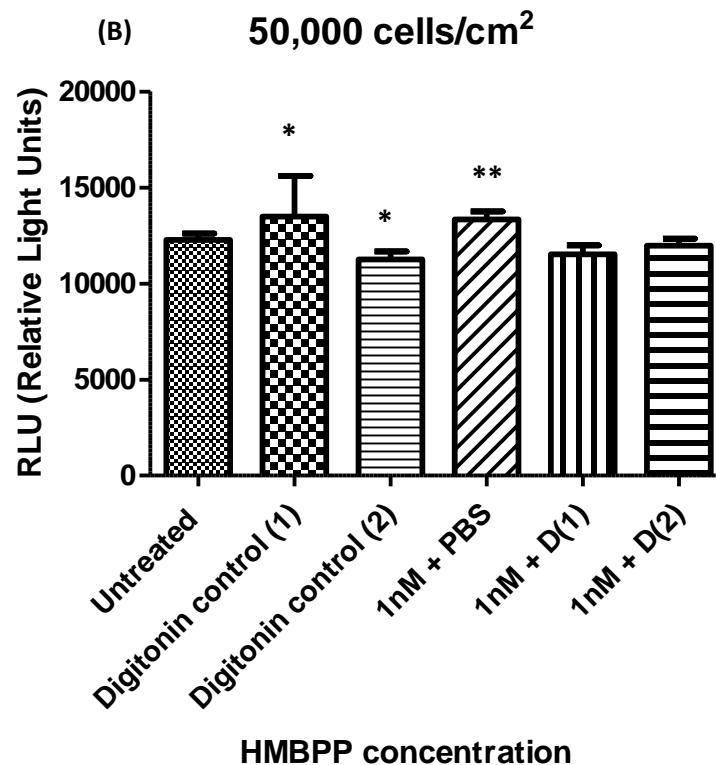
Fig. 3(B). Cell viability analysis of THP-1 cells treated and untreated with 1nm HMBPP, with or without digitonin controls.

Summary of T-test results: Digitonin control (2) vs. 1nM HMBPP + PBS (**p=0.0068), 1nM HMBPP + PBS vs. 1nM + Digitonin control (1) (*p=0.0112), 1nM HMBPP + PBS vs. 1nM Digitonin control (2) (*p=0.0486). All other groups compared were not found to be statistically significant. HMBPP on its own does not seem to adversely affect cell viability in the THP-1 cells compared to controls. HMBPP in combination with digitonin seems to negatively affect viability. Exogenous ATP/GTP did not seem to affect the cell viability assay.

Microscopy of THP-1 cells treated and untreated with HMBPP/digitonin:

10X magnification inverted light microscope images were captured of differentiated

THP-1 cells treated and untreated with HMBPP/digitonin. Cells were examined for

dendritic cell morphology and adherent patterns. HMBPP or digitonin did not

visually alter cell morphology in this study (Fig. 4).

Fig. 4. Inverted light microscope images (10X) of HMBPP/digitonin treated and untreated THP-1 cells.

THP-1 cells were observed to have dendritic cell morphology under the light microscope and a very adherent pattern on the cell monolayer. HMBPP or digitonin did not visually affect cell morphology.

MACE RNA-seq analysis of individual (triplicate) sample and grouped datasets for THP-1 treatments:

The Subio platform was used for analysing the complete MACE RNA-seq dataset in this study (Materials and Methods). A total of 28,538 potential signal reads from the entire human genome were identified for all treatment groups (Control, Digitonin, HMBPP only and HMBPP + Digitonin with n=3 per group). Further statistical analysis will be performed on the complete dataset under stringent criteria to begin to identify significant differentially expressed genes (Materials and Methods) Individual samples (A) and grouped (B) expression plots are illustrated (Fig. 5).

A. Individual (triplicate) analysed samples
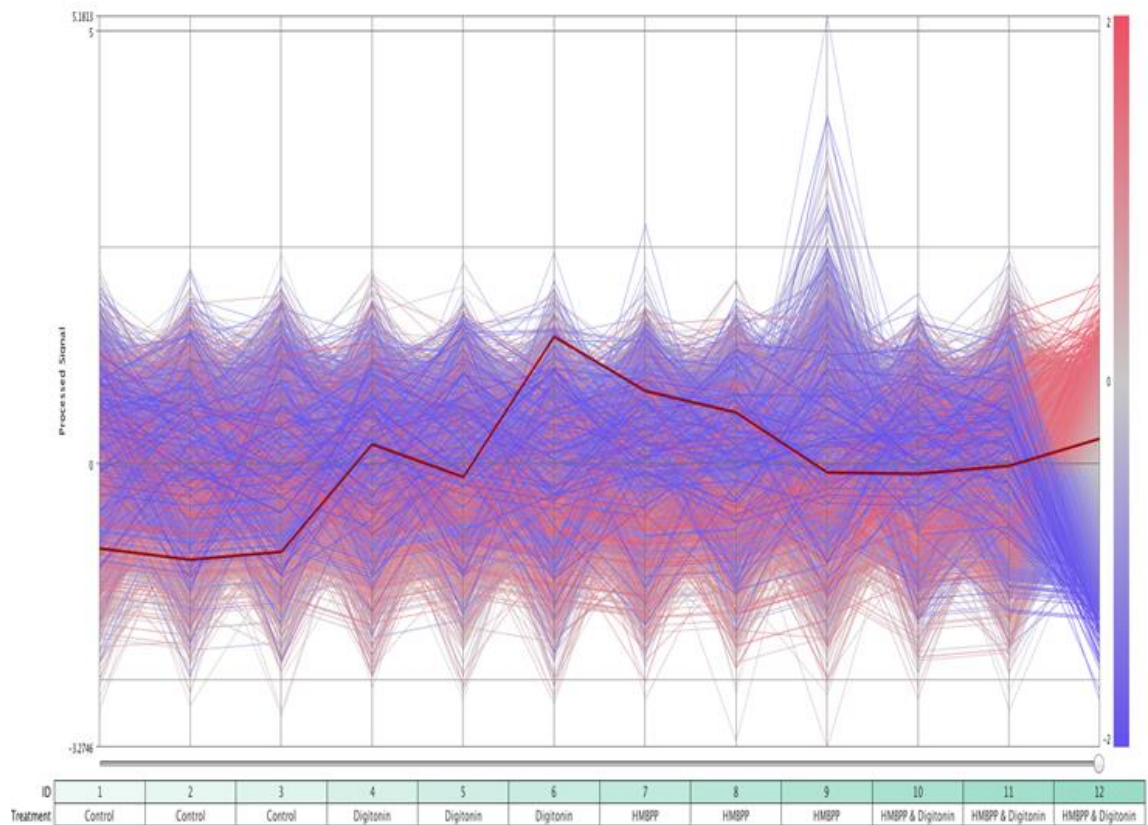
B. Samples grouped by treatment
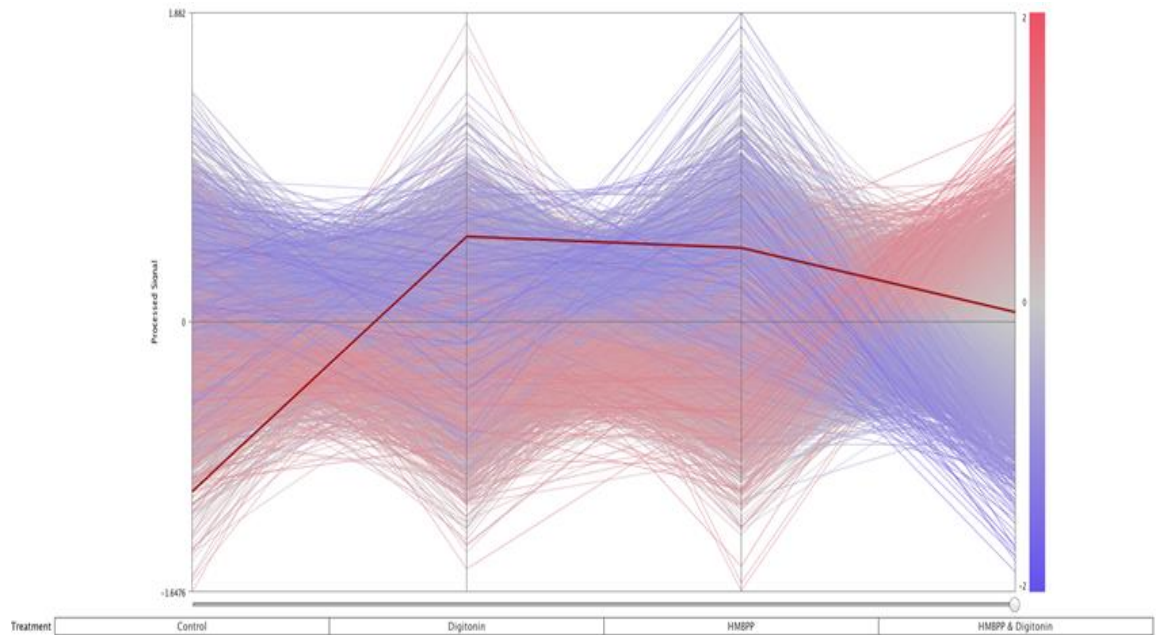
Fig.5. Subio expression plot of MACE RNA-seq dataset for all THP-1 treatments.

Illustration of differential expressed genes for individual triplicate samples (A) and grouped samples, n=3 per group (B) between groups (Control, Digitonin, HMBPP and HMBPP + Digitonin) for 28,538 candidate genes prior to statistical analysis. A randomly selected gene is highlighted in both figures. Red indicates an increase in expression and blue represents a decrease in expression relative to untreated cells (Control).

PCA analysis of complete MACE RNA-seq dataset:

Principle Component Analysis (PCA) was performed on the entire MACE RNA-seq dataset for all THP-1 treatment (Control (untreated), Digitonin, HMBPP and HMBPP + Digitonin) (Fig. 6). Differential expression profiles were demonstrated for each treatment that was generally satisfactory for grouped (A) and individual samples (B) in the overall dataset.
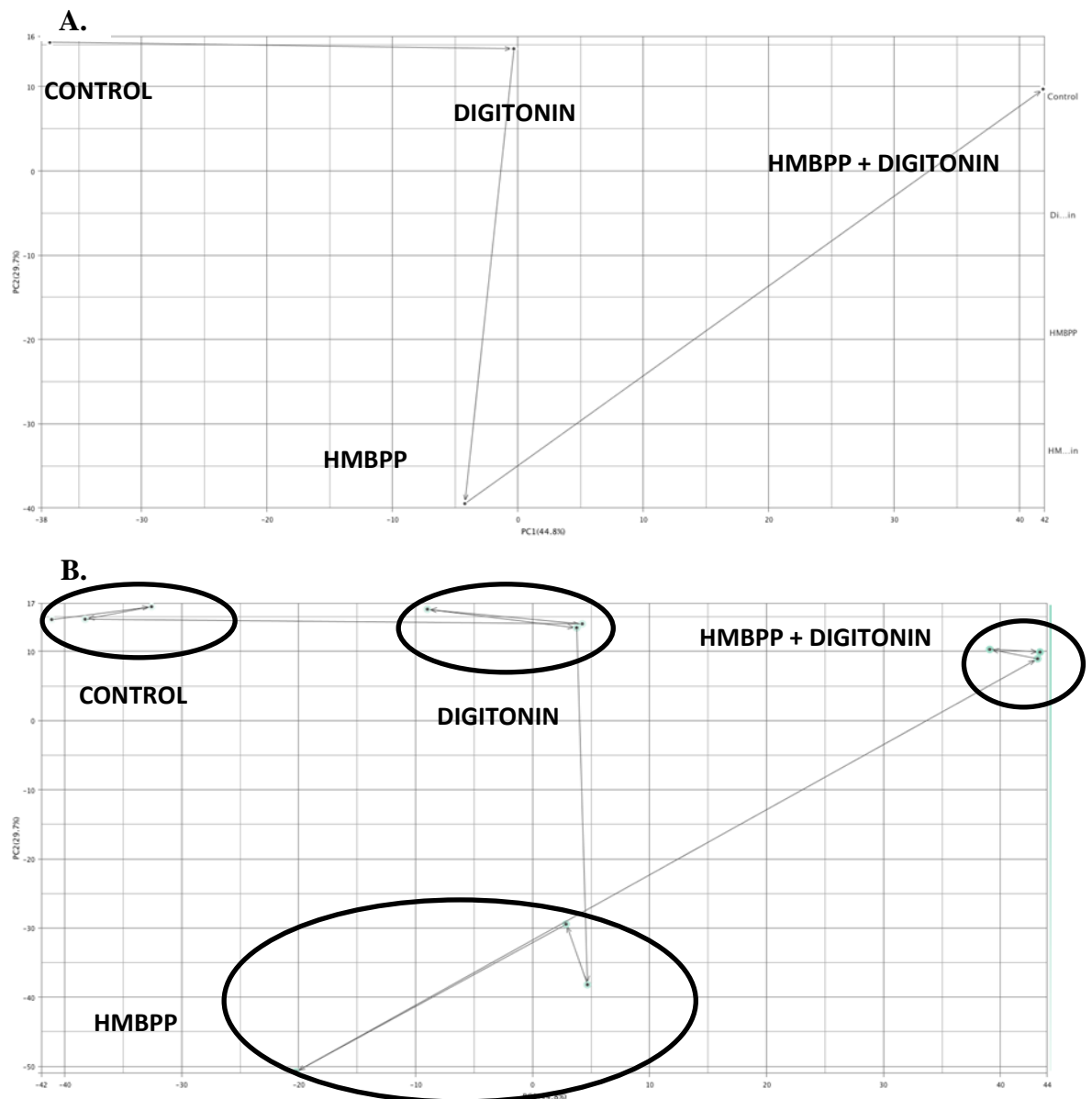
Fig. 6. Subio Principal Component Analysis (PCA) of complete THP-1 MACE RNA-seq dataset.

PCA analysis of grouped (n=3 per group) (A) and individual samples (B) for THP-1 treatments (Control (untreated), Digitonin, HMBPP and HMBPP + Digitonin).

Statistical analysis to determine differentially expressed genes:

Statistical analysis was performed on the complete dataset to narrow down candidate genes differentially expressed following THP-1 treatment (Control (untreated), Digitonin, HMBPP and HMBPP + Digitonin). A total of 589 genes were determined based on stringent selection criteria (1.5 fold differential and $P<0.05$ cut off) for all treatments and compared with Control (untreated) group (Fig. 7).

A.
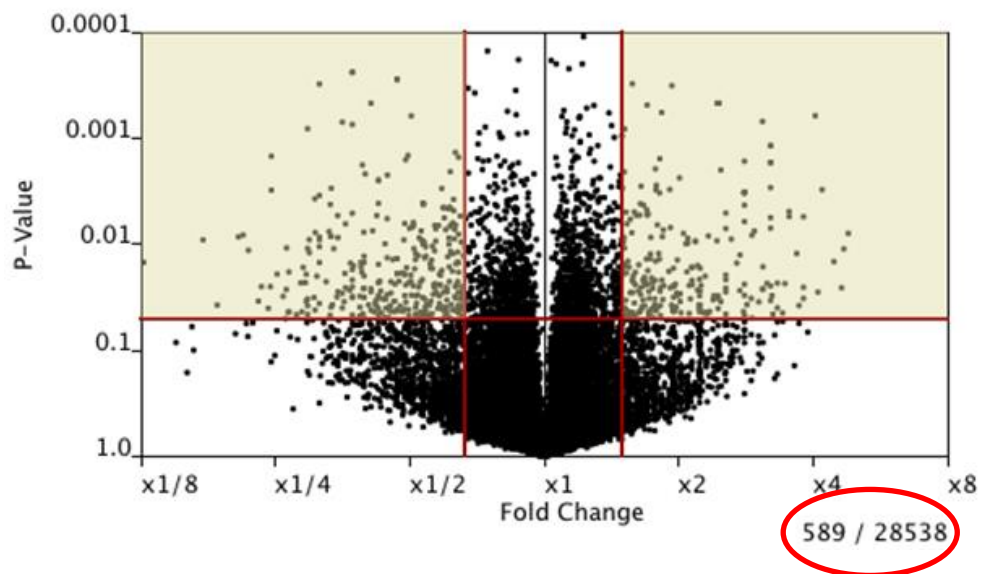
B.
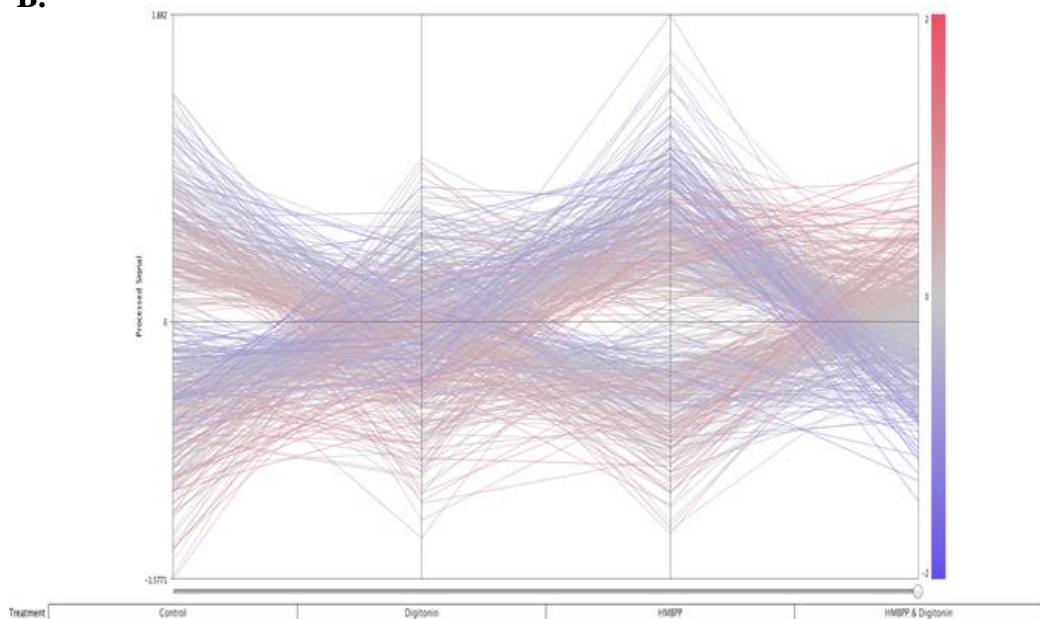
Fig.7. **Scatter plot (A) and expression plot (B) representation of 589 differentially genes selected by statistical analysis of THP-1 MACE RNA-seq dataset.**

589 genes were determined under stringent criteria (1.5 fold differential and P<0.05 cut off) for control and treatment groups (Control, Digitonin, HMBPP, HMBPP + Digitonin). Red indicates an increase in expression and blue represents a decrease in expression relative to control (untreated) group.

Heat map representation of 589 differentially expressed genes:

The Subio platform was used to configure genes into a clustered heat map

representative of differential expression. HMBPP alone was found to significantly

affect gene expression in THP-1 cells without the need for the permeabilisation

agent Digitonin stringent selection criteria (as above). Red indicates an increase in

expression and blue represents a decrease in expression relative to control

(untreated) group (Fig. 8).
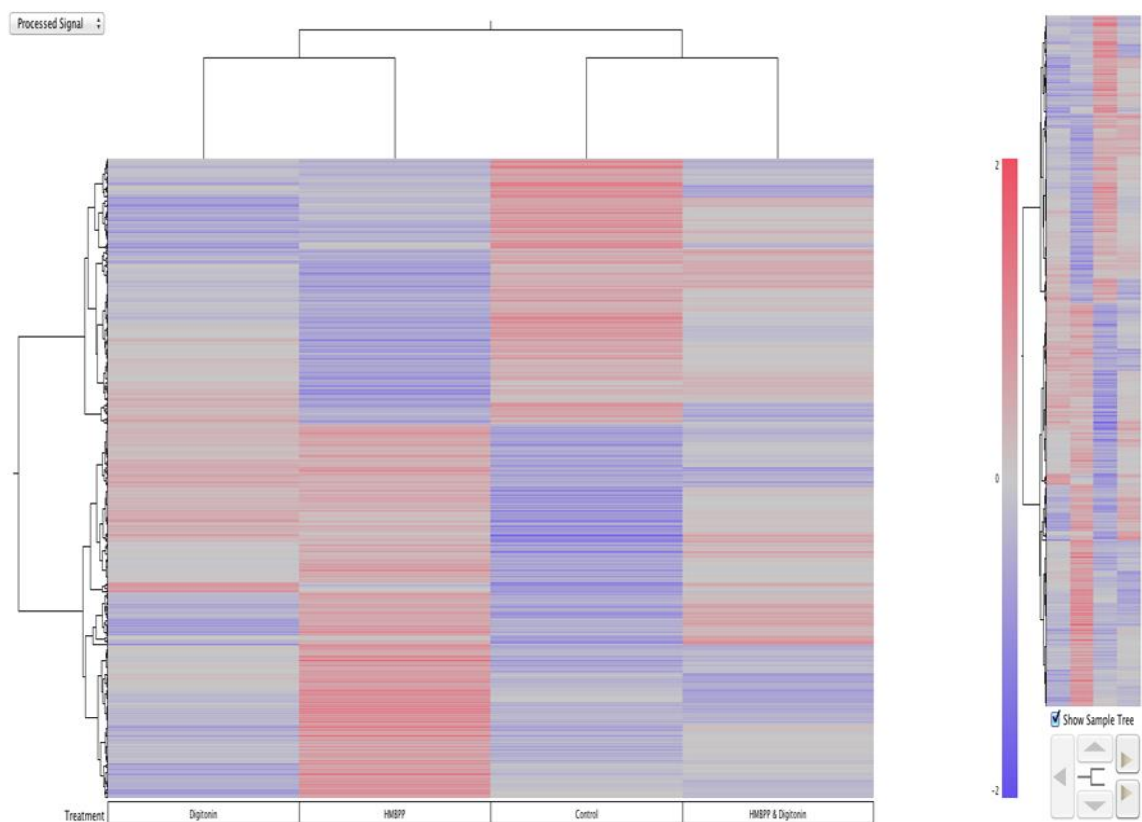
Fig. 8. Heat map representation of significant HMBPP-associated differential gene expression in THP-1 cells

Gene ontology analysis of HMBPP attributed differential expression:

Functional classification and annotation chart analysis was carried out using a web-based resource package (GATHER®) (Materials and Methods). HMBPP elicited significant changes in genes involved in the immune response, defence response, response to biotic stimulus, response to external biotic stimulus, organismal physiological response, taxis and chemotaxis (Fig. 9). The numbers and identity of genes affected by HMBPP in each category are described and assigned p-value and Bayes factor score.
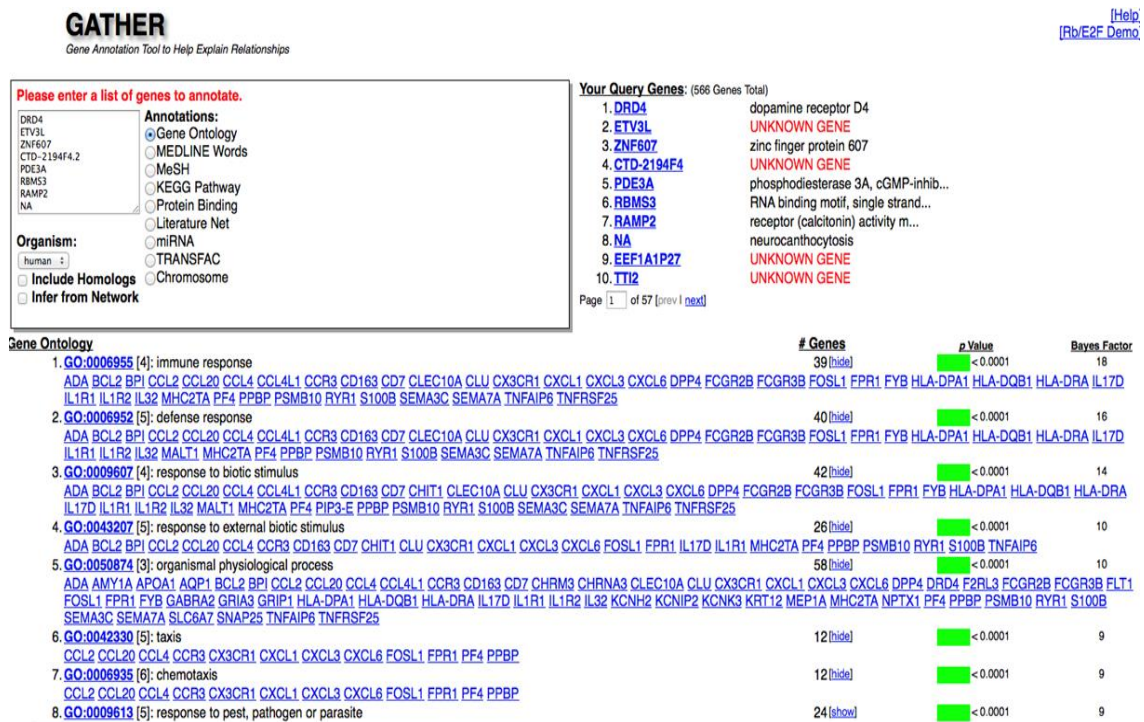
Fig. 9. Screen shot illustrating GATHER gene ontology of 589 differentially expressed genes altered by HMBPP in THP-1 cells.

Gene ontology demonstrates a significant effect of HMBPP in the immune response, defence response, response to biotic stimuli, response to external biotic stimuli, organismal physiological process, taxis and chemotaxis. Numbers and identity of differentially expressed genes are depicted and assigned p-value and Bayes factor score by GATHER®. Analysis represents differential expression of Control (untreated) vs. HMBPP under stringent criteria (1.5 fold change, P<0.05 cut off).
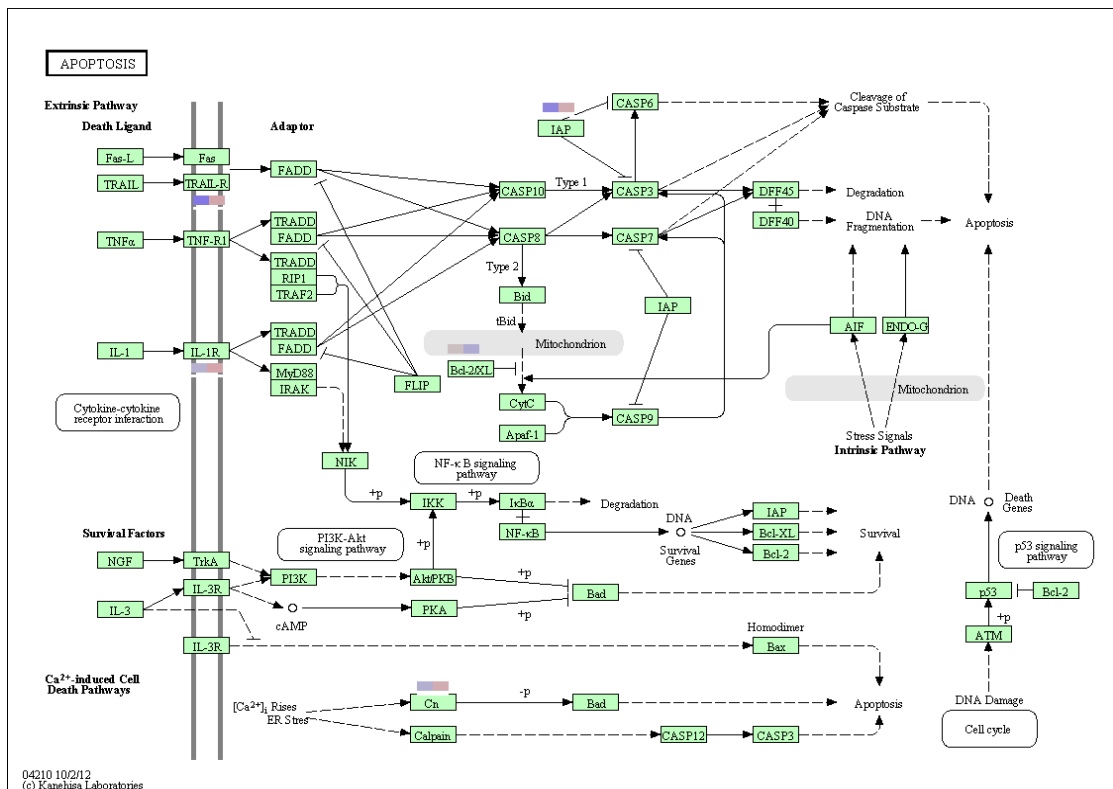
GATHER KEGG pathway analysis of HMBPP attributed differential expression:

The GATHER platform was used to rank HMBPP associated differential gene

expression changes according to major Kyoto Encyclopaedia of Genes and Genomes

(KEGG) pathways based on the number of changed genes identified. HMBPP was

found to significantly affect pathways associated with immunity and antigen

presentation (Cytokine-Cytokine receptor interactions, MAPK signalling, Apoptosis,

Oxidative phosphorylation, Toll-like receptor signalling) pathways (Fig. 10). The

numbers and identity of genes affected by HMBPP in each pathway are described

and are assigned a p-value and Bayes factor score.

Fig. 10. Screen shot illustrating GATHER KEGG pathway analysis of 589 differentially expressed genes altered by HMBPP in THP-1 cells.

GATHER KEGG pathway analysis revealed a significant effect of HMBPP on a number of immunity and antigen presentation pathways (illustrated). Numbers and identity of differentially expressed genes are depicted and assigned a p-value and Bayes factor score by GATHER®. Analysis represents differential expression of Control vs. HMBPP under stringent criteria (1.5 fold change, P<0.05 cut off).

KEGG pathway visualisation:

The Kyoto Encyclopaedia of Genes and Genomes (KEGG) pathway database was used for visualisation of pathways implicated by HMBPP attributed gene expression changes compared to control (untreated) cells. Differentially expressed genes are highlighted with red/blue symbols in each pathway (Cytokine-cytokine interactions, phagosome formation and apoptosis) (Fig. 11-13).
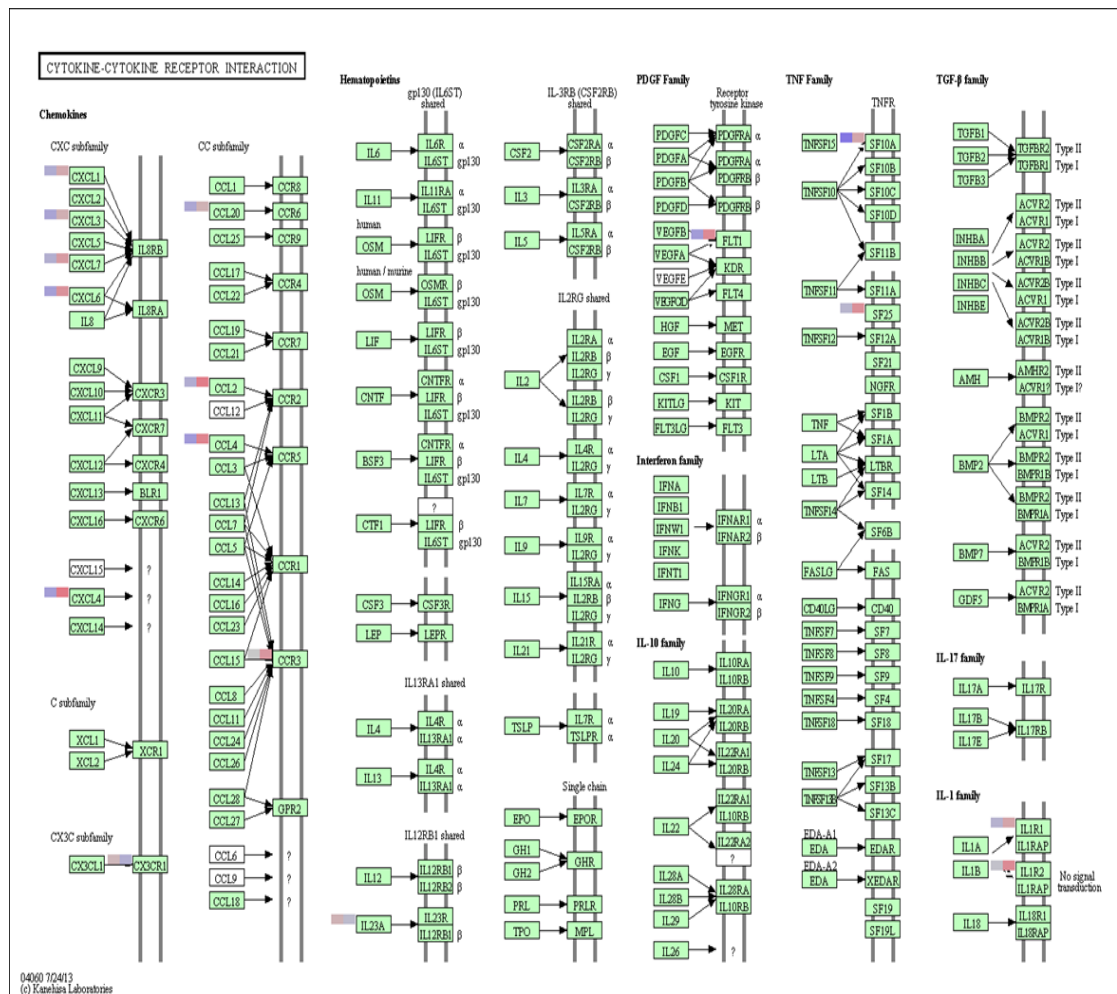
Fig. 11. Cytokine-cytokine interaction KEGG pathway.
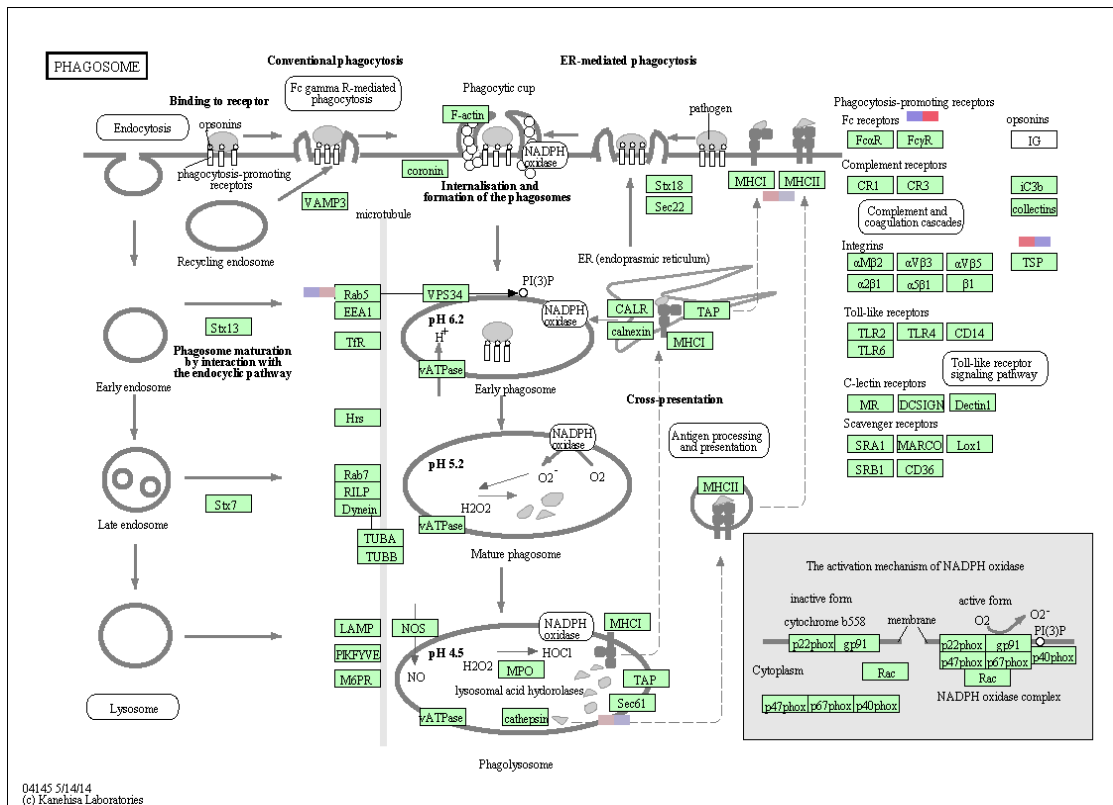
Fig. 12. Phagosome formation KEGG pathway.

Fig. 13. Apoptosis KEGG pathway.

218

Heat map representation of key genes of interest:

The Subio platform was utilised to identity key genes of interest for immunity and antigen presentation following GATHER and KEGG pathway analysis of HMBPP treatment of THP-1 cells. 42 such key genes were identified and assembled into a heat map for all treatment groups (Control, HMBPP, HMBPP + Digitonin and Digitonin) (Fig. 14). Differential expression was examined under stringent criteria (1.5 fold change and P<0.05). Analysis represents significant increases (red) and significant decreases (blue) for control (untreated) versus other groups. Heat maps were assembled (A) alphabetically and (B) from greatest to least overall expression for ease of interpretation. HMBPP in this study was observed to elicit significant increases in these key genes.
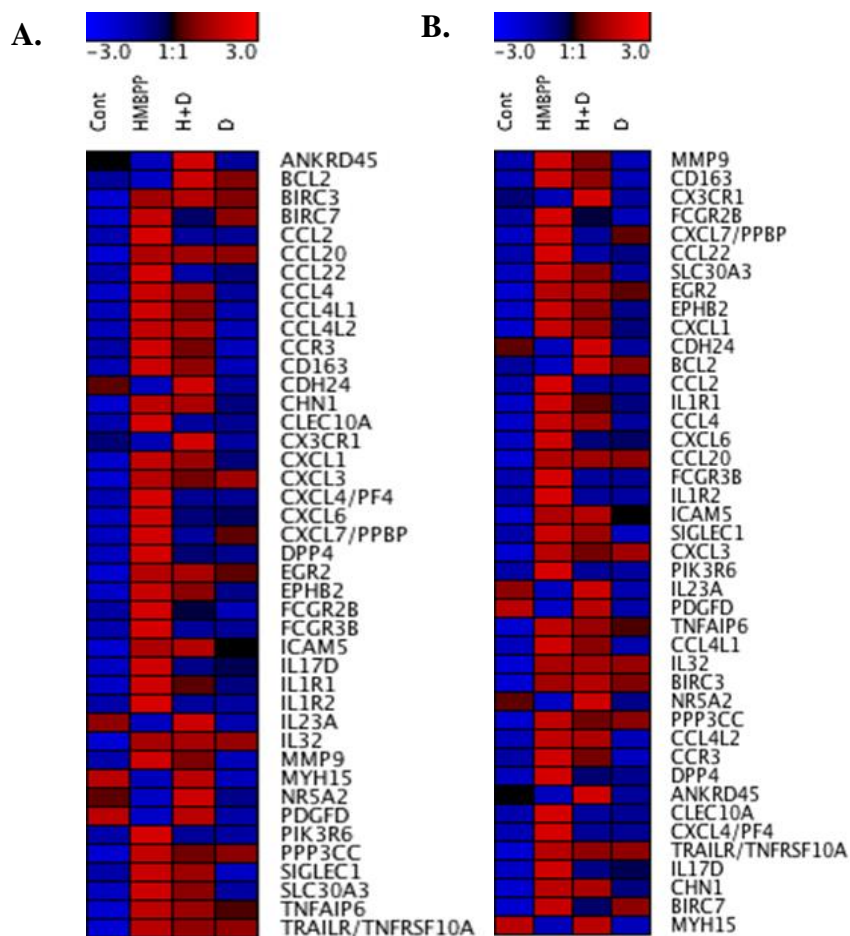
Fig. 14. Heat map illustrations of differential immunity and antigen presentation gene expression listed (A) alphabetically and (B) from overall greatest to least expression.

HMBPP alone elicited significant increased activation of genes (red) involved in immunity and antigenic presentation pathways relative to the control (untreated) while decreased activation are highlighted in blue. Digitonin (D) and HMBPP + Digitonin (H+D) elicited a different set of gene expression changes that are unrelated to the aim of the study. Selection of genes was based on GATHER and KEGG pathway analysis under stringent criteria (1.5 fold change and P<0.05 cut off).

Confirmation of MACE RNA-seq analysis by qRT-PCR:

Confirmatory qRT-PCR analysis was performed on genes identified as being significantly increased by HMBPP treatment of THP-1 following MACE RNA-seq analysis (Fig. 15 (A-F)). qRT-PCR analysis subsequently confirmed significant activation of the following genes in a replicate experiment. *CCL4* (*p=0.0443), *IL-17D* (*p=0.0201), *TNFAIP6* (**p=0.0086), *FCGR3B* (trend) confirm significant increases attributed to HMBPP stimulation (Fig.15). *CCL4* (*p=0.0107) and *TNFAIP6* (*p=0.0228) confirm a co-stimulatory activation effect of HMBPP (H) + Digitonin (D), while FCGR2B (*p=0.0313) and *FCGR3B* (*p=0.0126) confirm a HMBPP + Digitonin co down regulation relative to CONTROL. qRT-PCR also confirmed a down regulation of gene expression by Digitonin in *FCGR2B* (*p=0.013). Statistical significance was determined via Student's T-test.
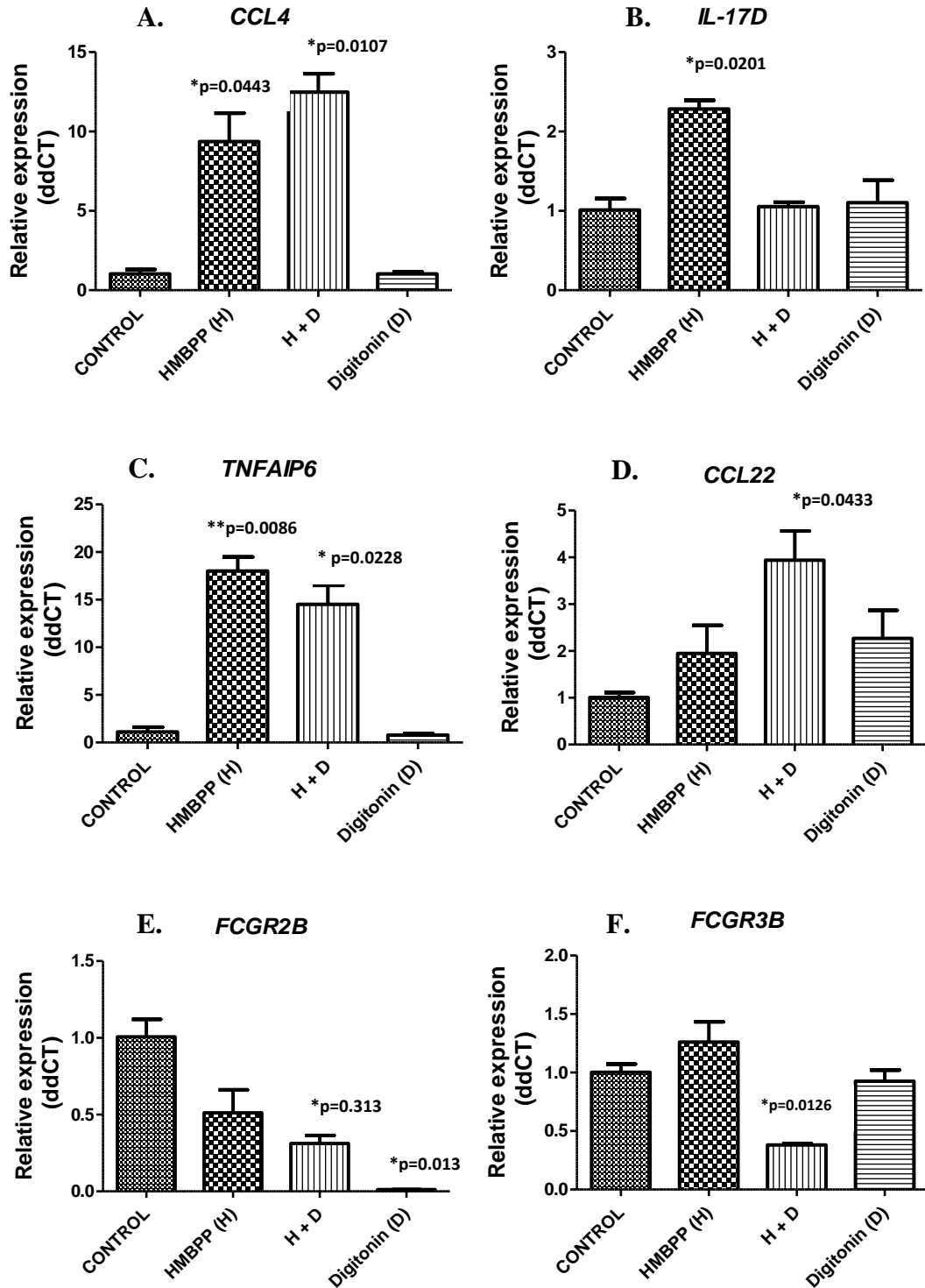
Fig. 15. Confirmation of MACE RNA-seq analysis for selected genes (A-F: *CCL4, IL-17D, TNFAIP6, CCL22, FCGR2B* and *FCGR3B*).

qRT-PCR of selected genes (A-F: *CCL4, IL-17D, TNFAIP6, CCL22, FCGR2B* and *FCGR3B*) confirmed expression changes from MACE RNA-seq in a replicate experiment. *CCL4* (*p=0.0443), *IL-17D* (*p=0.0201), *TNFAIP6* (**p=0.0086), *FCGR3B* (trend) show a significant increase by HMBPP stimulation. *CCL4* (*p=0.0107) and *TNFAIP6* (*p=0.0228) confirm a co-stimulatory activation effect of HMBPP (H) +

Digitonin. (D), while *FCGR2B* (*p=0.0313) and *FCGR3B* (*p=0.0126) confirm a HMBPP + Digitonin co down regulation. *FCGR2B* (*p=0.013) confirmed a significant down regulation by Digitonin treatment in the dataset. Student's T-test confirm statistical significance of genes analysed (*p>0.05).

Identical virulence of wild type and mutant L. monocytogenes EGDe:

THP-1 cells were seeded with 5 X 10^6 cells/ml (6-well plate) for 96-hours and differentiated (see Materials and Methods). Cells were infected with an M.O.I. of 10 with $5x10^6$ CFU/ml of wild type, lmo1441 (*ΔgcpE*) and lmo1451 (*ΔlytB*) strains of *L. monocytogenes* EGDe for 5 hours with gentamicin protection (Materials and Methods). Viable cell numbers (CFU/ml) were determined by plating on BHI agar overnight for uninfected and *Listeria*-infected cells, (Materials and Methods). Mean viable cell numbers recovered were as follows; (3 X 10^5 CFU/ml – wild type), (3.3 X 10^5 CFU/ml - *ΔgcpE*) and (1.8 X 10^5 CFU/ml - *ΔlytB*). Student's T-test analysis revealed no significant reduction in bacterial cell numbers for either mutant compared to wild type (Fig. 16).

CFU/ml bacteria
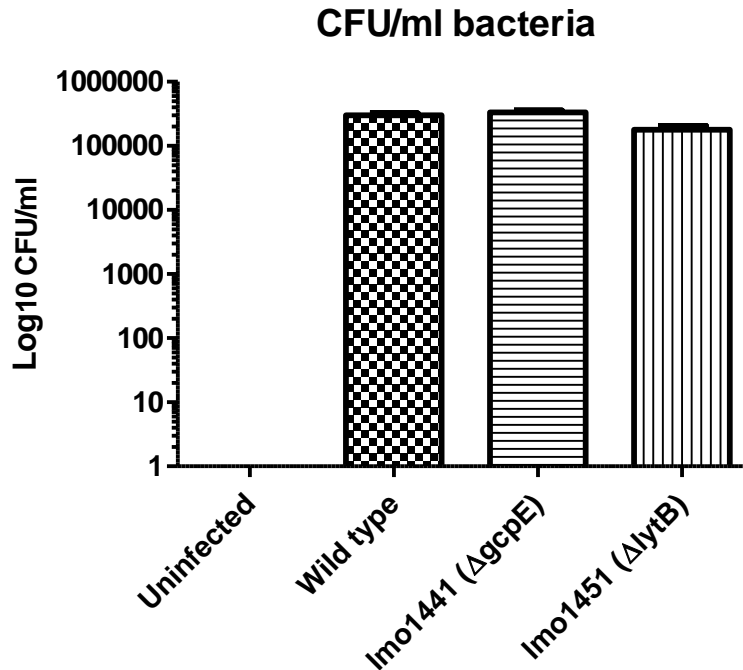
Fig. 16. Viable cell counts (CFU/ml) of uninfected, wild-type, lmo1441($\Delta gcpE$) and lmo1451 ($\Delta lytB$) *L. monocytogenes* **EGDe infected THP-1 cells**

THP-1 cells (5 X 10^6 cell/ml) were infected with 5 X 10^7 CFU/ml to a M.O.I. of 1:10 with wild type, lmo1441($\Delta gcpE$) and lmo1451($\Delta lytB$) mutant *L. monocytogenes* EGDe strains for 5 hours, following gentamicin protection. Error bars represent the standard deviation from the mean of a number of replicated experiments in triplicate. Viable cell numbers are expressed per $\log_{10}$ CFU/ml for each strain. Statistical significance (Student's T-test) showed no differences in mutants compared to the wild type.

HMBPP attributed gene expression was not affected by MEP deletion mutants in L. monocytogenes EGDe:

qRT-PCR analysis of uninfected (THP-1), wild type (WT) and mutant

lmo1441($\Delta gcpE$) and lmo1451($\Delta lytB$) *L. monocytogenes* EGDe after 5 hours

determined no significant effect of MEP deletion mutants on HMBPP-attributed

gene expression (Fig. 17). There is evidence that would suggest that deletion of the

HMBPP reductase (lmo1451$\Delta lytB$) enzyme in *L. monocytogenes* EGDe would result

in an over accumulation of HMBPP and conversely for deletion of HMBPP synthase

(lmo1441$\Delta gcpE$) (Begley, Gahan *et al*. 2004). We predicted this might stimulate

expression of predicted genes (A-F: *CCL4, IL-17D, TNFAIP6, CCL22, FCGR2B and FCGR3B*). qRT-PCR expression analysis failed to detect significant difference between wild type and either mutant *L. monocytogenes* EGDe expression for any of the predicted genes (Fig. 17).
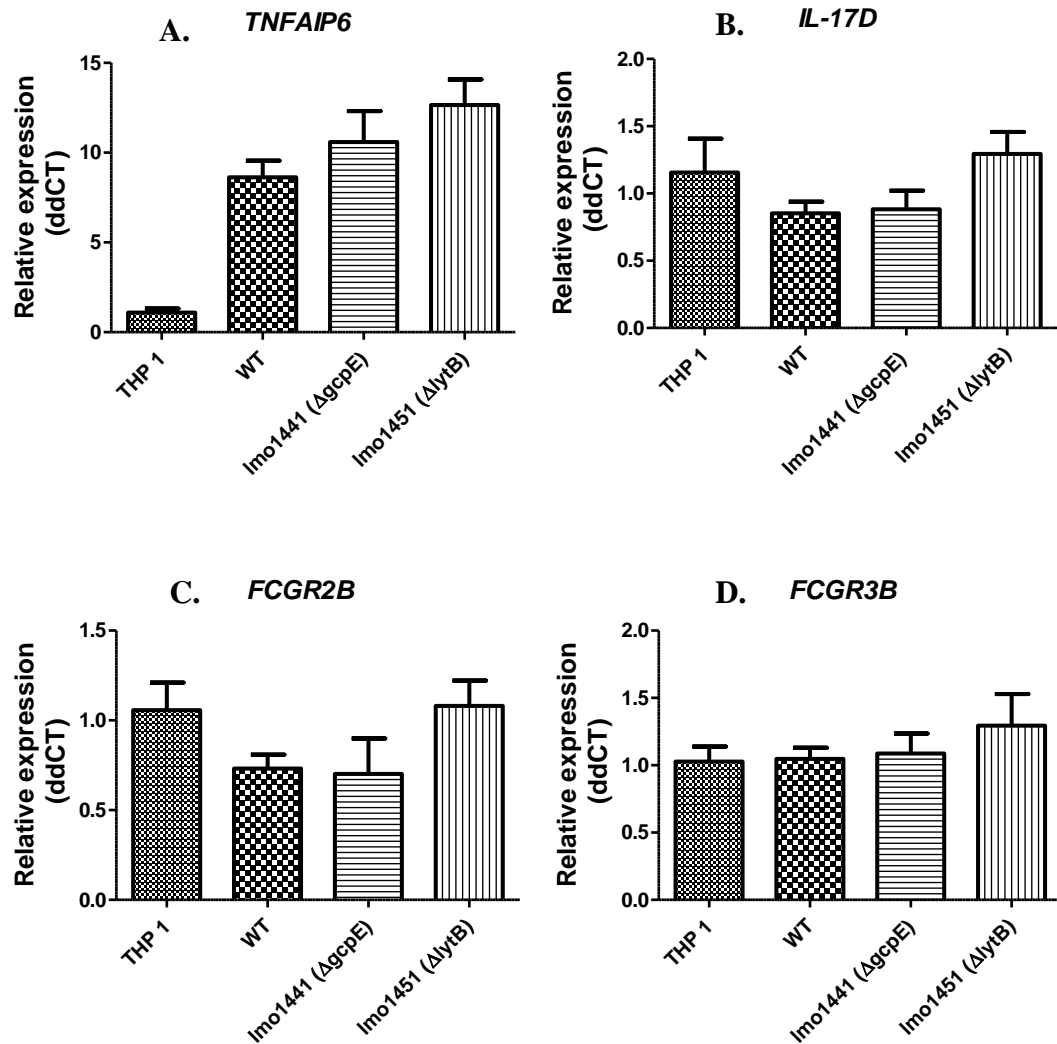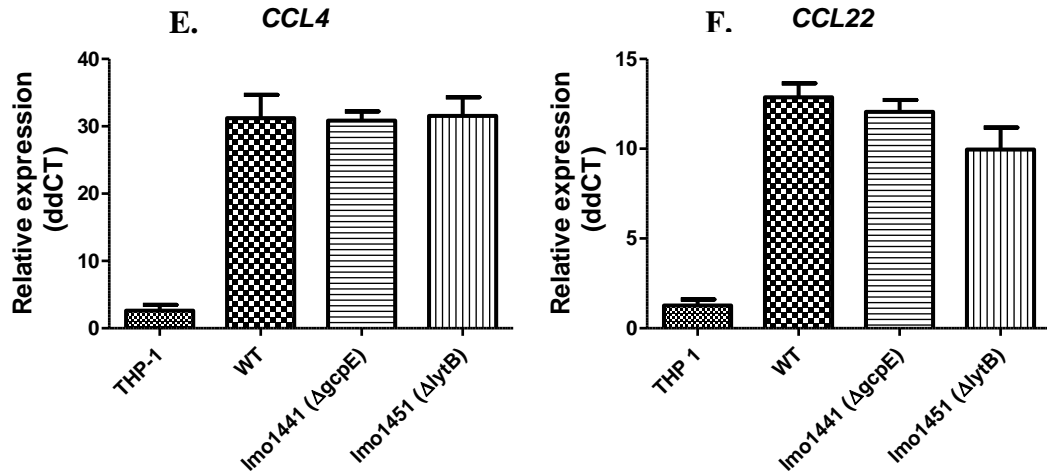
Fig.17. qRT-PCR expression analysis of HMBPP-associated genes (A-F) comparing wild type and mutant _L. monocytogenes_ EGDe

qRT-PCR expression analysis of THP-1 cells infected with wild type and mutant (lmo1441*ΔgcpE* and lmo1451*ΔlytB*) _L. monocytogenes_ EGDe. Statistical analysis (Student's T-test) determined no effect of either mutation on any of the predicted genes compared to wild type expression for all genes (A-F: _TNFAIP6, IL-17D, FCGR2B, FCGR3B, CCL4_ or _CCL22_). It should be noted that in comparison to the THP-1 (uninfected) cells expression was significantly increased for these genes in both wild type and mutants (up to 30 fold for _CCL4_, for example).

Discussion

The main aim of this study was to try and elucidate the previously undefined effect of a potential pathogen associated molecular pattern (PAMP), (E)-4-hydroxy-3-methyl-2-but-2-enyl pyrophosphate (HMBPP) on differentiated (dendritic-like) THP-1 cells. HMBPP is known to be a major stimulator of Vγ9/Vδ2 T cells for cellular proliferation and expansion (Eberl, Altincicek *et al.* 2002). A whole host of gut-associated microbes are known to synthesize this imunostimulatory molecule via the 2-C-methyl-$_D$-erythritol 4-phosphate (MEP) pathway (including *E. coli* and *L. monocytogenes*). Indeed we predict that this molecule is likely to contribute to immune homeostasis (Begley, Gahan *et al*. 2004). While there is much research available on the interaction of HMBPP with Vγ9/Vδ2 T cells (Eberl, Altincicek *et al.* 2002), (Jomaa, Feurle *et al.* 1999), relatively few studies have looked at the interaction of HMBPP with antigen presenting cells (dendritic cells) prior to cellular processing and antigenic presentation to T-lymphocytes (Bonneville and Scotet 2006). In our study, we used Massive Analysis of cDNA Ends (MACE) RNA-seq analysis to determine the effect of HMBPP on THP-1 cells. Furthermore, gene expression analysis (qRT-PCR) was performed following infection of THP-1 cells with wild type *L. monocytogenes* EGDe and knockout mutants (lmo1441*ΔgcpE*) and (lmo1451*ΔlytB*) that over- and under- produce HMBPP (Heuston, Begley *et al*. 2012).

Following optimisation of the experimental conditions, it was determined that 1nM of HMBPP, provided the highest optimal concentration that would not negatively impact on cell viability and provided the greatest possibility of observing gene expression changes. Previously, HMBPP for γδ T-cell activation has been

described as having an EC_{50} value of 0.1nM (Hintz, Reichenberg *et al.* 2001; Eberl, Hintz *et al*. 2003). Cell viability was determined based on measurement of cellular adenosine triphosphate (ATP) in THP-1 cells for both HMBPP and digitonin treatments. Digitonin has been used previously in order to ensure access of small molecules to the cell cytoplasm (Woodward, Iavarone *et al*. 2010).

MACE RNA-seq analysis identified a total of 589 genes significantly altered by all treatment groups (Control, HMBPP only, Digitonin only and HMBPP + Digitonin) identified under stringent statistical criteria (Materials and Methods). For this thesis, it was decided to focus on the gene changes associated with HMBPP only relative to untreated cells (69 genes) (Appendix to Chapter 5), as it provided a significant effect on gene expression without the need of the permeabilisation agent. These genes were subsequently categorised according to their gene ontology and involvement in KEGG pathways for immunity and antigen presentation. Cytokine-cytokine receptor interactions, phagosome formation and apoptosis as well as Toll-like receptor signalling and NFκB signalling were identified as major pathways that were significantly affected by HMBPP. The following representative genes were selected from the data set for MACE RNA-seq confirmatory analysis: *CCL4, IL-17D, TNFAIP6, CCL22, FCGR2B* and *FCGR3B* and again for further analysis in wild type and (HMBPP) mutant *L. monocytogenes* EGDe strains for potential HMBPP-attributed changes. HMBPP from this analysis stimulated a rich combination of genes that are known to be involved with immunostimulation and antigen presentation.

CCL4 (chemokine (C-C motif) ligand 4 also known as macrophage inflammatory protein-1β (MIP-1β), is a major activator protein and chemokine that specifically binds the *CCR5* receptor and is an important signalling molecule for

natural killer (NK) cells, monocytes and a wide variety of other immune cells such as T-lymophyctes (Bystry, Aluvihare *et al.* 2001). *CCL4* was identified as an inflammatory cytokine involved in toll-like receptor and *NFκB* signalling that was significantly up regulated by HMBPP in our study along with a number of other cytokine genes (*CXCL1, CXCL3, CXCL7, CXCL6, CXCL4* and *CCL2*). Chemokines are known to be important mediators between T-helper cells, effector cells and antigen presenting cells and are crucial for eliciting a controlled immune response (Roncarolo and Levings 2000).

CCL22 (chemokine (C-C motif) ligand 22, encodes a dendritic and macrophage cell associated secretory protein that is involved in immuoregulatory and inflammatory processes. *CCL22* is known to interact with numerous cell surface chemokine receptors for antigen processing (Vulcano, Albanesi *et al.* 2001) . *CCL22* is a potent chemokine that is strongly chemotactic for monocytes, dendritic cells and natural killer (NK) cells for activation, but mildly active for T-cells. *CCL22* is known not to be chemotactic (cytokine-cytokine signalling molecule) for neutrophils and eosinophils during inflammation (Vulcano, Albanesi *et al.* 2001), (Yanai, Sato *et al.* 2007). In our current study, expression of *CCL22* was found to be significantly increased in the presence of HMBPP. This would suggest that HMBPP is an important mediator of *CCL22* expression and could have potential implications for cell migration during microbial-associated infection of antigen presenting cells.

IL-17D (Interleukin-17D), is an important secretory protein that belongs to the IL-17 superfamily (*IL-17A-E*), all of which have similar protein structure. IL-17D represents 25% of all the various isoforms within the superfamily and is an important proinflammatory cytokine secreted by T-cells and a host of other immune cells (Kolls and Linden 2004). T-helper cell 17 (Th17) related cytokines such as IL-

17D have been shown to be essential for the expansion of γδ T cells following HMBPP-producing *M. tuberculosis* infection and antigen presentation in primates (Shen, Wang *et al*. 2014).

TNFAIP6 (tumour necrosis factor alpha-induced protein 6) encodes another important secreted protein (TSG-6) that is characterised by a hyaluronan-binding domain, an essential chemokine molecule involved in cellular migration. *TNFAIP6* has been shown to be induced by a number of other cytokine signalling molecules such as TNFα and IL-1. Studies by Dyer and co-workers (Dyer, Thomson *et al*. 2014), have previously demonstrated that TSG-6 suppresses cytokine-mediated chemotaxis of neutrophils as an anti-inflammatory mediator of inflammation. We speculate that HMBPP may fine tune local inflammatory response to bacteria.

FCGR2B (low affinity immunoglobulin gamma Fc region receptor 2-B - CD32B) and *FCGR3B* (Fc fragment of IgG, low affinity 3B, receptor - CD16B) were also identified by our MACE RNA-seq analysis as being significantly increased by HMBPP. *FCGR2B* and *FCGR3B* were found to be important receptors for the formation of the phagosome (KEGG pathway). Research by Lafont and colleagues (Lafont, Liautard *et al*. 2001), showed experimentally in cell culture assays that phosphoantigens such as isopentyl pyrophosphate (IPP) and HMBPP significantly prime γδ T-cells for activation and cytokine production. *FCGR3B* was an important specific cell surface receptor for the HMBPP directed expansion of γδ T-cells in co-culture with antigen presenting cells.

HMBPP significantly increased expression of the negative response regulator *TRAIL-R* for the innate immune response (Diehl, Yue *et al*. 2004) in the apoptotic pathway. Studies in human cell lines by Uchiyama and co-workers (Uchiyama,

Yonehara *et al*. 2013) have shown activation of apoptosis following infection of Natural Killer and macrophages with *L. monocytogenes* via Fas (CD95/Apo-1) leading to the production of the Fas ligand and inflammatory cytokines (IL-1β and IL-18) (Uchiyama, Yonehara *et al.* 2013). This demonstrates the importance of TRAIL-R for immune activation post infection and here we shown this to be an important target for HMBPP.

Viable cell counts of wild type *L. monocytogenes* EGDe and mutant Δ*gcpE* (lmo1441) and Δ*lytB* (lmo1451) strains did not show any significant difference in bacterial cells numbers (CFU/ml bacteria) comparing wild and both mutants infection of THP-1 cells. qRT-PCR expression analysis of all *L. monocytogenes* EGDe strains (wild type, *ΔgcpE* and *ΔlytB*) for HMBPP-attributed gene expression (*TNFAIP6, IL-17D, FCGR2B, FCGR3B*, *CCL4* and *CCL22*) showed no significant differences between wild type and either mutant strains. This would likely suggest that the overall effect of HMBPP in bacterial infection might be masked by other biological systems in the *L. monocytogenes* bacterium.

It is well known that a whole host of genes are activated in response to Listerial stimulation. *Nod1* and *Nod2* are two such cytosolic sensors critical for bacterial recognition and host defence (Kim, Park *et al.* 2008). However, as of yet a full understanding of the consequences of bacterial cell invasion is far from defined and it is likely that HMBPP may play an important role in this regard. In a wider context we showed a massive increase in expression of *TNFAIP6, CCL4* and *CCL22* (>15-fold) following infection with *L. monocytogenes* in general (regardless of phenotype) compared to uninfected cells. As previously mentioned, these genes are known to be important mediators of immunity and antigen presentation and we have

now shown these systems to be triggered following Listerial infection of THP-1 cells.

Recently published research identified an interesting gene Butyrophilin 3A1 (*BTN3A1*) located on human chromosome 6 that is involved in presenting phosphorylated antigens such as HMBPP to γδ T-cells (Vavassori, Kumar *et al.* 2013; Willcox, Mohammed *et al.* 2013). Unlike our study, in which we adopted a global investigation of the entire human genome (MACE RNA-seq analysis), they confined their investigation to genes located on chromosome 6 known to be associated with the butyrophillin family of immunoglobulin-like molecules. Interestingly, when we analysed our MACE RNA-seq dataset for genes identified in their study (Appendix to Chapter 5), we found that *BTN3A1* just came under the remit of being significantly increased (>1.5 fold) but was clearly increased in THP-1 cells following HMBPP treatment. Further explorations into our dataset might involve protein analysis by flow cytometry in the supernatant fractions of our samples for BTN3A1 expression (as well as other genes identified in our study) and subsequently blocking with the anti-CD277 antibody (Vavassori, Kumar *et al.* 2013) to determine potential differences related to HMBPP in THP-1 cells.

In conclusion, we have highlighted in this study the importance of HMBPP as a pathogen associated molecular pattern (PAMP) that is recognised by antigen presenting cells such as THP-1's. We show that the HMBPP molecule alone (without the aid of a permeabilisation agent) is able to elicit a significant number of gene expression changes in THP-1 cells, representing a number of biological pathways for immunity and antigen presentation such as cytokine-cytokine interactions, phagosome formation, apoptosis, toll-like receptor signalling, NFκB signalling and MAPK signalling without a detectable loss to cell viability. APCs are

generally necessary for optimal γδ T-cell cell response to HMBPP (Eberl, Roberts *et al*. 2009). Here we demonstrate that HMBPP provides a discrete signal to APCs which may co-ordinate the subsequent γδ T-cell response. Because many bacteria in the human gut microbiota produce HMBPP it is tempting to speculate that the molecule may play a significant role in immune homeostasis. However further work is necessary to examine this hypothesis.

References

Amslinger, S., S. Hecht, et al. (2007). "Stimulation of Vgamma9/Vdelta2 T-lymphocyte proliferation by the isoprenoid precursor, (E)-1-hydroxy-2-methyl-but-2-enyl 4-diphosphate." <u>Immunobiology</u> **212**(1): 47-55.

Anders, S. and W. Huber (2010). "Differential expression analysis for sequence count data." <u>Genome Biol</u> **11**(10): R106.

Asmann, Y. W., E. W. Klee, et al. (2009). "3' tag digital gene expression profiling of human brain and universal reference RNA using Illumina Genome Analyzer." <u>BMC Genomics</u> **10**: 531.

Begley, M., C. G. Gahan, et al. (2004). "The interplay between classical and alternative isoprenoid biosynthesis controls gammadelta T cell bioactivity of Listeria monocytogenes." <u>FEBS Lett</u> **561**(1-3): 99-104.

Begley, M., C. G. M. Gahan, et al. (2004). "The interplay between classical and alternative isoprenoid biosynthesis controls [gamma][delta] T cell bioactivity of Listeria monocytogenes." <u>FEBS Letters</u> **561**(1-3): 99-104.

Bonneville, M. and E. Scotet (2006). "Human Vgamma9Vdelta2 T cells: promising new leads for immunotherapy of infections and tumors." <u>Curr Opin Immunol</u> **18**(5): 539-546.

Bystry, R. S., V. Aluvihare, et al. (2001). "B cells and professional APCs recruit regulatory T cells via CCL4." <u>Nat Immunol</u> **2**(12): 1126-1132.

Diehl, G. E., H. H. Yue, et al. (2004). "TRAIL-R as a negative regulator of innate immune cell responses." <u>Immunity</u> **21**(6): 877-889.

Dyer, D. P., J. M. Thomson, et al. (2014). "TSG-6 inhibits neutrophil migration via direct interaction with the chemokine CXCL8." <u>J Immunol</u> **192**(5): 2177-2185.

Eberl, M., B. Altincicek, et al. (2002). "Accumulation of a potent gammadelta T-cell stimulator after deletion of the lytB gene in Escherichia coli." <u>Immunology</u> **106**(2): 200-211.

Eberl, M., M. Hintz, et al. (2003). "Microbial isoprenoid biosynthesis and human gammadelta T cell activation." FEBS Lett **544**(1-3): 4-10.

Eberl, M. and B. Moser (2009). "Monocytes and gammadelta T cells: close encounters in microbial infection." Trends Immunol **30**(12): 562-568.

Eberl, M., G. W. Roberts, et al. (2009). "A rapid crosstalk of human gammadelta T cells and monocytes drives the acute inflammation in bacterial infections." PLoS Pathog **5**(2): e1000308.

Hepworth, M. R. and G. F. Sonnenberg (2014). "Regulation of the adaptive immune system by innate lymphoid cells." Curr Opin Immunol **27**: 75-82.

Heuston, S., M. Begley, et al. (2012). "Isoprenoid biosynthesis in bacterial pathogens." Microbiology **158**(Pt 6): 1389-1401.

Hintz, M., A. Reichenberg, et al. (2001). "Identification of (E)-4-hydroxy-3-methyl-but-2-enyl pyrophosphate as a major activator for human gammadelta T cells in Escherichia coli." FEBS Lett **509**(2): 317-322.

Jomaa, H., J. Feurle, et al. (1999). "Vgamma9/Vdelta2 T cell activation induced by bacterial low molecular mass compounds depends on the 1-deoxy-D-xylulose 5-phosphate pathway of isoprenoid biosynthesis." FEMS Immunol Med Microbiol **25**(4): 371-378.

Kim, Y. G., J. H. Park, et al. (2008). "The cytosolic sensors Nod1 and Nod2 are critical for bacterial recognition and host defense after exposure to Toll-like receptor ligands." Immunity **28**(2): 246-257.

Kolls, J. K. and A. Linden (2004). "Interleukin-17 family members and inflammation." Immunity **21**(4): 467-476.

Lafont, V., J. Liautard, et al. (2001). "Production of TNF-alpha by human V gamma 9V delta 2 T cells via engagement of Fc gamma RIIIA, the low affinity type 3 receptor for the Fc portion of IgG, expressed upon TCR activation by nonpeptidic antigen." J Immunol **166**(12): 7190-7199.

Livak, K. J. and T. D. Schmittgen (2001). "Analysis of relative gene expression data using real-time quantitative PCR and the 2(-Delta Delta C(T)) Method." <u>Methods</u> **25**(4): 402-408.

Rekittke, I., E. Olkhova, et al. (2013). "Structure of the (E)-4-hydroxy-3-methyl-but-2-enyl-diphosphate reductase from Plasmodium falciparum." <u>FEBS Lett</u> **587**(24): 3968-3972.

Roncarolo, M. G. and M. K. Levings (2000). "The role of different subsets of T regulatory cells in controlling autoimmunity." <u>Curr Opin Immunol</u> **12**(6): 676-683.

Ryan-Payseur, B., J. Frencher, et al. (2012). "Multieffector-functional immune responses of HMBPP-specific Vgamma2Vdelta2 T cells in nonhuman primates inoculated with Listeria monocytogenes DeltaactA prfA*." <u>J Immunol</u> **189**(3): 1285-1293.

Sacchettini, J. C. and C. D. Poulter (1997). "Creating isoprenoid diversity." <u>Science</u> **277**(5333): 1788-1789.

Shen, H., Y. Wang, et al. (2014). "Th17-related cytokines contribute to recall-like expansion/effector function of HMBPP-specific Vgamma2Vdelta2 T cells after M. tuberculosis infection or vaccination." <u>Eur J Immunol</u>.

Uchiyama, R., S. Yonehara, et al. (2013). "Fas-mediated inflammatory response in Listeria monocytogenes infection." <u>J Immunol</u> **190**(8): 4245-4254.

Vavassori, S., A. Kumar, et al. (2013). "Butyrophilin 3A1 binds phosphorylated antigens and stimulates human [gamma][delta] T cells." <u>Nat Immunol</u> **14**(9): 908-916.

Vulcano, M., C. Albanesi, et al. (2001). "Dendritic cells as a major source of macrophage-derived chemokine/CCL22 in vitro and in vivo." <u>Eur J Immunol</u> **31**(3): 812-822.

Willcox, C. R., F. Mohammed, et al. (2013). "Resolving the mystery of pyrophosphate antigen presentation." <u>Nat Immunol</u> **14**(9): 886-887.

Woodward, J. J., A. T. Iavarone, et al. (2010). "c-di-AMP secreted by intracellular Listeria monocytogenes activates a host type I interferon response." <u>Science</u> **328**(5986): 1703-1705.

Yanai, M., K. Sato, et al. (2007). "The role of CCL22/macrophage-derived chemokine in allergic rhinitis." <u>Clin Immunol</u> **125**(3): 291-298.

Zawada, A. M., K. S. Rogacev, et al. (2014). "Massive analysis of cDNA Ends (MACE) and miRNA expression profiling identifies proatherogenic pathways in chronic kidney disease." <u>Epigenetics</u> **9**(1): 161-172.

Thesis Summary

The main aim of this body of work was to investigate the relevance of bacterial isoprenoid biosynthetic pathways for host-microbe interactions. In this study, specific enzymes and immunostimulatory metabolites of both the mevalonate and MEP pathways for isoprenoid (isopentyl pyrophosphate (IPP)) synthesis were investigated in light of potential implications for overall human health and relevance to microbial infections. Isoprenoids are essential organic molecules for both prokaryotic and eukaryotic organisms. They contribute too many key cellular functions including cellular structure formation, energy transport and even vitamin absorption. Bacteria are unusual in that they synthesize isoprenoids via one of two pathways. Most bacteria utilise the MEP pathway for IPP biosynthesis and this pathway generates an intermediate (HMBPP) which is a potent stimulator of human gamma delta ($\gamma\delta$) T-cells. A subset of bacteria (including gut bacteria such as *Lactobacillus* species, *Enterococcus* species and gut *Archaea*) utilise the classical mevalonate pathway for IPP biosynthesis. These bacteria express the enzyme HMG-R which is an isoform of the human HMG-R enzyme that is the target of statin drugs. It is likely that the mevalonate pathway represents the oldest evolutionary form of the pathway which was retained in higher *Eukarya* but replaced by the MEP pathway in the majority of bacteria.

The first chapter of this thesis provides an in-depth overview of the literature examining the biochemistry of HMG-R enzymes in bacteria and humans and outlining the specific and off-target effects of statins. The literature describes two isoforms of HMG-R (encoded by *hmgR*) that exist in the biosphere; Class 1 (human-like) and Class 2 (bacterial-like). Structural and sequence based analysis reveal

explanations for varying statin-sensitivity between both isoforms; Class 1 enzymes are much more susceptible to statins compared to their Class 2 counterparts. Historically, the first naturally discovered HMG-R inhibitor was compactin (modern day mevastatin), isolated form *Penicillium* species. To date, a wide diversity of statins are readily available as moieties modified from the original mevastatin structure or chemically synthesised. Rosuvastatin (RSV), is an example of a "super statin" with low lipophilicity, rapid absorption time and high bioavailability for hypercholesterolemia treatment. The literature clearly indicates that statins have been increasingly linked with off-target (pleiotropic) effects upon host responses. These include the promotion of antimicrobial activity through formation of neutrophil and macrophage extracellular traps against bacterial colonisation and a potential influence upon the production of host antimicrobial peptides. Furthermore statins are able to elicit a T-helper cell class switching response from Class 1 to Class 2, altering cytokine release and chemotaxis and even blocking the T-helper 17 cell responses.

Given the potential for statins to directly affect bacterial growth (through inhibition of HMG-R) or to indirectly influence bacterial survival *in-vivo* (through an influence upon host response and immunity), we investigated the influence of the statin RSV upon the composition of the gut microbiota in mice (Chapter 2). *In-silico* analysis of the MetaHIT database revealed several gut representative microorganisms containing both Class 1 (including methanogenic bacteria) and Class 2 (including *Lactobacilli* and *Coprococcus*) HMG-R isoforms. Through a range of *in-vitro* experiments we determined that RSV inhibits bacterial growth and MVAL formation in HMGR+ bacteria (*E. faecalis, E. faecium, L. monocytogenes* etc.) but only when administered at relatively high concentrations.

However *in-vivo* analysis of RSV is our murine model, determined a significant alteration to the community structure of the gut microbiota at a physiologically relevant dose. We noted a significant reduction in overall microbial biodiversity in the caecum of statin-treated mice as determined by α-diversity analysis (chao1, observed species, phylogenetic diversity), which was not apparent in the faeces. β-diversity (PCA) analysis confirmed a significant distant clustering of bacterial groups in the caecum of RSV-treated mice. It is well known that a rich biodiversity of microorganisms in the gastrointestinal tract is essential for maintaining a healthy homeostasis in metabolic, nutritional, physiological and immunological processes in the host. Disruption to this fine balance has been associated with increased susceptibility to metabolic disorders (metabolic syndrome) and a whole host of other health related effects (including increased obesity, diabetes, regulation of normal gut function and prevention of opportunistic infection) (Turnbaugh, Backhed *et al.* 2008; Clarke, Murphy *et al.* 2012; Kallus and Brandt 2012; Joyce and Gahan 2014). Overriding the obvious beneficial effects of statins our findings should prompt an investigation in human models for similar shifts in the microbiota biodiversity.

When we examined individual bacterial species (such as *Akkermansia*, *Bilophila* and the phylum *Desulfovibrionaceae*) more closely in our model we noted substantial reductions in these key microbial species in the presence of RSV. These groups have previously been associated with physiological parameters in the host and are known predictors of disease risk. For instance, the species, *Bilophila wadsworthia* has been strongly linked with the causation of colitis in knockout murine mice (Devkota, Wang *et al*. 2012). *Akkermansia muciniphila,* is now believed to be a strong indicator for lean phenotypes and inflammation in

mammalian models. A significant reduction in *Akkermansia* would predict towards a phenotype with a higher susceptibility for weight gain, Type 2 diabetes and increased intestinal inflammation (Everard, Belzer *et al.* 2013). Similarly, we determined a significant reduction in the phylum *Proteobacteria,* which almost exclusively contains gram negative bacteria members (such as *E. coli*). This group is well regarded as a driver of inflammation in the intestine through pathogen associated molecular patterns such as LPS (Yue, Ma *et al.* 2012). We can interfere from our findings that statins exhibit a strong propensity to alter the gut microbiota potentially with wider implications for the overall health of the host that should be followed up in humans.

We investigated a measureable marker of positive metabolic activity (SCFA's) in the host that are strongly linked to a bio diverse microbiota and as mentioned previously are strongly beneficial for gut health (Hamer, Jonkers *et al.* 2008; Cox, Jackson *et al.* 2009; Louis and Flint 2009). We identified significant decreases in key microbial groups (such as *Roseburia* and *Eyrsipelotrichaceae*) as well as a significant increase in *Lachnospiraceae* (*Coprococcus*) in the caecum and faeces of RSV-treated animals. Many of these groups are known to be important producers of the SCFA butyrate which exhibits strong anti-inflammatory and anti-cancerous in the gut (Machiels, Joossens *et al.* 2013) Similarly we examined a reduction in the family *Coriobacteriaceae* which is beneficial for polyphenol conversion, bile acid and lipid metabolism in the gut. However, in our model we determined no considerable effect on individual SCFA markers (butyrate, propionate, aceate) or total SFCA's in the caecum. This suggests that whilst the microbial community structure is altered by statins, there is no effect upon overall production of SCFA's. A similar investigation in humans is certainly warranted.

In Chapter 3 of this thesis, we aimed to link observed changes to the murine microbiota with respect to RSV (Chapter 2) with predicted in-direct (pleotropic) effects of statins (Chapter 1) regarding microbe-host and host-microbe feedback systems. We examined three main parameters in our model inflammation, bile acid synthesis and expression of antimicrobial effectors. We noted significant reductions in hepatic gene expression of pro inflammatory cytokines and cellular adhesion molecules (including *TNFα, CCL20, IL-1β* and *IL-18*) compared to an increased ileal response (including *ICAM-1, IL-17A, TGF-β* and *IL-1β*) in RSV-treated mice. This was confirmed by protein expression (MSD analysis) for systemic and hepatic cytokines (IL-1β and TNFα were both reduced by RSV administration). Our findings confirm previously reported pleiotropic effects of statins (Chapter 1) suggesting a strong involvement with local inflammation. We propose that statins have wider implications in respect of local and system inflammation and are likely to disrupt overall homeostasis with broad ranging implications for health.

Most importantly, RSV enhanced expression of genes encoding intestinal antimicrobials (*RegIIIγ, CAMP* and *iNOS2*) as well as local mucin production (*MUC2*). These antimicrobial agents are known to strongly influence microbial composition in the gastrointestinal tract and are active against a wide range of bacterial species. RegIIIγ is a potent inhibitor of peptidoglycan cell wall synthesis for bacterial replication. CAMP is a strongly antibacterial protein associated with the lysosomes of macrophages. *iNOS2* is essential for the synthesis of nitric oxide and acts as a key signalling molecule in the gut and can be stimulated by IL-1, TNFα in response to bacterial infection. Our findings confirm previous observations that statins can induce mucosal expression of *CAMP* (von Kockritz-Blickwede and Nizet 2009; Chow, von Kockritz-Blickwede *et al*. 2010). Similarly, it was reported that

individual bile acids (such as CDCA and UDCA) can considerably enhance CAMP activity in the gut (D'Aldebert, Biyeyeme Bi Mve *et al*. 2009). We deduce that in our model statin alterations to the gut microbiota are more likely due to effects on these key agents rather than direct antimicrobial activity.

Lastly we examined bile acid synthesis a well-defined microbe-directed physiological system with obvious implications for the host and indeed the gut microbiota. Bile acids are sterol compounds formed from the breakdown of cholesterol and are readily required for the absorption and emulsification of fats in the diet. It has been shown previously that bile acid feeding (cholic acid) significantly altered the gut microbiota prompting an increased outgrowth of *Firmicutes* (in particular *Clostridia* and *Erysipelotrich*i clusters) as well as *Proteobacteria* (*E.coli*) (Islam, Fukiya *et al*. 2011; Yokota, Fukiya *et al.* 2012). In our study we observed reduced hepatic expression of *CYP8b1* and *CYP27a1* genes that coincided with an overall reduction in hepatic and faecal bile acids (CA and CDCA). We note a concomitant effect on the microbiota that is broadly opposite to that seen in CA-treated rodents. Notably we witnessed a decrease in specific *Firmicutes* groups including specific *Clostridial* clusters (*Roseburia*), *Erysipelotrichaceae* and *Proteobacteria*. We therefore deduce that RSV resulted in reduced hepatic primary bile acid synthesis correlating with alterations to the microbiota that reflect these changes. These findings were confirmed by PCA plot analysis showing distinctive separation of control and RSV-treated animals for total hepatic, circulating and faecal bile acid profiles. Whilst inflammation and BA synthesis exert strong influences on the microbiota we recognise that other physiological parameters (including cholesterol homeostasis) may also potentially

influence the community structure within the gut microbiota. Our findings demonstrate a need to examine the potential for similar effects in humans.

When we examined the implications of RSV in GF mice, we observed contrasting effects compared to our conventional model. In this case RSV elicited an increase in the gene expression of hepatic inflammatory markers (including *IL-1β, TNFα, ICAM-1* and *Itgal*) which we confirmed by MSD protein analysis. RSV had no effect on the expression of genes encoding intestinal antimicrobial peptides (*RegIIIγ, CAMP, iNOS2*) or mucin genes (*MUC2*) in GF mice. We determined no effect of statin on genes encoding hepatic bile acid synthesis (*CYP7a1, CYP7b1, CYP8b1, CYP27a1* or *CYP46a1*), which was confirmed by UPLC-MS analysis for individual (including CA, CDCA and MCA) and total primary, secondary and tauro-conjugated bile acids. PCA plot analysis demonstrated no significant alterations for total hepatic, circulating, biliary or faecal bile profiles comparing control and RSV-treated GF animals. Our study confirms the importance of a functional, rich enteric microbiota for driving BA synthesis in the host. Similarly, it is known that the microbiota is a key determinant for intestinal inflammatory homeostasis (in particular ICAM-1 and IL-1β). With the exception of certain porcine models (simvastatin) the inflammatory effects of statins in GF animals are not well defined (Jung, Wang *et al.* 2012; Bui, Kocher *et al.* 2013). Our study is the first of its kind that examines such effects in gnotobiotic rodents and highlights the significance of altering the gut microbiota for both inflammation (and indeed BA synthesis) in the host with implications for health status.

Chapter 4 of this thesis was undertaken to investigate the contribution of the second enzyme (HMG-CoA synthase) in the mevalonate pathway of *L.*

monocytogenes EGDe (growth and virulence) following clean deletion of Δ*mvaS*.
Previously, our lab has shown that the third mevalonate pathway enzyme (HMG-R)
is essential in *L. monocytogenes* EGDe for normal growth and virulence (this mutant
could be rescued by addition of exogenous MVAL) (Heuston, Begley *et al*. 2012). *L.
monocytogenes* is a unique bacterium which has been identified as containing a
complete set of enzymes for both mevalonate and MEP pathways.

In our study we successfully knocked out the *mvaS* gene by deletion
mutagenesis. Surprisingly, we determined no effect on growth of this mutant in
complex and defined media compared to the parent wild type strain. This mutant
was capable of similar comparable growth without addition of exogenous MVAL.
This was in contrast compared to the *ΔhmgR* mutant which failed to grow in the
absence of exogenous MVAL. Phenotypic analysis under different environmental
stress conditions (cell wall autolysis, oxidative stress, cell wall antibiotics or HMG-
R inhibitors) revealed no increased susceptibility of this deletion for *L.
monocytogenes* EGDe. Similarly, *in-vivo* we observed no increased disadvantage of
this mutant for infection in cell culture (J774 macrophages) and animal models
(BALB/c mice) against the wild type. We reasoned from this that *mvaS* was non-
essential for the normal growth and virulence of *L. monocytogenes* EGDe.

Collectively our data suggested the possibility of an alternative enzyme
capable of generating the substrate of *mvaS* (HMG-CoA) encoded in *L.
monocytogenes* EGDe genome. KEGG pathway analysis highlighted an alternative
means of generating this substrate in other bacteria via activity of methylglutaconyl-
CoA hydratase involved in the degradation of amino acids (valine, leucine and iso-
leucine). Extensive bioinformatics analysis of *Listerial* genomes failed to identify a
properly annotated homologue of this gene in EGDe. We identified the presence of

this enzyme in the distantly related species (*L. fleischmanni*). Hence it is possible that an alternative mechanism for providing the HMG-CoA substrate in *L. monocytogenes* EGDe exists rendering HMG-CoA synthase activity redundant (at least under our test conditions) that may involve methylglutaconyl-CoA hydratase. We suggest that in order to investigate this hypothesis further a transposon bank could be generated within the *ΔmvaS* mutant and to screen this bank for clones incapable of growth in the absence of MVAL. Our study (at least for *L. monocytogenes* EGDe) suggests that much more remains to be discovered about isoprenoid biosynthesis concerning other potential pathways and metabolites that may feed into the mevalonate and MEP pathways as currently described with attendant implications for bacterial infection.

In Chapter 5, the focus of this thesis switched to the alternative pathway for isoprenoid biosynthesis i.e. the 2-C-methyl-$_D$-erythritol 4-phosphate (MEP) pathway and the penultimate metabolite (E)-4-hydroxy-3-methyl-2-but-2-enyl pyrophosphate (HMBPP), a potential pathogen associated molecular pattern (PAMP). HMBPP is a potent activator of Vγ9/Vδ2 human T cells which elicits proliferation and expansion of this T-cell subset. Many gut-associated microbes (such as *E.coli* and *Listeria monocytogenes*) are known to synthesize this immunostimulatory molecule with strong implications for immune homeostasis (Eberl, Hintz *et al*. 2003). Whilst much research has focussed on the on the interaction of HMBPP with T-cells, our study is one of the first to examine the interaction of HMBPP with antigen presenting cells (APC's) (dendritic cells) prior to cellular processing and presentation to γδ T-cells (Bonneville and Scotet 2006).

We determined that HMBPP at optimised nanomolar concentrations (without the aid of a cellular permeabilisation agent) significantly altered gene expression in

human THP-1 cells by MACE RNA-seq analysis. HMBPP significantly activated genes (including *CCL4, IL-17D, TNFAIP6, CCL22, FCGR2B, FCGR3B* and *TRAIL-R*) involved in pathways for immunity and antigen presentation (cytokine-cytokine receptor interactions, phagosome formation, apoptosis, toll-like receptor signalling, NFκB signalling and MAPK signalling). Further gene expression analysis of HMBPP-activated genes in THP-1 cells infected with wild type, HMBPP under-producing (*ΔgcpE*) and HMBPP over-producing (*ΔlytB*) mutant *L. monocytogenes* EGDe strains (available in our lab), showed that HMBPP likely plays a small yet significant role in overall bacterial infection. However we postulate that other biological interactions (such as with *Nod 1* and *Nod 2*) may mask the importance of effect (Kim, Park *et al*. 2008).

We also examined our dataset in relation to other previous studies that implicated other genes (such as butyrophilin (immunoglobulin-like) genes) involved in HMBPP presentation by APC's to γδ-T cells (Vavassori, Kumar *et al*. 2013; Willcox, Mohammed *et al.* 2013). Our dataset stands out as the first global investigation in relation to HMBPP antigen presentation compared to these previous localised (human chromosome 6) studies. *BTN3A1* was identified as one such potential target which we found to be just under the remit of significantly activated (along with a number of other butyrophilin associated genes located on chromosome 6) under our test conditions. Further exploration might involve protein (flow cytometry) analysis in supernatant fractions of our samples blocking *BTN3A1* activity (anti-CD277 antibody) to determine potential HMBPP-associated effects in our dataset. Overall we reveal the importance of HMBPP as a PAMP recognised by APC's (such as THP-1 cells) for immunity and antigen presentation in providing a discrete signal γδ T-cell proliferation and expansion. Our findings provide a greater

in depth molecular knowledge regarding the effects of HMBPP in early bacterial infection. Since many bacteria in the human gut microbiota synthesize this molecule it is tempting to speculate that HMBPP may play a significant role in immune homeostasis. However further investigation will be necessary to expand upon this hypothesis.

In summary, we provide a complex overview of host-microbe interactions involving different enzymes and intermediary metabolites of both the mevalonate and non-mevalonate (MEP) pathways for isoprenoid biosynthesis, building upon what is already known about these pathways. We have presented evidence for wider expansion of enzymes and metabolites that could be further linked to these pathways in bacteria. We examined the previously uncharacterised effects of a widely prescribed medication (RSV) which we show has a profound impact upon gut microbiota structure and concomitant host responses in murine studies. Given the number of individuals worldwide currently taking statins this could potentially have widespread implications for human medicine into the future. Finally, in this thesis we were successfully able to expand on previous knowledge regarding the early stages of bacterial infection which may in time change our current perceptions about host-microbe and indeed microbe-host dialogue.

References

Bonneville, M. and E. Scotet (2006). "Human Vgamma9Vdelta2 T cells: promising new leads for immunotherapy of infections and tumors." Curr Opin Immunol **18**(5): 539-546.

Bui, T., J. Kocher, et al. (2013). "Median infectious dose of human norovirus GII.4 in gnotobiotic pigs is decreased by simvastatin treatment and increased by age." J Gen Virol **94**(Pt 9): 2005-2016.

Chow, O. A., M. von Kockritz-Blickwede, et al. (2010). "Statins enhance formation of phagocyte extracellular traps." Cell Host Microbe **8**(5): 445-454.

Clarke, S. F., E. F. Murphy, et al. (2012). "The gut microbiota and its relationship to diet and obesity: new insights." Gut Microbes **3**(3): 186-202.

Cox, M. A., J. Jackson, et al. (2009). "Short-chain fatty acids act as antiinflammatory mediators by regulating prostaglandin E(2) and cytokines." World J Gastroenterol **15**(44): 5549-5557.

D'Aldebert, E., M. J. Biyeyeme Bi Mve, et al. (2009). "Bile salts control the antimicrobial peptide cathelicidin through nuclear receptors in the human biliary epithelium." Gastroenterology **136**(4): 1435-1443.

Devkota, S., Y. Wang, et al. (2012). "Dietary-fat-induced taurocholic acid promotes pathobiont expansion and colitis in Il10-/- mice." Nature **487**(7405): 104-108.

Eberl, M., M. Hintz, et al. (2003). "Microbial isoprenoid biosynthesis and human gammadelta T cell activation." FEBS Lett **544**(1-3): 4-10.

Everard, A., C. Belzer, et al. (2013). "Cross-talk between Akkermansia muciniphila and intestinal epithelium controls diet-induced obesity." Proc Natl Acad Sci U S A **110**(22): 9066-9071.

Hamer, H. M., D. Jonkers, et al. (2008). "Review article: the role of butyrate on colonic function." Aliment Pharmacol Ther **27**(2): 104-119.

Heuston, S., M. Begley, et al. (2012). "HmgR, a key enzyme in the mevalonate pathway for isoprenoid biosynthesis, is essential for growth of Listeria monocytogenes EGDe." Microbiology **158**(Pt 7): 1684-1693.

Islam, K. B., S. Fukiya, et al. (2011). "Bile acid is a host factor that regulates the composition of the cecal microbiota in rats." Gastroenterology **141**(5): 1773-1781.

Joyce, S. A. and C. G. Gahan (2014). "The gut microbiota and the metabolic health of the host." Curr Opin Gastroenterol **30**(2): 120-127.

Jung, K., Q. Wang, et al. (2012). "The effects of simvastatin or interferon-alpha on infectivity of human norovirus using a gnotobiotic pig model for the study of antivirals." PLoS One **7**(7): e41619.

Kallus, S. J. and L. J. Brandt (2012). "The intestinal microbiota and obesity." J Clin Gastroenterol **46**(1): 16-24.

Kim, Y. G., J. H. Park, et al. (2008). "The cytosolic sensors Nod1 and Nod2 are critical for bacterial recognition and host defense after exposure to Toll-like receptor ligands." Immunity **28**(2): 246-257.

Louis, P. and H. J. Flint (2009). "Diversity, metabolism and microbial ecology of butyrate-producing bacteria from the human large intestine." FEMS Microbiol Lett **294**(1): 1-8.

Machiels, K., M. Joossens, et al. (2013). "A decrease of the butyrate-producing species Roseburia hominis and Faecalibacterium prausnitzii defines dysbiosis in patients with ulcerative colitis." Gut.

Turnbaugh, P. J., F. Backhed, et al. (2008). "Diet-induced obesity is linked to marked but reversible alterations in the mouse distal gut microbiome." Cell Host Microbe **3**(4): 213-223.

Vavassori, S., A. Kumar, et al. (2013). "Butyrophilin 3A1 binds phosphorylated antigens and stimulates human [gamma][delta] T cells." Nat Immunol **14**(9): 908-916.

von Kockritz-Blickwede, M. and V. Nizet (2009). "Innate immunity turned inside-out: antimicrobial defense by phagocyte extracellular traps." <u>J Mol Med (Berl)</u> **87**(8): 775-783.

Willcox, C. R., F. Mohammed, et al. (2013). "Resolving the mystery of pyrophosphate antigen presentation." <u>Nat Immunol</u> **14**(9): 886-887.

Yokota, A., S. Fukiya, et al. (2012). "Is bile acid a determinant of the gut microbiota on a high-fat diet?" <u>Gut Microbes</u> **3**(5): 455-459.

Yue, C., B. Ma, et al. (2012). "Lipopolysaccharide-induced bacterial translocation is intestine site-specific and associates with intestinal mucosal inflammation." <u>Inflammation</u> **35**(6): 1880-1888.

Appendices

Appendix to Chapter 3

Bile acid standard curves:

Taurine: $R^2 = 0.975028$

Compound name: Taurine
Coefficient of Determination: R^2 = 0.975028
Calibration curve: 0.0101345 * x
Response type: Internal Std (Ref 5), Area * (IS Conc. / IS Area)
Curve type: Linear, Origin: Force, Weighting: Null, Axis trans: None
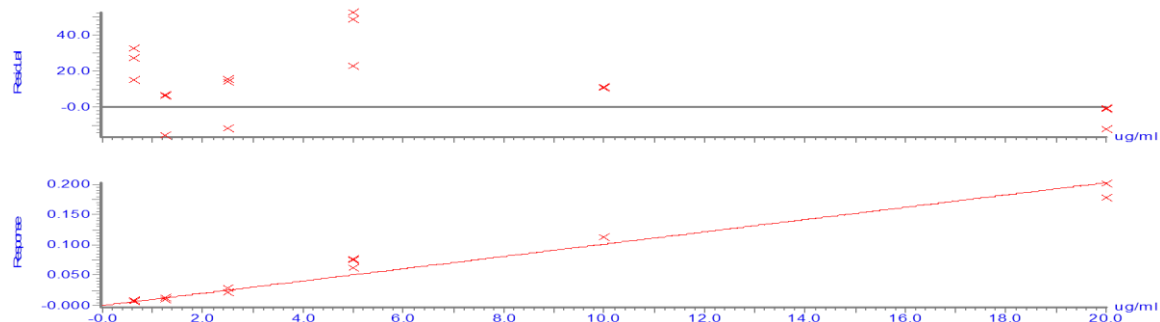
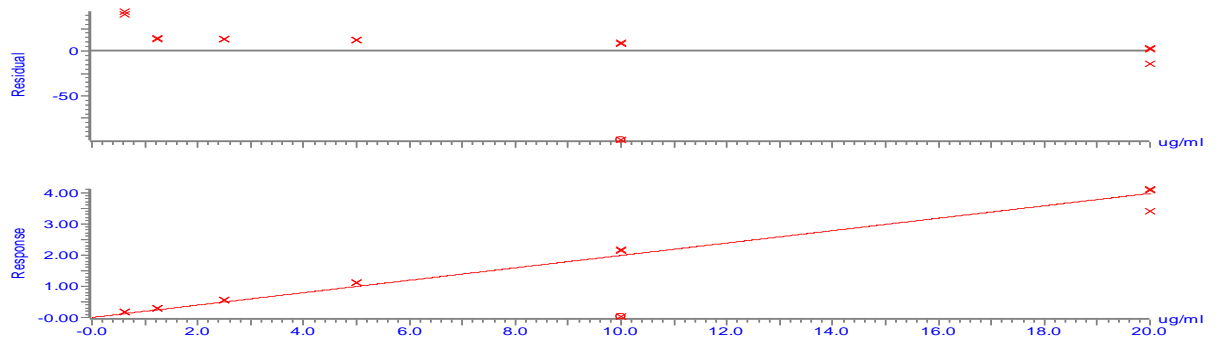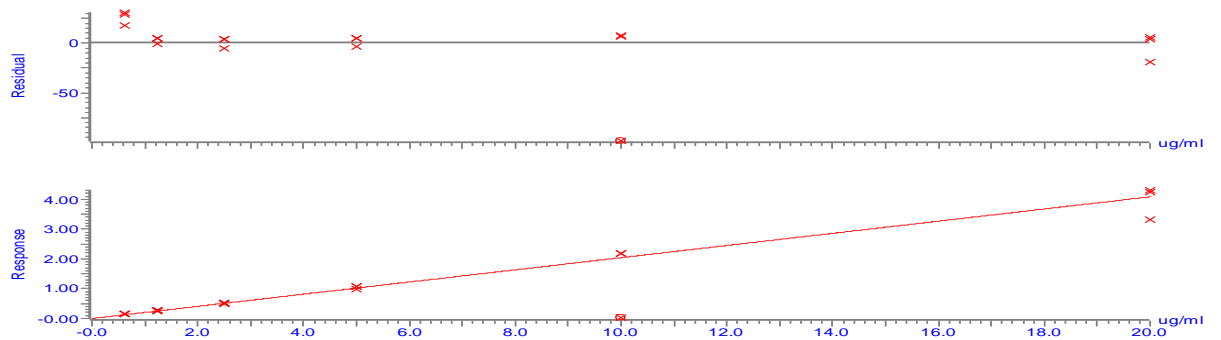## Cholic acid (CA): $R^2 = 0.999481$

Compound name: Cholic acid
Coefficient of Determination: R^2 = 0.999481
Calibration curve: 0.192316 * x
Response type: Internal Std (Ref 5), Area * (IS Conc. / IS Area)
Curve type: Linear, Origin: Force, Weighting: Null, Axis trans: None
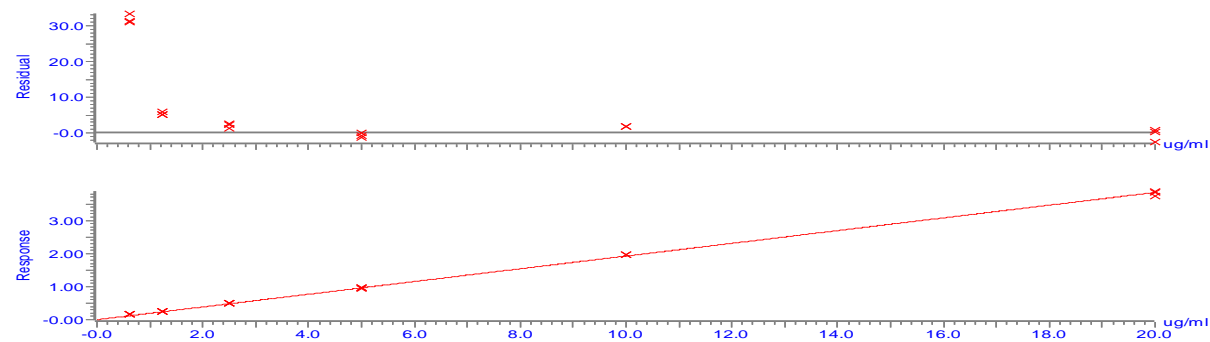
Chenodeoxycholic acid (CDCA): R^2=0.975284

Compound name: Chenodeoxycholic acid
Coefficient of Determination: R^2 = 0.975284
Calibration curve: 0.226256 * x
Response type: Internal Std (Ref 5), Area * (IS Conc. / IS Area)
Curve type: Linear, Origin: Force, Weighting: Null, Axis trans: None
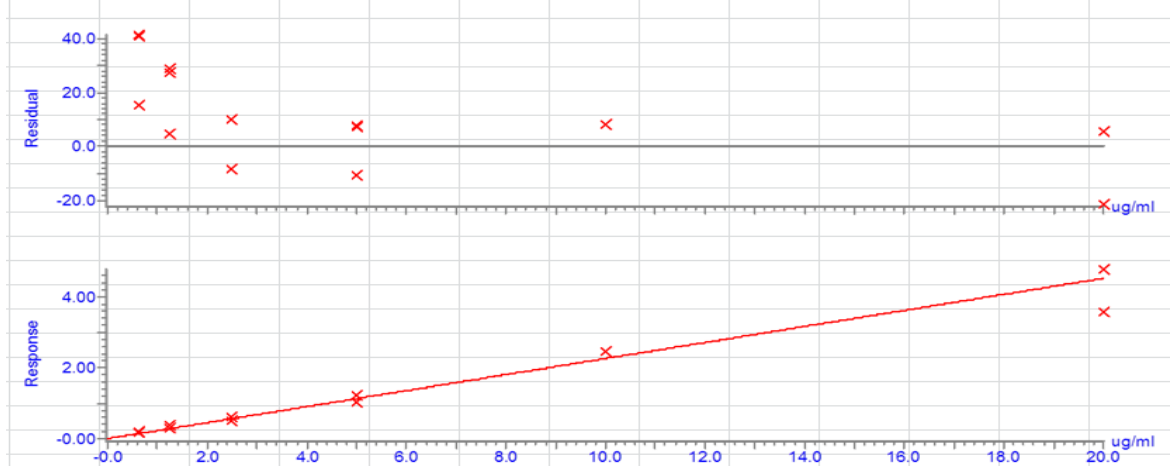
Lithocholic acid (LCA): R^2 = 0.000 (always difficult!)

Compound name: Lithocholic acid
Coefficient of Determination: R^2 = 0.000000
Calibration curve: 0.0682274 * x
Response type: Internal Std (Ref 5), Area * (IS Conc. / IS Area)
Curve type: Linear, Origin: Force, Weighting: Null, Axis trans: None
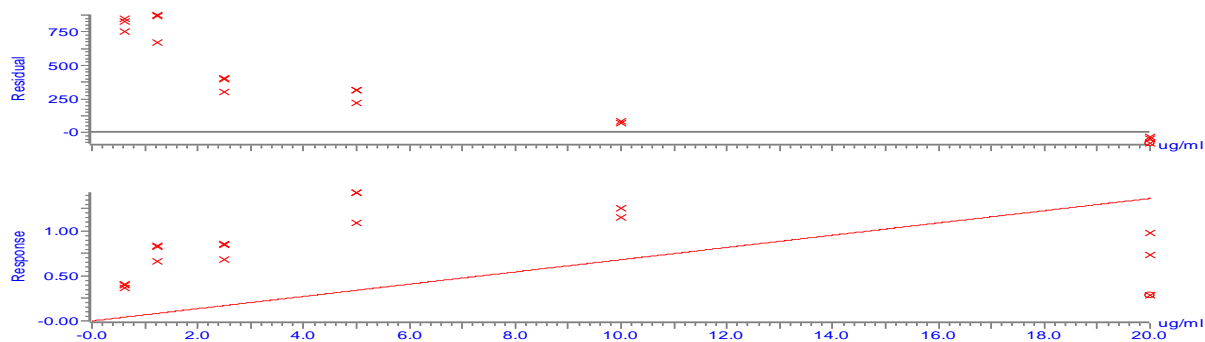
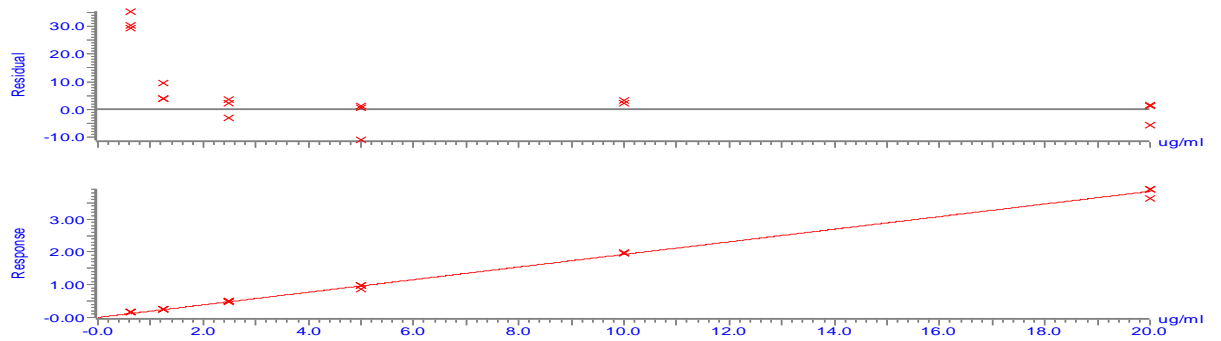## Deoxycholic acid (DCA): R^2 = 0.997885

Compound name: Deoxycholic acid
Coefficient of Determination: R^2 = 0.997885
Calibration curve: 0.241799 * x
Response type: Internal Std (Ref 5), Area * (IS Conc. / IS Area)
Curve type: Linear, Origin: Force, Weighting: Null, Axis trans: None

253
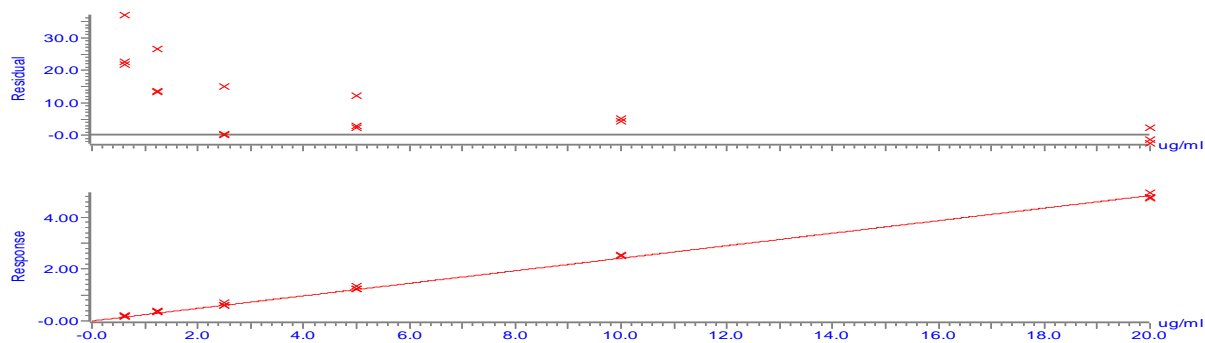
Ursodeoxycholic acid (UDCA): $R^2 = 0.976659$

Compound name: Ursodeoxycholic acid
Coefficient of Determination: R^2 = 0.976659
Calibration curve: 0.151834 * x
Response type: Internal Std (Ref 5), Area * (IS Conc. / IS Area)
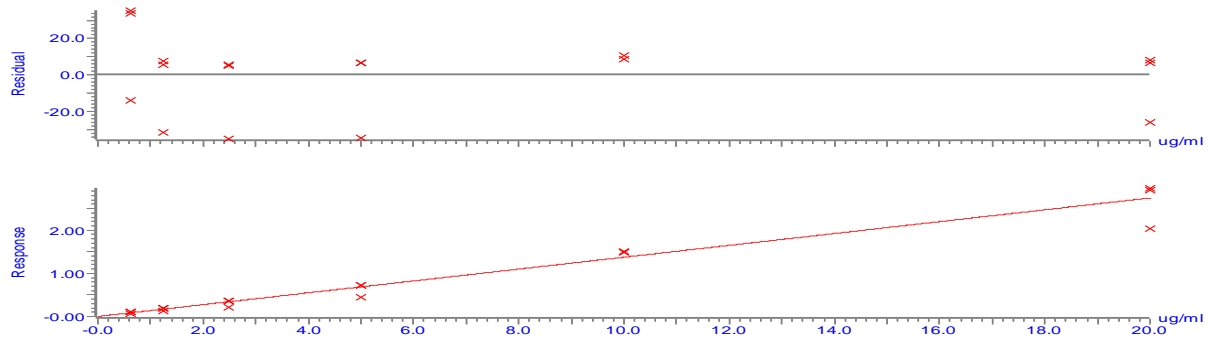Curve type: Linear, Origin: Force, Weighting: Null, Axis trans: None
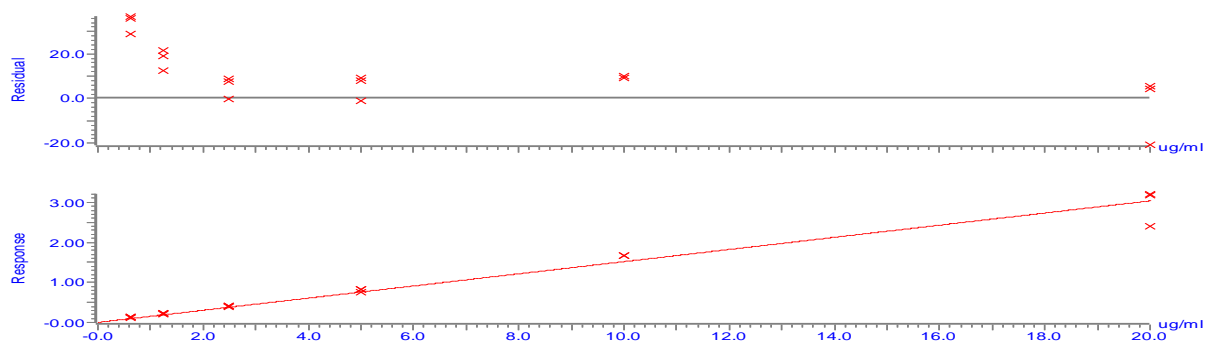
α –muricholic acid (α-MCA): $R^2 = 0.968570$

Compound name: alpha-muricholic acid
Coefficient of Determination: R^2 = 0.968570
Calibration curve: 0.42465 * x
Response type: Internal Std (Ref 5), Area * (IS Conc. / IS Area)
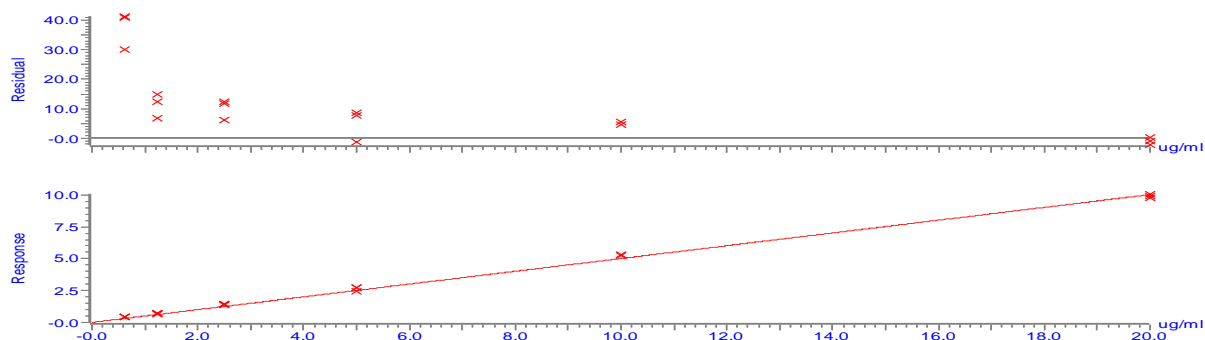Curve type: Linear, Origin: Force, Weighting: Null, Axis trans: None
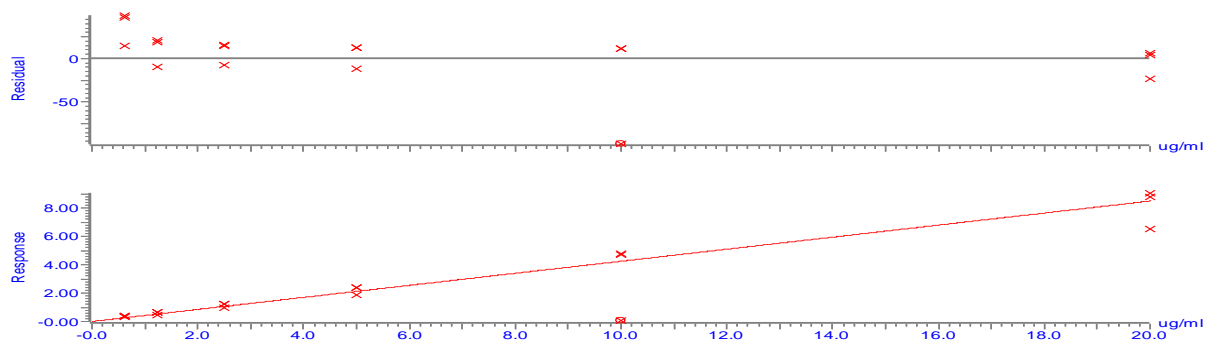
β-muricholic acid (β-MCA): $R^2 = 0.982533$

Compound name: B-Muricholic acid
Coefficient of Determination: R^2 = 0.982533
Calibration curve: 0.245306 * x
Response type: Internal Std (Ref 5), Area * (IS Conc. / IS Area)
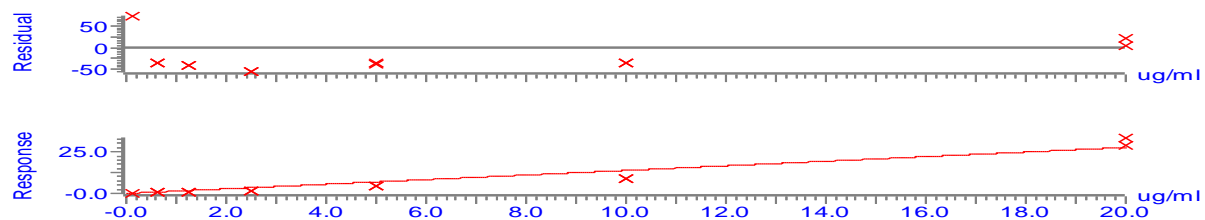Curve type: Linear, Origin: Force, Weighting: Null, Axis trans: None

254
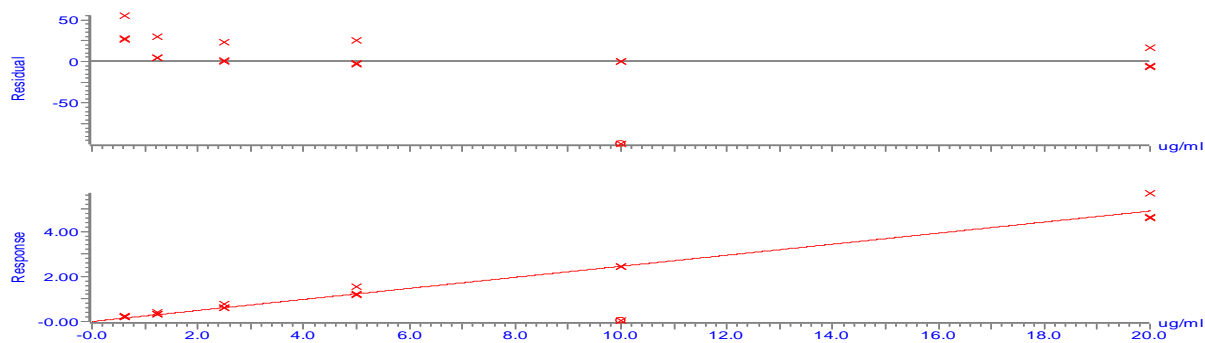
ω – muricholic acid (ω-MCA): $R^2 = 0.989249$

Compound name: omega Muracholic acid
Coefficient of Determination: R^2 = 0.989249
Calibration curve: 55767.8 * x
Response type: External Std, Area
Curve type: Linear, Origin: Force, Weighting: Null, Axis trans: None
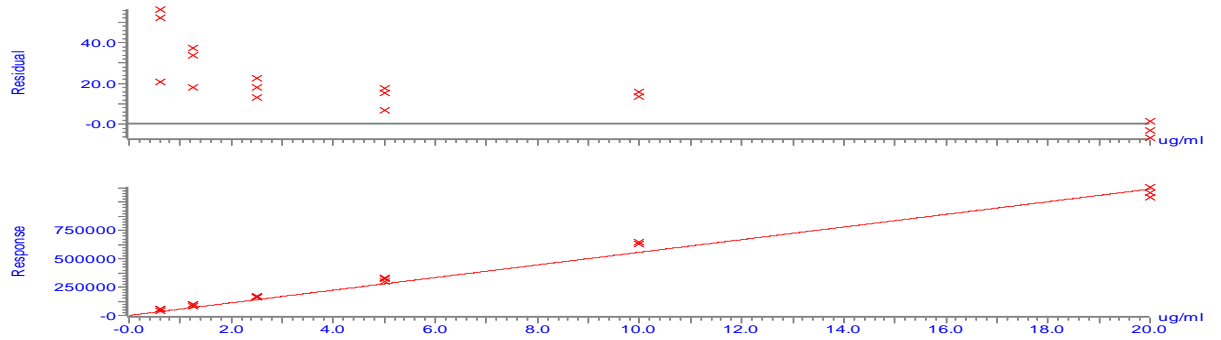
Taurocholic acid (TCA): $R^2 = 0.985264$

Compound name: Taurocholic acid
Coefficient of Determination: R^2 = 0.985264
Calibration curve: 0.198613 * x
Response type: Internal Std (Ref 5), Area * (IS Conc. / IS Area)
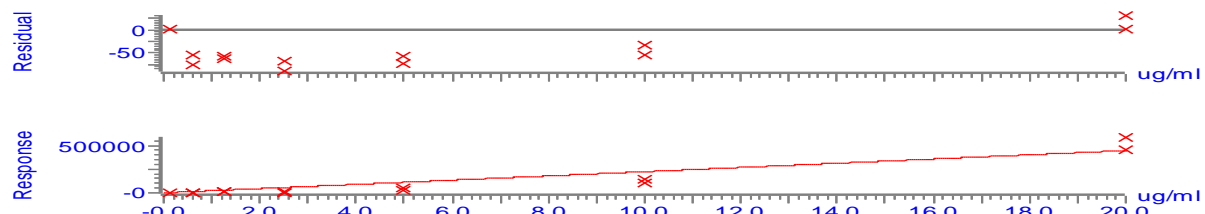Curve type: Linear, Origin: Force, Weighting: Null, Axis trans: None

Taurochenodeoxycholic acid (TDCA): $R^2 = 0.981316$

Compound name: Na Taurochenodeoxycholic acid
Coefficient of Determination: R^2 = 0.981316
Calibration curve: 0.204287 * x
Response type: Internal Std (Ref 5), Area * (IS Conc. / IS Area)
Curve type: Linear, Origin: Force, Weighting: Null, Axis trans: None

255

Taurolithocholic acid (TLCA): $R^2 = 0.977044$

Compound name: Taurolithocholic acid
Coefficient of Determination: R^2 = 0.977044
Calibration curve: 0.207965 * x
Response type: Internal Std (Ref 5), Area * (IS Conc. / IS Area)
Curve type: Linear, Origin: Force, Weighting: Null, Axis trans: None
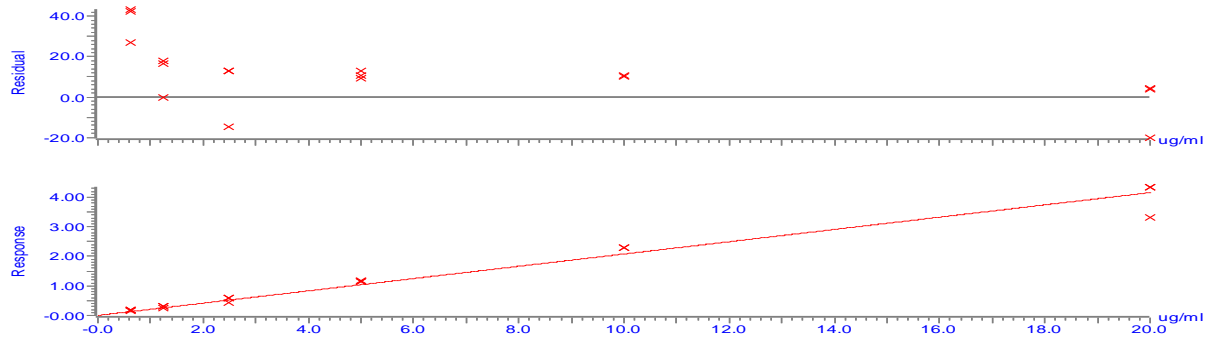
Taurodeoxycholic acid (TDCA): $R^2 = 0.997838$

Compound name: Na Taurodeoxycholic acid
Coefficient of Determination: R^2 = 0.997838
Calibration curve: 0.19235 * x
Response type: Internal Std (Ref 5), Area * (IS Conc. / IS Area)
Curve type: Linear, Origin: Force, Weighting: Null, Axis trans: None

Tauroursodeoxycholic acid (TUDCA): $R^2 = 0.961158$

Compound name: tauro UDCA
Coefficient of Determination: R^2 = 0.961158
Calibration curve: 0.137374 * x
Response type: Internal Std (Ref 5), Area * (IS Conc. / IS Area)
Curve type: Linear, Origin: Force, Weighting: Null, Axis trans: None

256

Taurobetamuricholic acid (TβCA): $R^2 = 0.998299$

Compound name: Taurobetamuricholic acid
Coefficient of Determination: R^2 = 0.998299
Calibration curve: 0.501312 * x
Response type: Internal Std (Ref 5), Area * (IS Conc. / IS Area)
Curve type: Linear, Origin: Force, Weighting: Null, Axis trans: None

Taurochenodeoxycholic acid (TCDCA): $R^2 = 0.927171$

Compound name: Na Taurochenodeoxycholic acid
Coefficient of Determination: R^2 = 0.927171
Calibration curve: 1.37791 * x
Response type: Internal Std (Ref 5), Area * (IS Conc. / IS Area)
Curve type: Linear, Origin: Force, Weighting: Null, Axis trans: None

Tauro-α-muricholic acid (TαMCA): $R^2 = 0.871911$

Compound name: tauroalphamuricholic acid
Coefficient of Determination: R^2 = 0.871911
Calibration curve: 22341.7 * x
Response type: External Std, Area
Curve type: Linear, Origin: Force, Weighting: Null, Axis trans: None

Tauro-β-muricholic acid (TβMCA): $R^2 = 0.909661$

Compound name: Taurobetamuricholic acid
Coefficient of Determination: R^2 = 0.909661
Calibration curve: 0.351872 * x
Response type: Internal Std (Ref 5), Area * (IS Conc. / IS Area)
Curve type: Linear, Origin: Force, Weighting: Null, Axis trans: None
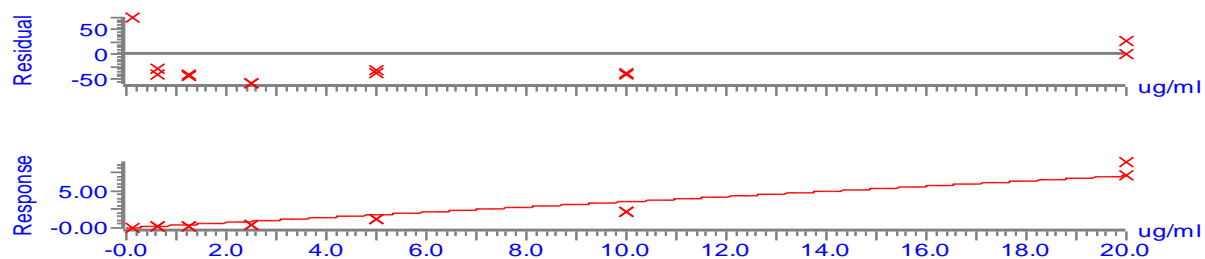
Fig. 1. UPLC-MS bile acid standard curves for individual BA's.

*Faecal UPLC-MS BA analysis (C57Bl/6 mice):*

258
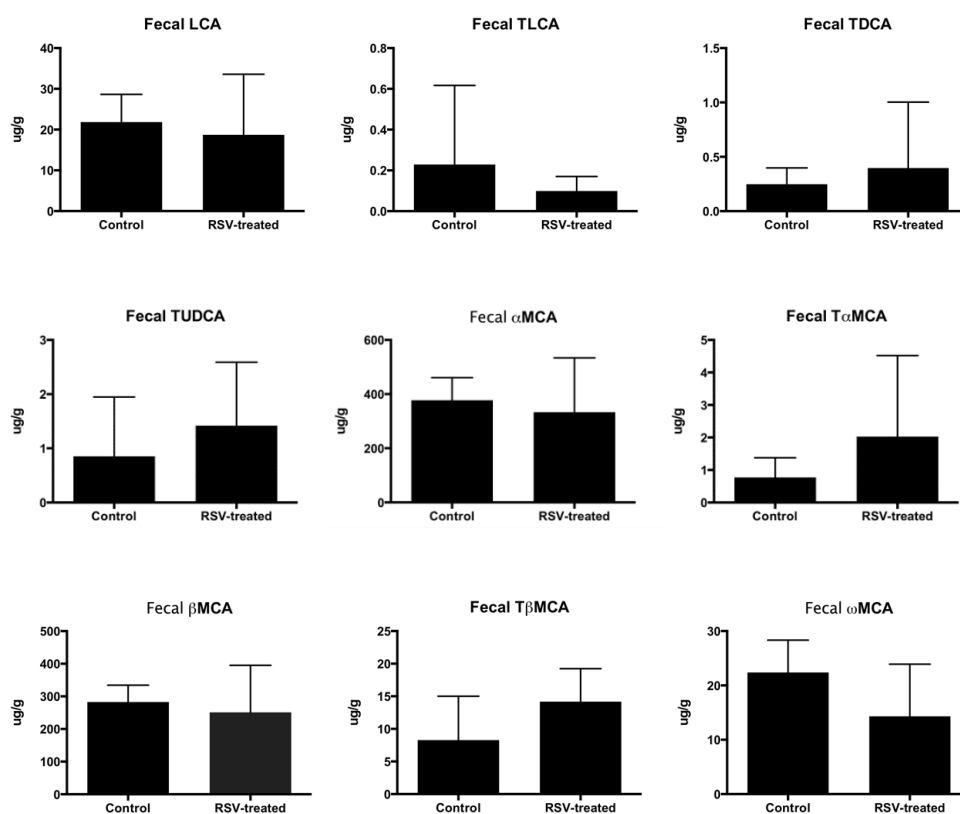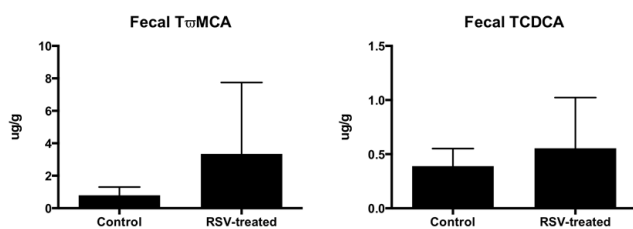
Fig.2. RSV unaffected certain faecal BA's in RSV-treated C57Bl/6 mice.

Individual graphs indicate levels of a number of faecal BA's (LCA, TLCA, TDCA, TUDCA, αMCA, TαMCA, βMCA, TβMCA, ωMCA, TωMCA and TCDCA) in control and RSV-treated mice. No significant differences where determined.

Hepatic (Liver) UPLC-MS BA analysis (C57Bl/6 mice):
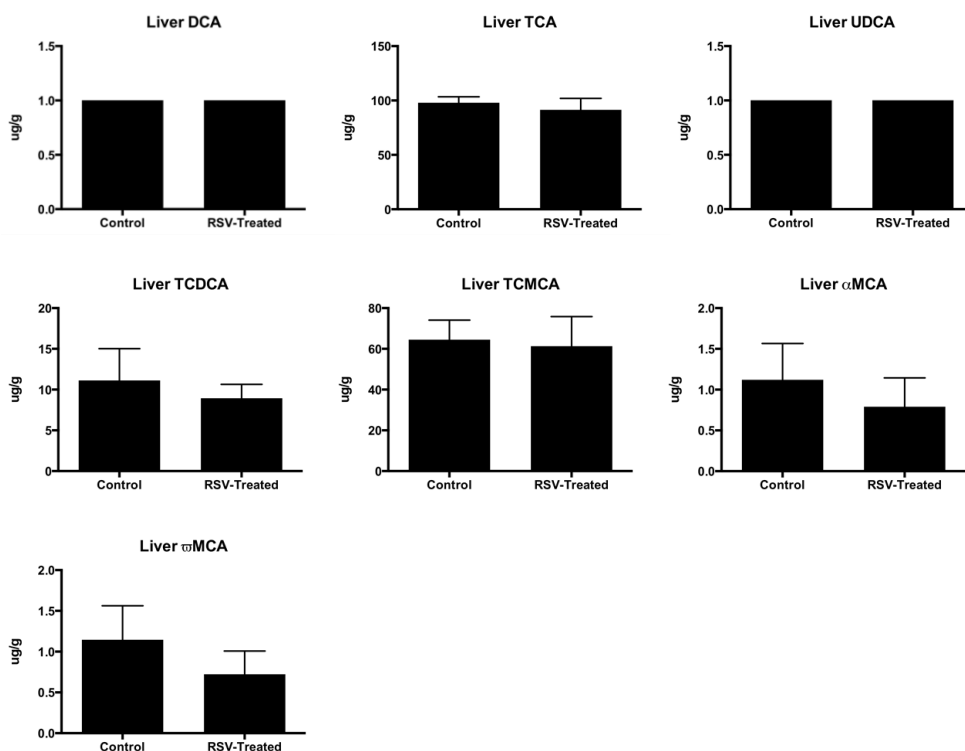
Fig. 3. RSV unaffected certain hepatic BA's in RSV-treated C57Bl/6 mice.

Individual graphs indicate levels of a number of liver BA's (DCA, TCA, UDCA, TDCA, TcMCA, αMCA and ωMCA) in control and RSV-treated mice. No significant differences where determined.
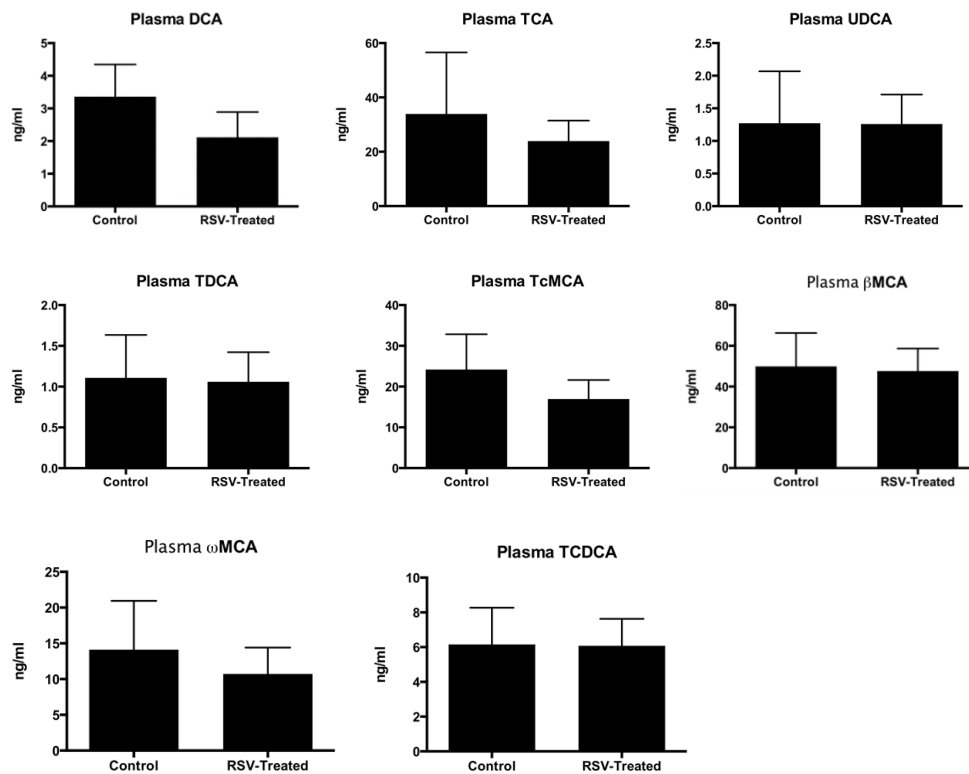
Fig. 4. RSV unaffected certain circulating BA's in RSV-treated C57Bl/6 mice.

Individual graphs indicate levels of a number of plasma BA's (DCA, TCA, UDCA, TDCA, TcMCA, βMCA, ωMCA and TCDCA) in control and RSV-treated mice. No significant differences were determined.
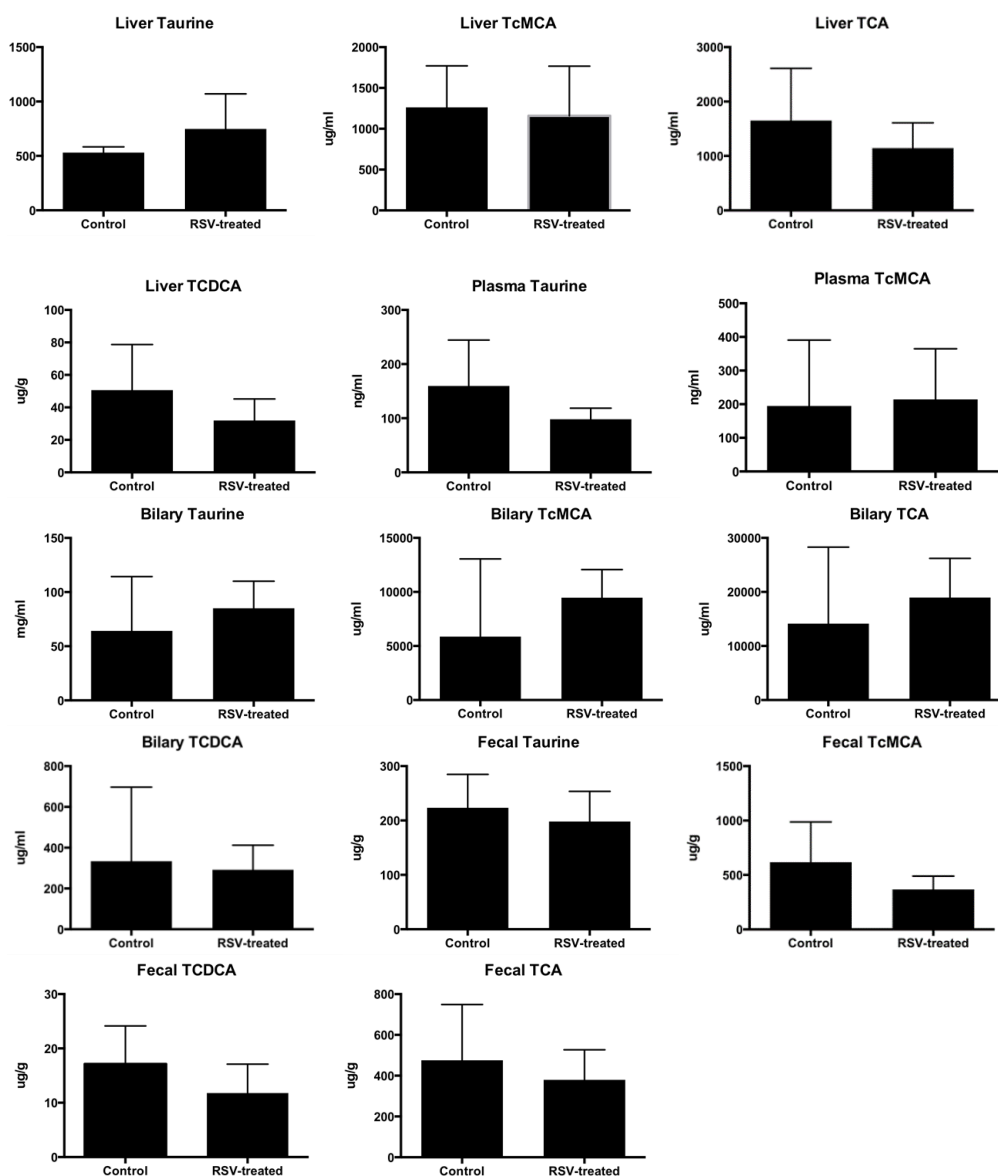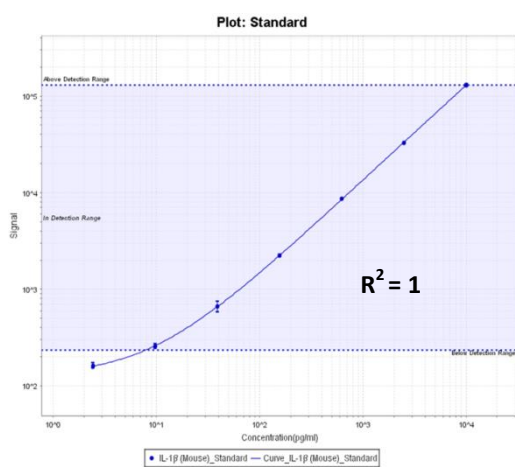
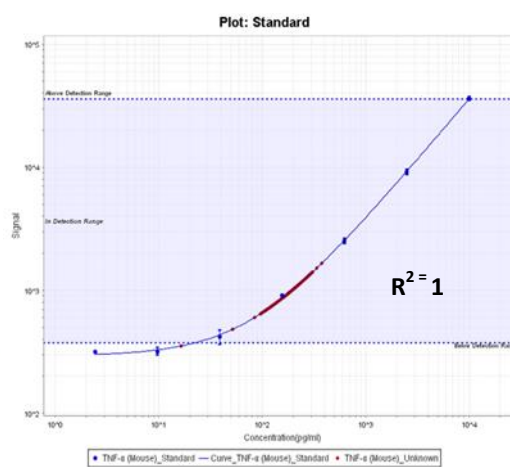**Fig.5. RSV unaffected a number of hepatic, circulating (plasma), biliary and faecal BA's in GF mice.**

Individual graphs indicate levels of a number of BA's (TcMCA, TCA, TCDCA and free taurine) between control and RSV-treated mice in liver, plasma, gall gladder (biliary) and faeces of GF animals. No significant differences were determined.
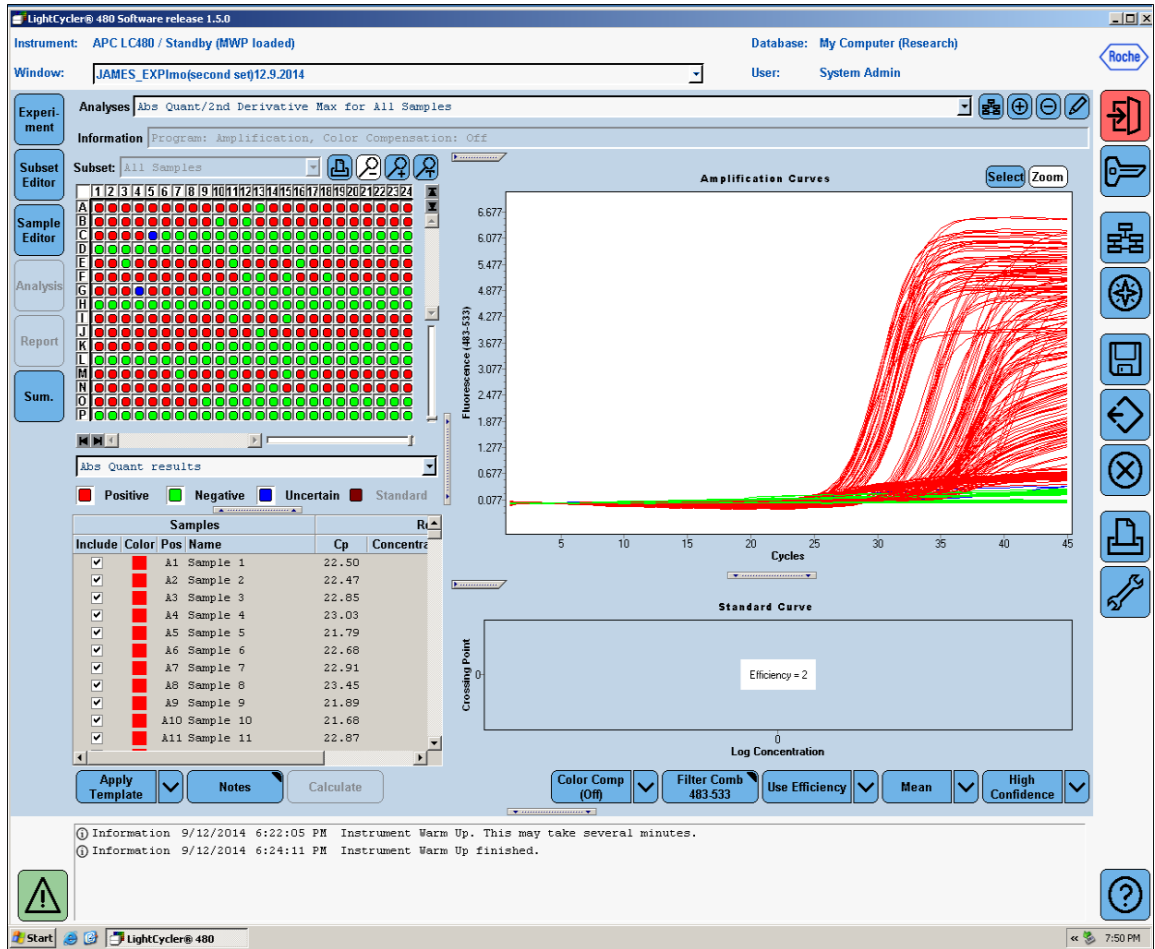
IL-1β:

TNFα:

Fig. 6. MSD standard curves for IL-1β and TNFα proinflammatory cytokines.

# Appendix to Chapter 5

Fig. 7. Example of qRT-PCT amplification curves.

Red circles indicate positive amplification, green circles indicate negative amplification and blue circles indicate uncertain values. Graphs represent fluorescence vs. cycle number for each amplification.

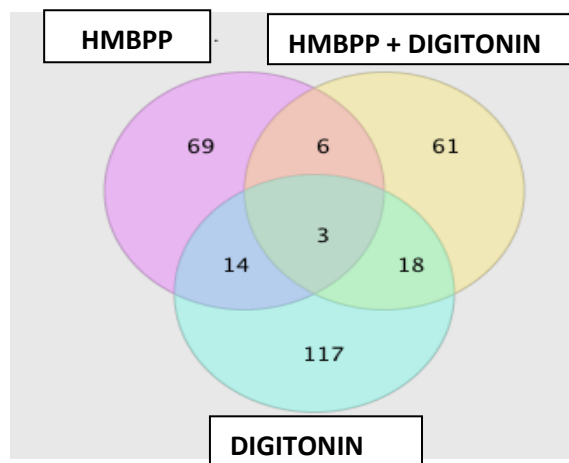*KEGG pathway analysis of differentially expressed genes in THP-1 cells by HMBPP for immunity and antigen presentation:*
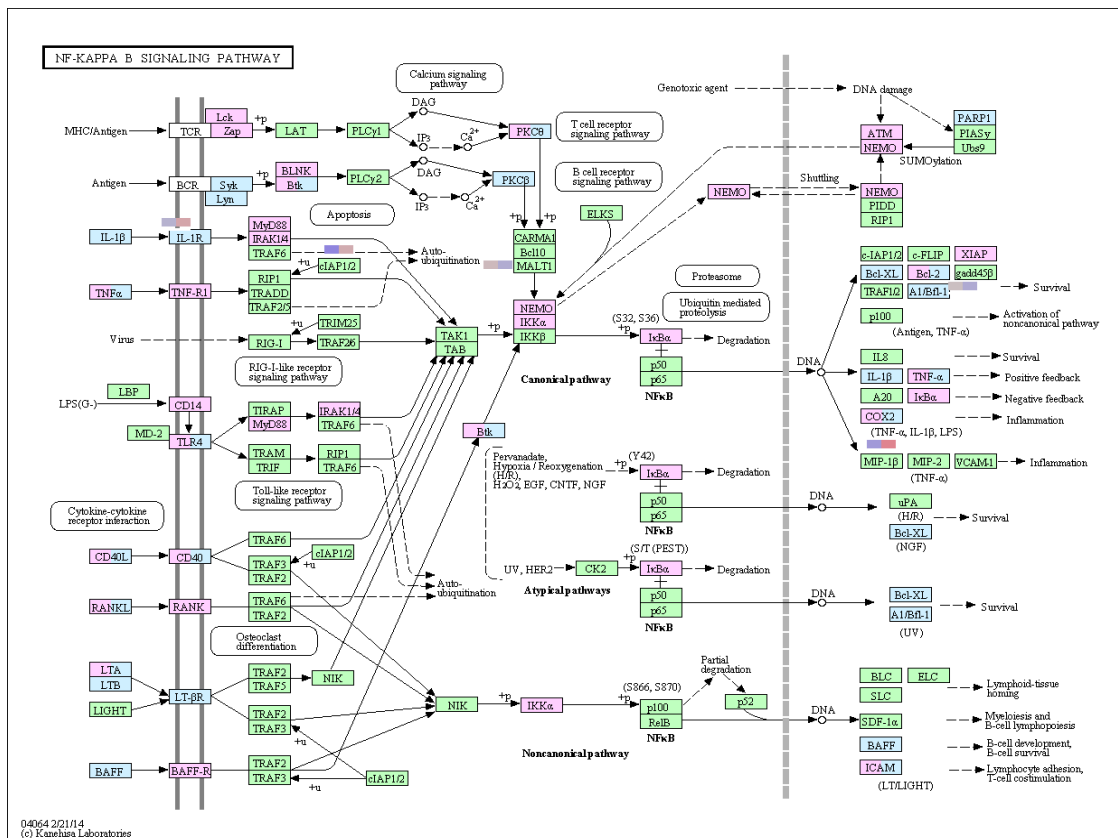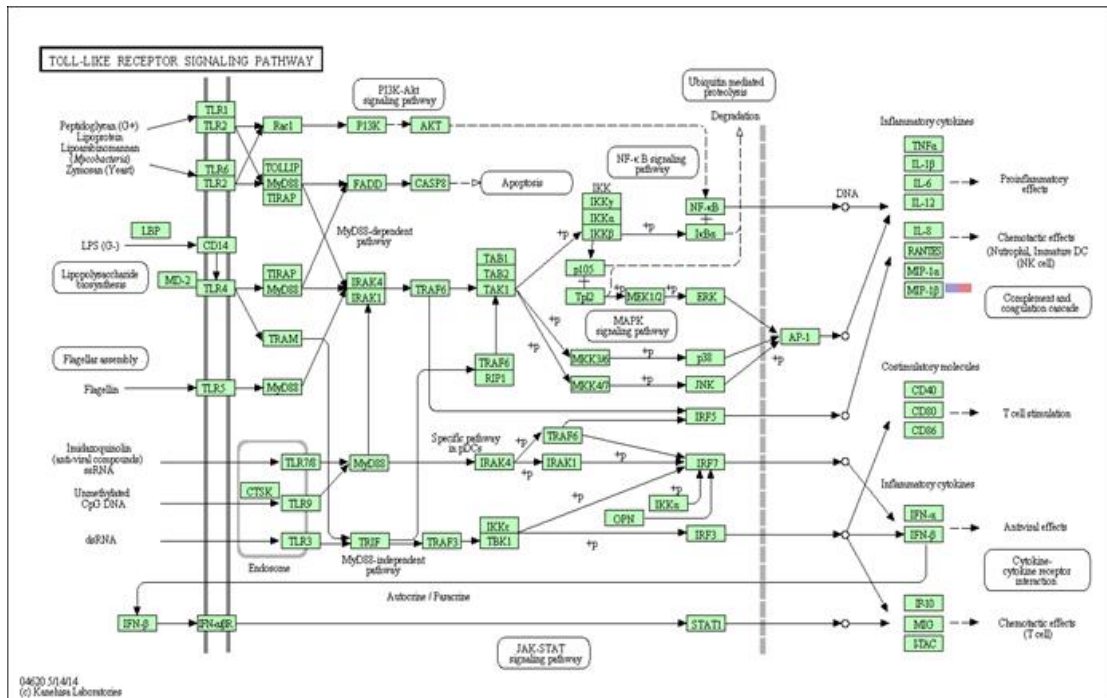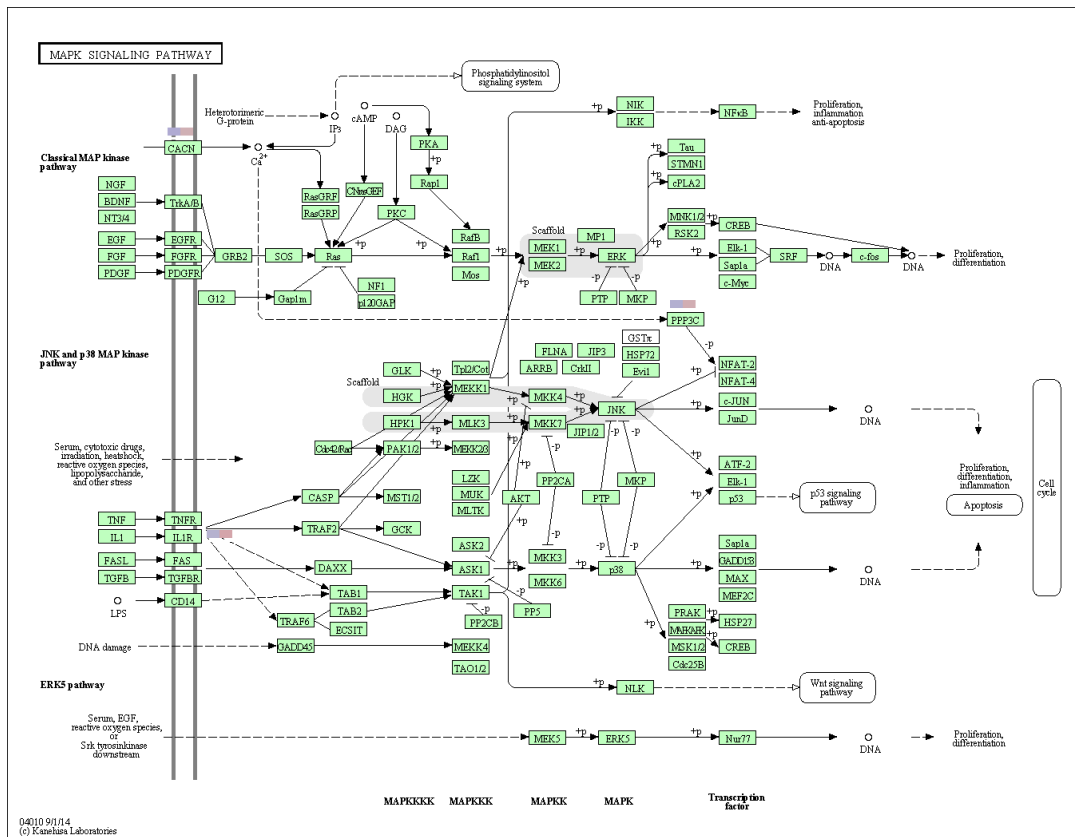
Fig. 8. **HMBPP attributed gene activation for immunity and antigen presentation in KEGG pathways for Toll-like receptor signalling, NFκB signalling and MAPK signalling in THP-1 cells.**

Fig. 9. Venn diagram representation of common and unique genes to each THP-1 treatment.

HMBPP did not significantly alter expression of the butyrophillin family of immunoglobulin-like molecules located on human chromosome 6 in THP-1 cells for antigenic presentation:

Gene	ID	Control	Digitonin	HMBPP	HMBPP & Digitonin	Sig. (CNTRL vs. HMBPP)
SSR1	ENSG000001 24783	921	868.3333	1172	1258	NO
SLC35B3	ENSG000001 24786	140	164	177.33333	183	NO
TMEM14C	ENSG000001 11843	699	740.3333	907	1057.6666	NO
TMEM14B	ENSG000001 37210	479	574	630.3333	819	NO
CCDC90A/MCUR1	ENSG000000 50393	70.3333	101.333336	81.666664	105.333336	NO
FAM8A1	ENSG000001 37414	58	59	80.333336	78.666664	NO
MBOAT1	ENSG000001 72197	50.6667	55.333332	66.666664	90.333336	NO
CDKAL1	ENSG000001 45996	68.3333	72.333336	71.333336	86.333336	NO
HDGFL1	ENSG000001 12273	0.33333	0.33333334	1.6666666	0.6666667	NO
NRSN1	ENSG000001 52954	2.66667	2.3333333	3.3333333	2.6666667	NO
NRSN2	ENSG000001 25841	49	62.666668	65.666664	75	NO
BTN3A2	ENSG000001 86470	173.667	190	250	255.66667	NO
BTN3A3	ENSG000001 11801	85.6667	96	123.666664	125.333336	NO
BTN3A1	ENSG000000 26950	82.6667	78	124	114	NO
BTN2A2	ENSG000001 24508	30	34	40.333332	49	NO
BTN2A1	ENSG000001 12763	103	131.66667	117	136.33333	NO

Fig. 10. MACE RNA-seq analysis of the butyrophillin family of immunoglobulin-like molecules (human chromosome 6) for control versus HMBPP.

Acknowledgements

I believe I have been very lucky to be given this opportunity to undertake a PhD in what has been a fascinating and very valuable experience going forward in my career. I would to acknowledge my supervisors Dr. Cormac Gahan and Prof. Colin Hill for allowing me integrate and become a value member of their research team. I would like to thank The Irish Research Council for Science and Technology (IRCSET), The Alimentary Pharmabiotic Centre (APC) and School of Microbiology, University College Cork (UCC) for awarding me an EMBARK postgraduate scholarship for the duration of my PhD. I would also like to thank our collaborators at the Teagasc Food Research Centre, School of Nutritional Sciences (UCC) and Genxpro (Germany) for their great help and assistance in my research.

I would like to give a special mention to particular individuals in my lab 4.23 (second home) and other labs (4.25, 4.28 and 4.35) in the APC for all the great times we spent together discussing science as well as all the other things we talked about during the last 4 years! Firstly, Dr. Cormac Gahan and Prof. Colin Hill for all the insightful and enlightening discussions that helped me grow as scientist/researcher and supporting me throughout. I want to give a very special mention to Dr. Susan Joyce in our group who has been so amazing in working with over the last few years. She has inspired me to reach for the stars in the lab and helped me no end my research. Without her valuable contribution, I would not be the microbiologist I am today. Dr. Kalai Govindarajan, who has spent many a late evening in the lab with me teaching and imparting her vast wealth of cell biology knowledge onto me. FYI, if you ever get a chance to try her cooking I would recommend it! It's yummy ☺!   Dr. John Mac Sharry, one of the nicest and friendliest guys I have been privileged to

have had the opportunity to work with. He also was someone that helped me so much during this PhD. Mr. Pat Casey, for all his help with the mouse trials. RIP to all those poor mice we put to sleep all in the name of science hahaha. Pat, you're a legend ☺!

To all my lab buddies past and present; Dr. Eamonn Culligan, Dr. Heather Mc Laughlin, Dr. Ruth Morrissey, Dr. Joanne Cummins, Dr. Aurelie Hanin, Dr. Sinead Heuston, Dr. Avelino Alvarez Ordonez, Dr. Tanya Clifford, Dr. Georgina O' Dowd Ciara, Sarah-Louise, Ann, Sinead – I could not have done this without guys! Thanks for putting up with me through the good times and the bad. Our escapades from nights out will forever be in my memory ☺. Also the guys and girls of Lab 4.25 next door I won't forget you guys either! (Mary, Debbie, Kerry, Lorena, Amy, Muireann, Kieran, Noreen, Emer, Pauline, Marita and anyone else I am forgetting!) I am sure will remain friends for years to come! And to all the other people in UCC I have met and worked with - the list is endless! To all the School of Microbiology staff (Carmel, Margaret, Collette, Ciorsdan, Pat, Paddy, Maire, Aine, Hilda, Dan, Liam, Maurice, apologises to anyone I am missing). To the wider lecturers and staff in the department. You all had a part to play!

To my family, friends and my dear partner who looked out for me over the last few years. Thank for supporting and having faith in me throughout. This has been my journey and yours! I dedicate this thesis in your honour ☺ I am sure you will support me to no end in my next endeavour!